



---

b  
**UNIVERSITÄT  
BERN**

Graduate School for Cellular and Biomedical Sciences  
University of Bern

**ENDOTHELIAL CELL PROTECTION IN XENOTRANSPLANTATION  
AND ISCHEMIA/REPERFUSION INJURY: ASSESSING THE EFFECT  
OF MULTIPLE TRANSGENES AND THE PATHOPHYSIOLOGICAL  
ROLE OF THE PLASMA CASCADE SYSTEMS**

PhD Thesis submitted by

**Riccardo Sfriso**

from **Italy**

for the degree of

PhD in Biomedical Sciences

Supervisor

Prof. Dr. Robert Rieben

Department for BioMedical Sciences

Faculty of Medicine of the University of Bern

Co-advisor

Prof. Dr. Jörg Seebach

Division of Immunology and Allergology

University Hospital and Medical Faculty of the University of Geneva



Accepted by the Faculty of Medicine, the Faculty of Science and the Vetsuisse  
Faculty of the University of Bern at the request of the Graduate School for Cellular  
and Biomedical Sciences

Bern,

Dean of the Faculty of Medicine

Bern,

Dean of the Faculty of Science

Bern,

Dean of the Vetsuisse Faculty Bern





## TABLE OF CONTENTS

|  |           |
|--|-----------|
| <b>ABSTRACT .....</b>  | <b>1</b>  |
| <b>INTRODUCTION .....</b>  | <b>1</b>  |
| ORGAN SHORTAGE: THE SITUATION OF ALLOGENEIC ORGAN TRANSPLANTATION .....  | 1         |
| XENOTRANSPLANTATION: A POSSIBLE SOLUTION TO ORGAN SHORTAGE? .....  | 3         |
| CONCORDANT OR DISCORDANT XENOTRANSPLANTATION? .....  | 5         |
| THE HURDLES TO XENOTRANSPLANTATION. ORGAN REJECTION: PIG ORGANS ARE SEEN AS ‘DANGEROUS’ AND ‘FOREIGN’ BY THE HUMAN IMMUNE SYSTEM.....                        | 6         |
| <i>Hyperacute rejection</i> .....  | 7         |
| <i>Acute vascular rejection</i> .....  | 8         |
| <i>T-cell mediated rejection</i> .....   | 9         |
| GENETIC MODIFICATION OF THE DONOR .....  | 11        |
| CURRENT PRECLINICAL SURVIVAL OF XENOGRAFTS IN NON-HUMAN PRIMATE MODELS .....   | 15        |
| THE COMPLEMENT SYSTEM AND ITS REGULATION.....  | 16        |
| <i>Overview of the complement system</i> .....   | 17        |
| <i>The classical pathway</i> .....   | 17        |
| <i>The lectin pathway</i> .....  | 18        |
| <i>The alternative pathway</i> .....   | 18        |
| <i>C3 independent pathways</i> .....   | 19        |
| <i>Regulation of the complement system</i> .....   | 19        |
| THE COAGULATION SYSTEM.....  | 22        |
| THE VASCULAR ENDOTHELIUM: A KEY PLAYER IN REJECTION .....  | 24        |
| <i>Flow and shear stress</i> .....   | 25        |
| <i>The endothelial glycocalyx</i> .....  | 26        |
| MICROFLUIDIC SYSTEM .....  | 30        |
| <b>HYPOTHESIS AND AIM OF THE THESIS.....</b>   | <b>32</b> |
| <b>REFERENCES .....</b>  | <b>35</b> |
| <b>RESULTS.....</b>  | <b>51</b> |
| PAPER I.....   | 53        |
| <i>Assessment of the Anticoagulant and Anti-inflammatory Properties of Endothelial Cells Using 3D Cell Culture and Non-anticoagulated Whole Blood.</i> ..... | 53        |
| PAPER II.....  | 61        |
| <i>3D artificial round section micro-vessels to investigate endothelial cells under physiological flow conditions.</i> .....                                 | 61        |
| PAPER III (BOOK CHAPTER).....  | 77        |

|  |            |
|--|------------|
| <i>3D cell culture models for the assessment of anticoagulant and anti-inflammatory properties of endothelial cells</i> .....  | 77         |
| PAPER IV.....  | 99         |
| <i>Release of pig leukocytes and reduced human NK cell recruitment during ex vivo perfusion of HLA-E/human CD46 double-transgenic pig limbs with human blood</i> .....   | 99         |
| PAPER V .....  | 115        |
| <i>Multiple genetically modified GTKO/hCD46/HLA-E/h<math>\beta</math>2–mg porcine hearts are protected from complement activation and natural killer cell infiltration during ex vivo perfusion with human blood</i> ..... | 115        |
| PAPER VI.....  | 127        |
| <i>Consistent success in life supporting porcine cardiac xenotransplantation</i> .....   | 127        |
| <b>OVERALL DISCUSSION AND OUTLOOK</b> .....  | <b>163</b> |
| <b>ACKNOWLEDGMENTS</b> .....   | <b>165</b> |

## Abstract

Worldwide, the critical and growing shortage of human donor organs represents a major concern which needs alternative solutions. Xenotransplantation – the transplantation of cells, tissues and organs between different species – has a long history and aims to provide a solution to the high demand of donor organs. Pigs are considered a suitable donor candidate, however organs from wildtype pigs are rapidly rejected by a process called hyperacute rejection. This consists of a massive antibody binding and subsequent complement activation with an inevitable graft destruction. Nowadays, hyperacute rejection can be overcome by genetic manipulation of the donor. However, a delayed rejection still occurs. It is defined as acute vascular rejection and is characterized by coagulation dysregulation resulting in thrombotic microangiopathy and leading to graft failure within days. Cellular rejection mediated by T cells as well as innate immune cells, including NK cells, macrophages and neutrophils is another hurdle which needs to be overcome in order to bring xenotransplantation closer to the clinical application. Advanced genetic engineering techniques such as the CRISPR-Cas9 technology allow to delete antigens from the porcine genome or to introduce human transgenes with the aim of reducing the molecular incompatibilities as well as the immunogenicity of the xenograft. The use of pigs with new multiple genetic modifications, including expression of human thrombomodulin, complement regulatory proteins and knock-out of xeno-antigens are now available for testing in nonhuman primates.

This thesis focuses on the study of the vascular endothelium, as this is the first tissue to come in contact with the recipient blood after transplantation. A novel *in vitro* 3D microfluidic system has been developed and used to explore the effects of multiple transgenes in a xenotransplantation setting. Endothelial cells cultured on the luminal surface of circular microchannels were exposed to shear stress and pulsatile flow, so that they experience a microenvironment similar to the *in vivo* situation. Perfusion of porcine endothelial cells with human serum allowed to study the effects of transgenes on prevention of complement and antibody mediated cytotoxicity. This thesis comprises of interesting and fruitful collaborations which gave light to real breakthroughs in the field of xenotransplantation.



# Introduction

## **Organ shortage: the situation of allogeneic organ transplantation**

Allogeneic organ transplantation – the transplantation between two genetically non-identical individuals from the same species – is, nowadays, a globally accepted life-saving medical treatment for end-stage organ failure. However, worldwide, the demand for organs largely exceeds their availability. On average, 20 people die each day in the U.S while waiting for a transplant and every 10 minutes a new person is added to the waiting list. At the end of 2015, there were 122,071 patients waiting for a donor organ, 30,975 transplants performed, and 15,068 donors recovered (Figure 1). Currently (August 2018) in the U.S, 114,400 people need a lifesaving organ transplant and 21,000 transplantations have been performed so far. (<https://optn.transplant.hrsa.gov/>).

According to the non-profit Swisstransplant Foundation, by the end of 2017, there were 1,480 Swiss residents waiting for a transplant, which represents a 38% increase as compare to 2010 (<https://www.swissinfo.ch>). In Switzerland, a patient in need of a kidney – the most requested organ – must wait on average 1,109 days. The shortage is likely to be exacerbated by Switzerland’s policy of explicit consent, known as ‘opt in’ system, according to which organs can be donated only with the patient’s permission, or the one of their next of kin. The majority of European countries adopt the policy of “presumed consent”, known as ‘opt out’ system, meaning that a deceased individual is classified as a potential donor in absence of explicit opposition to donation before death. In practice, regardless of the type of legislation, in most countries families are allowed to have the last word. A study carried out by Queen Mary University of London revealed that ‘the next of kin are more likely to quash a donation if their deceased relative has not given explicit consent’.<sup>1</sup> Indeed, approximately half of the families that are asked to decide for a donation refuse it in the U.S. and Great Britain, compared to around 20% in Spain and around 30% in France.<sup>2-4</sup>

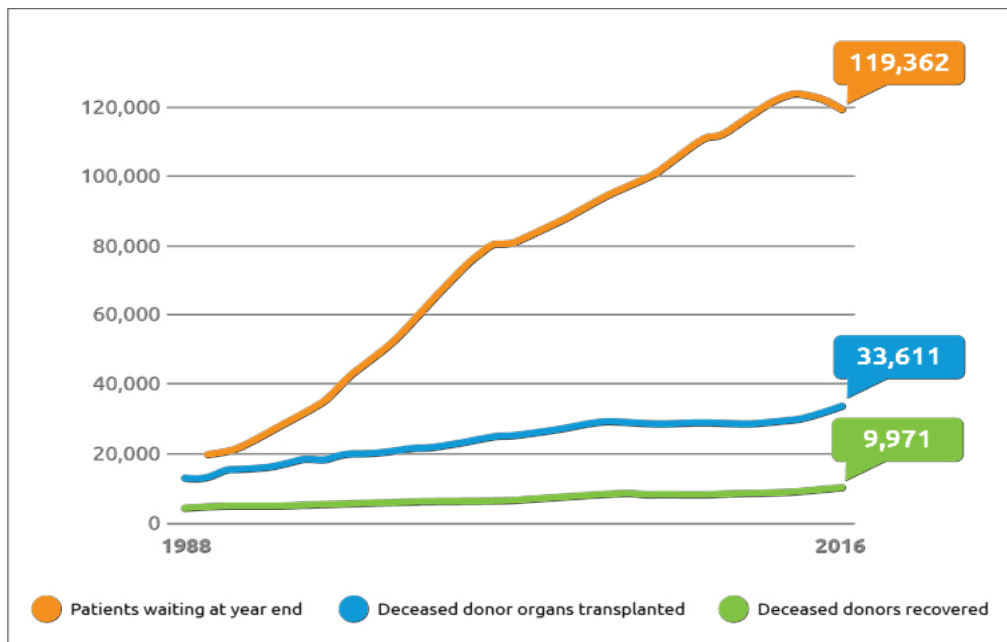


**Figure 1** The organ shortage increases and the gap between organ demand and supply widen.  
 (Data from United Network for Organ Sharing, <https://unos.org/bucketlist/>)

Spain is considered the world leader in organ donation and transplantation. A leadership which was maintained for 26 years reaching a total of 2,183 donors in 2017 (49.9 donors per million population). This success derives from a specific organizational approach. In 1989 the Spanish Government created the Organización Nacional de Trasplantes (ONT), an organism responsible for overseeing and coordinating donation and transplant activities in Spain. The Spanish model relies on the designation of specialized professionals (transplant coordinators) with the aim of making donation happen when a patient dies in conditions that allow organ donation, not only after cerebral death but also after circulatory death.<sup>5</sup> Following this approach, Italy was able to significantly increase the donation rate.<sup>6</sup> Very recently, Italy and Spain carried out the first international paired kidney exchange in Southern Europe (<http://www.ont.es>). The countries adhering to the paired exchange program offer the possibility to exchange living kidney donors between 2 or more pairs despite the fact that their partner or relative, who would like to make the donation, is incompatible. One patient in Spain and another in Italy received a living-donor kidney transplant thanks to the exchange of organs from their respective donors. Despite the manifold efforts aiming at increasing the donor pool, the need for solid organ transplantation

keeps growing, with rises in the number of patients on the waiting lists. Alternative solutions are therefore needed.

### **Xenotransplantation: a possible solution to organ shortage?**

Alternatives to allotransplantation include artificial organs, stem cell therapy and xenotransplantation. Despite the recent advances in stem cell biology and tissue engineering their clinical application remains in the far future.

Xenotransplantation, from the Greek '*xeno*' meaning 'foreign', is a cross-species transplantation aiming to resolve the shortage of human organs. It has the potential to offer virtually unlimited supply of organs and cells for clinical transplantation.<sup>7</sup> In addition to the unrestricted availability of organs, xenotransplantation offers additional advantages: Genetic manipulation of the donor organ/animal to improve molecular compatibility with the recipient; the organs would be available electively, allowing the planning of a pretreatment to enhance the acceptance of the graft. Lastly, donor organs would not be potentially damaged after brain death as they would be explanted from healthy anesthetized animals.<sup>8</sup>

Xenotransplantation has a long history since there have been a number of clinical attempts during the past 350 years. The first one known from the literature goes back to 1667, when Jean-Baptiste Denis, a French physician, performed lamb-to-human blood transfusion.<sup>9</sup> At that time, scientists believed that by transfusing blood from an animal that was considered innocent and pure, the lamb or a calf for instance, they would have been able to replace bad blood with a good one. Several transfusions were then performed in Europe until a patient called Antony Mauroy dying after being repeatedly transfused with calf blood to cure his mental illness. Even though the cause of the death was later found to be arsenic poisoning, a French court decided to ban transfusions. Since then, no one attempted to do it again until the 19<sup>th</sup> century.<sup>10</sup>

The first xenotransplantation of body parts was performed in 1682 when physicians successfully repaired a damaged skull of a Russian nobleman with a piece of bone retrieved from a dog's skull. In 19th century, Serge Voronoff, a famous French physician, performed several xenotransplantation using testicles of chimpanzee or

baboon aiming at rejuvenating men.<sup>11</sup> During the early 1900's many xenotransplantation attempts miserably failed. To mention few of them: In 1905, in France, Princeteau transplanted slices of rabbit kidney into a child with signs of renal failure who succumbed after 16 days of lung congestion. In 1906, after perfecting the anastomosis technique, Mathieu Jaboulay carried out two distinct heterotopic transplantations of a pig and goat kidneys to the bend of the elbow of a 48-year and 50-year old women, respectively. Both the patients died on the third day because of thrombosis. Lastly, there was a remarkable attempt of Harold Neuhof (USA) in 1923, consisting in the transplantation of a lamb kidney to a man with mercury poisoning. The patient survived for 9 days. Following these striking failures, for the next 40 years no other attempt was to be done.

The arrival of the first immunosuppressive drugs reawoke interest in transplantation. The modern history of clinical xenotransplantation is generally thought to begin in 1963 when Dr. Keith Reemtsma transplanted chimpanzee kidneys into 13 patients using immunosuppressive treatment.<sup>12-14</sup> Remarkably, one patient returned to work for almost 9 months before suddenly dying from electrolyte imbalance. Dr. Hardy in 1964 performed the first heart transplant in a human using a chimpanzee heart. However, the patient died within two hours as the heart proved too small to support the patient's circulation.<sup>15</sup> The first chimpanzee-to-human liver transplantation was carried out 1966 by Dr. Starzl.<sup>16</sup> Between 1966 and 1974 he performed one ex vivo chimpanzee liver perfusion and three chimpanzee liver transplants in humans with a maximum of 14 days of graft function. After that, Dr. Starzl did not use chimpanzees anymore as organ donors. Following the introduction of cyclosporine, in 1981, Dr. Starzl's group performed more than 600 transplantations in a year establishing what was considered the busiest transplant program in the world (nicely reviewed by Dr. Cooper<sup>17</sup>). In 1984, the most famous xenotransplantation so far was realized by Leonard Bailey. He transplanted a neonate ('Baby Fae') with an ABO-mismatched baboon heart to cure her hypoplastic left-heart syndrome.<sup>18</sup> Even though the conditions for the success were present: match in the organ size, immunological immaturity of the recipient, availability of cyclosporine, unfortunately, the baby recipient died 20 days after surgery. After this latest failure, xenotransplantation faced



a stalemate. Only in 1992, when FK506 (tacrolimus) became available, Dr. Starzl obtained patient survival for 70 days following a baboon liver transplant.<sup>19</sup>

### **Concordant or discordant xenotransplantation?**

Promising results were obtained in the past by using organs from concordant species (chimpanzee or baboons). However, the availability of great apes closely related to humans is poor. Even though the baboon is available in the wild in relatively large numbers, its usability is reduced due to several compelling ethical and practical reasons. Non-human primates are more likely than other animals to carry viruses which could infect humans (e.g., the HIV virus originated in chimpanzees)<sup>20</sup>. Besides that, the baboon's organ size would restrict transplantation to pediatric patients. Another practical issue is represented by the low breeding potential which consists of long pregnancies, very few offspring and their slow growth. Last but not least, the ethical concern: The public is reluctant to exploit animals sharing many features with humans as organ reservoir for transplantation.

The early attempts at clinical xenotransplantation using discordant donors (e.g., pigs) were all characterized by early failure. Even though the usage of pigs as organ donors would guarantee several advantages over the non-human primates (Table 1)<sup>21</sup>, it appeared to be less desirable from an immunological point of view reflecting the fact that pigs and humans are phylogenetically distant. This results in a very very strong response to pig organs by the human immune system. Nevertheless, given the numerous advantages (Table 1), the pig is generally accepted as 'the' discordant species of choice for xenotransplantation.<sup>7,22</sup>

**Table 1. The advantages and disadvantages of the pig vs baboon as a potential source of organs and cells for humans<sup>21</sup>**

|  | <b>Pig</b>                               | <b>Baboon</b>                        |
|--|--|--------------------------------------|
| Availability                                       | Unlimited                                | Limited                              |
| Breeding potential                                 | Good                                     | Poor                                 |
| Period to reproductive maturity                    | 4–8 months                               | 3–5 years                            |
| Length of pregnancy                                | 114 ± 2 days                             | 173–193 days                         |
| Number of offspring                                | 5–12                                     | 1–2                                  |
| Growth   | Rapid (adult human size within 6 months) | Slow (9 years to reach maximum size) |
| Size of adult organs                               | Adequate                                 | Inadequate                           |
| Cost of maintenance                                | Significantly lower                      | High                                 |
| Anatomical similarity to humans                    | Moderately close                         | Close                                |
| Physiological similarity to humans                 | Moderately close                         | Close                                |
| Relationship of immune system to humans            | Distant                                  | Close                                |
| Knowledge of tissue typing                         | Considerable (in selected herds)         | Limited                              |
| Necessity for blood type compatibility with humans | Probably unimportant                     | Important                            |
| Experience with genetic engineering                | Considerable                             | None                                 |
| Risk of transfer of infection (xenozoonosis)       | Low                                      | High                                 |
| Availability of specific pathogen-free animals     | Yes                                      | Yes                                  |
| Public opinion                                     | More in favor                            | Mixed                                |

## **The hurdles to xenotransplantation. Organ rejection: pig organs are seen as 'dangerous' and 'foreign' by the human immune system**

### **Hyperacute rejection**

Early experimental xenotransplantation studies in 1960s suggested that transplantation of vascularized xenografts between widely disparate species, such as pig-to-human, results in immediate destruction of the graft by hyperacute rejection (HAR). This type of reaction, occurring within minutes to hours, was recognized to be similar to the one occurring in ABO-incompatible allograft<sup>23</sup> and characterized by extensive intravascular thrombosis and extravascular hemorrhage.<sup>24,25</sup> Later on, during the 1990s, it was shown that HAR results predominantly from complement activation, through both the classical and alternative pathways<sup>26</sup>, following preformed antibody binding to specific carbohydrate antigens present on the graft endothelium.

An important finding in the past 20 years was that pigs, as all the other mammals except apes, Old-World monkeys and humans, express an epitope, Gal- $\alpha$ 1,3-Gal ( $\alpha$ Gal), synthesized by the enzyme  $\alpha$ -1,3galactosyltransferase, which is responsible for the binding of a large portion of preformed human natural antibodies.<sup>27,28</sup> Such antibodies are not present at birth<sup>29</sup>, but they are thought to arise as a result of exposure to environmental bacteria expressing the same antigen (e.g., the microorganisms of the intestinal flora). It is estimated that these antibodies constitute 1% of total immunoglobulins in the circulation.<sup>30</sup> Activation of complement and rapid destruction of the graft have been observed within the first hours after xenotransplantation.<sup>24,31</sup> Molecular incompatibilities between porcine complement regulatory proteins expressed on the surface of porcine endothelium and human complement components result in a lack of regulation and blockage of the complement activation.

Endothelial cells (EC) are the primary target of host immunity during HAR.<sup>32,33</sup> Under normal physiological conditions EC express an anti-inflammatory, anticoagulant and pro-fibrinolytic phenotype which is partly due to the presence of the endothelial glycocalyx consisting of proteoglycans and associated glycosaminoglycans (mostly

heparan sulfates). Activation of the vascular endothelium, following the binding of xenoreactive natural antibodies and deposition of complement, results in a phenotype transition of EC due to a loss of anticoagulants, such as thrombomodulin (TBM), tissue factor pathway inhibitor (TFPI)<sup>34</sup> and vascular ATP diphosphohydrolase (ATPDase)<sup>35</sup>. Furthermore, plasma proteins such as antithrombin III, superoxide dismutase, C1 inhibitor, etc. normally bound to the heparan sulfate are also lost following glycocalyx shedding<sup>32,36-38</sup>. This type of EC activation is defined as type I as it does not involve *de novo* protein synthesis and it is responsible for the manifestation of HAR.

### **Acute vascular rejection**

Early destruction of the xenografts could be prevented by depletion of complement using complement inhibitors such as cobra venom factor<sup>39,40</sup> or by removal of xenoreactive natural antibodies from the circulation by plasmapheresis, perfusion through immunoaffinity columns<sup>41,42</sup> or swine organs (e.g., liver, kidney). This reinforced the idea that antibodies and complement play a critical role in rejection of xenografts. However, further experiments revealed that rejection still occurred, but it was delayed by hours or some days because of the anti-complement therapy. This delayed rejection process was named acute vascular rejection (AVR) or delayed xenograft rejection.<sup>43,44</sup> It is the first form of rejection occurring when a transplantation between concordant species is performed. To study in detail AVR, transplantations between concordant species (e.g., hamster-to-rat<sup>45</sup>, or mouse-to-rat<sup>46</sup>) were performed since HAR does not occur due to the absence of preformed xenoreactive natural antibodies. Even though AVR might be seen as a delayed form of HAR<sup>47</sup> there was evidence that it is pathogenetically distinct from HAR.<sup>44</sup> The histopathology of AVR is characterized by EC swelling, focal ischemia, and fibrin deposition resulting in diffuse microvascular thrombosis.<sup>43</sup> The immunopathology of xenogeneic organs undergoing AVR reveals that immunoglobulin of recipient origin bound to the endothelial lining of graft blood vessels.<sup>24,43,48</sup> In addition, increased synthesis of anti-donor antibodies was found following exposure to the xenogeneic organ.<sup>49,50</sup> Also complement was shown to be involved in AVR though less prominent than in HAR.<sup>51</sup>

Antibodies alone, or together with a low level of complement activation, may be able to induce pathophysiological changes in the EC leading to their activation.<sup>52</sup> The kind of EC activation underlying AVR involve *de novo* protein synthesis and is called type II. It consists of activation of cytokine genes, expression of adhesion molecules (e.g., selectins) which allows adhesion of immune cells, and changes from an anticoagulant to a procoagulant phenotype on the endothelial surface due to shedding of heparan sulfate from the cell surface.

Beside activation of EC, also NK cells have been demonstrated to play an important role in the delayed xenograft rejection. Evidence of the involvement of natural killer cells in AVR was provided in 1994 by Hancock et al.<sup>53</sup> using a discordant guinea pig-to-rat heart transplantation model. It was noticed that in AVR an intense cellular infiltrate was seen resulting from accumulation of activated macrophages and NK cells. Inverardi et al. demonstrated *ex vivo* and *in vitro* that NK cells adhered rapidly and led to lysis of the xenogeneic endothelium by two distinct pathways, one dependent (antibody dependent cellular cytotoxicity, ADCC) and the other independent from IgG presence, since the selective removal of human IgG from the perfusion buffer markedly reduces but does not completely abrogate NK cell adhesion.<sup>54,55</sup> Later on, Seebach et al. demonstrated *in vitro* that unstimulated NK cells provide little or no xenogeneic cytotoxicity in serum free medium whereas IL-2 stimulated NK cells result in porcine EC destruction.<sup>56</sup> Morphologic changes and appearance of gaps between EC as well as the induction of a procoagulant state by human NK cells has also been observed *in vitro*.<sup>57</sup>

HAR and AVR represent the ways through which the recipient immune system responds to 'dangerous' signals provided by the xenograft.

### **T-cell mediated rejection**

T cell mediated rejection represent the result of the recipient's adaptive immune response to the 'foreign' donor xenograft. T cells in xenotransplantation are activated through direct and indirect pathways similarly to the allogeneic response. Direct activation means that recipient (non-human primate or human) T cell receptors bind

swine leukocyte antigen class I and class II on porcine antigen-presenting cells (APC). Porcine dendritic cells or endothelial cells function as APC.<sup>58</sup> This interaction results in T cell-mediated cytotoxicity directed against the xenograft endothelium. The indirect pathway of T cell activation refers to the recognition by recipient T cells of porcine donor peptide presented on recipient major histocompatibility complex (MHC) class II. This leads to CD4<sup>+</sup> T cell stimulation followed by B cell activation with consequent *de novo* antibody production resulting in humoral xenograft rejection. Furthermore, activated T cells produce cytokines that prime the innate immune system, including macrophages and NK cells, ultimately leading to xenograft dysfunction.<sup>59,60</sup> The CD4<sup>+</sup> T cell subset, in particular, is of central importance in xenograft rejection. It was demonstrated *in vivo* that CD4-specific, but not CD8-specific immunosuppression significantly prolonged xenogeneic skin graft survival in the mouse.<sup>61</sup>

T-cell response to a xenograft is believed to be stronger than the alloresponse in allotransplantation as the xenograft bears more antigens, and molecular incompatibilities between species cause disordered regulation of cell-mediated responses.<sup>62,63</sup> This is possibly because T-cell activation leads to a rapid antibody response that results in AVR before significant T-cell infiltration occurs in the graft. Cell mediated rejection is therefore typically not seen with intense immunosuppressive drug regimens.<sup>50,64,65</sup> Activation of T cell requires both binding of the T cell receptor to an MHC-peptide complex on the APC as well as a second costimulatory signal. Blocking these second signals through fusion proteins or antibodies is nowadays an established strategy to prevent both allogeneic and xenogeneic T cell responses. One of the first studies using the fusion protein CTLA4-Ig which impedes CD28-CD80/86 interactions, was a xenogeneic human-to-mouse islet model. The blockage of the CD28-CD80/86 resulted in a prolonged islet survival.<sup>66</sup> Recent xenotransplantation studies have focused on the usage of antibodies targeting the CD40-CD154 pathway (reviewed by Cooper et al.<sup>67</sup>). These potent costimulation blockage agents, together with genetic modification of the donor organ, led to significantly prolonged xenograft survival: Kidney xenograft >400 days with anti-CD154mAb<sup>68</sup>, heterotopic heart xenograft >900 days<sup>69</sup> and orthotopic heart xenograft 150 days (oral communication by Dr. Paolo Brenner at the international

meeting TTS 2018, both with anti-CD40mAb<sup>70</sup>). Liver xenografts survived up to 29 days with anti-CD40mAb<sup>71</sup> and in xeno-islets >600 days with anti-CD154mAb<sup>72</sup>.

### **Genetic modification of the donor**

Together with the immunosuppression strategies to prevent cell-mediated rejection, genetic manipulations of the donor pig have made it possible to prevent complement-mediated rejection, and thus markedly prolong graft survival in pig-to-non human primate xenotransplantation. The first transgenic pig goes back to 1992 when the company Imutran (Cambridge, UK) produced pigs transgenic for human decay-accelerating factor (hDAF, hCD55), a protein that inhibits complement activation in man. *Ex vivo* perfusion of hearts and livers explanted from such transgenic pigs were performed in order to assess the hypothetical resistance towards human complement activation.<sup>73</sup> Indeed, the heart showed resistance to HAR.<sup>74-76</sup> This has been confirmed also *in vivo* in a pig-to-baboon heart transplantation model.<sup>77</sup> In 1995, the company Nextran (Princeton, NJ, USA) produced transgenic pigs expressing both human DAF and human CD59.<sup>78</sup> Following the advent of the cloning technology (nuclear transfer)<sup>79,80</sup>, which made it possible to delete genes from the pig genome, efforts were made to delete GGTA1, the gene encoding for the galactosyltransferase enzyme that attaches the terminal Gal saccharides to the underlying carbohydrates on the pig vascular endothelium. In 2001, combining nuclear transfer with homologous recombination technology, pigs with heterozygous inactivation of the GGTA1, were produced<sup>81</sup>, and 1 year later, piglets with homozygous inactivation of the gene (GTKO) became available.<sup>82</sup> Heart and kidney transplantations were performed using baboons selected for low levels of the remaining anti-pig antibodies (anti-nonGal antibodies). GTKO pig hearts and kidneys prolonged graft survival significantly.<sup>83-87</sup>

Later, the transplantation of organs from GTKO pigs transgenic for human complement regulatory proteins (CD46, CD55, CD59) showed improved outcomes compared to GTKO or complement regulatory proteins alone.<sup>88,89</sup> However, thrombotic microangiopathy within the graft and frequently also consumptive coagulopathy in the recipients developed. In parallel endothelial cell activation due to

the increases in complement deposition and antibody binding followed by graft failure was the typical outcome.<sup>83,90,91</sup> Already in the 1990s both *in vitro* and *in vivo* studies suggested that the generation of activated protein C (APC), an important anticoagulant factor, may be significantly compromised by cross-species incompatibilities.<sup>92,93</sup> This was later on confirmed by a molecular analysis showing that porcine thrombomodulin binds human thrombin but is a poor cofactor for activation of the human protein C.<sup>94</sup> In addition, pig tissue factor pathway inhibitor does not successfully inhibit primate factor Xa<sup>34,95</sup>, and pig von Willebrand factor is associated with excessive primate platelet aggregation.<sup>96</sup> To compensate for these molecular incompatibilities and to neutralize thrombin generated by TF-dependent and -independent mechanisms as well as to exploit its potent anti-inflammatory effects<sup>97,98</sup>, human thrombomodulin (hTBM) has been expressed in transgenic pigs. Petersen et al. successfully generated hTBM transgenic pigs by somatic cell nuclear transfer. They demonstrated that its expression on porcine fibroblasts led to an elevated activated protein C production.<sup>99</sup>

The advent of the CRISPR/Cas9 technology (clustered regularly interspaced short palindromic repeats/CRISPR associate systems) which is an adaptable immune mechanism used by many bacteria to protect themselves from foreign nucleic acids, has made it possible to perform virtually any kind of genetic manipulation *in vitro* and therefore the prospect of producing multitransgenic pigs for xenotransplantation. The technology is characterized by simplicity and high efficiency and at the same time is able to shorten the process of generation of multitransgenic pigs. Using such technique, Yang and colleagues successfully inactivated the porcine endogenous retroviruses (PERV), which could potentially infect human cells, from the porcine genome first using PK15 cells, an immortalized kidney epithelial cell line (PK15)<sup>100</sup> and later on using a porcine primary cell line. This allowed for the generation of PERV-inactivated pigs via somatic cell nuclear transfer.<sup>101</sup> Petersen et al. were able to obtain biallelic knockouts of GGTA1 gene in three pigs out of six by microinjection of CRISPR/Cas9 into zygotes.<sup>102</sup>



With the aim of producing pigs resistant to antibody mediated rejection, further xenoantigens were studied and deleted from the pig genome. One of these is the Neu5Gc (N-glycolylneuraminic acid) which is not expressed in humans but is found on cell surfaces in Old World monkeys. Pigs lacking GGTA1 as well as the gene encoding CMAH (cytidine monophosphate-N-acetylneuraminic acid hydroxylase), which is responsible for catalyzing the reaction leading to the formation of the Neu5Gc antigen, were produced and the cells showed better protection against human serum.<sup>103</sup> Another porcine xenoantigen, to which humans and non-human primates have antibodies, is an immunogenic non-Gal glycan produced by the enzymatic activity of the porcine  $\beta$ 1,4-N-acetylgalactosaminyltransferase ( $\beta$ 4GalNT2).<sup>104</sup> Pigs with triple knockouts (GGTA1, CMAH and  $\beta$ 4GalNT2) were produced by Estrada et al. and showed reduced IgM and IgG binding to PBMC compared to cells from pigs lacking Gal and Neu5Gc.<sup>105</sup> However, the possibility to test these pig organs in established pig-to-NHP models is hampered by the expression of Neu5Gc – and thus the lack of anti-Neu5Gc – in non-human primates.<sup>106,107</sup>

Anti-inflammatory and antiapoptotic genes to inhibit delayed xenograft rejection were also introduced and tested. Heme oxygenase 1 (HO-1) is an enzyme degrading heme into iron, carbon monoxide and biliverdin. These degradation products are important biologically active compounds contributing to the protection of cells against apoptosis, free radical formation and inflammation.<sup>108</sup> It has been shown that porcine aortic endothelial cells overexpressing human HO-1 are protected against TNF- $\alpha$ -dependent apoptosis. Furthermore, in an *ex vivo* kidney perfusion model HO-1 overexpression increased the survival of transgenic organs compared to non-transgenic controls.<sup>109</sup> Another protein, which has been shown to provide significant protection from apoptosis and inflammation by inhibiting NF-kB signaling, is called A20 (tumor necrosis factor  $\alpha$ -induced protein 3).<sup>110,111</sup> The protective effects provided by the expression of HO-1 and A20 were confirmed by Fischer et al. which produced multitransgenic pigs expressing human HO-1, A20, CD46, CD55 and CD59 genes. The multiple xenoprotective transgenes were collocated at a single genomic locus;

this permits to avoid segregation when these genes are transmitted to the next generation.<sup>112</sup>

The transgenic modifications mentioned above were directed towards the protection of the xenograft from HAR as well as AVR. Strategies to provide protection against cellular rejection were also studied. Indeed, following the study by Sullivan and colleagues describing the inability of porcine MHC (swine leukocyte antigens, SLA) to inhibit lysis by human NK cells, the HLA-E gene was introduced in the pig genome. Expression of HLA-E on porcine endothelial cells has been shown to partially protect the cells *in vitro* against NK cell cytotoxicity.<sup>113</sup> Furthermore, limb xenoperfusion studies, in which amputated pig forelimbs were perfused with human blood, showed encouraging results with reduced complement activation, inflammatory cytokines, and NK cell infiltration in HLA-E transgenic pigs compared to wild-type controls.<sup>114</sup> Laird et al. as well as Abicht et al. showed that additional expression of HLA-E together with GTKO/hCD46 led to a reduced recruitment and activation of NK cells after *ex vivo* perfusions with human blood.<sup>115,116</sup>

A recent review by Meier et al. provides a nice overview of the genetic modifications available so far as shown here in Table 2. This long list of genetic modifications does not assume that all of them must coexist in the pig genome, instead it is important to find the right organ-specific combination.

**Table 2. Genetically modified pigs available for xenotransplantation<sup>117</sup>**

| Category                          | Abbreviation                        | Name/Alternate name  | Function  |
|-----------------------------------|-------------------------------------|--|---|
| Gal or non-Gal deletion           | GalT-KO                             | $\alpha$ 1,3-galactosyl-transferase KO (GGTA1 KO)  | Deletion of $\alpha$ Gal xenoantigen  |
|                                   | EndoGalC                            | Endo-B-Galactosidase transgene   | Reduction in $\alpha$ Gal xenoantigen   |
|                                   | GLA                                 | $\alpha$ -galactosidase transgene  | Reduction in $\alpha$ Gal xenoantigen   |
|                                   | NeuGc/CMAH KO                       | N-glycolylneuraminic acid/Cytidine monophosphate-N-acetylneuraminic acid hydroxylase                                 | Deletion in xenoantigen Neu5Gc  |
|                                   | $\alpha$ 2FucT                      | Human H-transferase transgene  | Masking of xenoantigens by adding H blood group antigen                                       |
| Complement regulation             | $\beta$ 4GalNT2 KO                  | $\alpha$ 2FucT   | Synthesize xenoantigens   |
|                                   | GnT-III                             | N-acetylglucosaminyltransferase III  | Masking of xenoantigens $\alpha$ Gal and NeuGc  |
|                                   | CD46                                | Human complement regulatory protein transgene  | Inactivation complement factors C3b and C4b   |
|                                   | CD55                                | Human complement decay-accelerating factor (DAF) precursor transgene   | Acceleration of complement decay  |
|                                   | CD59                                | Human MAC-inhibitory protein transgene   | Inhibition of the complement membrane attack complex C5b-9                                    |
| Cellular immune response          | CIITA-DN                            | MHC class II transactivator knockdown, major histocompatibility complex class II, swine leukocyte Ag II, SLA-II      | Transcription factor essential for porcine histocompatibility antigens II (SLA-II) expression |
|                                   | MHC Class I KO                      | Major histocompatibility complex class I, swine leukocyte Ag I, SLA-1, SLA-2, and SLA-3                              | Antigen presentation  |
|                                   | HLA-E/human $\beta$ 2-microglobulin | Human leukocyte antigen class I histocompatibility antigen transgene, $\alpha$ chain E/human $\beta$ 2-microglobulin | Inhibition of NK cells cytotoxicity   |
|                                   | CD178                               | FAS ligand transgene, CD95L  | Inhibition of NK cells cytotoxicity   |
|                                   | CTLA4-Ig                            | Cytotoxic T lymphocyte antigen 4 transgene, CD152, LEA29Y  | Inhibition of T-cell costimulation via CD86/CD80  |
|                                   | CD253/TRAIL                         | TNF- $\alpha$ -related apoptosis-inducing ligand transgene   | Induction of apoptosis of activated T cells   |
|                                   | CD47                                | Human integrin-associated protein transgene  | Regulation of macrophage activation and phagocytosis  |
|                                   | SIRP $\alpha$                       | Human signal regulatory protein- $\alpha$ transgene  | Regulation of macrophage activation and phagocytosis  |
|                                   | ASGR1-KO                            | Porcine asialoglycoprotein receptor 1  | Decreases human platelet phagocytosis by pig sinusoidal endothelial cells                     |
|                                   | iGb3s KO                            | Isoglobotrihexosylceramide, isogloboside 3 synthase  | Critical for NK cell development and self-recognition   |
| Anticoagulation and other         | VWF-deficient                       | Von Willebrand factor  | Platelet adhesion   |
|                                   | TFPI                                | Tissue factor pathway inhibitor  | Human protein C activation  |
|                                   | CD141                               | Human thrombomodulin transgene   | Human protein C activation  |
|                                   | CD73                                | 5'-nucleotidase  | Platelet aggregation  |
|                                   | CD201                               | Human endothelial protein C receptor, EPCR   | Human protein C activation  |
| Anti-inflammatory/ Anti-apoptotic | CD39                                | Human ectonucleoside triphosphate diphosphohydrolase-1 transgene   | Platelet aggregation  |
|                                   | A20                                 | Human tumor necrosis factor- $\alpha$ -induced protein 3 transgene   | Inhibition of NF- $\kappa$ B activation and TNF-mediated apoptosis                            |
|                                   | HO-1                                | Human heme oxygenase-1 transgene   | Degradation of heme   |
| Other                             | sTNFR1-Fc chimera                   | Human soluble TNF receptor inhibitor/Fc chimera  | Inhibition of TNF/receptor binding  |
|                                   | PERV inactivation                   | Porcine endogenous retroviral viruses  | Retroviruses  |

## Current preclinical survival of xenografts in non-human primate models

Meier et al. also exhaustively describe the progresses made in solid organ xenotransplantation.<sup>117</sup> The following table (Table 3) shows recent advances and combinations of genetic modifications tested so far.

**Table 3. Longest survival times of porcine organs in non-human primate recipients and respective genetic modifications (modified from Meier et al.<sup>117</sup>)**

| Year         | Organ             | Recipient     | Donor (pig)  | Longest survival (days) | References |
|--------------|-------------------|---------------|--|-------------------------|------------|
| 2014<br>2016 | Heterotopic heart | Baboon        | GTKO/hCD46/hTBM#   | 146, 616, 550, 945      | 69,118,119 |
| 2018<br>2011 | Orthotopic heart  | Baboon        | hCD46<br>or<br>GTKO/hCD46/hTBM   | 34, 40, 57, 90, 180     | 70,120     |
| 2017         | Kidney            | Baboon        | GTKO/hCD46/CD55/EPCR/TFPI/CD47   | 260, 237                | 121        |
| 2017         | Kidney            | Rhesus monkey | GTKO/hCD55   | 499                     | 68         |
| 2017         | Kidney            | Rhesus monkey | GTKO/ B4GALNT2-KO  | 435                     | 122        |
| 2017         | Liver             | Baboon        | GTKO   | 5, 8, 25, 29            | 71         |
| 2017         | Lung              | Baboon        | GTKO/hCD46/hvWF<br>or<br>GTKO/hCD46/hCD47/HO-1/EPCR/hTBM<br>or<br>GTKO/hCD46/hCD47/hCD55/EPCR/TFPI | 7-9                     | 123        |

#Abbreviations: GTKO – alpha-galactosyl transferase knockout, hCD46 – human membrane co-factor protein, hTBM – human thrombomodulin, CD55 – (human) decay accelerating factor, EPCR – endothelial protein C receptor, TFPI – tissue factor pathway inhibitor, CD47 – integrin associated protein, B4GALNT2-KO – beta 1,4 N-acetyl-galactosaminyl-transferase 1 knockout, hvWF – human von Willebrand factor, HO-1 – hemoxygenase-1.

### **The complement system and its regulation**

Because the vascular endothelium of the xenograft is the first to come in contact with the recipient blood, thus with the recipient's complement, this section will focus on

the role of the complement system in graft rejection and will describe strategies to overcome its unwanted activation.

### **Overview of the complement system**

The complement system is an effector mechanism part of the innate immunity. It was first identified in 1890s as a heat-labile principle in serum that “complemented” antibodies in the killing of bacteria.<sup>124</sup> It consists of more than 30 proteins in plasma and on cell surfaces. The complement system has three main physiologic activities: Early defense against bacterial infections<sup>125</sup>, it bridges the innate and the adaptive immunity<sup>126</sup> and it is responsible for the waste disposal, meaning clearance of immune complexes as well as apoptotic cells.<sup>127</sup> As part of the innate immunity, its role is paramount to fight pathogenic invasion. As such the complement system must be able to discriminate the self from non-self and it accomplishes this using the ‘missing self’ strategy.<sup>128,129</sup> Basically, anything not recognized as self is considered non-self and destroyed. The three pathways of the complement system are the ways through which this discrimination occurs: The classical, the lectin and the alternative pathway.(Figure 2<sup>124</sup>) Each pathways has its own mechanism of activation that results in the activation of the central factor C3, followed by common terminal complement pathway leading to the formation of the C5b-9 – the membrane attack complex (MAC).

### **The classical pathway**

The classical pathway was the first to be discovered. It begins when antibodies (IgM or IgG) recognize and bind to a cell surface antigen and ends with the lysis of the target cell. C1, a multimeric complex which comprises C1q, C1r and C1s molecules, recognizes and adheres to the antigen-antibody complex bound to pathogenic surfaces. The C1q adherence to the Fc region of the IgG or IgM activates C1s and C1r. C1s cleaves C4 and C2, resulting in the cleavage of C4 and C2 into C4a, C4b, C2a and C2b<sup>126,130</sup>. The larger fragments (C2a and C4b) build the C4bC2a complex, called C3 convertase of the classical pathway. This enzyme cleaves cleave C3 to release C3a and C3b. At this point all the different pathways converge. C3b acts as an opsonin leading to enhanced phagocytosis and further amplification of the

complement activation. The C3b fragment can also adhere to the C3 convertase to produce the C4bC2aC3b, the C5 convertase. C5 gets cleaved by the C5 convertase leading to the formation of C5a and C5b. C5b binds to the target cell surface followed by C6 and C7. C8 and several C9 molecules bind to the C5bC6C7 complex to build the MAC. Cell lysis is achieved by the formation of a pore (MAC) into the cell membrane. C3a and C5a produced along the cascade are called anaphylatoxins and act as chemoattractants for cells such as phagocytes (neutrophils, monocytes) to the site of injury or inflammation.

### **The lectin pathway**

The lectin pathway functions in a similar way but it is immunoglobulin-independent. It employs pattern-recognition receptors (PRR), i.e. mannose-binding lectin (MBL) and ficolins, to perform non-self recognition. In contrast to antigen-recognition receptors (antibodies or T-cell receptors) which hypothetically can recognize every possible antigen thanks to their diversity, PRR specifically scan for highly conserved structures expressed in large groups of microorganisms called pathogen-associated molecular patterns (PAMPs). MBL, a well characterized receptor of the collectin family, is able to bind to carbohydrate moieties on surfaces of pathogens including yeast, bacteria, parasites and viruses. Both MBL and Ficolin circulate in the serum in form of complexes with MBL-associated proteins (MASPs) which are similar in many aspects to C1s and C1r of the classical pathway. Four structurally related MASPs are known so far: MASP1, MASP2, MASP3 and a truncated MASP2 called MAP19<sup>131</sup>. Binding to pathogens results in activation of MASP2 which in turn cleaves C4 into C4a and C4b. C4b is able to stick to the surface of pathogens and gather C2 to bind to it. The C2 is then cleaved by MASP2 and lead to the formation of the C2b and C2a fragments. C4b and C2a converge and build the lectin pathway C3 convertase also known as C4bC2a. The role of the other MASPs is still under investigation although MASP1 can cleave C2 but not C4.<sup>132</sup>.

### **The alternative pathway**

Carbohydrates, lipids and proteins found on foreign and non-self surfaces are responsible for the activation of the alternative pathway. It does not only represent

an individual recognition pathway, but also functions as an amplification loop of both the classical and lectin pathways. It has been shown *in vivo* that the alternative pathway alone can contribute up to >80% of the total activation induced by either pathways.<sup>133</sup> C3 is constantly hydrolyzed at a low level (“tick over”) to form C3b, which binds to bacteria for instance. Factor B, a protein homologous to C2, is then recruited to the cell-bound C3b. Factor D cleaves Factor B resulting in the C3 convertase C3bBb. The convertase is stabilized by the presence of plasma properdin which is released by activated neutrophils and binds to C3b. Properdin prevents C3b cleavage by Factors H and I. The C3bBb represents the core of the amplification loop converting C3 into C3b and C3a in a similar way C3 convertase of the classical and lectin pathways.

### **C3 independent pathways**

In addition to the activation by the above-mentioned pathways, complement activation products can be generated by immune cells (neutrophils and macrophages)<sup>134,135</sup> as well as by factors involved in other plasma cascade systems such as kallikrein, plasmin, factor XIIa. Thrombin, for instance, has been shown to be able to generate C5a *in vivo* in C3 deficient mice.<sup>136</sup> This evidences indicate a strict interconnection between the plasma cascade systems.

### **Regulation of the complement system**

Under physiological conditions, the activation of complement cascade is tightly controlled by a series of soluble and membrane-bound complement regulatory proteins. Their presence ensures that autologous complement activation is prevented protecting host cells from accidental complement attack. Molecular incompatibilities between pigs and humans are known to be responsible for the loss of complement regulation leading to HAR and AVR episodes. Decay accelerating factors (DAF, CD55) and membrane co-factor proteins (MCP, CD46) inhibit complement activation at the C3 convertase step, while CD59 prevents formation of MAC. The phlogistic potential of both C3a and C5a is quickly reduced by plasma carboxypeptidases which cleaves the C-terminal Arginine leading to C3a des-Arg and C5a des-Arg, resulting in a reduction of 90% of their biological activity.<sup>130</sup> C3b and C4b are quickly inactivated

by proteolytic cleavage into fragments iC3b, C3dg, C3c, C4c, C4d by Factor I in the presence of cofactors: CD46 and complement receptor 1 (CR1, CD35) and Factor H bound to host surfaces. Furthermore, there is a series of serum phase complement regulatory factors, which include C1 inhibitor, C4 binding protein, factor H, clusterin (apo-J) and S protein (vitronectin). The fluid-phase regulators prevent uncontrolled activation of complement in the fluid phase, whereas the membrane-bound regulators directly protect the host cell from complement attack.<sup>137</sup>



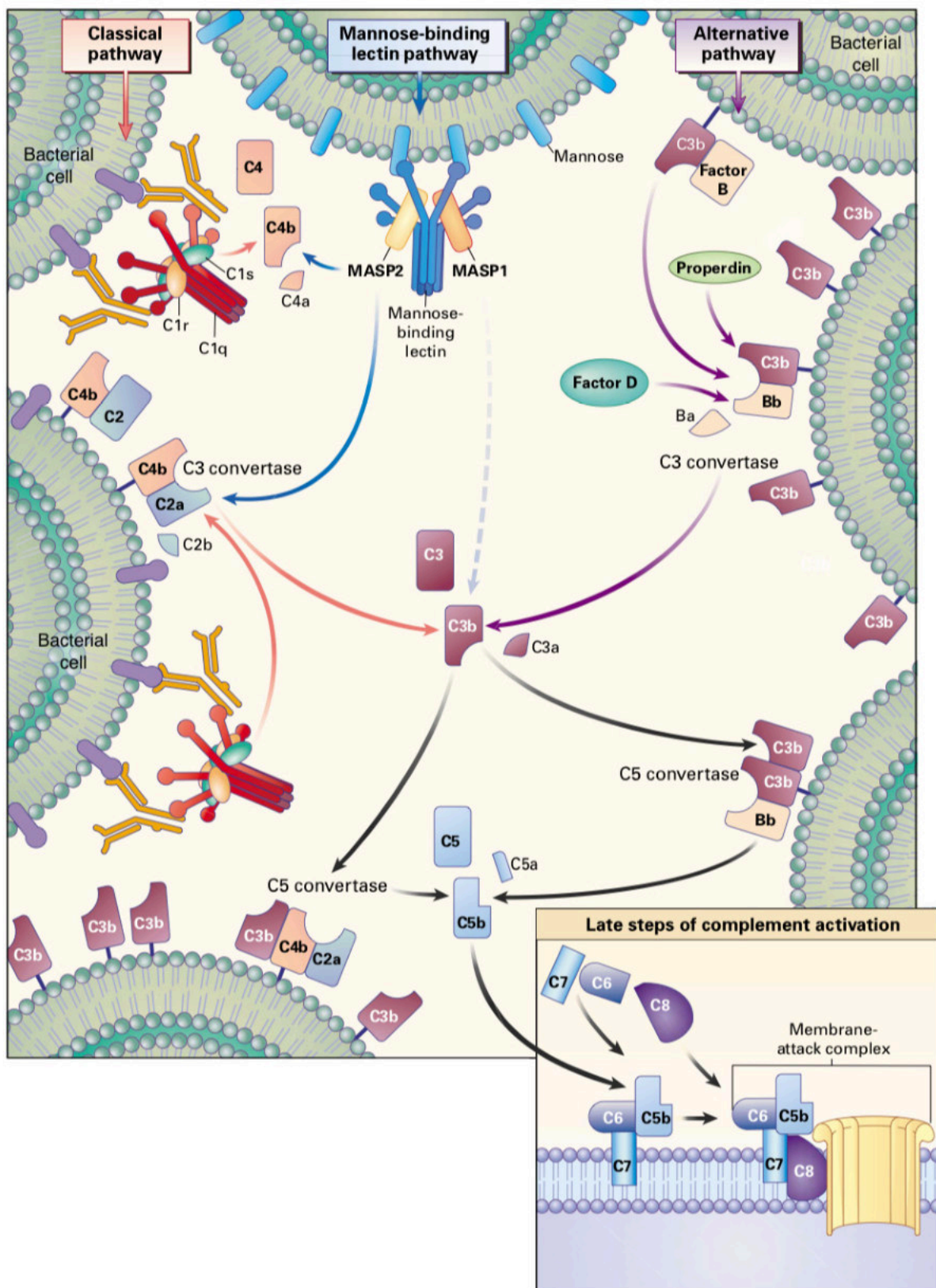


**Figure 2** The complement pathways - Overview of the three different pathways, classical pathway, lectin pathway and alternative pathway.<sup>124</sup>

## The coagulation system

Blood coagulation is a vital mechanism responsible for the normal hemostatic response to vascular injury. Under physiological circumstances, anticoagulation is maintained thanks to the expression of numerous inhibitors on the endothelial surface. Coagulation is a dynamic process subjected to a fine and meticulous regulation provided by the endothelium, the platelets and the fibrinolytic system. This delicate equilibrium is disturbed when the procoagulant activity of the coagulation factors is somehow enhanced or the inhibitory capabilities of the inhibitors is diminished.

The coagulation system consists of a series of inactive proteins that circulate in the blood. The majority of them circulate as precursors of proteolytic enzymes (zymogens). They are the core components of the coagulation system that lead to a cascade reaction resulting in the final conversion of soluble fibrinogen into insoluble fibrin strands. Zymogens undergo a vitamin K dependent post translational modification that enables them to bind calcium and other divalent cations and participate in clotting cascade.<sup>138</sup>

The coagulation cascade (fig. 3) is traditionally divided into the intrinsic and extrinsic pathways both of them converging at the level of factor X activation. The extrinsic pathway, also known as tissue factor pathway, is activated by tissue factor (TF) which is expressed by activated EC in the presence of trauma or any vascular insult.<sup>139</sup> The exposed TF interacts with factor VIIa and calcium to convert factor X into the active form Xa.<sup>140</sup> The tissue factor-factor VIIa complex also activates factor IX in the intrinsic pathway resulting in a positive feedback amplification loop.<sup>141,142</sup> The intrinsic pathway, also known as contact activation pathway, starts by contact activation of factor XII (Hageman factor), high molecular weight kininogen (HMWK) and prekallikrein into active factor XIIa. Factor XIIa converts factor XI into the active form XIa followed by activation of factors IX and X in the presence of the co-factor VIIIa to form the active factor Xa. The extrinsic pathway is believed to play a minor role in initiating clot formation as patients with deficiencies of factor XII, HMWK and prekallikrein do not experience bleeding disorders.<sup>143</sup> Both intrinsic and extrinsic

pathways share a common pathway that starts with active factor Xa. Factor Xa, in the presence of its co-factor (factor V), platelets and calcium for the prothrombinase complex which converts prothrombin into thrombin. The generated thrombin in turn cleaves soluble fibrinogen into insoluble fibrin and activates factor XIII which crosslinks fibrin polymers incorporated in the platelet plug resulting in clot formation.

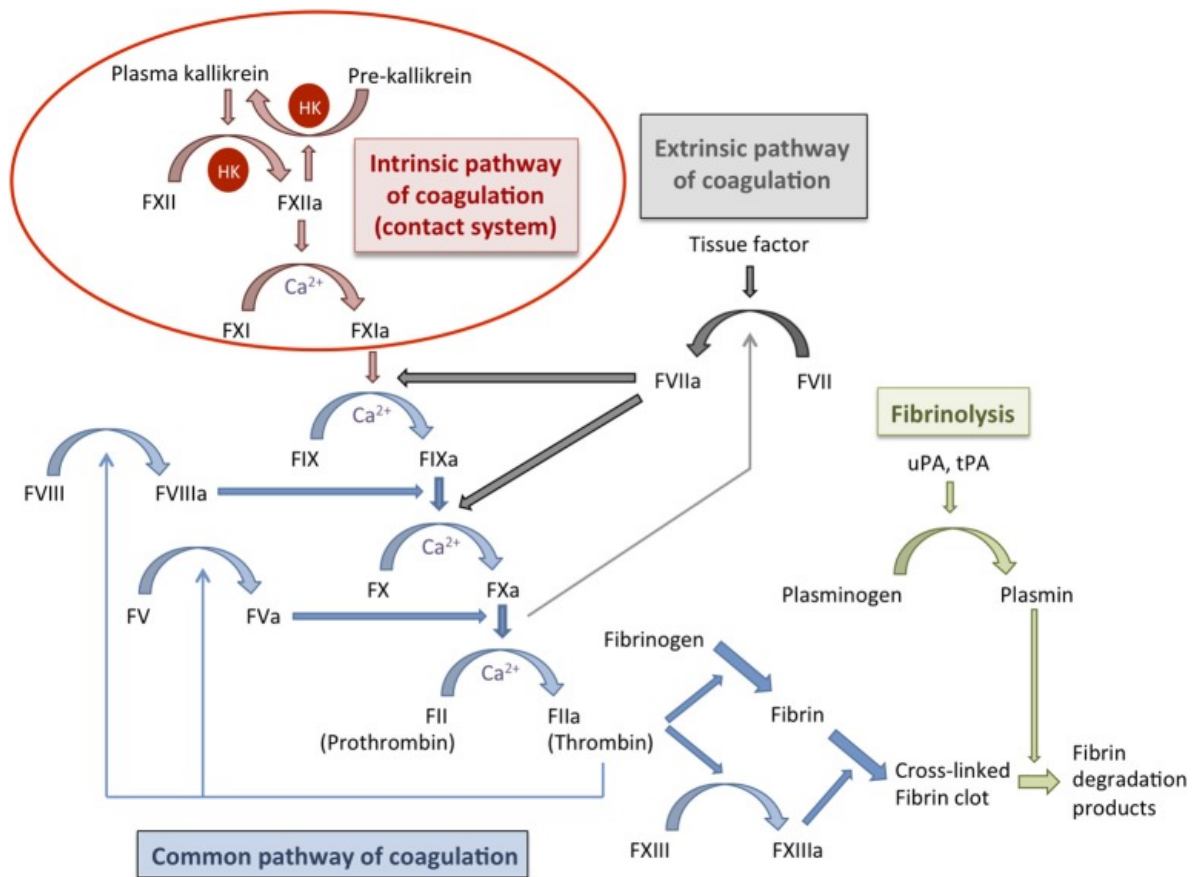


Figure 3 Overview of the coagulation system. <sup>144</sup>

## **The vascular endothelium: a key player in rejection**

In a (xeno)transplantation setting the endothelium lies at the interface between the recipient's blood and the transplanted donor organ. EC form the inner layer of blood vessels and, when quiescent, they are responsible for the maintenance of an anti-inflammatory, anti-coagulant and pro-fibrinolytic environment within the vascular lumen.<sup>145,146</sup> The endothelial surface layer, the glycocalyx, is a brush-like structure composed of glycoproteins, proteoglycans and associated glycosaminoglycans. It functions as a barrier to transvascular exchange of macromolecules as well as to leukocyte adhesion.<sup>147,148</sup> Heparan sulfate proteoglycans (HSPG) with a varying number of glycosaminoglycan (GAG) side chains (mainly heparan sulfate on EC) represents the majority of proteoglycans (50-90%) associated with the endothelium. Heparan sulfate, attached to the EC surface, provides anti-oxidant, anti-inflammatory and anti-coagulant effects via binding and activation of anti-thrombin III, superoxide dismutase, C1 inhibitor and other plasma proteins via their heparin binding domain.<sup>149-151</sup> In response to inflammatory mediators (interleukins, TNF, C5b-9), the endothelium switches to a proinflammatory, procoagulant and anti-fibrinolytic state by expressing tissue factor, enhancing prothrombinase assembly, attenuating thrombin inhibition as well as overproducing plasminogen activator inhibitor-1 (PAI-1), an inhibitor of fibrinolysis. These changes are also associated with the secretion of cytokines and the increased expression of adhesion molecules, such as E-selectin, vascular cell adhesion molecule (VCAM-1) on the endothelium. As mentioned above in the chapter describing the rejection mechanisms, this process of profound changes is defined as EC activation and it is a prominent feature of rejecting xenografts. EC activation can be divided into two phases: An early phase of which is independent of protein synthesis (type I EC activation) and a later phase, type II activation which is associated with *de novo* protein synthesis.(Table 4)<sup>152</sup>

**Table 4. Classification and biological consequences of endothelial cell (EC) activation.**<sup>152</sup>

| EC Activation  |   | Biological consequences                 |
|----------------|---|---|
| Type I         | Cellular retraction   | Exposure of thrombogenic subendothelium |
|                | P selectin  | PMN adhesion                            |
|                | vWF release   | Platelet adhesion to EC                 |
|                | Heparan sulphate release  | Loss of anti-thrombin III activity      |
|                | PAF release   | Platelet activation                     |
|                | Prostaglandin (I <sub>2</sub> ,E <sub>2</sub> )                 | Vascular tone and inflammation          |
|                | Nitric oxide (NO)   | Vasodilatation                          |
|                | Endothelin-1  | Vasoconstriction and mitogen            |
|                | Leukotriene (C <sub>4</sub> , D <sub>4</sub> , A <sub>4</sub> ) | vWF expression and secretion            |
| Type II        | Leukocyte-EC interactions                                       |   |
|                | E selectin  | PMN, lymphocyte, and monocyte adhesion  |
|                | ICAM-1  | Leukocyte adhesion ligand for LFA-1     |
|                | VCAM-1  | Leukocyte adhesion ligand for VLA-1     |
|                | MHC classes I, II   | Antigen presentation to T cells         |
|                | IL-8  | Chemokine                               |
|                | MCP-1   | Chemokine                               |
|                | IL-1β   | Inflammation                            |
|                | Growth factors  |   |
|                | M-CSF   | Monocyte differentiation                |
|                | GM-CSF  | Monocyte differentiation                |
|                | PDGF  | Smooth muscle cell mitogen              |
|                | TGF-β   | Growth regulation                       |
|                | bFGF  | Mitogen                                 |
|                | IL-6  | B cell growth                           |
|                | Vascular tone   |   |
|                | Cyclooxygenase  | Prostaglandin synthesis                 |
|                | NO synthase   | Synthesis of NO                         |
|                | Thrombosis/matrix remodelling                                   |   |
|                | PAI-1   | Inhibition of plasminogen activator     |
|                | Plasminogen activator   | Activation of plasminogen to plasmin    |
|                | Collagenase   | Matrix degradation and remodelling      |
|                | Vitronectin   | Extracellular matrix factor             |
| Tissue factor  | Cofactor for extrinsic coagulation pathway                      |   |
| Thrombomodulin | Regulation of aPC synthesis by thrombin                         |   |

## Flow and shear stress

*In vivo* EC are constantly exposed to shear stress as a consequence of the frictional forces created by the blood flow. Hemodynamic forces and chemical signals are sensed by the endothelium and influence its functional properties.<sup>153,154</sup> Pulsatile or steady unidirectional laminar flow stimulate EC production of factors that support their survival, quiescence and barrier function and at the same time suppress coagulation, leucocyte adhesion/extravasation and proliferation of vascular smooth muscle cells.<sup>155</sup> In contrast, sustained changes in hemodynamic forces, i.e. perturbed flow in atheroprone regions, challenge EC which consequently respond by altering

gene expression and cell morphology as well as undergo structural remodeling resulting in an increased permeability for plasma macromolecules, increased adhesion properties for monocytes and enhanced turnover (proliferation and apoptosis).<sup>156,157</sup> Mechanotransduction is a process through which EC are able to convert mechanical (physical) stimuli into intracellular biochemical mechanisms. Mechanosensing molecules present on EC include junctional proteins (VE-cadherin, occludin), receptor kinases (vascular endothelial growth factor (VEGF) receptor 2(VEGFR2) and others), integrins, focal adhesions (FAs), G-proteins, G-protein-coupled receptors (GPCRs), ion carriers and, last but not least the glycocalyx.<sup>157</sup>

### **The endothelial glycocalyx**

The endothelial glycocalyx (EG) has been briefly introduced in the previous sections. Here it will be described more in detail since it plays an important role in many crucial biological processes such as regulation of blood flow, prevention of coagulation, and modulation of inflammatory responses. The presence of this important layer was first observed 50 years ago in the microcirculation by perfusing the vasculature with a cationic dye (ruthenium red) which bound to the glycosylated proteins on the endothelial surface.<sup>158</sup> It is composed of proteoglycans and glycoproteins.<sup>159</sup> Its composition and thickness fluctuate as it continuously replaces material sheared by flowing plasma.<sup>160</sup> So far, the observed thickness varies between 0.1 and 4.5  $\mu\text{m}$ .<sup>159,161,162</sup> and changes throughout the body depending on the vessel type and the local shear stress. The EG is overall negatively charged and this is due to the sulfation of the glycosaminoglycans (GAG) side chains attached to the membrane bound proteoglycans. The net negative charge pushes away negatively charged molecules, white blood cells, red blood cells and platelets – essentially because they also carry a glycocalyx which is negatively charged.<sup>163</sup>

Proteoglycans consist of a core protein with one or more GAG chains linked to it. Syndecans and glypicans, two groups of core proteins, have a tight connection to the cell membrane through a membrane-spanning domain or a glycosylphosphatidylinositol anchor, respectively. Other proteoglycans, like perlecan, mimecan and biglycan are secreted after being assembled and modified in their GAG chains. The secreted soluble proteoglycans can either stay in the glycocalyx or

diffuse into the blood stream. Among the proteoglycans, hyaluronic acid is the only one to be synthesized on the cell surface and is not covalently attached to a core protein. GAG chains are composed of heparan sulfate, chondroitin sulfate, dermatan sulfate, keratan sulfate and hyaluronic acid. Heparan sulfate counts for the 50-90% of the total amount of proteoglycans in the glycocalyx.

Glycoproteins acts as adhesion molecules and can be grouped in three families: selectins, integrins and immunoglobulins.<sup>161</sup> Selectins that are mainly expressed on the activated vascular endothelium are E- and P-selectin which are responsible for the interaction with leukocytes and EC. Integrins are able to bind to collagen, fibronectin and laminin in the subendothelial matrix and play an important role in the interaction of platelets with EC. Intercellular adhesion molecules 1 and 2 (ICAM-1 and ICAM-2), vascular cell adhesion molecule 1 (VCAM-1) and platelet/endothelial cell adhesion molecule 1 (PECAM-1) belong to the immunoglobulin superfamily. These are ligands for integrins on leucocytes and platelets and are crucial for their adhesion to the endothelium and diapedesis.<sup>162</sup> All the known glycoproteins bound to the EG have an influence on coagulation, fibrinolysis and hemostasis.

It is well known that shear stress is sensed by the endothelial glycocalyx which transmit the hemodynamic forces acting as mechanotransducer and influencing vascular remodeling.<sup>164</sup> It has been shown that human umbilical vein endothelial cells under shear stress doubled their amount of hyaluronic acid in the glycocalyx and this could be a mechanism to control shear.<sup>165</sup> When the endothelial glycocalyx is degraded, for instance in atheroprone vessel regions, it deregulates vascular tone, by causing EC to lose their expression of endothelial nitric oxide synthase, antithrombin-III, superoxide dismutase and other important plasma proteins. Damage to the EG compromises these mechanisms and the response of the endothelium to shear stress. Treatment of EC with degrading enzymes such as heparanases led to the loss of response to shear stress suggesting a role of the glycocalyx in mechanotransduction.<sup>163</sup>

Different important factors can bind to the glycocalyx through their heparin binding domain (Figure 4).<sup>166</sup> For instance, antithrombin III, the thrombin inhibitor and activator of factors IX and X, binds to heparan sulfate and this enhances its anti-coagulant activity. The presence of plasma proteins on the glycocalyx supports the thromboresistant and antiflogistic nature of the healthy endothelium. Superoxide dismutase is also bound to the glycocalyx contributing to reduce the oxidative stress and to maintain nitric oxide bioavailability to prevent endothelial dysfunction.



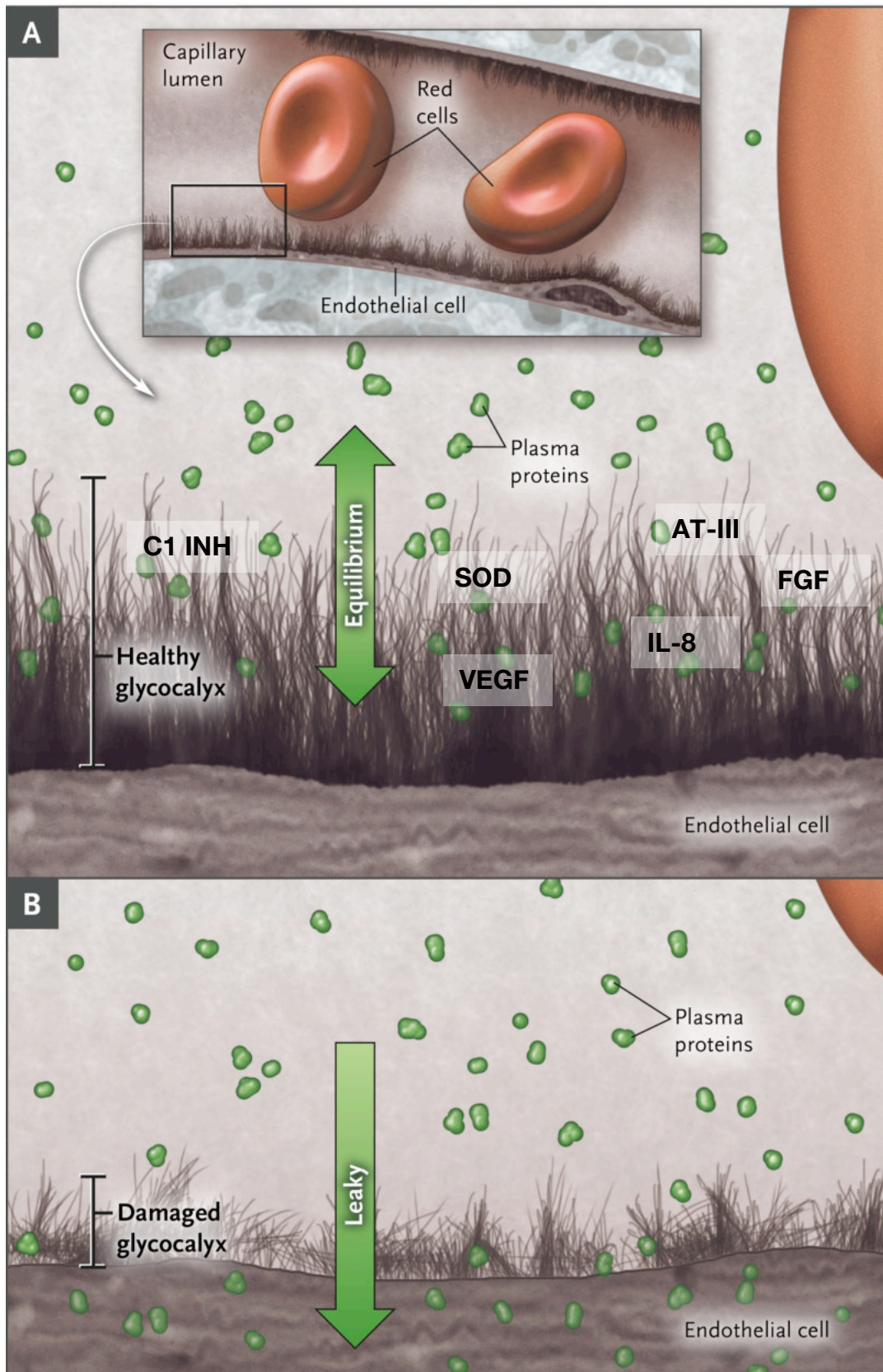


**Figure 4** Schematic representation of the endothelial glycocalyx. Panel A shows the situation of a healthy quiescent endothelium with an intact glycocalyx and plasma proteins bound to it. Panel B shows the shedding of the glycocalyx with consequent loss of plasma proteins which expose the endothelial surface. Adapted from: Myburgh JA, Mythen MG. Resuscitation fluids. *N Engl J Med* 2013; 369 (13): 1243-51.(7)

## Microfluidic system

Culturing cells using microfluidic systems is becoming more and more common nowadays. Microfluidics describes the science and technology of systems that use a small amount of fluids (in the order of  $\mu\text{L}$ , nL or pL) and work with channels in a range of tens to hundreds of micrometers. Microfluidics allows to create a microenvironment that is closer to the *in vivo* natural environment that cells are used to experience.

Polydimethylsiloxane (PDMS) is a widely used polymer for the fabrication of microfluidic chips and it brings several advantages. It has a high flexibility, is convenient (cost-effective), and allows the design of complex microfluidic systems. Furthermore, it is optically clear which allows real-time, high-resolution optical imaging, it can be polymerized and cross-linked (cured) to form a solid PDMS structure and it is permeable enough to gas<sup>167</sup> which makes it suitable for on-chip cells culture.<sup>168</sup>

Standard *in vitro* culture systems hardly mimic the physiological architecture of human organs or vessels. Microfluidic systems allow reproducing designs that are similar to the complex structures of human organs and vessels. It is possible to design microfluidic systems as perfusion systems. Medium will continuously flow through the system and this setup allows the removal of waste products and supplies the cells with fresh medium.

Moving cells from a macroscopic culture environment to a microscopic culture is a big change. Most of the culturing protocols are designed for macroscopic system and need therefore revision or extensive trials on the microscale culture system.

On Macroscale cell culture level, oxygen and  $\text{CO}_2$  diffuses from the air inside of the incubator into the culture medium and provide enough supply of oxygen for cell growth and proliferation, as well as  $\text{CO}_2$  for medium buffering. It is crucial to control the levels of oxygen and  $\text{CO}_2$  in microscale cell culturing because even minor changes have a huge impact on the condition of the cells because of the lower cell-to-media

ratio. Aerobic respiration and buffering of the medium pH is necessary and can be affected by low levels of CO<sub>2</sub> and O<sub>2</sub>.

Macroscopic cell cultures usually have medium unmoved and in excess to ensure a high amount of nutrients for the culture to feed over several days. Microscale systems rely on a regular exchange of medium to provide enough nutrients for the number of cells because, like mentioned above, the cell surface-to-volume ratio is lower.

## Hypothesis and Aim of the thesis

The overall aim of this thesis is to provide both basic fundamental research as well as important pre-clinical data which can support the clinical application of xenotransplantation. The specific aims are summarized below and follow the order of the publications reported in the results section.

1. The study of anti-inflammatory and anticoagulant properties of EC *in vitro* is fundamental not only in xenotransplantation research but also in other clinical conditions. Current *in vitro* models for the study of whole blood coagulation share the common limitation of using anticoagulants and overlook the important physiological anti-coagulant contribution of quiescent EC. The first aim was to provide a detailed and standardized methodology for the assessment of the anti-inflammatory and anti-coagulant properties of EC by using whole non-anticoagulated blood.
2. Reliable and high-throughput *in vitro* models mimicking the microenvironment present *in vivo* are required both to reduce avoidable animal experimentation (3R regulations: reduce, replace and refine) as well as to assess the hypothetical effects of transgenes before transgenic pigs are actually produced and pre-clinical pig-to-baboon xenotransplantation experiments are performed. Thus, the present study aimed at developing a novel *in vitro* 3D microfluidic model which include important parameters such as fluid flow, shear stress, recirculation.
3. Detailed experimental protocols are often missing in the scientific literature. A book chapter dedicated to 3D cell culture models for the assessment of endothelial cell function in xenotransplantation aims to provide the scientific community with a detailed and standardized protocol allowing the reproducibility of our state-of-the-art assays in 3D cell culture.
4. When hyperacute rejection is overcome by genetic manipulation of the donor or by complement inhibition, other mechanisms leading to acute vascular rejection play a crucial role in xenograft survival. Particularly NK cells-mediated graft

damage cannot be avoided using organs from GTKO/hCD46 pigs. NK cell activation is prevented by the binding of inhibitory NK receptors to MHC class I antigens on healthy, autologous cells. Porcine cells lack the human leucocyte antigen E (HLA-E) and are therefore recognized as 'dangerous' by human NK cells and lysed. Transgenic (over)expression of HLA-E on porcine endothelial cells might help to improve the xenograft survival. In this study, the potential of a combined overexpression of human CD46 and HLA-E to prevent both complement- and NK cell-mediated rejection was tested in an *ex vivo* perfusion system of pig limbs with human blood.

5. Following the rationale provided under aim 3 this study aims to assess the potential of a combined overexpression of hCD46/HLA-E to prevent both complement- and NK cell-mediated xenograft rejection in a pig-to-human *ex vivo* cardiac xenoperfusion model.
  
6. Heart transplantation is still the treatment of choice for patients with terminal cardiac failure, but the need for donated human organs far exceeds supply and alternatives are urgently required. Genetically multi-modified pig hearts lacking  $\alpha$  Gal epitopes (GTKO) and expressing human membrane cofactor protein (hCD46) and human thrombomodulin (hTM) have survived for up to 945 days (median 298 days) after heterotopic abdominal transplantation in baboons.<sup>69</sup> However, the maximum survival of an orthotopic life-supporting porcine xeno-heart is so far only 57 days and this was achieved only once. This study aims to prolong the survival of baboons transplanted with GTKO/hCD46/hTM pig hearts.



## References

1. Lin, Y., Osman, M., Harris, A. J. L. & Read, D. Underlying wishes and nudged choices. *J Exp Psychol Appl* (2018). doi:10.1037/xap0000183
2. Abadie, A. & Gay, S. The impact of presumed consent legislation on cadaveric organ donation: a cross-country study. *J Health Econ* **25**, 599–620 (2006).
3. Nathan, H. M. *et al.* Organ donation in the United States. *Am. J. Transplant.* **3 Suppl 4**, 29–40 (2003).
4. Barber, K. M. *et al.* The UK National Potential Donor Audit. *Transplantation Proceedings* **37**, 568–570 (2005).
5. Matesanz, R., Domínguez-Gil, B., Coll, E., Mahillo, B. & Marazuela, R. How Spain Reached 40 Deceased Organ Donors per Million Population. *Am. J. Transplant.* **17**, 1447–1454 (2017).
6. Simini, B. Tuscany doubles organ-donation rates by following Spanish example. *Lancet* **355**, 476–476 (2000).
7. David K C Cooper, Bernd Gollackner, A. & Sachs, D. H. Will the Pig Solve the Transplantation Backlog?  
<http://dx.doi.org/10.1146/annurev.med.53.082901.103900> (2003).  
doi:10.1146/annurev.med.53.082901.103900
8. Taniguchi, S. & Cooper, D. K. Clinical xenotransplantation: past, present and future. *Ann R Coll Surg Engl* **79**, 13–19 (1997).
9. Farr, A. D. *The first human blood transfusion. Medical history* **24**, 143–162 (Cambridge University Press, 1980).
10. Roux, F. A., Sai, P. & Deschamps, J.-Y. Xenotransfusions, past and present. *Xenotransplantation* **14**, 208–216 (2007).
11. Augier, F., Salf, E. & Nottet, J. B. [Dr. Samuel Serge Voronoff (1866-1951) or 'the quest for eternal youth']. *Histoire des sciences médicales* **30**, 163–171 (1996).
12. Reemtsma, K. *et al.* Renal heterotransplantation in man. *Annals of Surgery* **160**, 384–410 (1964).
13. Reemtsma, K. Renal heterotransplantation from nonhuman primates to man. *Ann. N. Y. Acad. Sci.* **162**, 412–418 (1969).

14. Reemtsma, K. *et al.* Reversal of early graft rejection after renal heterotransplantation in man. *JAMA* **187**, 691–696 (1964).
15. Hardy, J. D. *et al.* Heart transplantation in man. Developmental studies and report of a case. *JAMA* **188**, 1132–1140 (1964).
16. Starzl, T. E., Marchioro, T. L., Faris, T. D., McCardle, R. J. & Iwaski, Y. Avenues of future research in homotransplantation of the liver with particular reference to hepatic supportive procedures, antilymphocyte serum, and tissue typing. *The American Journal of Surgery* **112**, 391–400 (1966).
17. Cooper, D. K. C. Early clinical xenotransplantation experiences—An interview with Thomas E. Starzl, MD, PhD. *Xenotransplantation* **24**, e12306 (2017).
18. Bailey, L. L., Nehlsen-Cannarella, S. L., Concepcion, W. & Jolley, W. B. Baboon-to-human cardiac xenotransplantation in a neonate. *JAMA* **254**, 3321–3329 (1985).
19. STARZL, T. E. *et al.* Baboon-to-human liver transplantation. *The Lancet* **341**, 65–71 (1993).
20. Allan, J. S. The risk of using baboons as transplant donors. Exogenous and endogenous viruses. *Ann. N. Y. Acad. Sci.* **862**, 87–99 (1998).
21. Cooper, D. K. C. A brief history of cross-species organ transplantation. *Proc (Bayl Univ Med Cent)* **25**, 49–57 (2012).
22. Vadori, M. & Cozzi, E. The immunological barriers to xenotransplantation. *Tissue Antigens* **86**, 239–253 (2015).
23. Stussi, G., West, L., Cooper, D. K. C. & Seebach, J. D. ABO-incompatible allotransplantation as a basis for clinical xenotransplantation. in **13**, 390–399 (Wiley/Blackwell (10.1111), 2006).
24. Platt, J. L. *et al.* Immunopathology of hyperacute xenograft rejection in a swine-to-primate model. *Transplantation* **52**, 214–220 (1991).
25. Rose, A. G., Cooper, D., Human, P. A., Reichenspurner, H. & Reichart, B. Histopathology of Hyperacute Rejection of the Heart - Experimental and Clinical Observations in Allografts and Xenografts. *J. Heart Lung Transplant.* **10**, 223–234 (1991).



26. Johnston, P. S., Wang, M. W., Lim, S., Wright, L. J. & White, E. D. Discordant Xenograft Rejection in an Antibody-Free Model. *Transplantation* **54**, 573–576 (1992).
27. Sandrin, M. S., Vaughan, H. A. & McKenzie, I. F. C. Identification of Gal( $\alpha$ 1,3)Gal as the major epitope for pig-to-human vascularised xenografts. *Transplantation Reviews* **8**, 134–149 (1994).
28. Oriol, R., Ye, Y., Koren, E. & Cooper, D. K. Carbohydrate antigens of pig tissues reacting with human natural antibodies as potential targets for hyperacute vascular rejection in pig-to-man organ xenotransplantation. *Transplantation* **56**, 1433–1442 (1993).
29. Joziassse, D. H. & Oriol, R. Xenotransplantation: the importance of the Ga1 alpha 1,3Gal epitope in hyperacute vascular rejection. *Biochimica Et Biophysica Acta-Molecular Basis of Disease* **1455**, 403–418 (1999).
30. Galili, U., Buehler, J., Shohet, S. B. & Macher, B. A. The human natural anti-Gal IgG. III. The subtlety of immune tolerance in man as demonstrated by crossreactivity between natural anti-Gal and anti-B antibodies. *J. Exp. Med.* **165**, 693–704 (1987).
31. Stites, E., Le Quintrec, M. & Thurman, J. M. The Complement System and Antibody-Mediated Transplant Rejection. *J Immunol* **195**, 5525–5531 (2015).
32. Platt, J. L. *et al.* Release of heparan sulfate from endothelial cells. Implications for pathogenesis of hyperacute rejection. *J. Exp. Med.* **171**, 1363–1368 (1990).
33. Robson, S. C. *et al.* Role of endothelial cells in transplantation. *Int. Arch. Allergy Immunol.* **106**, 305–322 (1995).
34. Kopp, C. W. *et al.* Effect of porcine endothelial tissue factor pathway inhibitor on human coagulation factors. *Transplantation* **63**, 749–758 (1997).
35. Robson, S. C. *et al.* Loss of ATP diphosphohydrolase activity with endothelial cell activation. *J. Exp. Med.* **185**, 153–163 (1997).
36. Platt, J. L., Dalmaso, A. P., Lindman, B. J., Ihrcke, N. S. & Bach, F. H. The role of C5a and antibody in the release of heparan sulfate from endothelial cells. *Eur. J. Immunol.* **21**, 2887–2890 (1991).

37. Robson, S. C., Cooper, D. K. & d'Apice, A. J. Disordered regulation of coagulation and platelet activation in xenotransplantation. *Xenotransplantation* **7**, 166–176 (2000).
38. Sfriso, R. & Rieben, R. Real Time High-Resolution Imaging of Porcine Endothelial Glycocalyx Shedding by Human Serum in an in Vitro Microfluidic Model of Pig-to-Human Xenotransplantation. *Transplantation* **102**, S741 (2018).
39. Isolation of Complement Fractions Presents A New Approach to Immunosuppression. *JAMA* **191**, 30 (1965).
40. Gewurz, H. *et al.* Role of the complement system in graft rejections in experimental animals and man. *Ann. N. Y. Acad. Sci.* **129**, 673–713 (2006).
41. Watts, A. *et al.* Plasma perfusion by apheresis through a Gal immunoaffinity column successfully depletes anti-Gal antibody: experience with 320 aphereses in baboons. *Xenotransplantation* **7**, 181–185 (2000).
42. Brenner, P. *et al.* IG-therasorb immunoapheresis in orthotopic xenotransplantation of baboons with landrace pig hearts. *Transplantation* **69**, 208–214 (2000).
43. Leventhal, J. R. *et al.* The immunopathology of cardiac xenograft rejection in the guinea pig-to-rat model. *Transplantation* **56**, 1–8 (1993).
44. Parker, W. *et al.* Transplantation of discordant xenografts: a challenge revisited. *Immunol. Today* **17**, 373–378 (1996).
45. Chong, A. S. *et al.* Delayed xenograft rejection in the concordant hamster heart into Lewis rat model. *Transplantation* **62**, 90–96 (1996).
46. Matsumiya, G. *et al.* Analysis of rejection mechanism in the rat to mouse cardiac xenotransplantation. Role and characteristics of anti-endothelial cell antibodies. *Transplantation* **57**, 1653–1660 (1994).
47. Bach, F. H., Winkler, H., Ferran, C., Hancock, W. W. & Robson, S. C. Delayed xenograft rejection. *Immunol. Today* **17**, 379–384 (1996).
48. Magee, J. C. *et al.* Immunoglobulin prevents complement-mediated hyperacute rejection in swine-to-primate xenotransplantation. *J. Clin. Invest.* **96**, 2404–2412 (1995).

49. Cotterell, A. H., Collins, B. H., Parker, W., Harland, R. C. & Platt, J. L. The humoral immune response in humans following cross-perfusion of porcine organs. *Transplantation* **60**, 861–868 (1995).
50. McCurry, K. R. *et al.* Humoral responses to pig-to-baboon cardiac transplantation: implications for the pathogenesis and treatment of acute vascular rejection and for accommodation. *Hum. Immunol.* **58**, 91–105 (1997).
51. Loss, M. *et al.* Acute vascular rejection is associated with systemic complement activation in a pig-to-primate kidney xenograft model. *Xenotransplantation* **7**, 186–196 (2000).
52. Platt, J. L. *et al.* The role of natural antibodies in the activation of xenogenic endothelial cells. *Transplantation* **52**, 1037–1043 (1991).
53. Blakely, M. L. *et al.* Activation of intragraft endothelial and mononuclear cells during discordant xenograft rejection. *Transplantation* **58**, 1059–1066 (1994).
54. Inverardi, L. *et al.* Early Recognition of a Discordant Xenogeneic Organ by Human Circulating Lymphocytes. *J Immunol* **149**, 1416–1423 (1992).
55. Inverardi, L. & Pardi, R. Early Events in Cell-Mediated Recognition of Vascularized Xenografts: Cooperative Interactions between Selected Lymphocyte Subsets and Natural Antibodies. *Immunol. Rev.* **141**, 71–93 (1994).
56. Seebach, J. D., Yamada, K., McMorrow, I. M., Sachs, D. H. & DerSimonian, H. Xenogeneic human anti-pig cytotoxicity mediated by activated natural killer cells. *Xenotransplantation* **3**, 188–197 (1996).
57. Malyguine, A. M. *et al.* Induction of procoagulant function in porcine endothelial cells by human natural killer cells. *J Immunol* **159**, 4659–4664 (1997).
58. Murray, A. G., Khodadoust, M. M., Pober, J. S. & Bothwell, A. L. Porcine aortic endothelial cells activate human T cells: direct presentation of MHC antigens and costimulation by ligands for human CD2 and CD28. *Immunity* **1**, 57–63 (1994).
59. Yamada, K., Sachs, D. H. & DerSimonian, H. Human Antiporcine Xenogeneic T-Cell Response - Evidence for Allelic Specificity of Mixed Leukocyte

- Reaction and for Both Direct and Indirect Pathways of Recognition. *J Immunol* **155**, 5249–5256 (1995).
60. Scalea, J., Hanecamp, I., Robson, S. C. & Yamada, K. T-cell-mediated immunological barriers to xenotransplantation. *Xenotransplantation* **19**, 23–30 (2012).
  61. Pierson, R. N., Winn, H. J., Russell, P. S. & Auchincloss, H. Xenogeneic skin graft rejection is especially dependent on CD4<sup>+</sup> T cells. *J. Exp. Med.* **170**, 991–996 (1989).
  62. Moses, R. D., Winn, H. J. & Auchincloss, H. Evidence that multiple defects in cell-surface molecule interactions across species differences are responsible for diminished xenogeneic T cell responses. *Transplantation* **53**, 203–209 (1992).
  63. Alter, B. J. & Bach, F. H. Cellular basis of the proliferative response of human T cells to mouse xenoantigens. *J. Exp. Med.* **171**, 333–338 (1990).
  64. Cozzi, E. *et al.* Long-term survival of nonhuman primates receiving life-supporting transgenic porcine kidney xenografts. *Transplantation* **70**, 15–21 (2000).
  65. Cozzi, E. *et al.* Maintenance triple immunosuppression with cyclosporin A, mycophenolate sodium and steroids allows prolonged survival of primate recipients of hDAF porcine renal xenografts. *Xenotransplantation* **10**, 300–310 (2003).
  66. Lenschow, D. J. *et al.* Long-term survival of xenogeneic pancreatic islet grafts induced by CTLA4lg. *Science* **257**, 789–792 (1992).
  67. Cooper, D. K. C. *et al.* Progress in pig-to-non-human primate transplantation models (1998-2013): a comprehensive review of the literature. *Xenotransplantation* **21**, 397–419 (2014).
  68. Kim, S. *et al.* CD4 depletion is necessary and sufficient for long-term pig-to-nonhuman primate renal xenotransplant survival. *Xenotransplantation* **24**, (2017).
  69. Mohiuddin, M. M. *et al.* Chimeric 2C10R4 anti-CD40 antibody therapy is critical for long-term survival of GTKO.hCD46.hTBM pig-to-primate cardiac xenograft. *Nat Commun* **7**, 11138 (2016).

70. Brenner, P. *et al.* Worldwide First Successful Long-term Survival after Orthotopic Cardiac Xenotransplantation of Multitransgenic Pig Hearts into Baboons Using a CD40mAb or CD40L Costimulation Blockade. *Thorac cardiovasc Surg* **66**, S1–S110 (2018).
71. Shah, J. A. *et al.* Prolonged Survival Following Pig-to-Primate Liver Xenotransplantation Utilizing Exogenous Coagulation Factors and Costimulation Blockade. *Am. J. Transplant.* **17**, 2178–2185 (2017).
72. Shin, J. S. *et al.* Long-term control of diabetes in immunosuppressed nonhuman primates (NHP) by the transplantation of adult porcine islets. *Am. J. Transplant.* **15**, 2837–2850 (2015).
73. Cozzi, E. & White, D. J. The generation of transgenic pigs as potential organ donors for humans. *Nat. Med.* **1**, 964–966 (1995).
74. Luo, Y. *et al.* HDAF transgenic pig livers are protected from hyperacute rejection during ex vivo perfusion with human blood. *Xenotransplantation* **9**, 36–44 (2002).
75. Schmoeckel, M. *et al.* Prevention of hyperacute rejection by human decay accelerating factor in xenogeneic perfused working hearts. *Transplantation* **62**, 729–734 (1996).
76. Smolenski, R. *et al.* Reduction of hyperacute rejection and protection of metabolism and function in hearts of human decay accelerating factor (hDAF)-expressing pigs☆. *Cardiovasc. Res.* **73**, 143–152 (2007).
77. Waterworth, P. D. *et al.* Life-supporting pig-to-baboon heart xenotransplantation. *J. Heart Lung Transplant.* **17**, 1201–1207 (1998).
78. Byrne, G., McCurry, K., Martin, M., Platt, J. & Logan, J. Development and analysis of transgenic pigs expressing the human complement regulatory protein CD59 and DAF. *Transplantation Proceedings* **28**, 759 (1996).
79. Campbell, K. H., McWhir, J., Ritchie, W. A. & Wilmut, I. Sheep cloned by nuclear transfer from a cultured cell line. *Nature* **380**, 64–66 (1996).
80. Polejaeva, I. A. *et al.* Cloned pigs produced by nuclear transfer from adult somatic cells. *Nature* **407**, 86–90 (2000).
81. Lai, L. *et al.* Production of alpha-1,3-galactosyltransferase knockout pigs by nuclear transfer cloning. *Science* **295**, 1089–1092 (2002).

82. Phelps, C. J. *et al.* Production of alpha 1,3-galactosyltransferase-deficient pigs. *Science* **299**, 411–414 (2003).
83. Kuwaki, K. *et al.* Heart transplantation in baboons using alpha1,3-galactosyltransferase gene-knockout pigs as donors: initial experience. *Nat. Med.* **11**, 29–31 (2005).
84. Tseng, Y.-L. *et al.* alpha1,3-Galactosyltransferase gene-knockout pig heart transplantation in baboons with survival approaching 6 months. *Transplantation* **80**, 1493–1500 (2005).
85. Yamada, K. *et al.* Marked prolongation of porcine renal xenograft survival in baboons through the use of alpha1,3-galactosyltransferase gene-knockout donors and the cotransplantation of vascularized thymic tissue. *Nat. Med.* **11**, 32–34 (2005).
86. Hisashi, Y. *et al.* Rejection of cardiac xenografts transplanted from alpha1,3-galactosyltransferase gene-knockout (GalT-KO) pigs to baboons. *Am. J. Transplant.* **8**, 2516–2526 (2008).
87. Shimizu, A. *et al.* Thrombotic microangiopathic glomerulopathy in human decay accelerating factor-transgenic swine-to-baboon kidney xenografts. *J. Am. Soc. Nephrol.* **16**, 2732–2745 (2005).
88. McGregor, C. G. A. *et al.* Human CD55 expression blocks hyperacute rejection and restricts complement activation in Gal knockout cardiac xenografts. *Transplantation* **93**, 686–692 (2012).
89. Azimzadeh, A. M. *et al.* Early graft failure of GalTKO pig organs in baboons is reduced by expression of a human complement pathway-regulatory protein. *Xenotransplantation* **22**, 310–316 (2015).
90. Shimizu, A. *et al.* Thrombotic microangiopathy associated with humoral rejection of cardiac xenografts from alpha1,3-galactosyltransferase gene-knockout pigs in baboons. *Am. J. Pathol.* **172**, 1471–1481 (2008).
91. Houser, S. L. *et al.* Thrombotic microangiopathy and graft arteriopathy in pig hearts following transplantation into baboons. *Xenotransplantation* **11**, 416–425 (2004).
92. Siegel, J. B. *et al.* Xenogeneic endothelial cells activate human prothrombin. *Transplantation* **64**, 888–896 (1997).

93. Lawson, J. H., Daniels, L. J. & Platt, J. L. The evaluation of thrombomodulin activity in porcine to human xenotransplantation. *Transplantation Proceedings* **29**, 884–885 (1997).
94. Roussel, J. C. *et al.* Pig thrombomodulin binds human thrombin but is a poor cofactor for activation of human protein C and TAFI. *Am. J. Transplant.* **8**, 1101–1112 (2008).
95. Kopp, C. W. *et al.* Regulation of monocyte tissue factor activity by allogeneic and xenogeneic endothelial cells. *Thromb. Haemost.* **79**, 529–538 (1998).
96. Schulte Am Esch, J., Robson, S. C., Knoefel, W. T., Hosch, S. B. & Rogiers, X. O-linked glycosylation and functional incompatibility of porcine von Willebrand factor for human platelet GPIb receptors. *Xenotransplantation* **12**, 30–37 (2005).
97. Conway, E. M. *et al.* The lectin-like domain of thrombomodulin confers protection from neutrophil-mediated tissue damage by suppressing adhesion molecule expression via nuclear factor kappaB and mitogen-activated protein kinase pathways. *J. Exp. Med.* **196**, 565–577 (2002).
98. Van de Wouwer, M. *et al.* The lectin-like domain of thrombomodulin interferes with complement activation and protects against arthritis. *J. Thromb. Haemost.* **4**, 1813–1824 (2006).
99. Petersen, B. *et al.* Pigs transgenic for human thrombomodulin have elevated production of activated protein C. *Xenotransplantation* **16**, 486–495 (2009).
100. Yang, L. *et al.* Genome-wide inactivation of porcine endogenous retroviruses (PERVs). *Science* **350**, 1101–1104 (2015).
101. Niu, D. *et al.* Inactivation of porcine endogenous retrovirus in pigs using CRISPR-Cas9. *Science* **357**, 1303–1307 (2017).
102. Petersen, B. *et al.* Efficient production of biallelic GGTA1 knockout pigs by cytoplasmic microinjection of CRISPR/Cas9 into zygotes. *Xenotransplantation* **23**, 338–346 (2016).
103. Lutz, A. J. *et al.* Double knockout pigs deficient in N-glycolylneuraminic acid and galactose  $\alpha$ -1,3-galactose reduce the humoral barrier to xenotransplantation. *Xenotransplantation* **20**, 27–35 (2013).

104. Byrne, G. W., Du, Z., Stalboerger, P., Kogelberg, H. & McGregor, C. G. A. Cloning and expression of porcine  $\beta$ 1,4 N-acetylgalactosaminyl transferase encoding a new xenoreactive antigen. *Xenotransplantation* **21**, 543–554 (2014).
105. Estrada, J. L. *et al.* Evaluation of human and non-human primate antibody binding to pig cells lacking GGTA1/CMAH/ $\beta$ 4GalNT2 genes. *Xenotransplantation* **22**, 194–202 (2015).
106. Wang, Z.-Y. *et al.* Erythrocytes from GGTA1/CMAH knockout pigs: implications for xenotransfusion and testing in non-human primates. *Xenotransplantation* **21**, 376–384 (2014).
107. Varki, A. N-glycolylneuraminic acid deficiency in humans. *Biochimie* **83**, 615–622 (2001).
108. Loboda, A. *et al.* Heme oxygenase-1 and the vascular bed: from molecular mechanisms to therapeutic opportunities. *Antioxid. Redox Signal.* **10**, 1767–1812 (2008).
109. Petersen, B. *et al.* Transgenic expression of human heme oxygenase-1 in pigs confers resistance against xenograft rejection during ex vivo perfusion of porcine kidneys. *Xenotransplantation* **18**, 355–368 (2011).
110. Catrysse, L., Vereecke, L., Beyaert, R. & van Loo, G. A20 in inflammation and autoimmunity. *Trends in Immunology* **35**, 22–31 (2014).
111. Oropeza, M. *et al.* Transgenic expression of the human A20 gene in cloned pigs provides protection against apoptotic and inflammatory stimuli. *Xenotransplantation* **16**, 522–534 (2009).
112. Fischer, K. *et al.* Efficient production of multi-modified pigs for xenotransplantation by ‘combineering’, gene stacking and gene editing. *Sci Rep* **6**, 29081 (2016).
113. Lilienfeld, B. G., Crew, M. D., Forte, P., Baumann, B. C. & Seebach, J. D. Transgenic expression of HLA-E single chain trimer protects porcine endothelial cells against human natural killer cell-mediated cytotoxicity. *Xenotransplantation* **14**, 126–134 (2007).
114. Puga Yung, G. *et al.* Release of pig leukocytes and reduced human NK cell recruitment during ex vivo perfusion of HLA-E/human CD46 double-



- transgenic pig limbs with human blood. *Xenotransplantation* **23**, e12357 (2017).
115. Laird, C. T. *et al.* Transgenic expression of human leukocyte antigen-E attenuates GalkO.hCD46 porcine lung xenograft injury. *Xenotransplantation* **24**, (2017).
116. Abicht, J.-M. *et al.* Multiple genetically modified GTKO/hCD46/HLA-E/h $\beta$ 2-mg porcine hearts are protected from complement activation and natural killer cell infiltration during ex vivo perfusion with human blood. *Xenotransplantation* (2018). doi:10.1111/xen.12390
117. Meier, R. P. H. *et al.* Xenotransplantation: back to the future? *Transpl. Int.* **31**, 465–477 (2018).
118. Mohiuddin, M. M. *et al.* Genetically engineered pigs and target-specific immunomodulation provide significant graft survival and hope for clinical cardiac xenotransplantation. *Journal of Thoracic and Cardiovascular Surgery* **148**, 1106–1113 (2014).
119. Mohiuddin, M. M. *et al.* One-year heterotopic cardiac xenograft survival in a pig to baboon model. *Am. J. Transplant.* **14**, 488–489 (2014).
120. Byrne, G. W., Du, Z., Sun, Z., Asmann, Y. W. & McGregor, C. G. A. Changes in cardiac gene expression after pig-to-primate orthotopic xenotransplantation. *Xenotransplantation* **18**, 14–27 (2011).
121. Iwase, H. *et al.* Immunological and physiological observations in baboons with life-supporting genetically engineered pig kidney grafts. *Xenotransplantation* **24**, (2017).
122. Martens, G. *et al.* Porcine GGTA1/B4GalNT2 gene knockout reduces antibody binding and achieves one year life-supporting renal xenograft in pig-to-rhesus model. *Xenotransplantation* **24**, (2017).
123. Burdorf, L. *et al.* Progress and remaining challenges in xenogeneic lung transplantation. *Xenotransplantation* **24**, (2017).
124. Walport, M. J. Complement. First of two parts. *N. Engl. J. Med.* **344**, 1058–1066 (2001).
125. Figueroa, J., Andreoni, J. & Densen, P. Complement deficiency states and meningococcal disease. *Immunol Res* **12**, 295–311 (1993).

126. Dunkelberger, J. R. & Song, W.-C. Complement and its role in innate and adaptive immune responses. *Cell Res.* **20**, 34–50 (2010).
127. Sjöholm, A. G., Jonsson, G., Braconier, J. H., Sturfelt, G. & Truedsson, L. Complement deficiency and disease: An update. *Mol. Immunol.* **43**, 78–85 (2006).
128. Atkinson, J. P. & Farries, T. Separation of self from non-self in the complement system. *Immunol. Today* **8**, 212–215 (1987).
129. Meri, S. Self-nonsel self discrimination by the complement system. *FEBS Lett.* **590**, 2418–2434 (2016).
130. Sarma, J. V. & Ward, P. A. The complement system. *Cell Tissue Res.* **343**, 227–235 (2011).
131. Sørensen, R., Thiel, S. & Jensenius, J. C. Mannan-binding-lectin-associated serine proteases, characteristics and disease associations. *Springer Semin Immun* **27**, 299–319 (2005).
132. Wallis, R. Interactions between mannose-binding lectin and MASPs during complement activation by the lectin pathway. *Immunobiology* **212**, 289–299 (2007).
133. Harboe, M. & Mollnes, T. E. The alternative complement pathway revisited. *J. Cell. Mol. Med.* **12**, 1074–1084 (2008).
134. Ward, P. A. & Zvaifler, N. J. Quantitative phagocytosis by neutrophils. II. Release of the C5-cleaving enzyme and inhibition of phagocytosis by rheumatoid factor. *J Immunol* **111**, 1777–1782 (1973).
135. Huber-Lang, M. *et al.* Generation of C5a by phagocytic cells. *Am. J. Pathol.* **161**, 1849–1859 (2002).
136. Huber-Lang, M. *et al.* Generation of C5a in the absence of C3: a new complement activation pathway. *Nat. Med.* **12**, 682–687 (2006).
137. Meri, S. & Jarva, H. *Complement Regulatory Proteins and Related Diseases.* **124**, (John Wiley & Sons, Ltd, 2001).
138. Kaushansky, K. & Levi, M. M. *Williams Hematology Hemostasis and Thrombosis.* (McGraw Hill Professional, 2018).
139. Lasne, D., Jude, B. & Susen, S. From normal to pathological hemostasis. *Can J Anaesth* **53**, S2–11 (2006).

140. Owens, A. P. & Mackman, N. Tissue factor and thrombosis: The clot starts here. *Thromb. Haemost.* **104**, 432–439 (2010).
141. Osterud, B. & Rapaport, S. I. Activation of factor IX by the reaction product of tissue factor and factor VII: additional pathway for initiating blood coagulation. *Proc. Natl. Acad. Sci. U.S.A.* **74**, 5260–5264 (1977).
142. Bauer, K. A., Kass, B. L., Cate, ten, H., Hawiger, J. J. & ROSENBERG, R. D. Factor IX is activated in vivo by the tissue factor mechanism. *Blood* **76**, 731–736 (1990).
143. Wu, Y. Contact pathway of coagulation and inflammation. *Thromb J* **13**, 17 (2015).
144. Loof, T. G., Deicke, C. & Medina, E. The role of coagulation/fibrinolysis during *Streptococcus pyogenes* infection. *Front Cell Infect Microbiol* **4**, (2014).
145. Pober, J. S. & Cotran, R. S. The role of endothelial cells in inflammation. *Transplantation* **50**, 537–544 (1990).
146. Pober, J. S. & Sessa, W. C. Evolving functions of endothelial cells in inflammation. *Nature Reviews Immunology* **7**, 803–815 (2007).
147. Ihrcke, N. S., Wrenshall, L. E., Lindman, B. J. & Platt, J. L. Role of heparan sulfate in immune system-blood vessel interactions. *Immunol. Today* **14**, 500–505 (1993).
148. Constantinescu, A. A., Vink, H. & Spaan, J. A. E. Endothelial cell glycocalyx modulates immobilization of leukocytes at the endothelial surface. *Arterioscler Thromb Vasc Biol* **23**, 1541–1547 (2003).
149. ROSENBERG, R. D. & Rosenberg, J. S. Natural anticoagulant mechanisms. *J. Clin. Invest.* **74**, 1–6 (1984).
150. De Agostini, A. I., Watkins, S. C., Slayter, H. S., Youssoufian, H. & Rosenberg, R. D. Localization of Anticoagulant Active Heparan-Sulfate Proteoglycans in Vascular Endothelium - Antithrombin Binding on Cultured Endothelial-Cells and Perfused Rat Aorta. *J. Cell Biol.* **111**, 1293–1304 (1990).
151. Muñoz, E. M. & Linhardt, R. J. Heparin-binding domains in vascular biology. *Arterioscler Thromb Vasc Biol* **24**, 1549–1557 (2004).

152. Cooper, D. K. C., Kemp, E., Platt, J. & White, D. J. G. *Xenotransplantation*. (Springer Science & Business Media, 2012). doi:10.1007/978-3-642-60572-7
153. Davies, P. F. Hemodynamic shear stress and the endothelium in cardiovascular pathophysiology. *Nat Clin Pract Cardiovasc Med* **6**, 16–26 (2009).
154. Heo, K.-S., Fujiwara, K. & Abe, J.-I. Disturbed-flow-mediated vascular reactive oxygen species induce endothelial dysfunction. *Circ. J.* **75**, 2722–2730 (2011).
155. Reinhart-King, C. A., Fujiwara, K. & Berk, B. C. Physiologic stress-mediated signaling in the endothelium. *Meth. Enzymol.* **443**, 25–44 (2008).
156. Davies, P. F., Civelek, M., Fang, Y. & Fleming, I. The atherosusceptible endothelium: endothelial phenotypes in complex haemodynamic shear stress regions in vivo. *Cardiovasc. Res.* **99**, 315–327 (2013).
157. Zhou, J., Li, Y.-S. & Chien, S. Shear stress-initiated signaling and its regulation of endothelial function. *Arterioscler Thromb Vasc Biol* **34**, 2191–2198 (2014).
158. Luft, J. H. Fine Structure of Capillary and Endocapillary Layer as Revealed by Ruthenium Red. *Federation Proceedings* **25**, 1773–& (1966).
159. Pries, A. R., Secomb, T. W. & Gaehtgens, P. The endothelial surface layer. *Pflugers Arch.* **440**, 653–666 (2000).
160. Lipowsky, H. H. Microvascular rheology and hemodynamics. *Microcirculation* **12**, 5–15 (2005).
161. Alphonsus, C. S. & Rodseth, R. N. The endothelial glycocalyx: a review of the vascular barrier. *Anaesthesia* **69**, 777–784 (2014).
162. Reitsma, S., Slaaf, D. W., Vink, H., van Zandvoort, M. A. M. J. & oude Egbrink, M. G. A. The endothelial glycocalyx: composition, functions, and visualization. *Pflugers Arch.* **454**, 345–359 (2007).
163. Weinbaum, S., Tarbell, J. M. & Damiano, E. R. The structure and function of the endothelial glycocalyx layer. *Annu Rev Biomed Eng* **9**, 121–167 (2007).
164. Fu, B. M. & Tarbell, J. M. Mechano-sensing and transduction by endothelial surface glycocalyx: composition, structure, and function. *Wiley Interdiscip Rev Syst Biol Med* **5**, 381–390 (2013).

165. Gouverneur, M., Spaan, J. A. E., Pannekoek, H., Fontijn, R. D. & Vink, H. Fluid shear stress stimulates incorporation of hyaluronan into endothelial cell glycocalyx. *Am. J. Physiol. Heart Circ. Physiol.* **290**, H458–2 (2006).
166. Myburgh, J. A. & Mythen, M. G. Resuscitation fluids. *N. Engl. J. Med.* **369**, 1243–1251 (2013).
167. Charati, S. G. & Stern, S. A. Diffusion of Gases in Silicone Polymers: Molecular Dynamics Simulations. *Macromolecules* **31**, 5529–5535 (1998).
168. Leclerc, E., Sakai, Y. & Fujii, T. Cell Culture in 3-Dimensional Microfluidic Structure of PDMS (polydimethylsiloxane). *Biomedical Microdevices* **5**, 109–114 (2003).



## Results





## Paper I

### Assessment of the Anticoagulant and Anti-inflammatory Properties of Endothelial Cells Using 3D Cell Culture and Non-anticoagulated Whole Blood.

Riccardo Sfriso, Anjan Bongoni, Yara Banz, Nikolai Klymiuk, Eckhard Wolf, Robert Rieben

**Status:** Published in *Journal of Visualized Experiments*, 2017 May 9 (127), e56227

**Contribution:** All experiments and graphs were performed and made by Riccardo Sfriso.

**Background:** Culturing endothelial cells on the surface of microcarrier beads allows to increase the endothelial surface allowing to explore their natural anticoagulant properties without the necessity of anticoagulants.

**Aim:** To provide a detailed video-protocol through which the effects of advanced genetic modifications on porcine endothelial cells can be tested using whole non-anticoagulated human blood.

**Conclusion:** The *in vitro* model successfully provided interesting data on the capability of transgenic cells to prolong the clotting time of human blood.

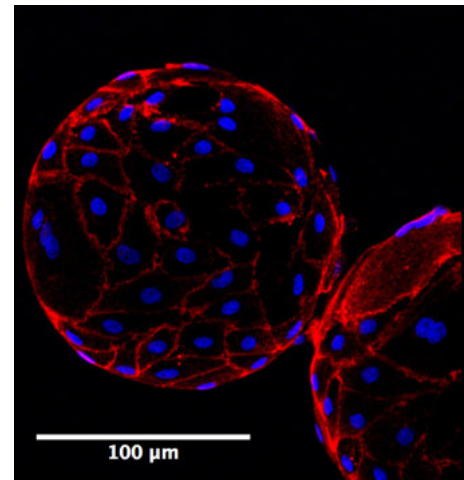


**Figure:** Confocal image of EC coated microcarrier beads. CD31 staining showing the membrane of EC (red). Nuclei are stained with DAPI (blue).



## Video Article

## Assessment of the Anticoagulant and Anti-inflammatory Properties of Endothelial Cells Using 3D Cell Culture and Non-anticoagulated Whole Blood

Riccardo Sfriso<sup>1,2</sup>, Anjan Bongoni<sup>3</sup>, Yara Banz<sup>4</sup>, Nikolai Klymiuk<sup>5</sup>, Eckhard Wolf<sup>5</sup>, Robert Rieben<sup>1</sup><sup>1</sup>Department of Clinical Research, University of Bern<sup>2</sup>Graduate School for Cellular and Biomedical Sciences, University of Bern<sup>3</sup>Immunology Research Centre, St. Vincent's Hospital Melbourne<sup>4</sup>Institute of Pathology, University of Bern<sup>5</sup>Institute of Molecular Animal Breeding and Biotechnology, Ludwig-Maximilian UniversityCorrespondence to: Robert Rieben at [robert.riegen@dkf.unibe.ch](mailto:robert.riegen@dkf.unibe.ch)URL: <https://www.jove.com/video/56227>DOI: [doi:10.3791/56227](https://doi.org/10.3791/56227)Keywords: Medicine, Issue 127, Endothelial cells, coagulation, whole blood, microcarrier beads, complement, 3D, *in vitro* model, clotting time.

Date Published: 9/5/2017

Citation: Sfriso, R., Bongoni, A., Banz, Y., Klymiuk, N., Wolf, E., Rieben, R. Assessment of the Anticoagulant and Anti-inflammatory Properties of Endothelial Cells Using 3D Cell Culture and Non-anticoagulated Whole Blood. *J. Vis. Exp.* (127), e56227, doi:10.3791/56227 (2017).

### Abstract

*In vivo*, endothelial cells are crucial for the natural anticoagulation of circulating blood. Consequently, endothelial cell activation leads to blood coagulation. This phenomenon is observed in many clinical situations, like organ transplantation in the presence of pre-formed anti-donor antibodies, including xenotransplantation, as well as in ischemia/reperfusion injury. In order to reduce animal experimentation according to the 3R standards (reduction, replacement and refinement), *in vitro* models to study the effect of endothelial cell activation on blood coagulation would be highly desirable. However, common flatbed systems of endothelial cell culture provide a surface-to-volume ratio of 1 - 5 cm<sup>2</sup> of endothelium per mL of blood, which is not sufficient for natural, endothelial-mediated anticoagulation. Culturing endothelial cells on microcarrier beads may increase the surface-to-volume ratio to 40 - 160 cm<sup>2</sup>/mL. This increased ratio is sufficient to ensure the "natural" anticoagulation of whole blood, so that the use of anticoagulants can be avoided. Here an *in vitro* microcarrier-based system is described to study the effects of genetic modification of porcine endothelial cells on coagulation of whole, non-anticoagulated human blood. In the described assay, primary porcine aortic endothelial cells, either wild type (WT) or transgenic for human CD46 and thrombomodulin, were grown on microcarrier beads and then exposed to freshly drawn non-anticoagulated human blood. This model allows for the measurement and quantification of cytokine release as well as activation markers of complement and coagulation in the blood plasma. In addition, imaging of activated endothelial cell and deposition of immunoglobulins, complement- and coagulation proteins on the endothelialized beads were performed by confocal microscopy. This assay can also be used to test drugs which are supposed to prevent endothelial cell activation and, thus, coagulation. On top of its potential to reduce the number of animals used for such investigations, the described assay is easy to perform and consistently reproducible.

### Video Link

The video component of this article can be found at <https://www.jove.com/video/56227/>

### Introduction

The vascular endothelium consists of a monolayer of endothelial cells (EC) which line the lumen of blood vessels. In a physiological state, quiescent EC are responsible for the maintenance of an anticoagulant and anti-inflammatory environment.<sup>1</sup> This is mediated by the expression of anticoagulant and anti-inflammatory proteins on the EC surface. For example, EC activation caused by ischemia/reperfusion injury or vascular rejection of (xeno-)transplanted organs results in a change of the endothelial surface from an anticoagulant and anti-inflammatory state to a pro-coagulant and pro-inflammatory state.<sup>1</sup>

To study the fascinating and complex interaction between the endothelium and coagulation factors, *in vitro* models which mimic as closely as possible the *in vivo* situation are highly desirable. A common limitation which characterizes conventional *in vitro* coagulation assays is the use of anticoagulated blood which makes the analysis of coagulation-mediated effects arduous and even recalcification of citrated whole blood cannot reproduce results obtainable with fresh non-anticoagulated blood.<sup>2</sup> Besides, in traditional flat-bed cell culture systems it is impossible to exploit the anticoagulant properties of the endothelium as a sufficient endothelial cell surface per blood volume cannot be reached. The model presented here overcomes these limitations by culturing EC on the surface of spherical microcarrier beads, so that an EC surface-to-blood ratio of >16 cm<sup>2</sup>/mL can be reached, which is similar to the situation in small arterioles or veins, and which was described to be sufficient to allow "natural" anticoagulation of the blood by the EC surface.<sup>3,4</sup> Whole blood can be used without added anticoagulants in this setting. Blood samples can be collected during the experiment and cytokines, coagulation factors and soluble complement activation markers can be detected and quantified. Furthermore, EC-coated microcarrier beads may be analyzed for complement and immunoglobulin deposition as well as the expression of EC activation markers by confocal microscopy. Another interesting application includes the testing of drugs which are supposed to prevent endothelial cell activation and, thus, coagulation.<sup>5</sup> Although this model cannot completely replace animal experimentation, it offers a

method to test specific functional hypotheses *ex vivo* using cells and thus reduce the number of animals used in basic research on ischemia/reperfusion injury or (xeno)transplantation.

The described model was used to mimic a xenotransplantation setting in which porcine aortic endothelial cells (PAEC) are grown on the microcarrier beads and incubated with whole, non-anticoagulated human blood. Different transgenic PAEC, carrying several human genes such as CD46 for the regulation of the complement system and/or thrombomodulin (hTBM) for the regulation of the coagulation system, were analyzed for their anticoagulant properties. Endothelial cell activation, complement, and coagulation systems are tightly controlled and interconnected.<sup>6</sup> It is therefore important to understand how the different transgenic cells behave after exposure to human blood with regard to adhesion molecule expression and cytokine release, shedding of the glycocalyx and loss of anticoagulant proteins.<sup>7</sup>

## Protocol

German Landrace pigs (wild type bred in a local farmhouse and transgenic bred at the Institute of Molecular Animal Breeding and Biotechnology, Ludwig-Maximilian University, Munich, Germany), weighing between 30 kg to 40 kg, were used in this study. All animals were housed under standard conditions with water and food *ad lib*. All animal experiments were performed in accordance with the U.K. Animals Act (scientific procedures) and the NIH Guide for the Care and Use of Laboratory Animals, as well as the Swiss animal protection law. All animal studies complied with the ARRIVE guidelines. The animal experimentation committee of the cantonal veterinary service (Canton of Bern, Switzerland) approved all animal procedures, permission no. BE70/14. Experimental protocols were refined according to the 3R principles and state-of-the-art anesthesia and pain management were used to minimize the number of animals and reduce the exposure of the animals to stress and pain during the experiments.

Blood was drawn from healthy individuals by closed system venipuncture in accordance with Swiss jurisdiction and ethics guidelines of the Bern University Hospital. The phrase "non-anticoagulated blood" means that the blood has not been treated with any anticoagulant.

The following steps are performed under sterile conditions. Familiarity with basic cell culture sterile technique is required.

### 1. Isolation of PAEC

NOTE: Thoracic aorta segments of 6 to 10 cm were obtained from euthanized German Landrace pigs of 3 to 6 months of age (used for other *in vivo* experiments) and immediately transferred into a 500-mL glass bottle containing transport medium (DMEM + 1% penicillin/streptomycin).

1. Pre-coat a 6-well plate with fibronectin 12.5 µg/mL in PBS 1x and place it in an incubator at 37 °C for 1 h.
2. Pre-warm sterile PBS 1x and cell culture medium (DMEM).
3. Take out the porcine aorta from transport medium.
4. Place the aorta on a polystyrene plate.
5. Flush with warm PBS gently beforehand.
6. Cut the aorta longitudinally and fix it with needles.
7. Add warm cell culture medium on the inner vessel surface.
8. Aspirate fibronectin-cell culture medium and add fresh cell culture medium (DMEM supplemented with 10% FBS, 1% penicillin/streptomycin and 0.4% of Endothelial Cell Growth Medium Supplement Mix).
9. Soak one cotton swab in the cell culture medium. Swab the cotton wool bud on the very top of the inner vessel surface gently and slowly in the same direction.
10. Rub the cells in one well of 6-well plate round by round.
11. Do the same for the rest of the wells.
12. Check cells under the microscope and place the 6-well plate in incubator at 37 °C, 5% CO<sub>2</sub>.
13. Change the medium on the second day and change it again every 2 - 3 days.
14. When cells are going to be confluent, trypsinize cells and seed them into a T75 flask (PAEC P1).

### 2. PAEC Characterization

1. Pre-coat an 8-well chamberslide with fibronectin 12.5 µg/mL in PBS 1x and place it in an incubator at 37 °C for 1 h.
2. Seed 5 x 10<sup>4</sup> cells/well and incubate overnight in the incubator at 37 °C.
3. Wash the cells twice with PBS<sup>++</sup> (PBS supplemented with CaCl<sub>2</sub> and MgCl<sub>2</sub>), 300 µL/well.
4. Fix cells with 3.7% paraformaldehyde for 10 min at room temperature, 200 µL/well.
5. Wash cells 3 times with PBS<sup>++</sup>, 300 µL/well.
6. Add 300 µL of PBS 1x-3% BSA (blocking buffer) and leave 30 min at room temperature.
7. Apply primary antibodies (anti-VE-cadherin, anti-CD31, anti-vWF) diluted in PBS 1x-1%BSA-0.05% detergent, 160 µL/well and incubate for 1 h at room temperature.
8. Wash 3 times with PBS<sup>++</sup> (200 µL/well).
9. Apply secondary antibodies and DAPI diluted in PBS 1x-1%BSA-0.05% detergent, 160 µL/well, and incubate for 1 h at room temperature.
10. Wash 3 times with PBS<sup>++</sup> (200 µL/well).
11. Mount slides with glycerol based mounting medium and verify endothelial cell markers expression under a fluorescence microscope.

NOTE: Culture porcine aortic endothelial cells in a T175 flask (DMEM low glucose medium + 10% FBS, 1% penicillin/streptomycin and 0.4% of Endothelial Cell Growth Medium Supplement Mix) until 90% confluence is reached. (seeding density 1 x 10<sup>6</sup> cells, 90% confluence correspond roughly to 5 x 10<sup>6</sup> cells).



### 3. Coating of Microcarrier Beads

1. Mix 7 mL of microcarrier beads with 42 mL of collagen solution in a 50-mL tube (100 µg/mL, diluted in a 0.2% acetic acid solution) and incubate for 1 h at room temperature.
2. Wash beads two times with 25 mL of PBS pH 7.4 (add 25 mL of PBS, mix well with the pipet and wait until the beads are settled down then discard the supernatant and repeat) and one time with 25 mL of DMEM medium.
3. Cover the beads in the 50-mL tube with 10 mL of medium 199 supplemented with 10% FBS, 1% penicillin/streptomycin, 1% L-Glutamine, 0.4% of Endothelial Cell Growth Medium Supplement Mix and 25 µL of heparin (5000 IU/mL) and allow equilibration for 10 min before further use.

### 4. Collecting Cells

1. Remove the cell culture medium from the T175 flask containing PAEC and add 5 mL of PBS pH 7.4.
2. Remove PBS from the T175 flask.
3. Add 5 mL of Trypsin-0.05% EDTA and incubate for 3 - 4 min at 37 °C.
4. Collect the cells by rinsing the flask with 15 mL of cell culture medium and transfer the suspension in a 50-mL tube.
5. Centrifuge cells at 1,200 x g for 8 min at room temperature, remove excess medium and resuspend the pellet in 5 mL of cell culture medium.

### 5. Seeding Cells into the Stirrer Flask

1. Add 20 mL of cell culture medium to the cell suspension and resuspend.
2. Add 20 mL cell culture medium (w/o cells) into the 500-mL magnetic stirrer flask.
3. Add the cells to the washed microcarrier beads from step 3.3 and mix carefully with a 25-mL serological pipette.
4. Transfer the beads/cell mixture into the magnetic spinner flask.
5. Rinse the 50-mL tube with 10 mL of cell culture medium to collect the remaining cells.
6. Add an additional 85 mL of cell culture medium into the spinner flask and place it into the incubator overnight at 37 °C on a shaker (100 x g, mixing interval: 3 min every 45 min).
7. Add 50 mL of cell culture medium (total volume 200 mL) and continue stirring for additional 24 h at 37 °C on a shaker (100 x g, mixing interval: 3 min every 45 min).
8. Add colorless RPMI medium (supplemented with 10% FBS, 1% penicillin/streptomycin, 1% L-Glutamine, 0.4% of Endothelial Cell Growth Medium Supplement Mix and 25 µL of Heparin) until 320 mL of total volume is reached.
9. Replace the medium every 48 h: Remove 100 mL of old medium and add 100 mL of fresh supplemented colorless RPMI.
10. Culture the cells for 5 to 7 days. The time depends on the confluence state of the cell-coated beads.

### 6. Confluence Verification

1. Collect 200 µL of cell-coated beads using a pipette and transfer them into a polypropylene tube.
2. Wash the beads 3 times with 600 µL of PBS 1x (add PBS, tilt the tube and mix gently to avoid detachment of the cells, wait the beads to settle down, discard the PBS and repeat).
3. Fix the beads for 10 min by adding 200 µL of parapiacic acid.
4. Wash 3 times with 600 µL of PBS 1x.
5. Add DAPI diluted in PBS 1x and incubate for 10 min.
6. Transfer the beads on a glass slide and apply a coverslip using glycerol based mounting medium.
7. Visualize the beads under a confocal microscope.

### 7. Experimental Procedure

1. Remove the cell-coated beads from the magnetic stirrer flask (procedures do not have to be done under sterile conditions) with a 10-mL serological pipette and transfer them into 12 mL round-bottom polypropylene tubes.
2. Let the beads settle down (around 1 - 2 min) and remove excess medium.
3. Add more beads to the tubes until every tube contains exactly 2 mL of beads.
4. Add 5-mL clear RPMI to each tube and mix carefully using a 10-mL serological pipette.
5. Let the beads settle down and remove excess medium.
6. Repeat the washing procedure one more time with RPMI and remove all excess medium.

### 8. Incubation with Non-anticoagulated Blood

1. Carefully and slowly (using neither jet nor vacutainers) draw blood from a healthy volunteer and collect it in 9 mL neutral polypropylene tubes (no anticoagulant).
2. Slowly transfer 8 mL of blood with a 10-mL serological pipette into each of the polypropylene tubes containing 2 mL of cell-coated beads (the total volume will be 10 mL). Always avoid rough handling of blood or beads to avoid premature EC activation. The procedure takes 1 - 2 min.
3. Carefully tilt the blood/bead mixture to ensure equal mixing and seal the cap with paraffin film.
4. Place the tubes on a horizontal tilting table (with gentle tilting settings only) inside a 37 °C incubator and record clotting times.
  1. At set time intervals, e.g. after 10, 20, 30, 50, 70, 90 min, remove at least 1.5 - 2 mL of blood-bead mixture for serum or plasma analysis.

- NOTE: for 6 time points we suggest having more than 3 replicates within one group of cells, as the blood sampling will be done in different tubes.
- For collection of serum, leave the blood to coagulate. To collect the plasma, add EDTA or citrate to 2 mL tubes before adding blood samples.
  - Store the tubes on ice, centrifuge at 2,500 x g for 10 min at 4 °C and store serum/plasma at 80 °C until use.
- NOTE: Details on materials are provided in **Table of Materials**

## Representative Results

After 7 - 10 days of culture in the spinner flask (**Figure 1**) the cells were confluent, covering the whole surface of the microcarrier beads (**Figure 2**). Verification of the confluency state is an important step because a non-confluent monolayer of EC on the microbeads will lead to a marked decrease in the clotting time, given the microcarrier beads' surface is strongly pro-coagulant (clotting time:  $4 \pm 1$  min) (**Figure 3**).

Another important point which needs attention is the speed of the tilting plate. A high tilting speed will enhance blood clotting. A prolongation of the clotting time could be observed if a monolayer of EC was present on the surface of the microcarrier beads. The use of GalTKO/hCD46/hTBM transgenic PAEC showed a significant increase in the clotting time compared to WT PAEC (**Figure 3**). The absence of the Gal- $\alpha$ -1,3-Gal xenoantigen on the PAEC (GalTKO) showed an increase in clotting time ( $25 \pm 8$  min for PAEC WT and  $68 \pm 30$  min for PAEC GalTKO). Another strong increase in clotting time was observed when PAEC GalTKO/hCD46/hTBM were present on microcarrier beads ( $205 \pm 32$  min), which suggests a successful modulation of both the complement (hCD46) and coagulation systems (hTBM). The end of the experiment is defined when a visible clot is formed. The variability within samples of the same of group is due both to inter assay-variability and the blood donor. Every experiment had 3 replicates and each time a different blood donor was used to increase the reliability of the data. For each donor, a blood analysis (platelet count, WBC, RBC, HCT and other parameters) was performed by external healthcare laboratories. The results shown in **Figure 3** are obtained from different experiments performed with different blood donors.

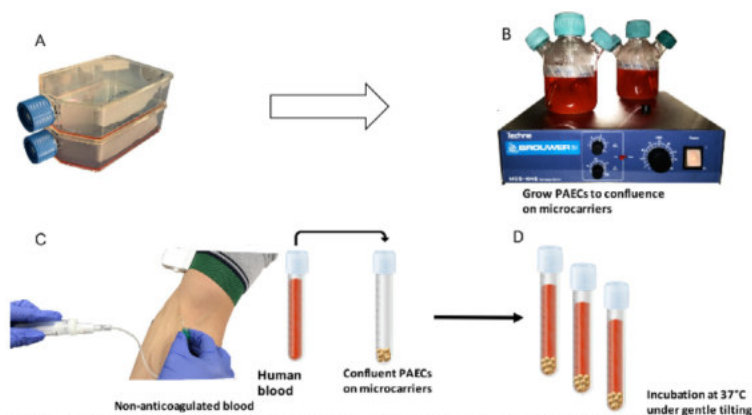


**Figure 1: Schematic Representation of the Microcarrier-based Assay.** (A) EC are expanded in T175 flasks and (B) transferred into spinner flasks together with collagen-coated microcarrier beads. (C) Fresh non-anticoagulated blood is collected from a healthy volunteer, (D) mixed with EC-coated microcarrier beads, and incubated at 37 °C. The phrase "non-anticoagulated blood" means that the blood has not been treated with any anticoagulant. [Please click here to view a larger version of this figure.](#)

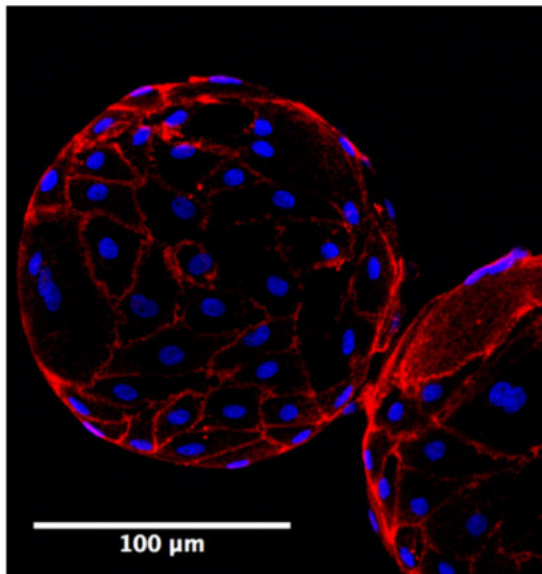


**Figure 2: Immunofluorescence Staining on EC-coated Microcarrier Beads.** Microcarrier beads were retrieved and stained for CD31 (PECAM-1) to assess the confluency. The nuclei were stained in blue (DAPI) and CD31 was stained in red (Cy3). Scale bar: 100  $\mu$ m. [Please click here to view a larger version of this figure.](#)

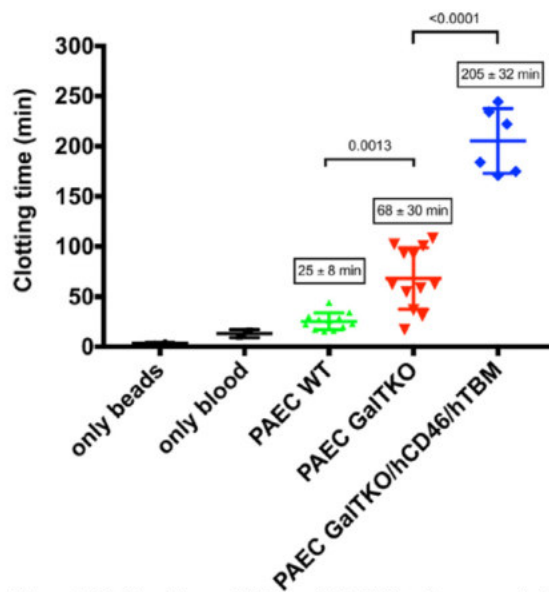


**Figure 3: Clotting Times of Different EC.** Clotting times were determined visually and the end of the experiment was defined when a visible clot was observed. A strong procoagulant effect was observed when non-EC-coated microcarrier beads were exposed to whole non-anticoagulated human blood. The absence of the Gal- $\alpha$ -1,3-Gal xenoantigen on the PAEC (GalTKO) showed an increase in clotting time (25  $\pm$  8 min for PAEC WT and 68  $\pm$  30 min for PAEC GalTKO). A further increase in clotting time was observed when PAEC GalTKO/hCD46/hTBM were present on microcarrier beads, which suggests a successful modulation of both the complement (hCD46) and coagulation systems (hTBM). Data are shown as mean  $\pm$  standard deviation. Statistical analysis has been done using ANOVA for multiple comparisons with Bonferroni correction. [Please click here to view a larger version of this figure.](#)



## Discussion

The model presented here is suitable for coagulation related studies allowing the analysis of different aspects of coagulation and its interaction with EC.<sup>8</sup> In xenotransplantation research, it is a useful system to test the anticoagulant properties of different genetically modified porcine ECs after incubation with human blood<sup>9</sup>.

The most critical steps of the protocol are those ensuring complete cell coverage (confluency) of the microbeads before starting the experiment and those pertaining to the careful collection and handling of the non-anticoagulated whole blood to avoid premature platelet activation due to high shear stress, which may occur if vacutainers are used to collect the blood.<sup>10</sup> Nevertheless, this system has some limitations, including the absence of a recirculating closed system and the absence of physiological shear stress which would better represent the *in vivo* conditions.

Despite these limitations, the described model offers significant advantages over currently existing models. Due to the use of microcarrier beads, the EC surface to blood volume ratio is increased, allowing the establishment of the anti-coagulant and anti-inflammatory environment and use of non-anticoagulated whole blood. In current flat-bed cell culture models, this is not possible and mechanisms which involve blood clotting due to EC activation therefore often require the use of animal experimentation. In part, this can be avoided using the described microcarrier bead model.

Furthermore, this system allows for a broad spectrum of applications. Its versatility resides in the possibility of testing different drugs or compounds which are not only related to (xeno-) transplantation but also to human diseases. The effects of the drugs on the endothelium and on the coagulation system can be easily assessed by immunofluorescence, ELISA and multiplex suspension array analysis. This was previously done in a study on the effect of transgenic expression of human thrombomodulin in a xenotransplantation setting.<sup>11</sup>

A possible modification of the described method could be the collection of non-anticoagulated whole blood directly into tubes which are filled previously with cell-coated beads in order to reduce air-contact and blood activation by using the pipette. The use of human aortic endothelial cells (HAEC) may be an interesting control and is already incorporated into future plans. Argon topping of the tubes might be used to reduce the contact of non-anticoagulated blood with air, which is known to lead to contact activation of the clotting cascade. If the blood is drawn too quickly, for example by using vacuumed tubes with rubber stopcocks and introducing blood into the tube in a fine jet, then platelets become activated and coagulation will occur sooner. To avoid platelet activation, use large diameter hypodermic needles (21G - 16G).

## Disclosures

The authors have nothing to disclose.

## Acknowledgements

This study was supported by the Swiss National Science Foundation (SNSF, Grant No. 320030\_156193). The authors thank Dr. Benoît Werlen for providing the Biosilon microcarrier beads. We also thank Prof. Hans Peter Kohler and Prof. André Haeberli for help with setting up the microcarrier bead model.

## References

1. Rajendran, P. *et al.* The vascular endothelium and human diseases. *Int. J. Biol. Sci.* **9**, 1057-1069, (2013).
2. Rajwal, S., Richards, M., & O'Meara, M. The use of recalcified citrated whole blood - a pragmatic approach for thromboelastography in children. *Pediatric Anesthesia*. **14**, 656-660 (2004).
3. Kohler, H. P., Muller, M., Mombeli, M., Mtraub, M. M. Maeberli, M. The Suppression of the Coagulation of Nonanticoagulated Whole-Blood in-Vitro by Human Umbilical Endothelial-Cells Cultivated on Microcarriers Is Not Dependent on Protein-C Activation. *Thromb. Haemost.* **73**, 719-724 (1995).
4. Biedermann, B., Rosenmund, A., Muller, M., Kohler, H. P., Haeberli, A., Straub, P. W. Human endothelial cells suppress prothrombin activation in nonanticoagulated whole blood in vitro. *J. Lab. Clin. Med.* **124**, 339-347 (1994).
5. Banz, Y., Cung, T., Korchagina, E. Y., Bovin, N. V., Haeberli, A., Rieben, R. Endothelial cell protection and complement inhibition in xenotransplantation: a novel in vitro model using whole blood. *Xenotransplantation*. **12**, 434-443 (2005).
6. Cowan, P. J., d'Apice, A. J. Complement activation and coagulation in xenotransplantation. *Immunology and Cell Biology*. **87**, 203-208 (2009).
7. Reitsma, S., Slaaf, D. W., Vink, H., van Zandvoort, M. A. M. J., oude Egbrink, M. G. A. The endothelial glycocalyx: composition, functions, and visualization. *Pflügers Arch.* **454**, 345-359 (2007).
8. Wiegner, R., Chakraborty, S., Huber-Lang, M. Complement-coagulation crosstalk on cellular and artificial surfaces. *Immunobiology*. **221**, 1073-1079 (2016).
9. Bongoni, A. K. *et al.* Transgenic Expression of Human CD46 on Porcine Endothelium: Effect on Coagulation and Fibrinolytic Cascades During Ex Vivo Human-to-Pig Limb Xenoperfusions. *Transplantation*. **99**, 2061-2069 (2015).
10. Miyazaki, Y. *et al.* High shear stress can initiate both platelet aggregation and shedding of procoagulant containing microparticles. *Blood*. **88**, 3456-3464 (1996).
11. Wuensch, A. *et al.* Regulatory Sequences of the Porcine THBD Gene Facilitate Endothelial-Specific Expression of Bioactive Human Thrombomodulin in Single-and Multitransgenic Pigs. *Transplantation*. **97**, 138-147 (2014).



## Paper II

### 3D artificial round section micro-vessels to investigate endothelial cells under physiological flow conditions.

Riccardo Sfriso, Shengye Zhang, Colette Andrea Bichsel, Oliver Steck, Alain Despont, Olivier Thierry Guenat & Robert Rieben

**Status:** Published in *Nature Scientific Reports*, 2018 April 12; 8:5898

**Contribution:** Figure 1, figure 3, figure 4, figure 6, figure 7, figure 8, and all the supplementary data.

**Background:** *In vivo* endothelial cells, the cell type lining the luminal side of blood vessels, live in a 3D microenvironment and experience shear stress caused by the flowing blood. According to the 3R regulations (reduce, replace and refine animal experimentation) we developed a closed circuit microfluidic *in vitro* system in which endothelial cells are cultured in 3D round section microchannels and subjected to physiological, pulsatile flow.

**Aim:** To establish an *in vitro* model able to mimic as close as possible the *in vivo* situation where endothelial cells grown in artificial cylindrical microchannels experience pulsatile laminar flow and shear stress.

**Conclusion:** The microfluidic *in vitro* system revealed to be able to reproduce the structure of a 3D microvessel formed by a monolayer of elongated endothelial cells. Furthermore, we provided interesting data on the feasibility of drug testing.

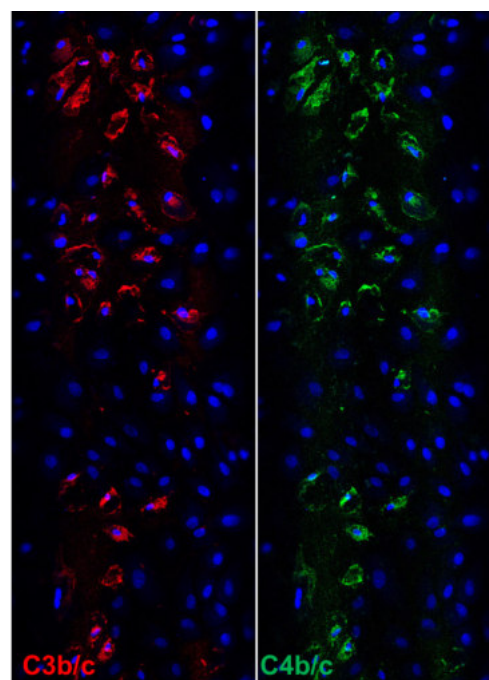


**Figure:** Complement activation fragments (C3b/c and C4b/c) deposited on porcine cells after perfusion with allogeneic porcine serum.



# SCIENTIFIC REPORTS

OPEN

## 3D artificial round section microvessels to investigate endothelial cells under physiological flow conditions

Received: 6 November 2017  
Accepted: 28 March 2018  
Published online: 12 April 2018

Riccardo Sfriso<sup>1,2</sup>, Shengye Zhang<sup>1,2,3</sup>, Colette Andrea Bichsel<sup>4</sup>, Oliver Steck<sup>1</sup>, Alain Despont<sup>1</sup>, Olivier Thierry Guenat<sup>5</sup> & Robert Rieben<sup>1</sup>

In the context of xenotransplantation, in ischemia/reperfusion injury as well as in cardiovascular research, the study of the fascinating interplay between endothelial cells (EC) and the plasma cascade systems often requires *in vitro* models. Blood vessels are hardly reproducible with standard flat-bed culture systems and flow-plate assays are limited in their low surface-to-volume ratio which impedes the study of the anticoagulant properties of the endothelial cells. According to the 3R regulations (reduce, replace and refine animal experimentation) we developed a closed circuit microfluidic *in vitro* system in which endothelial cells are cultured in 3D round section microchannels and subjected to physiological, pulsatile flow. In this study, a 3D monolayer of porcine aortic EC was perfused with human serum to mimic a xenotransplantation setting. Complement as well as EC activation was assessed in the presence or absence of complement inhibitors showing the versatility of the model for drug testing. Complement activation products as well as E-selectin expression were detected and visualized *in situ* by high resolution confocal microscopy. Furthermore, porcine pro-inflammatory cytokines as well as soluble complement components in the recirculating fluid phase were detected after human serum perfusion providing a better overview of the artificial vascular environment.

Endothelial cell (EC) activation plays an important role in the pathophysiology of ischemia/reperfusion injury, sepsis, vascular rejection of transplanted organs, and other diseases linked to the vascular system. In transplantation, the vascular endothelium of the donor organ is the first tissue to come in contact with the blood of the recipient. If pre-formed anti-donor antibodies are present in the recipient's blood, an immediate activation of the donor endothelium occurs due to antibody binding followed by activation of the complement system. This is for example the case in blood group ABO incompatible transplantations, recipients sensitized to donor HLA antigens, and in experimental pig to primate xenotransplantation. EC activation in turn triggers the coagulation cascade and leads to the clinical picture of hyperacute or acute vascular rejection<sup>1,2</sup>. Xenotransplantation experiments in animal models have been carried out extensively to investigate mechanisms of EC activation<sup>3,4</sup>, but also *ex vivo* perfusions of porcine organs with human blood, plasma or serum have been used for this purpose<sup>5,6</sup>. In order to reduce – in accordance with the 3R principles – the number of animals used for investigation of EC activation in hyperacute and acute vascular rejection, we developed an *in vitro* system to grow and investigate EC under physiological, pulsatile flow conditions, simulating shear stress as occurring in small to medium sized arteries. Furthermore, the system provides additional scientific advantages over *in vivo* models such as a reduced amount of drugs needed for the experiments, better controlled and lower variability, as well as the possibility to scale up as a high throughput system capable of parallel investigation of dozens or even more parameters like drugs or genetic modifications of EC.

<sup>1</sup>Department for BioMedical Research, University of Bern, Bern, Switzerland. <sup>2</sup>Graduate School for Cellular and Biomedical Sciences, University of Bern, Bern, Switzerland. <sup>3</sup>First Affiliated Hospital of Zhengzhou University, Zhengzhou, China. <sup>4</sup>Vascular Biology Program, Boston Children's Hospital and Harvard Medical School, Boston, MA, USA. <sup>5</sup>ARTORG Center for Biomedical Engineering Research, University of Bern, Bern, Switzerland. Riccardo Sfriso and Shengye Zhang contributed equally to this work. Correspondence and requests for materials should be addressed to R.R. (email: robert.rielen@dbmr.unibe.ch)

In standard 2D cell culture the amount of serum, plasma or whole blood in contact with EC grown on the bottom of the wells is small and may often be the limiting factor for activation or cytotoxicity of EC *in vitro*: in a typical experiment using 96-well microtiter plates, the ratio of fluid volume to EC surface is only  $0.2 \text{ ml/cm}^2$  ( $100 \mu\text{l}$  per well with a bottom surface of  $0.5 \text{ cm}^2$ ). This ratio is much lower than in a physiological situation in which blood circulates through vessels and where ratios from  $1.3 \text{ ml/cm}^2$  (in the aorta) up to  $5000 \text{ ml/cm}^2$  (in capillaries) are reached. Using *in vitro* systems based on 3D culture of EC on the inner surface of 'artificial blood vessels' and perfusion with a physiological flow the *in vivo* ratio of fluid volume to EC surface can be reached making it possible to exploit the natural anticoagulant properties of EC<sup>10</sup>.

Over the last decade, microfluidic technologies have been developed, and commercial systems have been made available in which cells can be cultured under flow using convenient slide- or microtiter plate-based setups<sup>11,12</sup>. These systems are normally used to grow EC two-dimensionally, on the bottom of a rectangular shaped micro channel. Such systems have for example been used to assess the effect of complement inhibition on thrombus formation in a xenotransplantation setting<sup>13–15</sup>. Also 3D growth of EC has been reported on the inner surface of rectangular channels<sup>16–18</sup>. However, the geometry of these rectangular microfluidic channels poorly replicates the shape of the microvasculature, in particular in terms of shear stress. In order to fabricate circular microchannels, different technologies have been reported such as a combination of mechanical micromilling and soft lithography, or introducing a pressurized air stream into liquid uncured PDMS filled microchannels<sup>19–21</sup>. Most often, however, these "circular cross-sections" were rather irregular, making it difficult to standardize the respective assays and reproduce experimental findings.

Based on the use of needles as molds published by Chrobak *et al.*<sup>22</sup>, we therefore produced microfluidic chips with evenly circular microchannels. We inserted the needles directly in polydimethylsiloxane (PDMS) in a petri dish and extract them after casting the gel. This results in an even, round inner diameter of the microchannels, which remains constant at  $37^\circ\text{C}$ . The inner surface of the microchannels is then chemically modified and functionalized to adsorb extracellular matrix proteins and allow cell attachment.

Existing microfluidic models often use syringe pumps kept outside the incubator with consequent temperature changing of the perfusate which might influence the behavior of the sensitive EC. The model presented here involves the use of a peristaltic pump and reservoir tubes which can be kept inside the incubator at  $37^\circ\text{C}$  avoiding temperature changes of the medium while perfusing the cells. Recirculation is an interesting feature of the system as it allows for cell-cell communication through soluble messenger molecules such as cytokines, chemokines as well as amplification of plasma cascade systems.

In the present study porcine EC grown under physiological shear stress were perfused with normal human serum (NHS) as a source of xenoreactive natural antibodies and complement under physiological flow conditions in the context of xenotransplantation.

## Results

**Endothelial cell characterization.** To confirm that EC isolated from porcine aortas still expressed typical endothelial markers when cultured in microfluidic channels, staining for CD31 and VE-cadherin was performed by immunofluorescence (IF). All of these markers were expressed on PAEC after culturing in the 3D microfluidic system under both static and flow conditions, demonstrating successful PAEC culture in the microfluidic channels (Fig. 1). However, expression of the respective markers was different depending on flow conditions. In cells cultured under static conditions, CD31 and VE-cadherin were expressed in arbitrary patterns, whereas CD31 and VE-cadherin were aligned with the direction of the pulsatile flow when the cells were cultured for 2 days at  $10 \text{ dyn/cm}^2$ . This indicates that the expression of these endothelial cell markers is affected by shear stress dependent mechanotransduction<sup>23</sup>.

**Cell morphology, alignment, and distribution along the direction of pulsatile flow.** Cells started to attach to the inner surface of the microchannels 1 h after seeding. They then became elongated and a confluent EC monolayer was formed on day 1. When a pulsatile flow was applied, cells started to align with the flow over time. After 2 days of pulsatile flow, cells were completely aligned as shown by bright field microscopy pictures and F-actin staining at days 2 and 4 (Fig. 2a). Cell alignment in the direction of flow was assessed by staining of the cytoskeleton protein F-actin as well as CD31. For F-actin, after 2 days of pulsatile flow, the average angle of the cells with respect to the flow direction of the microchannels was  $9.6 \pm 8.1^\circ$ , which was significantly smaller than under static conditions ( $70.7 \pm 32.1^\circ$ ,  $p = 0.007$ ). For CD31, the respective values were  $21.8 \pm 26.3^\circ$  and  $74.2 \pm 13.7^\circ$ , respectively;  $p = 0.047$  (Fig. 2b,c).

This cell alignment was described earlier in microfluidic studies and is supposed to be due to mechanically affected distribution of cytoskeleton proteins as soon as exposure to shear stress occurs, which is induced by pulsatile perfusion with cell culture medium<sup>24,25</sup>.

In our microfluidic system, the formation of an EC monolayer on the whole inner surface of the microchannels was assessed by IF and confocal microscopy. VE-cadherin staining showed elongated EC covering the entire microchannel and forming a typical monolayer on both  $550 \mu\text{m}$  and  $100 \mu\text{m}$  channel diameters (double staining with F-actin in  $100 \mu\text{m}$  channels, Fig. 3a and supplementary movie 1). This observed staining pattern mimics the *in vivo* impression of a small artery as shown in 3D rendering views in Fig. 3a and b. In contrast to the *in vivo* situation, biological phenomena on a molecular or cellular level could be directly observed in our microfluidic assay by real time *in vivo* cell imaging even though the data presented here were obtained at the end of the experiments only. High resolution confocal laser scanning microscopy as well as spinning disk microscopy for high speed acquisition of pictures can be used and provide detailed insights into biological mechanisms.

**Complement activation in a xenotransplantation setting.** After establishment of our *in vitro* model, we aimed to reproduce complement activation as occurring in hyperacute or acute vascular rejection in

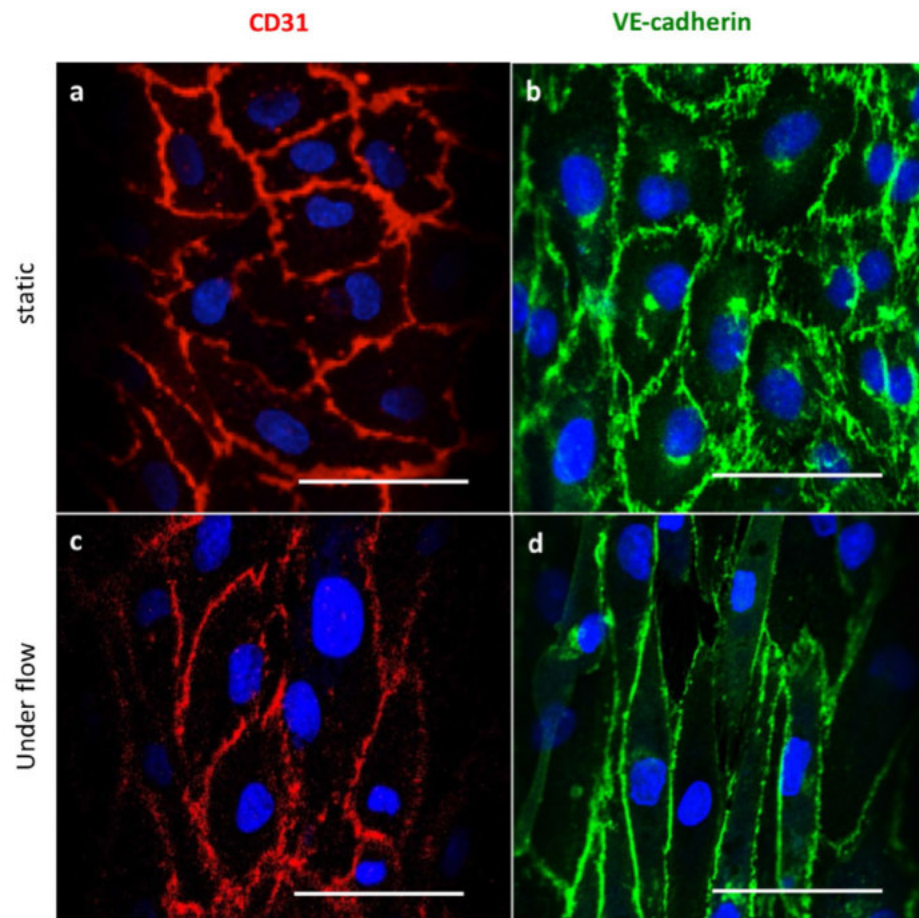


**Figure 1.** EC characterization and overview of cell distribution in microfluidic channels both under static and flow conditions. EC characterization by expression of CD31 and VE-cadherin. (a–b) Representative images for CD31 and VE-cadherin expression under static conditions; (c–d) representative images for CD31 and VE-cadherin expression under flow conditions. Scale bars represent 50  $\mu\text{m}$ .

a xenotransplantation setting<sup>1</sup>. We therefore perfused PAEC-microchannels with 1:10 diluted normal human serum. Dilution of the human serum is necessary to evaluate EC activation and complement deposition while minimizing cell loss as the immune reaction triggered by undiluted serum will result in rapid cell death and cell release from the channel surface. A monolayer of PAEC is essential to mimic an intact endothelium, therefore the intactness and the confluency of PAEC-coated microchannels were assessed before performing any experiment. However, since bovine collagen was used to coat the microchannels to allow a better cell adhesion and proliferation, binding of human antibodies was assessed by perfusing fibronectin/collagen coated microchannels with 1:10 NHIS to verify the absence of xeno-reactions (Supplementary Fig. 1). The assessment of EC activation and complement deposition was performed by IF staining for E-selectin and C3b/c, respectively, after different serum incubation times: 10 min, 30 min, 60 min and 120 min. The results confirmed a time-dependently increased EC activation as shown by strong E-selectin expression and increased complement deposition as shown by C3b/c staining (Fig. 4a). Furthermore, another experiment was done by perfusing PAEC for 120 min with different volumes of 1:10 diluted NHS: 200  $\mu\text{l}$ , 3 ml, 5 ml, 10 ml corresponding to 20  $\mu\text{l}$ , 300  $\mu\text{l}$ , 500  $\mu\text{l}$  and 1 ml of undiluted NHS (Fig. 4b). The perfusion rate was kept constant at 600  $\mu\text{l}/\text{min}$  except for the channels kept under static conditions which were filled with 200  $\mu\text{l}$  of 1:10 diluted NHS. Significantly increased E-selectin expression and C3b/c deposition were observed when 5 ml and 10 ml of diluted NHS were used, corresponding to 500  $\mu\text{l}$  and 1 ml of undiluted NHS, respectively. As control experiments both PAEC and human aortic endothelial cells (HAEC) were perfused with normal porcine serum (NPS) and NHS respectively (Supplementary Fig. 2). The data obtained support the idea that this microfluidic system, specifically optimized for the assessment and quantification of complement deposition thanks to the possibility to use relatively large volumes for perfusion of the artificial microvessels, is able to mimic the *in vivo* situation in which EC are continuously perfused with blood containing



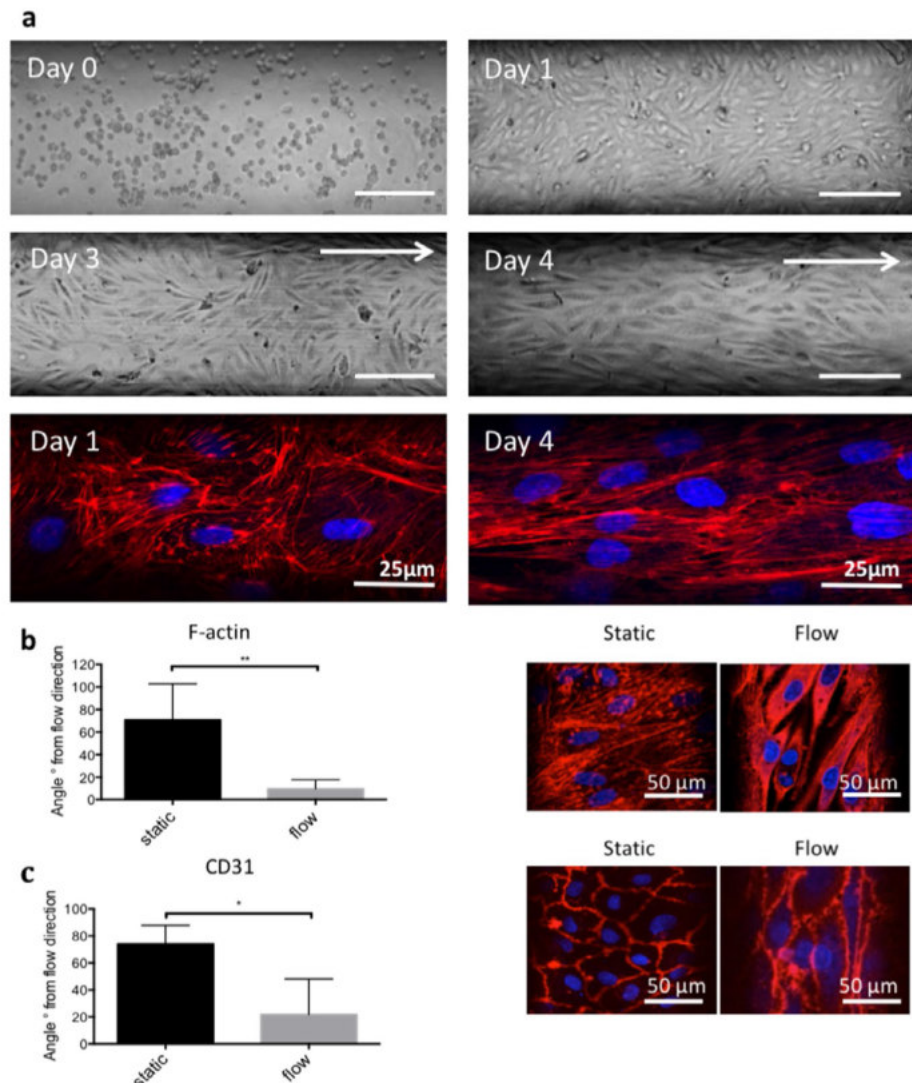


**Figure 2.** Cell morphology and quantification of cell alignment. **(a)** Cell morphology over time. **(a)** day 0, cells are randomly distributed immediately after seeding; **(b)** day 1, cells attach and elongate under static conditions; **(c)** day 3, cells start to become aligned under flow for one day; **(d)** day 4, most of the cells are aligned under flow for two days. Arrows indicate the direction of pulsatile flow in the microfluidic channels. **(e)** F-actin staining of PAEC in static conditions and **(f)** under flow. If not specified scale bar represents 100  $\mu\text{m}$ . **(b,c)** Quantification of cell alignment to the x-axis of the microfluidic channels by immunofluorescence staining for the cytoskeleton protein F-actin and CD31, respectively. On the left panel, column graphs of the average cell angle in degrees to the x-axis are shown under static and pulsatile flow conditions (mean values  $\pm$  SD, p-value: \*  $< 0.05$ , \*\*  $< 0.01$ ). Representative immunofluorescence images are shown on the right panel (a-b). Arrows show the flow direction. Scale bar represents 50  $\mu\text{m}$ .

active proteins of the complement and coagulation cascade. Indeed, compared with standard chamber slides where the amount of serum is low (data not shown), our 3D microfluidic assay gave a better quantification of human immunoglobulin binding and complement deposition on porcine endothelial cells allowing to screen the protective role of transgenes.

An interesting application of our microfluidic system could be the screening of complement inhibitors or other drugs in general. Three known complement inhibitors were therefore tested in our model: C1 INH (10 IU/ml), APT070 (0.25 mg/ml), and DXS (0.3 mg/ml). C1 INH is a physiological, fluid phase inhibitor of complement and coagulation, acting mainly on the C1 complex, which initiates the classical pathway of complement activation<sup>23</sup>.

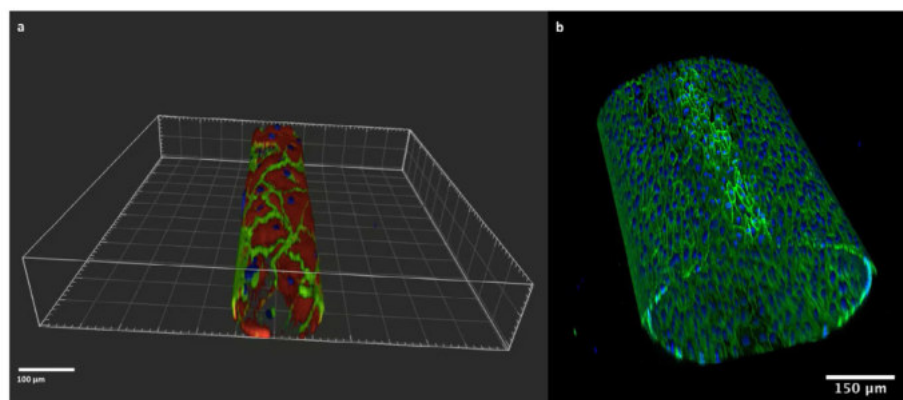


**Figure 3.** Confocal images of EC coated microchannels. **(a)** 3D rendering of the 100 µm round section channel. EC monolayer was stained for VE-cadherin (green) and F-Actin (red). Nuclei were stained with DAPI (blue). **(b)** 3D z-stack of the 550 µm round section channel. EC monolayer was stained for VE-cadherin (green). Nuclei were stained with DAPI (blue).

APT070 is a recombinant derivative of the soluble complement receptor 1, regulating complement activation at the level of C4/C3<sup>24</sup>. DXS, finally, is a highly sulfated polyglucose and a member of the glycosaminoglycan family. It acts as an EC protectant and a complement inhibitor<sup>25,26</sup>. Activation of the complement cascade was confirmed by positive staining for C3b/c, C4b/c, and C6. As expected, all inhibitors blocked complement activation on the C4/C3 level and further downstream. Deposition of C3b/c, C4b/c, and C6 was significantly reduced by all of the used complement inhibitors compared to perfusion by NHS alone. The respective data are shown in Fig. 5, both quantitated as column graphs and as representative immunofluorescence images. Our results confirm earlier data on successful complement inhibition using C1 INH, APT070 and DXS<sup>25,27,28</sup>. Furthermore, the model could reproduce data obtained *ex vivo* in a pig lung xenotransplantation model by using the same amount of C1 INH (10 IU/ml) which was shown to effectively prolong the survival time of the xenoperfused organ by diminishing complement activation after perfusion with human blood<sup>29</sup>.

**Proinflammatory cytokines, growth factors and soluble complement activation markers in perfusate samples.** Perfusate samples were collected and analyzed for the presence of porcine specific inflammatory cytokines, growth factors and soluble complement components. The assay specifically detects cytokines produced by porcine endothelial cells after being stimulated with NHS, with the exception of bFGF and sC5b-9 for which also the human proteins are detected. Analysis of NHS pre-perfusion as well as normal pig serum (NPS) were performed in order to show the specificity of the assay (Supplementary Fig. 3). Among all the pro-inflammatory cytokines which were elevated by perfusion of the microchannels with NHS, IL-1 $\beta$  was reduced by treatment with DXS ( $p = 0.0095$ , Fig. 6) while C1 INH and APT070 did not show an effect. High levels of the soluble terminal complement complex sC5b-9 and C5a were found when cells were perfused with NHS alone (sC5b-9:  $30547 \pm 2932$  ng/ml, C5a:  $3298 \pm 184.6$  pg/ml), while addition of complement inhibitors significantly reduced both sC5b-9 and C5a generation [sC5b-9 (C1 INH:  $19019 \pm 10501$  ng/ml,  $p = 0.004$ ; APT070:  $725 \pm 585$  ng/ml,  $p < 0.0001$ ; DXS:  $18605 \pm 4181$  ng/ml, C5a (C1 INH:  $2123 \pm 538$  pg/ml,  $p = 0.002$ ; APT070:  $1543 \pm 805.3$  pg/ml,  $p < 0.0001$ ; DXS:  $808.4 \pm 325.4$  pg/ml,  $p < 0.0001$ ; Fig. 7). Elevated levels of IL-1 $\beta$  and sC5b-9 as found in our *in vitro* system were also found in earlier *ex vivo* perfusion experiments performed with pig forelimbs<sup>30</sup>. We also found elevated levels of the growth factor bFGF in the perfusate when APT070 was used as compared to NHS alone ( $p < 0.05$ , Fig. 6). The significance of this finding is still unclear, also because APT070 has only rarely been used in xenotransplantation settings so far.

### Discussion

We have established an *in vitro* system for 3-dimensional growth of EC in microfluidic channels with circular cross sections under physiological flow conditions, mimicking small to medium sized arteries *in vivo*<sup>31</sup>. This microfluidic system was used to investigate endothelial cell activation in the context of a xenotransplantation setting.

Endothelial cells seeded into the microfluidic channels and grown under static conditions for the first two days aligned in the direction of flow as soon as exposure to shear stress was induced by pulsatile perfusion with cell culture medium. A frequent medium exchange after seeding the cells into the microchannels is required due to the high cell surface-to-volume ratio. After flow application, the EC monolayer covering the inner surface of the channels is continuously perfused with recirculating medium, reducing the need for medium exchange. In contrast to microchannels with a rectangular cross-section, the shear stress along the endothelial walls is homogeneous in our system and enables a better quantification of the effects of the flow on EC behaviour. Thanks to the transparency of the PDMS the system allows visualization as well as analysis of the microchannels by high resolution confocal microscopy. This is an advantage over *in vivo* systems and allows insights into molecular and cellular biological mechanisms which are not possible in animal models. Thanks to advanced settings of the



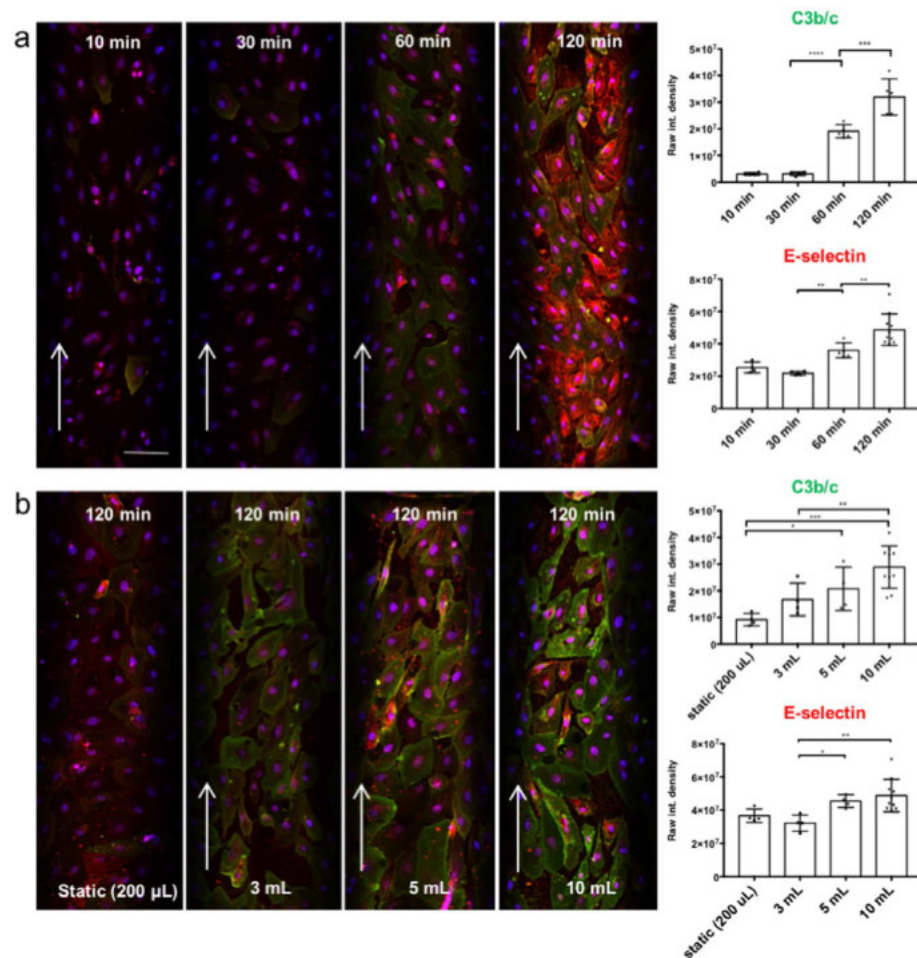


**Figure 4.** Impact of incubation time on EC activation and complement deposition. Confocal pictures of EC coated microchannels. **(a)** Perfusion with 10 ml of 1:10 diluted NHS, recirculating at 600  $\mu$ l/min for 10, 30, 60, 120 min. **(b)** Incubation for 120 min with different volumes of 1:10 diluted NHS: 200  $\mu$ l (static conditions), 3 ml, 5 ml, and 10 ml (all recirculating at 600  $\mu$ l/min). Quantification of C3b/c deposition (green) and E-selectin expression (red) was done by immunofluorescence. Nuclei were stained with DAPI (blue). Arrows show the flow direction. Shown are mean values  $\pm$  SD with indication of statistically significant differences between the time points,  $n = 5$ ,  $p$ -value: \* $p = 0.01$ , \*\* $p < 0.01$ , \*\*\* $p = 0.0001$ , \*\*\*\* $p < 0.0001$ ). Sera from different donors with different blood groups were used as pool of at least 3 donors. Scale bar represents 100  $\mu$ m.

confocal microscope we could show complete coverage of the inner surface of the round microchannels, both of 550  $\mu$ m and 100  $\mu$ m of diameter, by a confluent monolayer of EC, creating the impression of artificial small to medium sized arteries in a three-dimensional view. Furthermore, the closed system and recirculation of cell culture medium, with or without human serum or drugs, allows for the assessment of both acute and chronic effects on EC. Effector molecules in the fluid phase, which are an important way of communication between both adjacent and distant cells in the vasculature as well as in the blood stream, can develop their effects in the recirculatory microfluidic system and they can also be analyzed by ELISA or multi-plex assays.

After establishment of our *in vitro* model, we wanted to further validate the system by reproducing findings on complement activation as occurring *in vivo* in hyperacute or acute vascular rejection in xenotransplantation settings. A time- and volume-dependent increase of EC activation (E-selectin) and complement deposition (C3b/c) was observed. Indeed, the possibility to continuously perfuse the artificial blood vessels with high volumes of fresh serum as occurring *in vivo* is one of the main advantages of our system as compared for example to conventional 96-well plate assays. The results obtained from the testing of complement inhibitors – C1 INH, AP1070 and DXS – regarding deposition of complement components and the prevention of EC activation revealed another important aspect of the new *in vitro* system, which is the possibility to assess the effects of different drugs in a purified system composed of an artificial endothelium exposed to pulsatile flow.



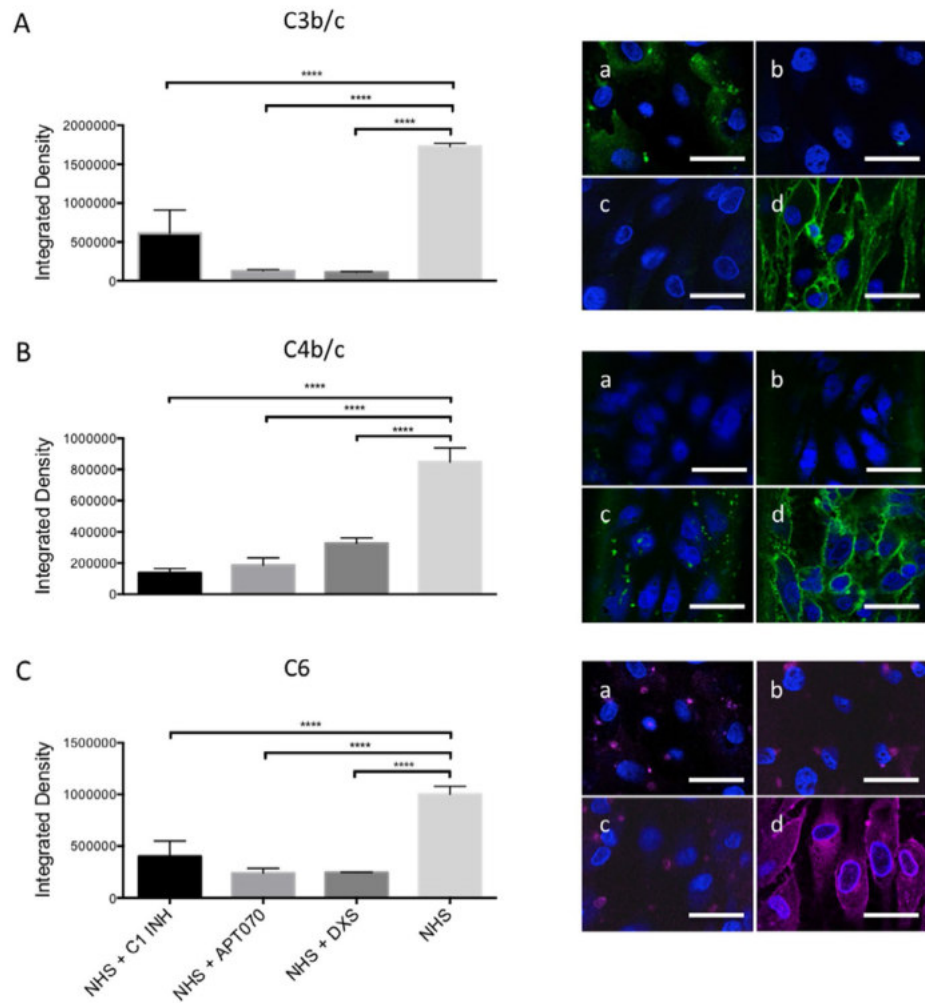


**Figure 5.** Deposition of C3b/c, C4b/c, and C6 on PAEC assessed by immunofluorescence after perfusion with NHS with or without complement inhibitors. Column graphs on the left panels show quantification of immunofluorescence staining for deposition of C3b/c (A), C4b/c (B) and C6 (C). Shown are mean values  $\pm$  SD with indication of statistically significant differences between complement inhibitor groups and NHS alone. \*\*\*\* $p < 0.0001$ ,  $n = 5$ . Representative images are shown on the right panels. PAEC in microfluidic channels were perfused for 60 min with 1:10 NHS + C1 INH (a), 1:10 NHS + APT070 (b), 1:10 NHS + DXS (c), and 1:10 NHS alone (d). Sera from different donors with different blood groups were used as pool of 8 donors. Scale bar represents 50  $\mu$ m.

The reproducibility of the results is high as long as a confluent monolayer of cells is achieved and the cells are kept healthy before any kind of perfusion either with drugs or with serum.

A limitation of the current model is the use of serum to study activation of the EC growing on the inner surface of the microfluidic channels. *In vivo*, EC activation in transplantation, ischemia/reperfusion injury and other clinical settings occurs in the whole blood environment. Our study only includes the effect of complement and omits possible effects of the other plasma cascade systems, namely coagulation, fibrinolysis and kallikrein/kinin, as well as blood cells. Coating of the silicon tubings and connectors with heparin might allow the use of whole, non-anticoagulated blood for perfusion of the EC-microchannels and further improve the model. In the microchannels the ratio of EC-surface to blood volume is 73  $\text{cm}^2/\text{ml}$  for 550  $\mu\text{m}$  diameter and 400  $\text{cm}^2/\text{ml}$  for 100  $\mu\text{m}$  diameter, respectively. This would allow the exploitation of the natural, anticoagulant properties of EC when working with non-anticoagulated whole blood<sup>10</sup>. Modification of the model for use with whole, non-anticoagulated blood is currently under way.

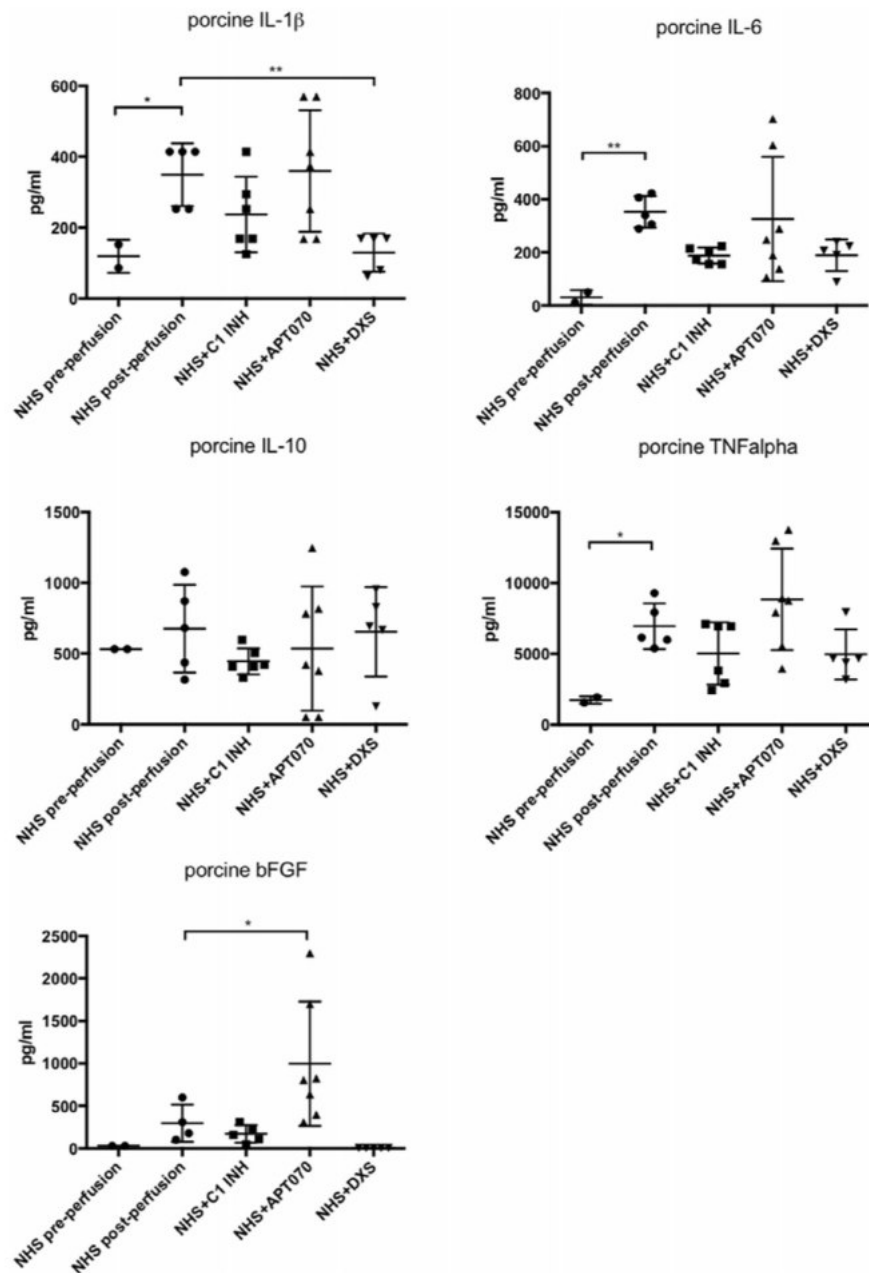


**Figure 6.** Concentrations of inflammatory cytokines/growth factors after perfusion with NHS with or without complement inhibitors. Porcine-specific cytokines [interleukin (IL)-6, IL-1 $\beta$ , IL-10, tumor necrosis factor alpha (TNF- $\alpha$ )] and basic fibroblast growth factor (bFGF) levels were measured by Bio-Plex analysis. Data are presented as scattered dot plot with mean values, error bars indicate standard deviations, NHS post-perfusion n = 5, NHS + C1INH n = 6, NHS + APT070 n = 7, NHS + DXS n = 5, p-values: \*p < 0.05, \*\*p < 0.01, \*\*\*p < 0.0001. Sera from different donors with different blood groups were used as pool of 8 donors.

## Methods

**Isolation and culture of porcine aortic endothelial cells.** Porcine aortic endothelial cells (PAEC) were isolated from aortas by using a mechanical procedure. In brief, aortas were cut open and PAEC were isolated by gently rubbing the inner surface with a cotton wool bud. The cells were transferred into fibronectin-coated tissue

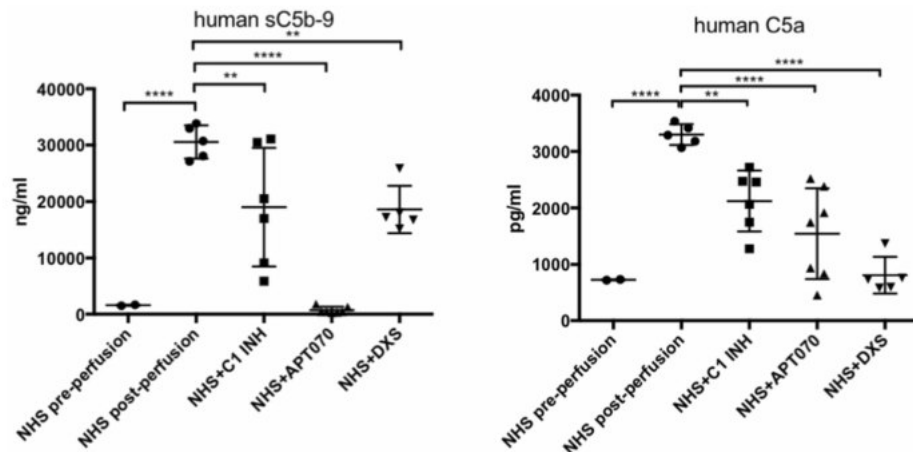


**Figure 7.** Concentrations of soluble complement markers after perfusion with NHS with or without complement inhibitors. Human soluble complement activation markers in the perfusate were detected by ELISA (human C5a) and Bio-Plex [human soluble (s)C5b-9]. Data are presented as scattered dot plot with mean values, error bars indicate standard deviations, NHS post-perfusion  $n = 5$ , NHS + C1INH  $n = 6$ , NHS + APT070  $n = 7$ , NHS + DXS  $n = 5$ ,  $p$ -values: \*\* $p < 0.01$ , \*\*\*\* $p < 0.0001$ . Sera from different donors with different blood groups were used as pool of 8 donors.

culture flasks (Nalge Nunc International, Kamstrup, DK) and placed at 37 °C in a 5% CO<sub>2</sub> incubator until confluence. DMEM cell culture medium (Thermo Fisher Scientific, Waltham, MA, USA) was used, supplemented with 10% heat-inactivated fetal bovine medium (FBS, Biochrom, Berlin, Germany), 100 IU/ml penicillin and 100 µg/ml streptomycin (Thermo Fisher Scientific), and 0.4% Endothelial Cell Growth Medium (ECGM) Supplement Mix (PromoCell, Heidelberg, Germany). Cells between passage 3 and 6 were used in the present study.

No animals were used specifically for the present study. Porcine aortas used for PAEC isolation were from animal experiments with pigs in the context of evaluation of surgical techniques and devices, as well as studies on xenotransplantation. All animal experiments were approved by the Veterinary Service of the Canton of Bern, Switzerland, and performed in accordance with national and international 3 R and ARRIVE guidelines<sup>32</sup>.

**Construction of microfluidic channels with round cross section.** Polydimethylsiloxane (PDMS, Sylgard 184, Dow Corning, Wiesbaden, Germany) was prepared by mixing 10 parts of elastomer silicone and 1 part of curing agent, and casted in a petri dish (Thermo Fisher Scientific). Sterile and pyrogen free needles with a diameter of 120 µm and a length of 3 cm (Seirin, Hamburg, MA, USA) were laid in parallel in the liquid uncured PDMS, at the bottom of the petri dish. Four mold needles of 550 µm or 100 µm diameter and 2.5 cm length (BD Biosciences, New Jersey, USA) were placed at a 90° angle on top of the thinner needles. The Luer connectors of the needles were cut off with a diagonal cutter before using the needles as molds. The PDMS with the needle-molds was cured at 60 °C overnight. PDMS chips were cut out, while needles were extracted horizontally. Inlet and outlet connectors to the microchannels were made with 2 mm biopsy punches (Shoney Scientific, Waukesha, USA). The hole, left from extraction of needles, between the edge of the PDMS gel and the inlet and outlet, respectively, was sealed with liquid PDMS and cured at 60 °C overnight. The final microfluidic chips contained four microchannels, mimicking small to medium sized arteries, with a diameter of 550 µm or 100 µm, respectively, and a length of 1 cm. The schematic for microchannel fabrication is shown in Fig. 8.

**Modification of PDMS surface in microchannels.** Before seeding cells in the microfluidic channels, the inner surface of PDMS was modified to covalently bond extracellular matrix molecules<sup>53</sup>. Briefly, PDMS chips and standard glass slides were cleaned, activated in an oxygen plasma cleaner (Harrick Plasma, New York, USA) at 650 mTorr for 3 min, and bonded together. Immediately after bonding, the hydrophobic PDMS surface in the microchannels was silanized to make it hydrophilic by filling the channels with 5% 3-triethoxysilylpropylamine (APTES, Sigma-Aldrich, Buchs, Switzerland) and incubation for 20 min at room temperature. The channels were then washed with ultrapure water and treated with 0.1% glutaraldehyde (Sigma-Aldrich) for 30 min to provide a crosslinking substrate for the immobilization of extracellular matrix proteins. Microchannels were incubated with 50 µg/ml human fibronectin (Millipore, Schaffhausen, Switzerland) in PBS for 1 h at 37 °C or at room temperature overnight under UV light, followed by 100 µg/ml bovine collagen I in 0.2 mol/l acetic acid (Gibco, Thermo Fisher Scientific) at room temperature for 1.5 h. Cell culture medium containing 10% FBS was then rinsed through the microfluidic channels to block unspecific protein binding sites as well as to wash out unbound collagen I before cell loading.

**Cell loading and pulsatile flow.** PAEC grown to confluence in T75 flasks were trypsinized with 0.05% EDTA-trypsin (Gibco, Thermo Fisher Scientific) and suspended in ECGM- and FBS-supplemented cell culture



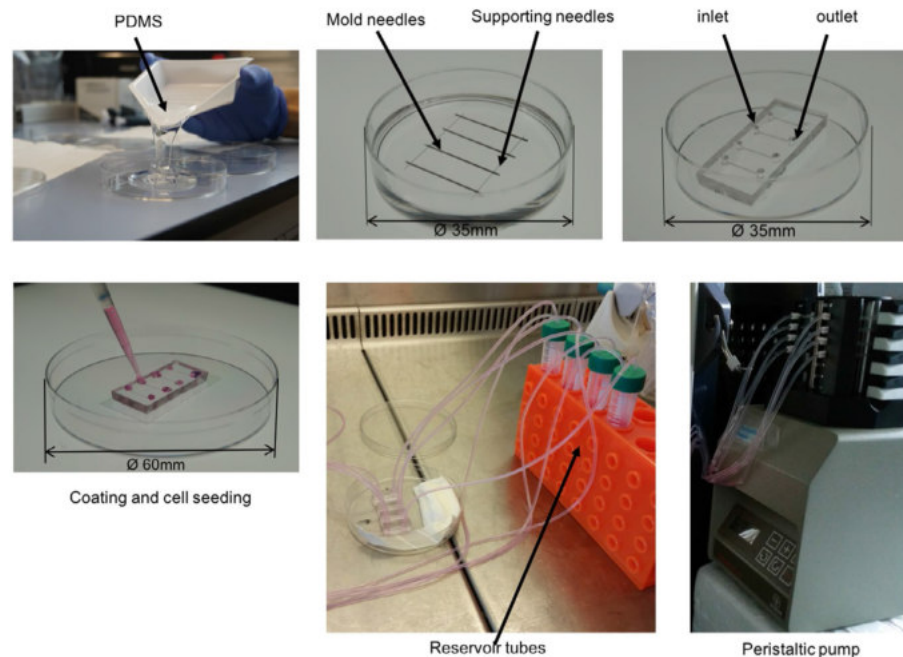


**Figure 8.** Schematic of microchannel fabrication and pump connecting. PDMS is poured into a Petri dish (Ø 60 mm). Supporting and mold needles are placed as shown in the picture and the whole Petri dish is incubated overnight at 60 °C. Needles are removed, inlet and outlet holes are made with a 2 mm biopsy puncher. Lateral holes are sealed with more PDMS. The second and the third steps show the device inside a Ø 35 mm Petri dish for a demonstration purpose. Normally everything is done using a Ø 60 mm Petri dish which can host up to 4 microchips. After plasma oxygen treatment, the microchip is bonded to a glass slide, coated with fibronectin and collagen I, and ultimately cells are seeded within the microchannels. One day after seeding a peristaltic pump is connected and a shear stress of 10 dyn/cm<sup>2</sup> is applied.

medium (DMEM) with 4% dextran from *Leuconostoc* spp. (Mw ~ 70,000, Sigma-Aldrich), to increase viscosity and promote cell adhesion. Cells at a density of  $1 \times 10^6$ /ml were loaded into the microfluidic channels. The whole device was flipped upside down and placed in an incubator at 37 °C/5% CO<sub>2</sub> for 10–15 minutes to promote cell adhesion on the upper part of the microchannel. Subsequently cell attachment was checked under the microscope and if necessary more cells were added and the unflipped device placed back in the incubator. Cells were then cultured under static conditions with 2–3 cell culture medium changes at intervals of 2 h, followed by overnight incubation. Growth of the cells was checked daily under an inverted microscope. After confluency was reached, a peristaltic pump – Minipuls 3 with 8 channels (Gilson, Villiers le bel, France) – was connected to the microfluidic channels via sterile silicon tubing with stoppers (Gilson) and extension silicon tubings (Gobatec, Bern, Switzerland). These tubes were autoclaved and extensively flushed with distilled water and PBS, followed by cell culture medium with 4% dextran. A medium reservoir in a 15 ml sterile tube (Corning, Berlin, Germany) was connected to each microchannel and placed in the 37 °C incubator together with the microfluidic device. PAEC in the microfluidic channels were maintained in DMEM under pulsatile flow, starting overnight with a low shear stress of 0.04 dyn/cm<sup>2</sup>, corresponding to 0.5 pump head rotations per minute, equaling 5 beats per minute (bpm) because of the presence of 10 rollers on the pump head. Thereafter the shear stress and pulse rate was gradually increased by 10 bpm per hour, until the desired shear stress of 10 dyn/cm<sup>2</sup> at 70 bpm was reached. This shear stress of 10 dyn/cm<sup>2</sup>, corresponding to a flow of 600 µl per minute for 550 µm channels, was maintained for two days in the present study. Calculations of the shear stress were performed based on the equation (1):

$$SS = 4\mu Q / \pi R^3$$

where  $\mu$  is the viscosity of the medium,  $Q$  is the flow rate and  $R$  represents the radius of the microchannel. The system can be maintained for at least 7 days with exchange of the medium every 2–3 days. Cell morphology was assessed under a bright field microscope (DMI 4000B, Leica Microsystems Schweiz, IHeerbrugg, Switzerland).

**Human serum preparation.** Human blood was drawn from healthy volunteers into polypropylene tubes containing glass beads (S-Monovette, Sarstedt, Germany) and allowed to clot for 30 min at room temperature. The clot was removed by centrifugation for 10 min at  $2000 \times g$  in a refrigerated centrifuge (4 °C) and the supernatant collected and stored at –80 °C. In the present study sera from different donors with different blood groups were

used, mostly as pool of at least 3 donors. Details are given in the respective figure legends. All experimental protocols were reviewed and approved by the University of Bern and carried out in accordance with the University of Bern regulations. All human blood samples were obtained with informed consent according to Swiss jurisdiction and ethics guidelines of the Bern University Hospital.

**Perfusion of PAEC with normal human serum and complement inhibitors.** After two days of pulsatile flow, cell culture medium was replaced with normal human serum (NHS) 1:10 diluted in 1% dextran DMEM without supplements. PAEC were perfused for different periods of time (10 min, 30 min, 60 min, 120 min). The perfusate (1:10 diluted NHS in 4% dextran DMEM with or without complement inhibitors) was present in 15 ml reservoir tubes (Nalge NUNC) and perfusion was performed in a closed circuit so that the perfusate was recirculated. Usually 10 ml of perfusate were used, but for some experiments the amount was varied from 3 to 10 ml, with a control of static incubation with 200  $\mu$ l. Four groups were made: Group 1: NHS alone, Group 2: NHS + 10 IU/ml C1 inhibitor (C1 INH, Bermer, provided by CSL Behring, Marburg, Germany), Group 3: NHS + 0.25 mg/ml APT070 (a recombinant, membrane-targeted complement inhibitor based on complement receptor 1, provided by Richard Smith, King's College, London, UK), Group 4: NHS + 0.3 mg/ml low molecular weight dextran sulfate (DXS, Mw ~5000, provided by Tikomed, Viken, Sweden). For each group, experiments with 3–5 channels were performed. Finally, perfusate was collected and stored at  $-80^{\circ}\text{C}$ . EC in the microchannels were used for immunofluorescence staining.

**Immunofluorescence staining.** Immunofluorescence staining was performed to assess the establishment of a confluent EC monolayer on the inner surface of the microchannels, to characterize endothelial cells and to assess disposition of complement components as well as EC activation. In brief, cells in the microfluidic channels were washed with PBS, fixed with 4% formaldehyde for 15 min, and blocked with PBS-3% BSA for 45 min. Incubation with primary antibodies was done at  $4^{\circ}\text{C}$  overnight, followed by secondary antibodies and 4',6-diamidino-2-phenylindole (DAPI). The primary antibodies used were: rat anti-porcine CD31 (mAB33871, R&D, Minneapolis, USA), goat anti-human VE-cadherin (sc-6458, Santa Cruz, Texas, USA), rabbit anti-human von Willebrand factor (vWF, A0082, Dako, Glostrup, Denmark), rabbit anti human C3b/c FITC (F0201, Dako), rabbit anti human C4b/c FITC (F0169, Dako), Goat anti human C6 (A307, Quidel, San Diego, USA), mouse anti human E selectin (S 9555, Sigma Aldrich). The secondary antibodies were goat anti rat IgG Cy3 (112 166 003, Jackson ImmunoResearch, West Grove, PA, USA), donkey anti goat alexa488 (A21082, Thermo Fisher Scientific), sheep anti rabbit IgG Cy3 (C2306, Sigma Aldrich), donkey anti goat IgG alexa488 (A11055, Thermo Fisher Scientific), goat anti-mouse IgM FITC (115-097-020, Jackson ImmunoResearch), goat anti-mouse IgG alexa488 (A21121, Thermo Fisher Scientific). Nuclei were stained with DAPI (Boehringer, Roche Diagnostics, Indianapolis, IN, USA). In addition, cytoskeleton filamentous actin (F-actin) was stained with Rhodamine Phalloidin (PHDRI, Cytoskeleton, Inc., Denver, USA). Images were taken at 10x and 63x with a confocal laser scanning microscope (LSM 710, Zeiss, Feldbach, Switzerland) and analyzed by ImageJ (National Institutes of Health, Bethesda, MD, USA). The thickness of the entire microfluidic device is 0.5 cm and the distance between the bottom of the device and the bottom of the microchannel is 120  $\mu\text{m}$  which allows a good imaging. In addition, z stack images were processed by Imaris 8.2 software (Bitplane, Zurich, Switzerland).

**Quantification of cellular alignment.** To quantify cellular alignment with the direction of flow, cell orientation was analyzed and quantified using the Fibril Tool plugin function in Fiji (<http://ij.usc.edu/Fiji>) following the published protocol<sup>34</sup> both under static and flow conditions. Fluorescent signals from CD31 and F actin staining were used. Three images per channel were analyzed to obtain the mean fluorescence intensity.

**Detection of porcine cytokines and complement activation markers by Bio-Plex/ELISA.** To determine the concentrations of porcine-specific cytokines [interleukin (IL)-6, IL-1 $\beta$ , IL-10, tumor necrosis factor alpha (TNF- $\alpha$ )], basic fibroblast growth factor (bFGF), as well as the complement activation marker soluble (s)C5b-9 in perfusate samples, a multiplex xMAP technology (Luminex) assay was performed according to a custom made protocol developed by our group<sup>37</sup>. In brief, microbeads (Luminex) were coupled with respective capture antibodies using the Bio-Plex amine coupling kit (Bio-Rad). Coupled beads were then incubated with samples, followed by biotinylated detection antibodies and Streptavidin R-PE (922721, Qiagen, Hilden, Germany). Measurement and data analysis were performed with a Flexmap 3D reader and the Bio-Plex Manager software version 6.1 (Bio-Rad). Concentrations of human C5a were detected by ELISA using a commercially available kit (DuoSet, R&D Systems, Minneapolis, USA).

**Statistical analysis.** All data are presented as mean  $\pm$  standard deviation (SD). Statistical analyses were performed by GraphPad Prism 6 software (GraphPad, San Diego, CA, USA) using one-way analysis of variance (ANOVA) followed by Fisher's LSD post hoc test to compare means of all groups. For comparison of cell orientation, Mann-Whitney U test was used. P values  $< 0.05$  were considered statistically significant.

**Data availability.** The complete data sets of this article are available upon request.

## References

- Gallili, T. Interaction of the natural anti-Gal antibody with alpha-galactosyl epitopes: a major obstacle for xenotransplantation in humans. *Transplantation* **14**, 480–482 (1993).
- Gullackner, E. et al. Acute vascular rejection of xenografts: roles of natural and elicited xenoreactive antibodies in activation of vascular endothelial cells and induction of procoagulant activity. *Transplantation* **77**, 1735–1741 (2004).
- Orlitz, R., Ye, Y., Koen, K. & Cooper, D. K. Carbohydrate antigens of pig tissues reacting with human natural antibodies as potential targets for hyperacute vascular rejection in pig-to-man organ xenotransplantation. *Transplantation* **56**, 1455–1463 (1993).

- Tauntoner, T. et al. Multimeric tyrosine sulfate acts as an endothelial cell protectant and prevents complement activation in xenotransplantation models. *Xenotransplantation* **11**, 262–268 (2004).
- Dornéscu, N. et al. Porcine endothelial cell activation in hMx1 pig hearts transplanted in baboons with prolonged survival and lack of rejection. *Transplantation Proceedings* **35**, 2045–2046 (2003).
- Xu, H. et al. The *in vitro* and *in vivo* effects of anti galactose antibodies on endothelial cell activation and xenograft rejection. *J Immunol* **170**, 1531–1539 (2003).
- Baquertzo, A. et al. Characterization of human xenoreactive antibodies in liver failure patients exposed to pig hepatocytes after bioartificial liver treatment: an *ex vivo* model of pig to human xenotransplantation. *Transplantation* **67**, 5–18 (1999).
- Kroslos, T. I., Polman, R. M. & Paganasso, A. P. Selective fluid depletion prolongs organ survival in an *ex vivo* model of pig-to-human xenotransplantation. *Transplantation* **62**, 5–12 (1996).
- Guarnera, I. V. et al. A novel *ex vivo* porcine renal xenotransplantation model using a pulsatile machine preservation system. *Ann. Transplant.* **16**, 86–82 (2011).
- Kohler, H. B., Muller, M., Pembeli, T., Straub, P. W. & Haslerich, A. The Suppression of the Coagulation of Human-activated Whole-Blood *in-Vitro* by Human Umbilical Endothelial-Cells Cultivated on Microcarriers Is Not-Dependent on Protein-C Activation. *Transf. Haemost.* **73**, 719–724 (1995).
- Wilson, D. & Huba, B. Hgc1 mediates dynamic *Candida albicans* endothelium adhesion events during circulation. *Eukaryotic Cell* **9**, 278–287 (2010).
- Conrad, C. G., Schwartz, M. A. & Ionesco-Zanetti, C. Well plate-coupled microfluidic devices designed for facile image-based cell adhesion and transmigration assays. *J Biomater. Sci.* **15**, 102–106 (2010).
- Rataj, D. et al. Inhibition of complement component C5 prevents clotting in an *ex vivo* model of xenogeneic activation of coagulation. *Xenotransplantation* **23**, 117–127 (2016).
- Harris, D. G. et al. Four-dimensional characterization of thrombotic in a live-cell, shear-flow assay: development and application to xenotransplantation. *PLoS ONE* **10**, e0123015 (2015).
- Lesch, M. B., Post, D. I., Stulen, M. L. & Stokel, T. Characterization of *in vitro* endothelial linings grown within microfluidic channels. *Lab Chip* **11**, 2965–2971 (2011).
- Hattori, K. et al. Microfluidic perfusion culture chip providing different strengths of shear stress for analysis of vascular endothelial function. *J. Biosci. Bioeng.* **118**, 327–332 (2011).
- Wilson, M. E. et al. Fabrication of circular microfluidic channels by combining mechanical micromilling and soft lithography. *Lab Chip* **11**, 1550–1555 (2011).
- Abdelgawad, M. et al. A fast and simple method to fabricate circular microchannels in polydimethylsiloxane (PDMS). *Lab Chip* **11**, 545–551 (2011).
- Chrobak, K. M., Potter, D. R. & Tien, J. Formation of perfused, functional microvascular tubes *in vitro*. *Microvascular Research* **71**, 185–196 (2006).
- Látna, L. et al. A mechanosensory complex that mediates the endothelial cell response to fluid shear stress. *Nature* **437**, 426–431 (2005).
- Vuyyudic, P. L., Min, D. & Baker, A. B. A multichannel dampened flow system for studies on shear stress-mediated mechanotransduction. *Lab Chip* **12**, 3322–3330 (2012).
- Günget, C. T. M., Hwang, Y. & Barakat, A. T. Model of cellular mechanotransduction via actin stress fibers. *Biomater. Biodes. MechanoBiol* **15**, 331–344 (2016).
- Arlaud, G. I., Reboul, A., Sim, R. F. & Colemb, M. G. Interaction of C1-inhibitor with the C1r and C1s subcomponents in human C1. *Biochim. Biophys. Acta* **576**, 151–162 (1979).
- Xiao, F. et al. APT179 (microcept), a membrane-localizing C5 convertase inhibitor, attenuates early human islet allograft damage *in vitro* and *in vivo* in a humanized mouse model. *British Journal of Pharmacology* **173**, 575–587 (2016).
- Tauntoner, T. et al. Dextran sulfate acts as an endothelial cell protectant and inhibits human complement and natural killer cell mediated cytotoxicity against porcine cells. *Transplantation* **76**, 838–843 (2003).
- Spirig, R., Gajjarayak, T., Kersgen, O., Nilsson, B. & Rieben, R. Low molecular weight dextran sulfate as complement inhibitor and cytoprotectant in solid organ and islet transplantation. *Am. J. Transplant.* **43**, 4084–4094 (2004).
- Banz, Y. & Rieben, R. Endothelial cell protection in xenotransplantation: looking after a key player in rejection. *Xenotransplantation* **13**, 19–30 (2006).
- Duchekup, C. et al. C1 esterase inhibitor reduces lower extremity ischemia/reperfusion injury and associated lung damage. *PLoS ONE* **8**, e72059 (2013).
- Schödel, C. et al. Effect of complement fragment 1 esterase inhibition on survival of human decay accelerating factor pig lungs perfused with human blood. *J. Heart Lung Transplant.* **22**, 1365–1375 (2003).
- Bongoni, A. K. et al. Complement dependent early immunological responses during *ex vivo* xenoperfusion of hCD16/HLA-E double transgenic pig forelimbs with human blood. *Xenotransplantation* **21**, 230–243 (2014).
- Papadimitrou, T. G. & Stefanadis, C. Vascular wall shear stress: basic principles and methods. *Hellenic J. Cardiol.* **46**, 9–15 (2005).
- Kilkenny, C., Browne, W. J., Cullill, I. C., Emerson, M. & Altman, D. G. Improving bioscience research reporting: the ARRIVE guidelines for reporting animal research. *PLoS Biology* **8**, e100112 (2010).
- Kudannasa, S. et al. Surface chemical modification of polydimethylsiloxane for the enhanced adhesion and proliferation of mesendodermal stem cells. *ACS Appl. Mater. Interfaces* **5**, 9777–9784 (2013).
- Bondarod, A. et al. Fibrin lock an ImageJ plug-in to quantify fibrillar structures in raw microscopy images. *Nat. Protoc.* **9**, 477–483 (2014).
- Bongoni, A. K., Lanz, J., Rieben, R. & Banz, Y. Development of a bead-based multiplex assay for the simultaneous detection of porcine inflammation markers using xMAP technology. *Cytometry A* **83**, 656–617 (2013).

## Acknowledgements

We thank Prof. Peter J. Cowan, Melbourne, for critical comments. We also thank Drs Rolf Spirig, CSL Behring AG, Bern, Switzerland; Marc W. Nolte, CSL Behring GmbH, Marburg, Germany; Anders Waas, Thkomed AB, Viken, Sweden; and Richard Smith, King's College, London, UK, for providing complement inhibitors used in this study. Help with text editing and technical support by Jane Shaw-Boden is gratefully acknowledged. This work was supported by the Microscopy Imaging Center (MIC), University of Bern. Funding was provided by the 3R Research Foundation for Animal Use Alternatives Switzerland, project no. 133\_12 and the Swiss National Science Foundation, project no. 320030\_156193. SZ was supported by the China Scholarship Council (CSC).

## Author Contributions

R.S. and S.Z. contributed equally to this work. R.S., S.Z. and R.R. designed the study. R.S., S.Z., O.S. and A.D. performed the experiments and did the imaging. C.A.B. and O.T.G. provided technical support for creation of the microfluidic devices. R.S., S.Z. and R.R. wrote the paper. R.S., S.Z., C.A.B., O.T.G. and R.R. critically reviewed and revised the manuscript.

### Additional Information

**Supplementary information** accompanies this paper at <https://doi.org/10.1038/s41598-018-24273-7>.

**Competing Interests:** The authors declare no competing interests.

**Publisher's note:** Springer Nature remains neutral with regard to jurisdictional claims in published maps and institutional affiliations.



**Open Access** This article is licensed under a Creative Commons Attribution 4.0 International License, which permits use, sharing, adaptation, distribution and reproduction in any medium or format, as long as you give appropriate credit to the original author(s) and the source, provide a link to the Creative Commons license, and indicate if changes were made. The images or other third party material in this article are included in the article's Creative Commons license, unless indicated otherwise in a credit line to the material. If material is not included in the article's Creative Commons license and your intended use is not permitted by statutory regulation or exceeds the permitted use, you will need to obtain permission directly from the copyright holder. To view a copy of this license, visit <http://creativecommons.org/licenses/by/4.0/>.

© The Author(s) 2018





### Paper III (Book Chapter)

#### 3D cell culture models for the assessment of anticoagulant and anti-inflammatory properties of endothelial cells

Riccardo Sfriso, Robert Rieben

**Status:** Accepted for publication in *Methods in Molecular Biology*, published by Springer Nature.

**Contribution:** Written the book and contributed to the development of the *in vitro* microfluidic assay.

**Aim:** The aim of the present book chapter is to provide detailed protocols of state-of-the-art 3D cell culture *in vitro* models to study EC function in xenotransplantation setting.

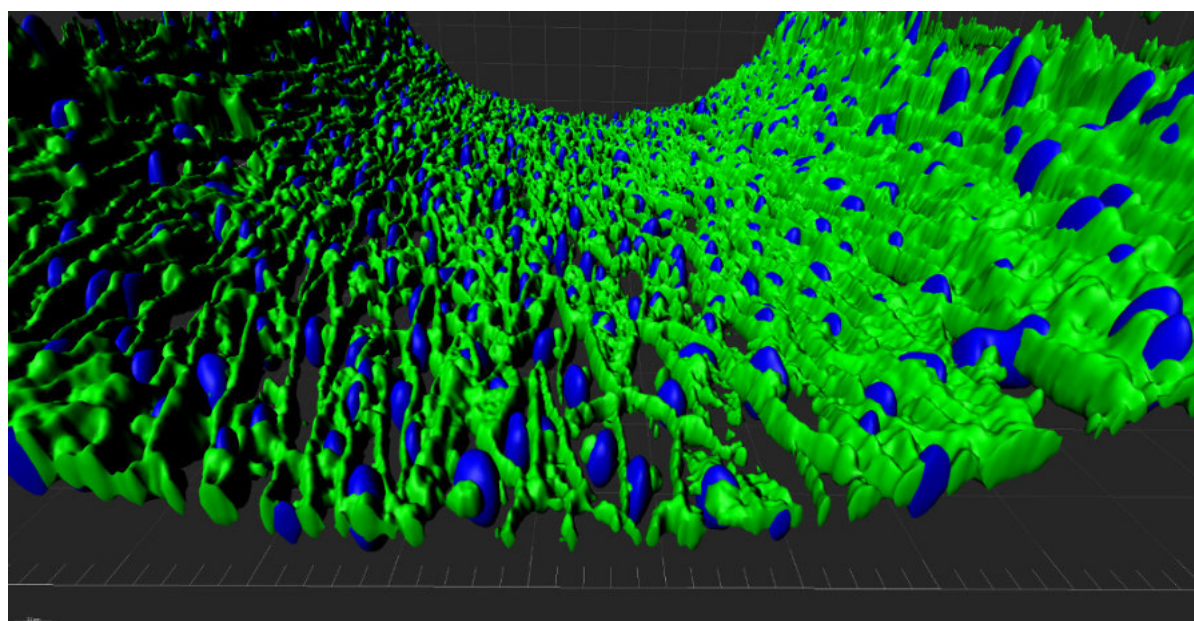


**Figure:** 3D rendering (Imaris software) of EC coated microchannel. The endothelial cells are stained for VE-cadherin (green) and the nuclei are stained with DAPI (blue).



# **3D cell-culture models for the assessment of anticoagulant and anti-inflammatory properties of endothelial cells**

**Riccardo Sfriso<sup>1,2</sup>, Robert Rieben<sup>1\*</sup>**

<sup>1</sup>University of Bern, Department for BioMedical Research (DBMR), Bern, Switzerland

<sup>2</sup>Graduate School for Cellular and Biomedical Sciences, University of Bern, Bern, Switzerland

\*Correspondence and requests for material should be addressed to R.R.

[robert.riegen@dbmr.unibe.ch](mailto:robert.riegen@dbmr.unibe.ch)

**Running Head:** Functional analysis of endothelial cells in 3D culture

**Abstract**

Endothelial cells (EC) play a crucial role in the pathophysiology of cardiovascular diseases, ischemia/reperfusion injury and graft rejection in (xeno-)transplantation. In such non-physiological conditions EC are known to lose their quiescent phenotype and switch into an actively pro-inflammatory, pro-coagulant and anti-fibrinolytic state. This happens essentially because the endothelial glycocalyx – a layer of proteoglycans and glycoproteins covering the luminal surface of the endothelium – is shed. Heparan sulfate, one of the main components of the endothelial glycocalyx, contributes to its negative charge. In addition, many plasma proteins such as antithrombin III, superoxide dismutase, C1 inhibitor as well as growth factors and cytokines bind to heparan sulfate and by this contribute to the establishment of an anticoagulant and anti-inflammatory endothelial surface. Shedding of the glycocalyx results in a loss of plasma proteins from the endothelial surface and this causes the switch in phenotype. Particularly in xenotransplantation, both hyperacute and acute vascular rejection are characterized by coagulation dysregulation, a situation in which EC are the main players.

Since many years EC have been used *in vitro* in 2D flatbed cell culture models, with or without the application of shear stress. Such models have also been used to assess the effect of human transgenes on complement- and coagulation-mediated damage of porcine EC in the context of xenotransplantation. The methods described in this chapter include the analysis of endothelial cell-blood interactions without the necessity of using anticoagulants as the increased EC surface-to-volume ratio allows for natural anticoagulation of blood. Furthermore, the chapter contains the description of a novel microfluidic *in vitro* model carrying important features of small blood vessels, such as a 3D round-section geometry, shear stress, and pulsatile flow – all this in a closed circuit, recirculating system aiming at reproducing closely the *in vivo* situation in small vessels.

**Key Words** 3D cell culture, Coagulation, Complement, Endothelial cells, Genetic modifications, Microcarrier beads, Microfluidics, Vascular biology, Xenotransplantation

## 1. Introduction

The endothelium consists of a monolayer of endothelial cells (EC) which constitute the inner lining of blood vessels. Given their location, EC are directly in contact with blood and circulating cells. Blood fluidity, the vascular tone and platelet aggregation are all actively regulated by EC which carry also a physical semi-selective barrier function and are responsible for the maintenance of blood vessel homeostasis by surface expression and secretion of different key molecules **(1, 2)**. The endothelial glycocalyx – a carbohydrate-rich layer covering the endothelial surface – serves several functions acting as a mechanotransducer and influencing blood-EC interactions **(3)**.

EC activation is characterized by a change of the endothelial phenotype which loses its anti-inflammatory, anticoagulant and pro-fibrinolytic features as a consequence of endothelial glycocalyx shedding. Coagulation dysregulation is a hallmark of acute vascular rejection in xenotransplantation, leading to thrombotic microangiopathy as well as systemic consumptive coagulopathy which culminate in organ failure **(4)**. This is mainly due to genetic differences between the donor and recipient.

Recent developments in genetic engineering techniques (CRISPR-Cas9) paved the way to quick and efficient production of new, multi-transgenic source pigs (over)expressing human regulators of both the complement and coagulation systems **(5)**. The effects of different combinations of transgenes and knockouts in preventing rejection need to be tested before pre-clinical pig to non-human primate xenotransplantation experiments are performed. Since the graft endothelium is the first site in contact with the recipient blood, many *in vitro* models use porcine endothelial cells to analyze the effect of human transgenes on complement and coagulation. However, the majority of *in vitro* experiments involving EC are still carried out in flat bed tissue culture systems, which are far from the physiological environment of EC and have only limited validity for the assessment of the anticoagulant, anti-inflammatory and pro-fibrinolytic functions of EC. We therefore developed a 3D cell culture model of EC on microcarrier beads, in which the increased cell surface-to-volume ratio allows for the study of the natural anticoagulant properties of EC **(6, 7)**. In addition, culturing of porcine EC on the inner surface of cylindrical microchannels (Fig. 1) and exposing them to pulsatile flow of cell culture medium (or human serum/plasma during the experiments) allows to assess the function of anticoagulant and anti-inflammatory properties of the EC under near-natural conditions.

This chapter focuses on the description of 3D cell culture techniques to assess anti-coagulant and anti-inflammatory properties of EC. It does not directly cover techniques for measuring coagulation markers in blood samples since most of them have been extensively described in the previous book by Bulato C. et al (**8**). However, the whole blood collected after incubation of EC coated microcarrier beads as well as the perfusate (plasma) collected from the microfluidic system can be easily analyzed to detect coagulation activation markers such as thrombin-antithrombin complex (TAT), prothrombin fragments (F1+F2) as well as tPA-PAI-1 complexes using commercial ELISA kits.

## **2. Materials**

### **2.1 Microcarrier bead assay**

#### **2.1.1 Coating of microcarrier beads**

The following materials must be of cell culture grade. A cell culture laminar flow hood is required.

1. Microcarrier beads (Biosilon, polystyrene beads with a diameter of 160-300  $\mu\text{m}$ , a density of 1.05 g/cm<sup>3</sup> and carry a negative surface charge).
2. Ultra-pure water.
3. 0.2% acetic acid solution (prepared in a 50 mL falcon tube by adding 57  $\mu\text{l}$  of acetic acid (60.05 g/mol) in 50 mL of sterile ultrapure water).
4. 100  $\mu\text{g/mL}$  bovine collagen I in 0.2% acetic acid.
5. Phosphate-buffered saline (PBS): 137 mM NaCl, 2.6 mM KCl, 8 mM Na<sub>2</sub>HPO<sub>4</sub>, 1.4 mM KH<sub>2</sub>PO<sub>4</sub>, pH 7.4.
6. Medium 199
7. Endothelial cell growth medium supplement mix and 25  $\mu\text{L}$  of heparin (5000 IU/mL).

#### **2.1.2 Collecting cells**

The following materials must be of cell culture grade. A cell culture laminar flow hood is required.

8. Subconfluent (85-90%) T175 flask with EC.
9. PBS 1X at 37°C.
10. Trypsin-0.05% EDTA.
11. Cell culture incubator at 37°C with 5% CO<sub>2</sub> in a humid atmosphere.
12. Medium 199 supplemented with 10% FBS, 1% penicillin/streptomycin, 0.4% endothelial cell growth medium supplement mix.
13. 50 mL falcon tube.

#### **2.1.3 Seeding cells into the spinner flask**

The following materials must be of cell culture grade. A cell culture laminar flow hood is required.

14. Subconfluent (85-90%) T175 flask with EC.
15. 500 mL spinner flasks.
16. 10 mL and 25 mL serological pipettes.

17. Medium 199
18. Colorless RPMI medium supplemented with 10% FBS, 1% penicillin/streptomycin, 1% L-glutamine, 0.4% endothelial cell growth medium supplement mix and 25  $\mu$ L of heparin.

#### **2.1.4 Confluence verification**

The following materials do not need to be of cell culture grade unless otherwise specified.

19. 200  $\mu$ L pipette.
20. PBS 1x at room temperature.
21. Fixative: Parapicric acid.
22. Nuclear labeling solution: 1  $\mu$ g/ mL of 4,6'-diamidino-2-phenylindole (DAPI) in PBS 1x.
23. Glass slides.
24. Mounting media (Glycergel).
25. Confocal microscope.

#### **2.1.5 Experimental procedure**

26. 10 mL serological pipette and pipetboy.
27. Colorless RPMI not supplemented.

#### **2.1.6 Incubation with non-anticoagulated blood**

28. Butterfly sterile syringe needle.
29. 9 mL neutral polypropylene tubes (see **Note 1**).
30. 10 mL sterile serological pipette.
31. 12 mL polypropylene tubes.
32. Parafilm.
33. Horizontal tilting table.
34. 37°C incubator.
35. Timer.
36. 2 mL tubes for serum/plasma collection.

#### **2.1.7 Immunofluorescence staining of EC-coated microcarrier beads**

37. PBS at room temperature.
38. PBS containing 3% BSA.



39. Fixative: Parapicric acid.
40. Antibody dilution buffer: 1% BSA in PBS (see **Note 2**).
41. 1  $\mu\text{g}/\text{mL}$  of 4,6'-diamidino-2-phenylindole (DAPI) in PBS.
42. Mounting medium: Glycergel.
43. Microscope slides (26×76 mm) and sterile coverslips.
44. Confocal microscope.

## **2.2 Microfluidic Model**

### **2.2.1 Microfluidic chip preparation**

1. PDMS silicon elastomer.
2. Curing agent.
3.  $\varnothing$  90mm Petri Dish.
4. Supporting needles ( $\varnothing$  120 $\mu\text{m}$ ).
5. Mold needles ( $\varnothing$  550 $\mu\text{m}$ ).
6. Vacuum chamber.
7. 60°C incubator.
8.  $\varnothing$  2mm biopsy punch.
9. Scalpel.

### **2.2.2 PDMS-glass bonding**

10. Scotch tape.
11. Plasma oxygen cleaner.
12. 100% Isopropanol.
13. Soap water.
14. Ultrapure water.
15. Nitrogen gun.
16. Glass slides (24x60mm).

### 2.2.3 Coating of microchannels

The following materials must be of cell culture grade. A cell culture laminar flow hood is required.

1. Ultrapure water.
2. 5% (3-Aminopropyl)triethoxysilane (APTES) (prepared by adding 250  $\mu$ L of APTES to 4.75 mL of ultrapure water, corresponding to a 1:20 dilution, in a 5 mL tube and mixing well).
3. 0.1% glutaraldehyde in ultrapure water (prepared by diluting 40  $\mu$ L of the 25% glutaraldehyde stock solution in 9'960  $\mu$ L of ultrapure water, corresponding to a 1:250 dilution).
4. 15 mL falcon tubes.
5. 50  $\mu$ g/mL human fibronectin in PBS (dilute 75  $\mu$ L of the 1mg/mL fibronectin stock solution in 1425  $\mu$ L of sterile PBS 1x). The volume of this solution is calculated for the coating of 4 microchannels. Please adjust the volume accordingly if more microchannels need to be coated.
6. 100  $\mu$ g/mL bovine collagen I in 0.2% acetic acid.
7. DMEM Glutamax supplemented with 10% FBS, 1% penicillin/streptomycin, 0.4% endothelial cell growth medium supplement mix.

### 2.2.4 Cell seeding

The following materials must be of cell culture grade. A cell culture laminar flow hood is required.

17. DMEM Glutamax supplemented with 10% FBS, 1% penicillin/streptomycin, 0.4% endothelial cell growth medium supplement mix and 4% dextran.
18. Subconfluent (85-90%) T75 flask with EC.
19. Trypsin-0.05% EDTA.
20. Phosphate-buffered saline (PBS): 137 mM NaCl, 2.6 mM KCl, 8 mM Na<sub>2</sub>HPO<sub>4</sub>, 1.4 mM KH<sub>2</sub>PO<sub>4</sub>, pH 7.4.

### 2.2.5 Peristaltic pump connection

The following materials must be of cell culture grade. A cell culture laminar flow hood is required.

21. Peristaltic pump.
22. Silicon extension tubings (inner diameter 1 mm).
23. Silicon pump head tubings with stoppers (Gilson).
24. Adapters (Bio-Rad).

25. Autoclaved ultra pure water.

26. Autoclaved PBS 1x.

27. DMEM Glutamax supplemented with 10% FBS, 1% penicillin/streptomycin, 0.4% endothelial cell growth medium supplement mix and 4% dextran.

15 mL falcon tubes (reservoir tubes) with two holes in the cap ( $\varnothing$  2mm made with a driller).

### 3. Methods

Carry out all procedures under cell culture laminar flow hood unless otherwise specified.

#### 3.1 Microcarrier bead assay ([6])

##### 3.1.1 Coating of microcarrier beads

28. Mix 7 mL of microcarrier beads with 42 mL of the 100 µg/mL collagen solution in a 50 mL tube and incubate for 1 h at room temperature.
29. Wash beads two times with 25 mL of PBS pH 7.4 (add 25 mL of PBS, mix well with the pipet and wait until the beads are settled down then discard the supernatant and repeat) and one time with 25 mL of medium 199.
30. Cover the beads in the 50 mL tube with 10 mL of the supplemented medium 199 and allow equilibration for 10 min before further use.

##### 3.1.2 Collecting cells

31. Remove the cell culture medium from the T175 flask containing PAEC and add 5 mL of PBS.
32. Remove PBS from the T175 flask.
33. Add 5 mL of Trypsin-0.05% EDTA and incubate for 3-4 min at 37 °C.
34. Collect the cells by rinsing the flask with 15 mL of cell culture medium and transfer the suspension to a 50 mL tube.
35. Centrifuge cells at  $1200 \times g$  for 8 min at room temperature, remove excess medium and resuspend the pellet in 5 mL of cell culture medium.

##### 3.1.3 Seeding cells into the spinner flask

36. Add 20 mL of cell culture medium to the cell suspension and resuspend.
37. Add 20 mL of cell culture medium (w/o cells) into the 500 mL magnetic spinner flask.
38. Add the cells to the washed microcarrier beads and mix carefully with a 25 mL serological pipette.
39. Transfer the beads/cell mixture into the magnetic spinner flask.
40. Rinse the 50 mL tube with 10 mL of cell culture medium to collect the remaining cells.
41. Add an additional 85 mL of cell culture medium into the spinner flask and place it into the incubator overnight at 37 °C on a shaker ( $100 \times g$ , mixing interval: 3 min every 45 min).

42. Add 50 mL of cell culture medium (total volume 200 mL) and continue stirring for an additional 24 h at 37 °C on a shaker (100 × *g*, mixing interval: 3 min every 45 min).
43. Add the colorless supplemented RPMI medium up to 320 mL of total volume.
44. Replace the medium every 48 h: Remove 100 mL of old medium and add 100 mL of fresh supplemented colorless RPMI.
45. Culture the cells for 5 to 7 days. The time depends on the confluence state of the cell-coated beads.

#### **3.1.4 Confluence verification**

46. Collect 200 µL of cell-coated beads using a pipette and transfer them into a polypropylene tube (see **Note 3**).
47. Wash the beads 3 times with 600 µL of PBS (add PBS, tilt the tube and mix gently to avoid detachment of the cells from the beads, wait for the beads to settle down, discard the PBS and repeat).
48. Fix the beads for 10 min by adding 200 µL of paraformaldehyde.
49. Wash 3 times with 600 µL of PBS as in step 2.
50. Add DAPI diluted in PBS and incubate for 10 min.
51. Transfer the beads on a glass slide and apply a coverslip using glycerol based mounting medium (see **Note 4**).
52. Visualize the beads under a confocal microscope. (Fig. 2)

#### **3.1.5 Experimental procedure**

53. Remove the cell-coated beads from the magnetic spinner flask with a 10 mL serological pipette and transfer them into 12 mL round-bottom polypropylene tubes.
54. Let the beads settle down (around 1-2 mins) and remove excess medium.
55. Add more beads to the tubes until every tube contains exactly 2 mL of beads (see **Note 5**).
56. Add 5 mL of clear RPMI to each tube and mix carefully using a 10 mL serological pipette.
57. Let the beads settle down and remove excess medium.
58. Repeat the washing procedure one more time with RPMI and remove all excess medium.

### 3.1.6 Incubation with non-anticoagulated blood

59. Carefully and slowly (using neither jet nor vacutainers) draw blood from a healthy volunteer and collect it in 9 mL neutral polypropylene tubes (without anticoagulant).
60. Slowly transfer 8 mL of blood with a 10 mL serological pipette into each of the polypropylene tubes containing 2 mL of cell-coated beads (the total volume will be 10 mL). Always avoid rough handling of blood or beads to avoid premature EC activation. The procedure takes 1- 2 min.
61. Carefully tilt the blood/bead mixture to ensure equal mixing and seal the cap with paraffin film.
62. Place the tubes on a horizontal tilting table (with gentle tilting settings only) inside a 37 °C incubator and record clotting times.
63. At set time intervals, e.g. after 10, 20, 30, 50, 70, 90 min, remove 1.5 - 2 mL of blood-bead mixture for serum or plasma analysis (see **Note 6**).
64. For collection of serum, leave the blood to coagulate (see **Note 7**). To collect the plasma, add EDTA or citrate to 2 mL tubes before adding blood samples.

### 3.1.7 Immunofluorescence staining of EC-coated microcarrier beads

1. Collect 200  $\mu$ L of cell-coated beads using a pipette and transfer them into a polypropylene tube (see **Note 3**).
2. Wash the beads 3 times with 600  $\mu$ L of PBS (add PBS, tilt the tube and mix gently to avoid detachment of the cells from the beads, wait for the beads to settle down, discard the PBS and repeat).
3. Fix the beads for 10 min by adding 200  $\mu$ L of parapiatric acid.
4. Wash 3 times with 600  $\mu$ L of PBS as in step 2.
5. Block using 600  $\mu$ L of PBS-3% BSA for 30 min at room temperature.
6. Add primary antibodies diluted in PBS-1%BSA and incubate for 1 h at room temperature.
7. Wash 3 times with 600  $\mu$ L of PBS as in step 2.
8. Add fluorescent secondary antibodies diluted in PBS-1% BSA and incubate for 1 h at room temperature.
9. Wash 3 times with 600  $\mu$ L of PBS as in step 2.
10. Add DAPI diluted in PBS and incubate for 10 min.
11. Wash 3 times with 600  $\mu$ L of PBS as in step 2.

12. Transfer the beads on a glass slide and apply a coverslip using glycerol based mounting medium (see **Note 4**).
13. Visualize the beads under a confocal microscope.

## **3.2 Microfluidic Model**

### **3.2.1 Microfluidic chip preparation**

1. Mix silicon elastomer and curing agent in proportion 10:1 (see **Note 8**).
2. Mix well the two components with a plastic spoon for 3 - 5 min.
3. Apply vacuum to remove air bubbles.
4. Clean the needles ( $\varnothing$  550  $\mu$ m and  $\varnothing$  120  $\mu$ m) with isopropanol and leave them to dry on a tissue.
5. Transfer liquid PDMS into a Petri dish ( $\varnothing$  90 mm, see **Note 9**) and vacuum it to remove further air bubbles.
6. Place support needles ( $\varnothing$  120  $\mu$ m) on the bottom of the Petri dish.
7. Place mold needles ( $\varnothing$  550  $\mu$ m) orthogonally on top of support needles (Figure 3)
8. Carefully transfer the Petri dish into the incubator (60°C).
9. Cure overnight at 60°C.
10. Remove the solidified PDMS and cut four equal chips.
11. Remove the needles with forceps ( $\varnothing$  550  $\mu$ m and  $\varnothing$  120  $\mu$ m). Store the 550- $\mu$ m needles (reusable) and discard the small needles.
12. Punch holes, distance 1 cm (use a ruler), as inlets and outlets using a  $\varnothing$  2.0 mm biopsy puncher.
13. Seal the side holes left by the needles with liquid PDMS (see **Note 10**).
14. Cure at 60°C for at least 2 h.
15. Chips can be stored at this point, tape the structures to protect them from dust.

### **3.2.2 PDMS-glass bonding (Figure 4)**

1. Cut a chip in four parts with a scalpel. Every single part must contain a microchannel.
2. Tape a PDMS chip with scotch tape on the bottom side while keeping the channel side on top and leave a small space between the channels.
3. Clean a glass slide with 70% Ethanol, soap water and rinse with ultrapure water.

4. Dry the glass slide with a nitrogen gun (see **Note 11**).
5. Place PDMS-chip & glass slide into the oxygen plasma cleaner.
6. Turn on the oxygen tank, the pressure Indicator, the plasma cleaner and the vacuum pump.
7. Wait the pressure decreases until ca. 300 mTorr, turn the O<sub>2</sub> valve into position.
8. Wait until the pressure stabilizes at ca. 650 mTorr.
9. Turn on plasma to a high level for glass-PDMS bonding. Leave 3 min under oxygen plasma.
10. Open the valve to let the pressure normalize by room air (see **Note 12**).
11. Place the PDMS chip in the center of the glass slide and gently press them together to allow a covalent bonding formation.

### 3.2.3 Coating of microchannels (Figure 5)

1. After oxygen-plasma bonding, modify the PDMS surface immediately by filling the microchannels with 5% APTES (the shorter the time between plasma oxygen treatment and APTES, the more APTES-groups will bind to the surface), and leave 20 min (see **Note 13**).
2. Wash channels 3 times with distilled water.
3. Replace the water with 0.1% glutaraldehyde 3 times. Leave it for 30 min.
4. Wash 3 times with distilled water.
5. Replace the water with 50 µg/mL fibronectin (3 times), incubate 60 min at 37°C, or place it in the laminar flow overnight at room temperature under UV light.
6. Fill the channels with the 100 µg/mL collagen-I solution (3 times) and leave it in the laminar flow at room temperature for 1.5 h.
7. Add cell culture medium and place the Petri dish with the chip in the 37°C incubator for 30 min or longer before cell seeding.

### 3.2.4 Cell seeding

1. Harvest the cells of interest and adjust cell density at 10<sup>6</sup>/mL by adding cell culture medium supplemented with dextran (4% final dextran concentration).
2. Inject 10<sup>6</sup> cells/mL into the channels from both ends using 200 µL pipette (make sure using a single cell suspension, avoid cell clumps!).
3. Place the microfluidic chip upside down in the incubator and leave it for 15 min. The cells should have enough time to attach to the surface (block the glass slide with a tape to the Petri



dish).

4. Aspirate the unattached cells and add new cells. Incubate the microfluidic chip upright for 30 minutes.
5. Verify cell attachment using a microscope.
6. Wash the channels with 4% dextran medium to get rid of unattached cells.
7. Wait until the cells are confluent (normally the next day) and change the medium regularly (every 2 hours).

### **3.2.5 Peristaltic pump connection (4 channels)**

1. Connect the peristaltic pump only when the endothelial cells are confluent.
2. Flush tubings with 30 mL of autoclaved ultrapure water then with 30 mL of autoclaved PBS.
3. Check the tubings for leakage and continue flushing with 20 mL 4% dextran medium.
4. Be sure that the medium runs through all the channels with the same speed. If not, adjust the flow with the screws on the back of the pump.
5. Fill 15 mL falcon tubes (reservoir tubes) with 10 mL of 4% dextran medium and insert the inlet and outlet of the tubings through the cap. Adjust the inlet at the level of 8 ml and the outlet at 2 mL so that mixing of the medium is ensured.
6. Insert the ends with the adapters in the inlet and outlet of the microchannels.
7. Start the pump at 7 rpm (flow 600  $\mu$ L/min).
8. Increase to desired rpm or leave the cells at 7 rpm.
9. Keep the desired rpm for 48 h or longer if you change medium reservoir every 2 days.

## **4. Notes**

1. For example Sarstedt blood collection system – do not use open systems to reduce blood-air contact and don't use vacutainers because of blood activation due to formation of a blood jet.
2. Always use fresh PBS - 1% BSA solution for antibody dilution. Since it does not contain antibiotics contamination may occur if stored for long time.
3. Carefully pipet and handle the cell coated microbeads to avoid cell detachment and/or activation.
4. Use a tissue to absorb excess PBS after pipetting the microbeads on the glass slide. Afterwards apply the mounting medium and place the coverslip without applying excessive pressure.

5. Pipet the cell-coated microbeads carefully into the polypropylene tubes without stirring them to prevent cell detachment.
6. For 6 time points we suggest having at least 3 replicates within each group of cells, as the blood sampling will be done in different tubes.
7. Appropriate collection of serum samples is necessary to prevent complement degradation. The blood must be allowed to coagulate at room temperature for 30 minutes. Immediately after placing the tubes in a 4°C centrifuge and centrifuging the samples at 2000 × g for 10 minutes. After centrifugation, place the tubes on ice and collect the serum in 1.5 mL tubes and store them immediately at -80°C for further analysis.
8. Example for 1 Petri dish (4 microchips): 35 g of silicon elastomer, 3.5 g of curing agent.
9. Use a nitrogen gun to clean the surface of the Petri dish before pouring the PDMS.
10. Prepare 5 g of PDMS: 5 g of silicon elastomer, 0.5 g of curing agent.
11. Clean the glass slide carefully and extensively. If not properly cleaned, a good bonding cannot be achieved and the microchannels will leak.
12. Slowly open the valve letting the pressure to normalize. Avoid opening the valve too fast, the microchips and the glass slides might be blown against the walls of the plasma oxygen cleaner chamber. After oxygen plasma treatment, the PDMS and the glass slide are strongly reactive and if they come in contact with other surfaces inside the chamber they could stick to them.
13. Fill the microchannel by pipetting the solution on the inlet until it reaches the outlet. Remove the excess solution from the outlet with a pipet paying attention not to dry the channel. Add more solution on the inlet and repeat the partial removal from the outlet two times more. This step has to be followed throughout the whole coating protocol.

## 5. References

1. Félétou M (2011) *The Endothelium*. Morgan & Claypool Publishers
2. Kása A, Csontos C, Verin AD (2015) Cytoskeletal mechanisms regulating vascular endothelial barrier function in response to acute lung injury. *Tissue Barriers* 3:e974448. doi: 10.4161/21688370.2014.974448

3. Reitsma S, Slaaf DW, Vink H, et al (2007) The endothelial glycocalyx: composition, functions, and visualization. *Pflugers Arch* 454:345–359. doi: 10.1007/s00424-007-0212-8
4. Lin CC, Cooper DKC, Dorling A (2009) Coagulation dysregulation as a barrier to xenotransplantation in the primate. *Transplant Immunology* 21:75–80. doi: 10.1016/j.trim.2008.10.008
5. Hryhorowicz M, Zeyland J, Słomski R, Lipiński D (2017) Genetically Modified Pigs as Organ Donors for Xenotransplantation. *Mol Biotechnol* 59:435–444. doi: 10.1007/s12033-017-0024-9
6. Sfriso R, Bongoni A, Banz Y, et al (2017) Assessment of the Anticoagulant and Anti-inflammatory Properties of Endothelial Cells Using 3D Cell Culture and Non-anticoagulated Whole Blood. *J Vis Exp* e56227–e56227. doi: 10.3791/56227
7. Sfriso R, Zhang S, Bichsel CA, et al (2018) 3D artificial round section micro-vessels to investigate endothelial cells under physiological flow conditions. *Sci Rep* 8:5898. doi: 10.1038/s41598-018-24273-7
8. Bulato C, Radu C, Simioni P (2012) Studies on coagulation incompatibilities for xenotransplantation. *Methods Mol Biol* 885:71–89. doi: 10.1007/978-1-61779-845-0\_6

## 6. Figure Captions

**Fig. 1.** Confocal images of EC coated microchannels. (a) 3D rendering of the 120  $\mu\text{m}$  round section channel. EC monolayer was stained for VE-cadherin (green) and F-Actin (red). Nuclei were stained with DAPI (blue). (b) 3D z-stack of the 550  $\mu\text{m}$  round section channel. EC monolayer was stained for VE-cadherin (green). Nuclei were stained with DAPI (blue). (c) 3D rendering of the 550  $\mu\text{m}$  round section channel, detail. EC were stained for VE-cadherin (green). Nuclei were stained with DAPI (blue).

**Fig. 2.** Confluence verification of endothelial cells grown on microcarrier beads. Confocal microscopy picture of endothelial cell nuclei (stained with DAPI, blue) after 7 days of culture.

**Fig. 3.** Position of supporting needles and mold needles.

**Fig. 4.** Schematic representation of the bonding procedure. The plasma oxygen treatment removes hydrocarbon groups (C<sub>x</sub>H<sub>y</sub>) leaving behind silanol groups on the PDMS and OH groups on the glass substrate, respectively. This allows strong Si – O – Si covalent bonds to form between the two materials.

**Fig. 5.** Schematic representation of PDMS surface modification to crosslink extracellular matrix proteins. GA: glutaraldehyde.

## 7. Figures

**Figure 1**

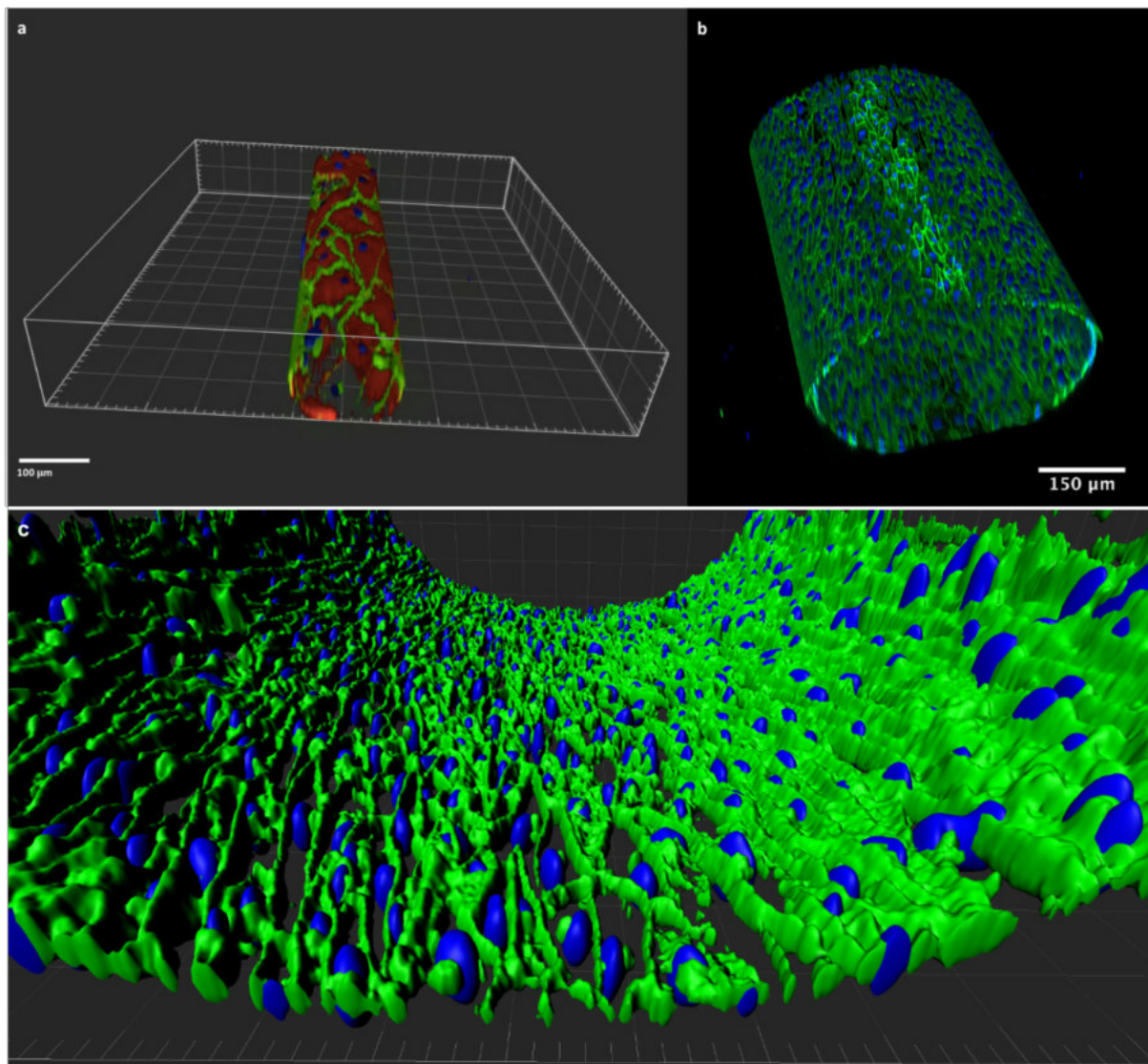


Figure 2

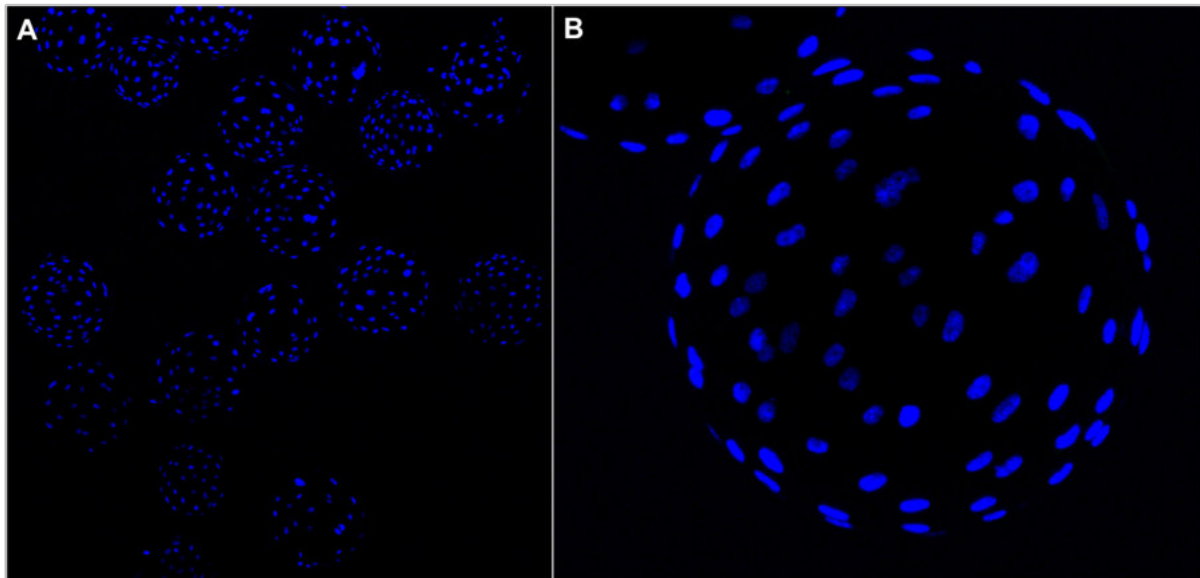


Figure 3

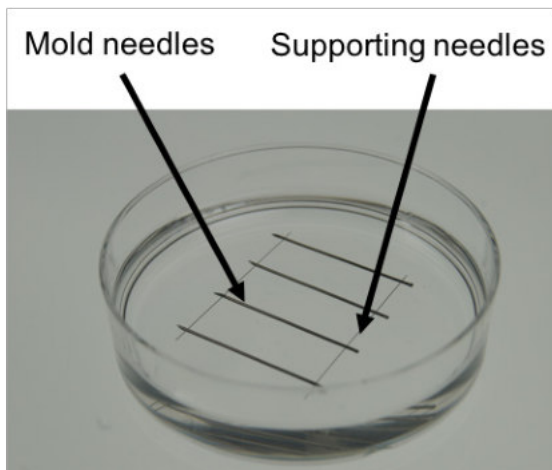


Figure 4

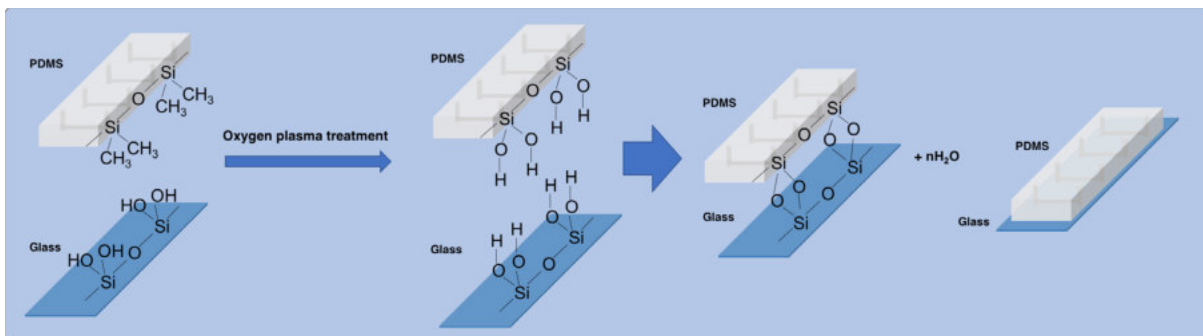
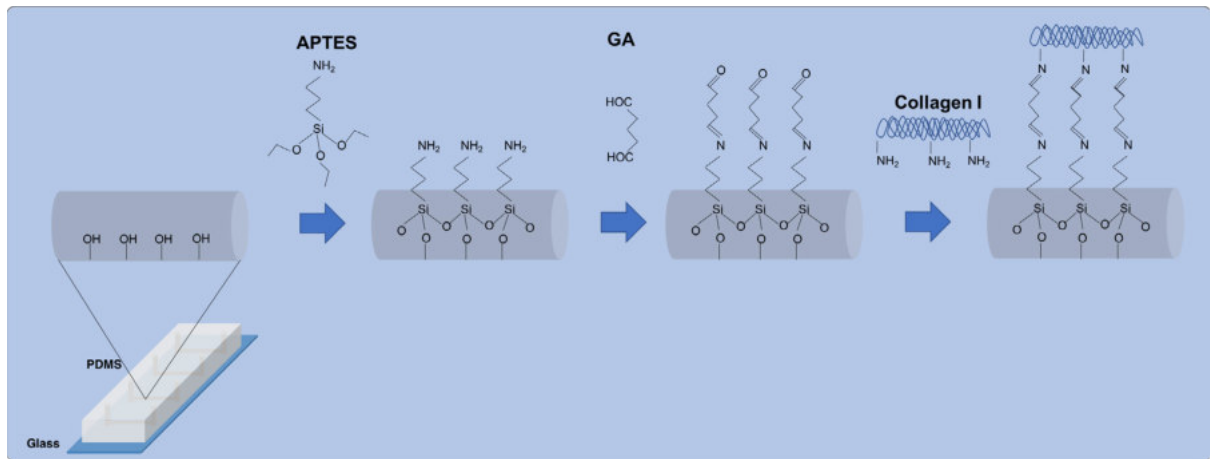


Figure 5



## Paper IV

### Release of pig leukocytes and reduced human NK cell recruitment during *ex vivo* perfusion of HLA-E/human CD46 double-transgenic pig limbs with human blood.

Gisella Puga Yung, Anjan K. Bongoni, Amandine Pradier, Natacha Madelon, Maria Papaserafeim, Riccardo Sfriso, David L. Ayares, Eckhard Wolf, Nikolai Klymiuk, Andrea Bähr, Mihai A. Constantinescu, Esther Voegelin, David Kiermeir, Hansjörg Jenni, Robert Rieben, Jörg D. Seebach

**Status:** Published in *Xenotransplantation*, 2017 Sep 1;e12357

**Contribution:** Performed immunofluorescence staining of NKp46 on muscle biopsies, imaging and relative quantification.

**Background:** In pig-to-human xenotransplantation, interactions between human natural killer cells and porcine endothelial cells result in cytotoxicity. Protection from xenogeneic NK cytotoxicity can be achieved *in vitro* by the expression of the non-classical human leukocyte antigen-E (HLA-E) on porcine endothelial cells.

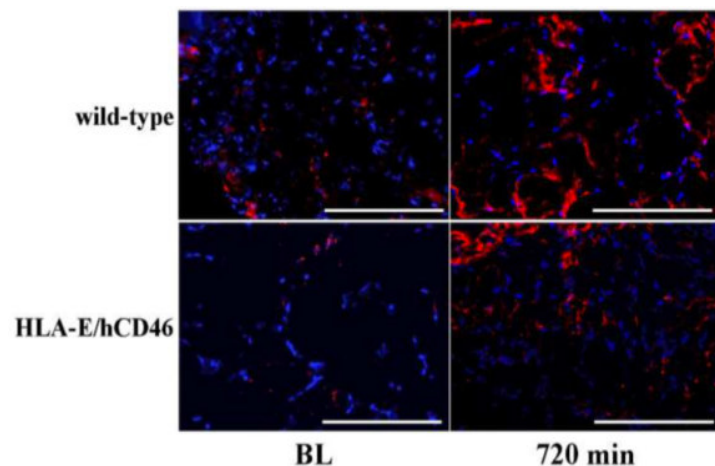


**Figure:** NKp46 staining (red) on pig limb muscle tissue. The figure shows reduced NK cells presence on the xeno-perfused transgenic porcine limbs compared to wild-type controls.

**Aim:** To analyze NK cell responses to vascularized xenografts using an *ex vivo* perfusion system of pig limbs with whole human blood.

**Conclusion:** Transgenic expression of HLA-E/hCD46 in pig limbs provides partial protection from human NK cell-mediated xeno responses. Furthermore, we could show the emergence of a pig cell population during xenoperfusions with evident implications for the immunogenicity of xenografts.





# Release of pig leukocytes and reduced human NK cell recruitment during ex vivo perfusion of HLA-E/human CD46 double-transgenic pig limbs with human blood

Gisella Puga Yung<sup>1</sup>  | Anjan K. Bongoni<sup>2</sup> | Amandine Pradier<sup>1</sup> | Natacha Madelon<sup>1</sup> | Maria Papaserafeim<sup>1</sup> | Riccardo Sfriso<sup>2</sup>  | David L. Ayares<sup>3</sup> | Eckhard Wolf<sup>4</sup> | Nikolai Klymiuk<sup>4</sup> | Andrea Bähr<sup>4</sup> | Mihai A. Constantinescu<sup>5</sup> | Esther Voegelin<sup>5</sup> | David Kiermeir<sup>5</sup> | Hansjörg Jenni<sup>6</sup> | Robert Rieben<sup>2</sup>  | Jörg D. Seebach<sup>1</sup> 

<sup>1</sup>Division of Immunology and Allergy, University Hospital and Medical Faculty, Geneva, Switzerland

<sup>2</sup>Department of Clinical Research, University of Bern, Bern, Switzerland

<sup>3</sup>Revisior Inc., Blacksburg, VA, USA

<sup>4</sup>Institute of Molecular Animal Breeding and Biotechnology, Ludwig-Maximilians-University, Munich, Germany

<sup>5</sup>Clinic of Plastic and Hand Surgery, University Hospital, Bern, Switzerland

<sup>6</sup>Clinic of Cardiovascular Surgery, University Hospital, Bern, Switzerland

## Correspondence

Jörg D. Seebach, Division of Immunology and Allergy, University Hospital Geneva, Geneva, Switzerland.

Email: jocrs,seebach@hcuge.ch

## Funding information

Swiss National Science Foundation (#320030\_118316 and 320000\_109921 to JDS and #32003B\_135177 and #32003B\_138437 to RR), in addition to a Private Foundation and the Gernar Research Foundation (TRK127).

## Abstract

**Background:** In pig-to-human xenotransplantation, interactions between human natural killer (NK) cells and porcine endothelial cells (pEC) are characterized by recruitment and cytotoxicity. Protection from xenogeneic NK cytotoxicity can be achieved in vitro by the expression of the non-classical human leukocyte antigen-E (HLA-E) on pEC. Thus, the aim of this study was to analyze NK cell responses to vascularized xenografts using an ex vivo perfusion system of pig limbs with human blood.

**Methods:** Six pig forelimbs per group, respectively, stemming from either wild-type (wt) or HLA-E/hCD46 double-transgenic (tg) animals, were perfused ex vivo with heparinized human blood for 12 hours. Blood samples were collected at defined time intervals, cell numbers counted, and peripheral blood mononuclear cells analyzed for phenotype by flow cytometry. Muscle biopsies were analyzed for NK cell infiltration. In vitro NK cytotoxicity assays were performed using pEC derived from wt and tg animals as target cells.

**Results:** Ex vivo, a strong reduction in circulating human CD45 leukocytes was observed after 60 minutes of xenoperfusion in both wt and tg limb groups. NK cell numbers dropped significantly. Within the first 10 minutes, the decrease in NK cells was more significant in the wt limb perfusions as compared to tg limbs. Immunohistology of biopsies taken after 12 hours showed less NK cell tissue infiltration in the tg limbs. In vitro, NK cytotoxicity against hCD46 single tg pEC and wt pEC was similar, while lysis of double tg HLA-E/hCD46 pEC was significantly reduced. Finally, circulating cells of pig origin were observed during the ex vivo xenoperfusions. These cells expressed phenotypes mainly of monocytes, B and T lymphocytes, NK cells, as well as some activated endothelial cells.

**Conclusions:** Ex vivo perfusion of pig forelimbs using whole human blood represents a powerful tool to study humoral and early cell-mediated rejection mechanisms of

**Abbreviations:** BL, basilic; FSC, forward scatter; hCD45<sup>+</sup>, human CD45 positive cells; hCD45<sup>neg</sup>, human CD45 negative cells; HLA, human leukocyte antigen; mAb, monoclonal antibody; MHC, major histocompatibility complex; NK, natural killer; pC, pig; C, CD45-positive cells; pCD45<sup>+</sup>, pig; C, CD45-negative cells; pEC, porcine endothelial cells; p-38, phospho-ribosomal kinase; pMNC, peripheral blood mononuclear cells; SJA, swine lymphocyte antigen; SSC, side scatter; tg, transgenic; WBC, white blood cells; wt, wild type.

vascularized pig-to-human xenotransplantation, although there are several limitations of the model. Here, we show that (i) transgenic expression of HLA-E/hCD46 in pig limbs provides partial protection from human NK cell-mediated xeno responses and (ii) the emergence of a pig cell population during xenoperfusions with implications for the immunogenicity of xenografts.

#### KEYWORDS

human leukocyte antigen-E/human CD46, limb perfusion, natural killer cells, release of pig cells, transgenic pigs, xenoperfusion

## 1 | INTRODUCTION

The use of porcine organs or cells to overcome the current shortage in transplantation medicine faces several challenges, including innate and adaptive immune responses. From the clinical point of view, adaptive responses might be controlled by immunosuppressive drugs currently used in allotransplantation; however, therapeutic approaches to control innate immunity remain to be developed. Cellular innate immunity causing early endothelial damage following xenotransplantation of vascularized organs is mediated by granulocytes, monocytes, and NK cells.<sup>1–6</sup> The activity of human NK cells is tightly regulated by a balance between activating and inhibiting NK cell receptors, the latter predominantly recognizing self-MHC class I molecules.<sup>11</sup> In the pig-to-human setting, pig MHC class I, that is swine leukocyte antigen I (SLA-I), is poorly recognized by human inhibitory NK cell receptors.<sup>6</sup> Indeed, overexpression of SLA-I on porcine endothelial cells (pEC) by stimulation with tumor necrosis factor reduced but did not fully abrogate human anti-pig NK cytotoxicity.<sup>7</sup> As a strategy to control xenogeneic human anti-pig NK cytotoxicity, we and others have previously shown that transgenic expression of various human leukocyte antigen (HLA) class I molecules including HLA-A2, HLA-B27, HLA-Cw3, HLA-Cw4, and HLA-G in pEC provides partial protection against NK cytotoxicity and reduces NK cell recruitment.<sup>8–11</sup> In contrast to the classical, highly polymorphic HLA-A/B/C alleles, HLA-E alleles are restricted to only 2 functional variants recognized by the ubiquitous inhibitory NK receptor CD94/NKG2A.<sup>12–15</sup> Consequently, transgenic expression of HLA-E in pig xenografts might inhibit a large majority of NK cells in human recipients and avoids the introduction of potentially allogeneic HLA molecules. Thus, we and others have used different HLA-E constructs to transfect porcine endothelial cells, including a trimer consisting of mature human  $\beta 2$  m, a canonical HLA-E binding peptide VMAPRTLIL, and mature HLA-E<sup>R</sup> heavy chain, E\*0103.<sup>12–23</sup> Subsequently, HLA-E and human  $\beta 2$  m contained in 2 separated vectors were used to generate HLA-E/ $\beta 2$  m transgenic pigs as a strategy to regulate human anti-pig NK cell responses.<sup>24</sup> Whereas in vitro NK cytotoxicity against HLA-E expressing pEC was reduced, this strategy is only now being tested under more physiological conditions such as ex vivo perfusion systems.

Ex vivo perfusion models have been used in xenotransplantation for many years to test early xenograft events and more recently to evaluate the potential of genetic modifications in pigs. Preferential

recruitment of human NK cells, to rat hearts perfused with human peripheral blood lymphocytes, was reported in a seminal paper by Inverardi et al<sup>25</sup> in 1992. A predominance of perivascular xenograft infiltration by NK cells was also demonstrated by Khalifoun et al<sup>26</sup> during pig kidney xenoperfusions with human peripheral blood lymphocytes and by Ramos et al<sup>27</sup> in a short report. Using a pig lung xenoperfusion model, Laird et al<sup>28</sup> reported recently that transgenic expression of HLA-E limited endothelial damage by preventing NK cell activation and cytotoxicity resulting in improved pig lung survival and function. This finding was corroborated in the Munich heart model showing reduced tissue infiltration by NK cells in HLA-E transgenic pig hearts perfused with human blood, as recently reported in abstract form.<sup>29,31</sup>

During the past years, our collaborative group has established a novel model of ex vivo xenoperfusion with human blood using porcine forelimbs of genetically modified pigs.<sup>32</sup> In the current work, a combined strategy to reduce humoral and cellular innate xenoresponses by overexpression of HLA-E and hCD46, respectively, was used to study interactions between human NK cells and the porcine vascular system. While HLA-E expression, tissue damage, and the effects on complement activation and coagulation all have been reported in detail elsewhere,<sup>32–34</sup> we describe here the effect of combined HLA-E/hCD46 expression on NK cell recruitment and tissue infiltration. Additionally, the release into the circulating blood of an important population of pig cells was observed during these xenoperfusions and further characterized.

## 2 | MATERIAL AND METHODS

### 2.1 | Animals and pig limb perfusion model

Ex vivo perfusion was performed as described in detail elsewhere.<sup>32</sup> Six HLA-E/hCD46 double-transgenic (tg)<sup>32</sup> and 6 wild-type (wt) pig forelimbs were perfused with heparinized whole human blood (xenoperfusion). Animal care was performed according to the Swiss National Guidelines and the Guide for the Care and Use of Laboratory Animals (NIH Publication No. 85-23, revised 1996). The local animal experimentation committee of the Canton Bern approved this study (permission # BE45/11). Serial blood samples of 10 mL were collected from the perfusion system at predefined intervals, starting at baseline (BL) before the blood was added to the perfusion system, and after 10, 60, 180, and 720 minutes of perfusion. Muscle biopsies were

obtained for analysis of cellular tissue infiltration before perfusion and at the end-point (720 minutes).

## 2.2 | White blood cell counts

Complete hemograms including white blood cell (WBC) counts were performed on each blood sample using an analyzer (Sysmex Europe GmbH, Norderstedt, Germany).

## 2.3 | Human and pig cell isolation from perfused blood

Peripheral blood mononuclear cells (PBMC) were isolated from xenogeneic and autologous perfused blood samples by gradient centrifugation using Ficoll-Paque (GE Healthcare, Glattbrugg, Switzerland) the morning following the end of the perfusion, typically at midnight. Thereafter, the cells were extensively washed with PBS, counted, and split for flow cytometry staining. A sample was stained with LIVE/DEAD<sup>®</sup> Fixable Aqua Dead Cell Stain according to manufacturer's instructions (Life Technologies, Basel, Switzerland). In some samples, reduced PBMC numbers or a high degree of hemolysis was noted (Table S1).

## 2.4 | Estimates of cell number changes

Absolute numbers of total viable hCD45 cells, hCD45 lymphocytes, and NK cells (CD3<sup>+</sup>CD56<sup>+</sup>) were calculated using the amount of PBMC (cells/mL of blood) purified from each blood sample (Table S1) and the corresponding cell percentages obtained by flow

cytometry and gating of the respective cell population. The absolute cell numbers were used to determine the relative percentage of the drop of cell numbers compared to base line (BL) values.

## 2.5 | Cell surface phenotype analysis by flow cytometry

The characteristics of the antibodies used for flow cytometry analysis are listed in Table 1. For staining, cells were incubated for 30 minutes at 4°C with saturating amounts of directly fluorochrome-labeled antibodies in PBS containing 1% bovine serum albumin. Secondary polyclonal goat anti-mouse antibody was used for indirect staining (IgG-PE, Poly4053, Biologend). All analyses were performed using isotype-matched control antibodies. The Attune (Life Technologies) flow cytometer was used for data acquisition, and FlowJo software, version X0.7 (TreeStar Inc, Ashland, OR, USA), for data analysis. Gating strategy for human cell populations is depicted in Fig. S1. For the characterization of pig cells, a panel of anti-pig antibodies was used (Table 1). Of note, some but not all of the anti-monocyte/macrophage pig markers were cross-reactive with human cells (Fig. S3). However, since the key pan-leukocyte marker CD45 was clearly species-specific, misinterpretation of data was excluded.

## 2.6 | Immunofluorescence

Snap-frozen biopsies from 6 wt and 6 HLA-E/hCD46 transgenic limbs were collected before and at the end of the perfusions (720 minutes) (a total of 24 biopsies), cut into 5-µm-thick sections, air-dried, and stored at -80°C until analysis. After fixation with acetone and rehydration,

**TABLE 1** Antibodies used in phenotype analysis by flow cytometry

| Specificity | Marker         | Clone     | Fluorochrome <sup>a</sup> | Source <sup>b</sup> |
|-------------|----------------|-----------|---------------------------|---------------------|
| Pig         | CD1a           | 76-7-4    | PE                        | SouthernBiotech     |
|             | CD3a           | BH23 B8-6 | PE                        | Novus Biologicals   |
|             | CD11b (CD11R3) | 2F4/11    | FITC                      | AbD Serotec         |
|             | CD14           | MIL2      | FITC                      | AbD Serotec         |
|             | CD16           | G7        | PE                        | AbD Serotec         |
|             | CD45           | K252 B7   | FITC, Dylight405          | AbD Serotec         |
|             | CD106          | 10.2C7    | Purified, PE              | Homemade            |
|             | CD172a (SWC3)  | BL1H7     | FITC                      | AbD Serotec         |
|             | SLA-I          | SCR3      | Purified, PE              | Homemade            |
|             | SLA-1          | 7/11-10   | Purified                  | VMRI <sup>c</sup>   |
|             | Pig and human  | CD31      | LC1-4                     | FITC                |
| Human       | CD45           | HK10      | PerCP-Cy5.5               | Biologend           |
|             | CD3            | UCTH11    | AF405                     | Life Technologies   |
|             | CD56           | HCD56     | BV605                     | Biologend           |
|             | CD19           | LT        | FITC                      | Miltenyi            |

AF405, Alexa Fluor<sup>®</sup>405; BV605, Brilliant<sup>™</sup>Volet<sup>™</sup>605; FITC, fluorescein isothiocyanate; PE, phycoerythrin; PerCP-Cy5.5, peridinin-chlorophyll protein cyanin 5.5.

<sup>a</sup>Directly labeled monoclonal antibodies were used for staining unless otherwise indicated. For indirect staining, secondary polyclonal goat anti-mouse antibody was used (IgG-PE, Poly4053, Biologend).

<sup>b</sup>Addresses of antibody distributors are as follows: AbD Serotec (Auchheim, Germany); Biologend (Luxem, Switzerland); Life Technologies (Dase, Switzerland); Miltenyi (Dergisch Gladbach, Germany); Novus Biologicals (Cambridge, UK); Southern Biotech (Birmingham, Switzerland); VMRI (Pullman, WA, USA).

the sections were stained with anti-human NKp46 (2 µg/mL, clone 195314, R&D Systems, Zug, Switzerland), a marker previously shown to identify human NK cells in frozen biopsies,<sup>27</sup> by indirect immunofluorescence using goat anti-mouse IgG conjugated with Alexa Fluor<sup>®</sup>546 (Molecular Probes, Carlsbad, CA, USA) as secondary antibody. Nuclei were stained using 4',6-diamidino-2-phenylindole (DAPI, Boehringer, Ingelheim, Germany). The slides were analyzed using a DMI4000 B fluorescence microscope (Leica, Heerbrugg, Switzerland) in different fields. At BL, 1 field was analyzed in 5 wt and 6 CD46/HLA-E tg limb biopsies. Whereas at the end-point, 1-3 fields per biopsy from independent wt perfusions and 2 fields per biopsy in the case of CD46/HLA-E tg limb perfusions were acquired. In summary, at BL, 5 fields were obtained from 5 different wt animals, and 6 fields from 6 different CD46/HLA-E animals, whereas at the end-point, a total of 11 fields were analyzed from 6 different wt biopsies and 12 fields from 6 different CD46/HLA-E tg limbs. Fluorescence intensity quantification was measured as raw integrated density by ImageJ software (version 10.2, National Institutes of Health) on non-manipulated TIFF images.<sup>30,39</sup>

## 2.7 Cells

Primary pEC were derived from pigs of different genetic background (wild-type, wt; hCD46; and HLA-E/hCD46 double-transgenic animals; respectively, see Weiss et al<sup>24</sup>). Cells were cultured in DMEM/GlutaMAX<sup>™</sup> medium (Gibco-BRL, Basel, Switzerland) supplemented with 10% heat-inactivated fetal calf serum (Sigma, Buchs, Switzerland), 100 U/mL penicillin, 100 µg/mL streptomycin (Gibco-BRL), and 0.8% endothelial cell growth medium II supplement mix (PromoCell, Baar, Switzerland) in a humidified atmosphere, at 37°C and 5% CO<sub>2</sub>. Polyclonal human NK cells were purified from 4 different healthy donors by negative magnetic bead selection according to the manufacturer's instructions (Miltenyi, Bergisch Gladbach, Germany) and expanded in the presence of 100 U/mL IL-2 as previously described.<sup>5</sup>

## 2.8 Direct NK cytotoxicity

Cytotoxicity was analyzed using the non-radioactive Delfia assay (PerkinElmer, Schwerzenbach, Switzerland) according to the

manufacturer's instructions.<sup>40</sup> IL-2-expanded human NK cell lines were used as effector cells. Target cells consisted of primary pEC derived from human CD46 (hCD46) tg, HLA-E/hCD46 double tg, or wt pigs. Labeling of cells with the non-radioactive BAFTA was previously optimized. Specific target cell lysis was calculated by subtracting background lysis (spontaneous lysis) of target cells in the absence of effector cells and the maximum release (100%) induced by detergent (Triton X-100) according to the following formula:

$$\text{Specific lysis(\%)} = \frac{\text{experimental} - \text{spontaneous}}{\text{maximum} - \text{spontaneous}} \times 100$$

Different effector to target ratios (E:T) was examined in 2 hours assay.

## 2.9 | Statistical analysis

Analysis was performed using GraphPad software, version 6 (GraphPad, La Jolla, CA, USA). Two-way ANOVA (considering pig genetic background and perfusion time as analysis factors) followed by multiple comparisons was performed in time-course experiments. For in vitro functional assays, a one-way ANOVA was used. Sidak's multiple comparison post-test was applied comparing groups at given perfusion time points. Significance is indicated by \*\*\* extremely significant,  $P < .001$ ; \*\* very significant,  $P < .01$ ; \* significant,  $P < .05$ ; and ns not significant,  $P \geq .05$ .

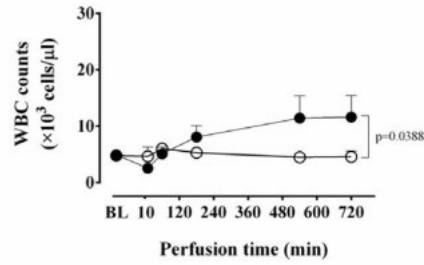
## 3 RESULTS

### 3.1 | Total white blood cell counts do not decrease during xenoperfusion

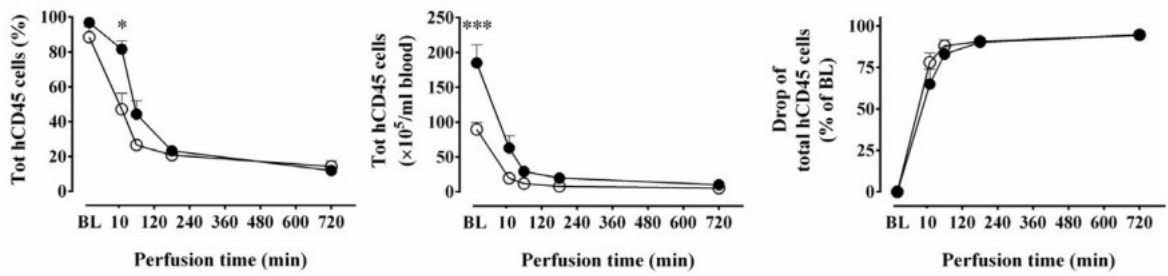
Perfusion of wt pig limbs with human blood did not induce significant changes in total WBC counts (Figure 1A). In contrast, when human blood was used to perfuse HLA-E/hCD46 tg pig limbs, we noted a significant increase in WBC counts after 720 minutes (from  $4.9 \times 10^3$  to  $11.6 \times 10^3/\mu\text{L}$ ,  $P < .05$ ). A small albeit statistically significant difference in WBC counts was detected between wt and tg limbs ( $P = .0388$ ). Control autologous perfusions with pig blood did not show an increase in total WBC counts, although the blood of tg animals contained higher levels of WBC at BL (Fig. S2).

**FIGURE 1** Time-course of circulating human CD45-positive leukocytes during perfusion. Blood samples were taken at predefined time points during ex vivo xenoperfusions. (A) Pooled data of total WBC counts as quantified by the Sysmex system during 6 wt and 6 HLA-E/hCD46 tg pig limb xenoperfusions are shown. The difference of total WBC counts in xenoperfusions between wt and HLA-E/hCD46 tg pig limbs was slightly significant,  $P < .0388$ , when tested by 2-way ANOVA. (B) For flow cytometry, PBMC were isolated and stained for viability followed by monoclonal antibody staining. The gating strategy for the analysis of viable human CD45<sup>+</sup> (hCD45) PBMC is shown in Fig. S1. Pooled data of the percentages of hCD45 PBMC (left plot); of the absolute numbers of hCD45 cells (middle plot); and the percentages of the drop of hCD45 cells numbers compared to base line values (right plot) are shown over time. (C) Pooled data of the percentages of human lymphocytes (left plot); of the absolute numbers of human lymphocytes (middle plot); and the percentages of the drop of human lymphocytes numbers compared to base line values (right plot) are shown over time. Data are shown as mean±SEM of 6 wt and 5 HLA-E/hCD46 pig limb perfusions. Wild-type (wt) limbs are shown with open circles (○), whereas HLA-E/hCD46 with filled circles (●). Differences between wt and HLA-E/hCD46 tg were obtained using 2-way ANOVA. Sidak's multiple comparison post-test was applied comparing groups at given perfusion time points. Significance is indicated by \*\*\*\* extremely significant,  $P < .001$ ; \*\* very significant,  $P < .01$ ; \* significant,  $P < .05$ . (D) Representative hCD45 and side scatter (SSC) flow cytometry plots during a HLA-E/hCD46 tg pig limb xenoperfusion are shown. Thick lined rectangles indicate total hCD45 cells and ovals lymphocytes; the respective percentages are given as numbers

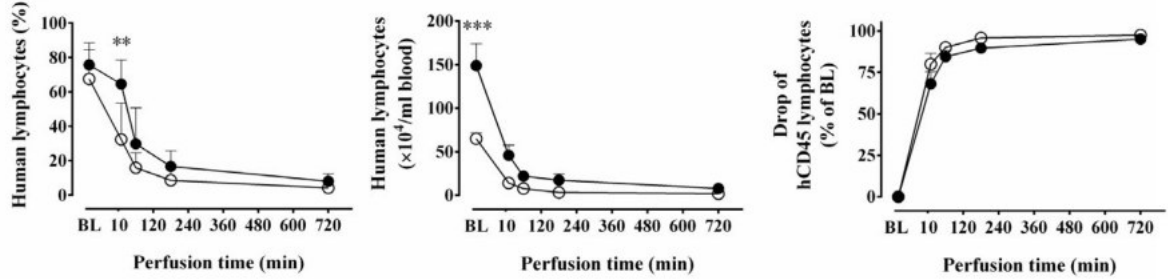
(A)



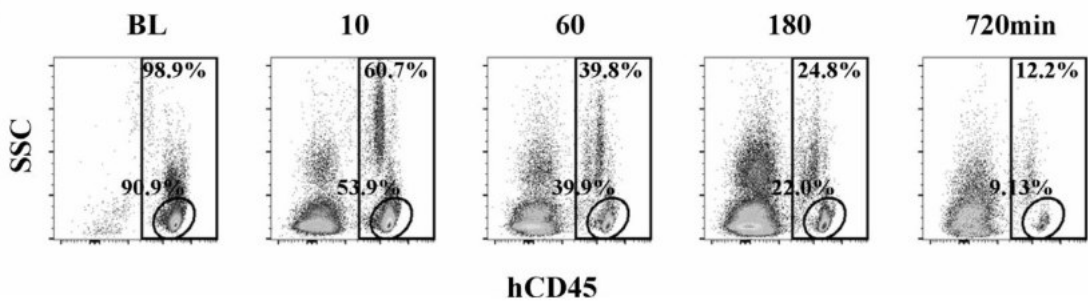
(B)



(C)



(D)





### 3.2 | Rapid consumption of circulating human leukocytes during xenoperfusion

To directly address the question whether human leukocytes decreased and were replaced by porcine cells during xenoperfusions, PBMC obtained from serial blood samples were analyzed by flow cytometry. The percentages of hCD45 cells in the viable PBMC gate revealed a striking drop over time ( $P < .001$ ) with a small, albeit statistically significant difference ( $P = .0229$ ) between limbs from wt and HLA-E/hCD46 pigs (Figure 1B, left plot). At baseline (BL), nearly 90% of the viable cells stained positive for hCD45, whereas after 720 minutes, the percentage of hCD45 PBMC was below 14%. This decrease became highly significant compared to BL after 60 minutes of perfusion of HLA-E/hCD46 tg pig limbs ( $P < .001$ ), in contrast the difference was already highly significant after only 10 minutes of perfusion of wt limbs ( $P < .001$ ). Next, we compared the absolute numbers of hCD45 cells over time (Figure 1B, middle plot) and calculated the relative drop of total hCD45 cells compared to BL (Figure 1B, right plot). For the relative drop of total hCD45 cells, no differences were found at any time-point between xenoperfusions of limbs from wt or HLA-E/hCD46 tg pigs. Moreover, human lymphocytes defined as  $SSC^{low}/hCD45$  PBMC declined in a similar manner as hCD45 cells (Figure 1C). Plotting of hCD45 vs SSC illustrated the presence of more

granular human cell populations including monocytes, contaminating neutrophils, and presumably early apoptotic cells, as well as cells of non-human origin appearing during xenoperfusions (Figure 1D). The quality of several blood samples, especially after many hours of perfusion, was compromised and showed signs of hemolysis and cell aggregates. Consequently, the numbers and purity of the recovered cells after Ficoll isolation revealed significant variations of neutrophil contaminations and apoptotic cells (Table S1 and data not shown).

### 3.3 | Recruitment of NK cells during xenoperfusion

One of the major aims of this study was to investigate whether the expression of HLA-E protects the endothelium of the perfused limbs from NK cell recruitment and NK cell-mediated damage, as previously demonstrated *in vitro*.<sup>24</sup> Therefore, NK cell percentages, defined by  $CD3^+CD56^+$  expression in the viable lymphocyte gates, and absolute NK cell numbers, calculated as described in the material and methods section, were analyzed during pig limb perfusions and compared to the BL values. Due to the random assignment of the blood, HLA-E/hCD46 tg pig limb perfusions were in most cases performed with a higher initial percentage and overall higher numbers of NK cells (Figure 2A). The percentage of NK cells revealed a striking drop over time (Figure 2B, left plot). Next, we analyzed the absolute numbers of NK cells during

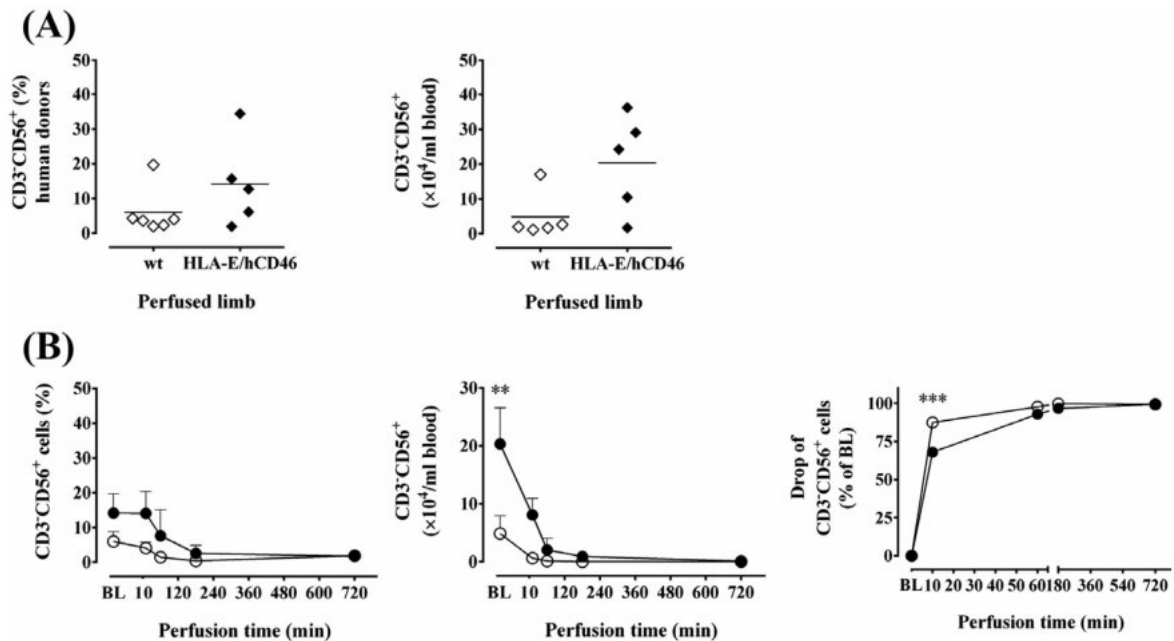


**FIGURE 2** Human NK cells are quickly removed from the circulation during xenoperfusion. Blood samples were taken at predefined time points during *ex vivo* xenoperfusions. PBMC were isolated and stained for viability followed by monoclonal antibody staining. (A), The percentages (left plot) and absolute numbers (right plot) of  $CD3^+CD56^+$  NK cells at baseline (BL) of wt (open diamonds,  $\diamond$ ) and HLA-E/hCD46 tg (filled diamonds,  $\blacklozenge$ ) xenoperfusions are shown, indicating the variability among different blood donors. The difference was tested by *t* test ( $P = .052$ ). (B), Pooled data of the percentages of NK cells (left plot); of the absolute numbers of NK cells (middle plot); and the percentages of the relative drop of NK cell numbers compared to BL values (right plot) are shown over time. Pooled data are shown from 4 and 3 xenoperfusions for wt and HLA-E/hCD46 pig limbs, respectively. Data shown as mean + SEM. Wild-type (wt) limbs are shown with open circles (o), whereas HLA-E/hCD46 is shown with filled circles (●). Differences between wt and HLA-E/hCD46 tg were obtained using 2-way ANOVA. Sidak's multiple comparison post-test was applied comparing groups at given perfusion time points. Significance is indicated by \*\*\* extremely significant,  $P < .001$ ; \*\* very significant,  $P < .01$

perfusion (Figure 2B, middle plot) and calculated the relative drop of NK cells compared to BL (Figure 2B, right plot). These data showed a significant difference in the early consumption of circulating NK cells between wt and HLA-E/hCD46 tg limbs 10 minutes after xenoperfusion ( $P < .001$ ). At 720 minutes, an almost complete absence of human NK cells was noted, without any difference between wt and HLA-E/hCD46 tg limb perfusions. Similar results were obtained when the absolute NK cells numbers were estimated using the results of WBC counts obtained by Sysmex system (data not shown). In brief, NK cells disappeared quickly from the circulation, slightly more rapidly during xenoperfusions of wt as compared to HLA-E/hCD46 tg pig limbs.

### 3.4 | Reduced recruitment of human NK cells into HLA-E/hCD46 transgenic pig muscle tissue

To determine the fate of the human NK cells which disappeared from the circulation during xenoperfusions, snap-frozen muscle biopsies taken at BL and the end-point at 720 minutes were analyzed by immunohistochemistry using the NK cell marker NKp46. As compared to CD56, NKG2A, and NKG2D, NKp46 (NCR1) is by far the best tissue NK cell marker reported in the literature. Whereas BL samples revealed only background staining, infiltrating NK cells were demonstrated after 720 minutes of perfusion (Figure 3A). Quantification of these NKp46-positive cells at 720 minutes using ImageJ software indicated lower recruitment of NK cells into HLA-E/hCD46 tg limbs as compared to wt pig limbs ( $P < .05$ ); however, more damaged wt tissue might have given rise to higher unspecific background staining (Figure 3B).

### 3.5 | Human NK cytotoxicity against pig endothelial cells derived from HLA-E/hCD46 double- and hCD46 single-transgenic pigs

To evaluate the relative effect of HLA-E and hCD46 expression on xenogeneic NK cytotoxicity, lysis of primary pEC isolated from pigs of different genetic background was tested. A representative experiment and pooled data from 3 independent experiments performed at ET ratios from 40:1 to 5:1 are shown (Figure 4). No differences were observed between the lysis of wt and hCD46 single tg pEC; however, HLA-E/hCD46 double tg pEC were partially protected from NK cytotoxicity. Overall, the difference of NK cytotoxicity found between pEC targets of wt vs HLA-E/hCD46 tg origin was highly significant, with 64.3% less NK cytotoxicity compared to wt ( $P < .001$ ), whereas lysis of hCD46 tg pEC did not differ from lysis of wt pEC. Thus, hCD46 expression on pEC did not alter human anti-pig xenogeneic NK cytotoxicity, whereas expression of HLA-E in combination with hCD46 reduced the lysis of pEC equally to HLA-E expression alone, as previously shown.<sup>13-21</sup>

### 3.6 | Emergence of pig cells into the circulation during perfusion

Next, hCD45<sup>pos</sup> cells of non-human origin were analyzed in blood samples taken at BL and 180 minutes by staining with a panel of antibodies directed at pig surface markers. Indeed, after 180 minutes of

xenoperfusion, pig CD45-positive (pCD45) PBMC were detected, as shown in a representative experiment in Figure 5A. To further characterize the phenotype of these cells, viable PBMC were gated as shown in Figure 5B. Three pCD45 cell populations, all of them negative for hCD45, were defined and distinguished according to their cellular granularity: (i) low granularity cells corresponding to pig lymphocytes (48%); (ii) intermediate granularity cells corresponding to pig monocytes (33%); (iii) and high granularity cells corresponding to pig granulocytes (14%), respectively. The phenotyping results of these populations are presented as percentages of expression in Table 2.

Population A, strongly resembling lymphocytes according to pCD45 vs SSC plotting, was predominantly positive for pig MHC class I (SLA-I, 88%) and expressed variable amounts of lymphocyte subset markers corresponding to T cells (CD3a<sup>+</sup>, 21%), NK cells (pCD16<sup>+</sup>CD172a<sup>-</sup>, 10%),<sup>11</sup> and a B-cell subpopulation (CD1a<sup>+</sup>, 9%). There was a modest contamination of myeloid cells, monocytes and granulocytes, respectively (CD14<sup>+</sup>, 2.7%; CD11R3<sup>+</sup>, 2.7%; pCD172a<sup>+</sup>, 13%). However, this analysis did not account for approximately 40% of the cells present in population A.

Population B, strongly resembling monocytes based on pCD45 vs SSC plotting, was predominantly positive for pig MHC class I (SLA-I, 83%), the myeloid markers CD11R3 (76%), pCD14 (84%) and exhibited double expression of pCD16 and CD172a (82%). In addition, this population contained small numbers of circulating porcine endothelial cells which were double-positive for pCD106 and CD31 (8.6%).

Population C, with the highest granularity, was positive for pig granulocyte markers including CD11R3 (73%); pCD172a (99%); only subsets of these granulocytes expressed pCD16 (54%) and pCD14 (65%), respectively. Intriguingly, 43% of the cells were SLA-I negative, indicating either the presence of MHC class I negative granulocytes, the loss or low expression of this marker, or technical staining artifacts. Furthermore, staining for circulating pCD106<sup>+</sup>CD31<sup>+</sup> porcine endothelial cells was detected on 7% of the cells.

In conclusion, the large majority of the pig cells emerging during limb perfusions expressed various lymphocyte subsets and myeloid markers, whereas only a small percentage represented endothelial cells.

## 4 | DISCUSSION

The primary aim of the current study was to test the potential of transgenic HLA-E expression on pig endothelial cells to control human NK cell recruitment during *ex vivo* pig limb xenoperfusions. Early studies with rat and pig hearts perfused with human blood or lymphocytes demonstrated recruitment of human NK cells into the xenoperfused hearts<sup>25,26</sup> and were supported later by the findings of xenoperfused pig kidneys.<sup>24,27</sup> Of note, the current xenoperfusion model is performed on pig limbs expressing alpha-Gal xenoantigen. To control xenoantibody-mediated endothelial damage via complement activation, pigs transgenic for human CD46 in addition to HLA-E were used as previously reported.<sup>25</sup> In the latter experiments, xenoperfusions of HLA-E/hCD46 double tg limbs were characterized by less

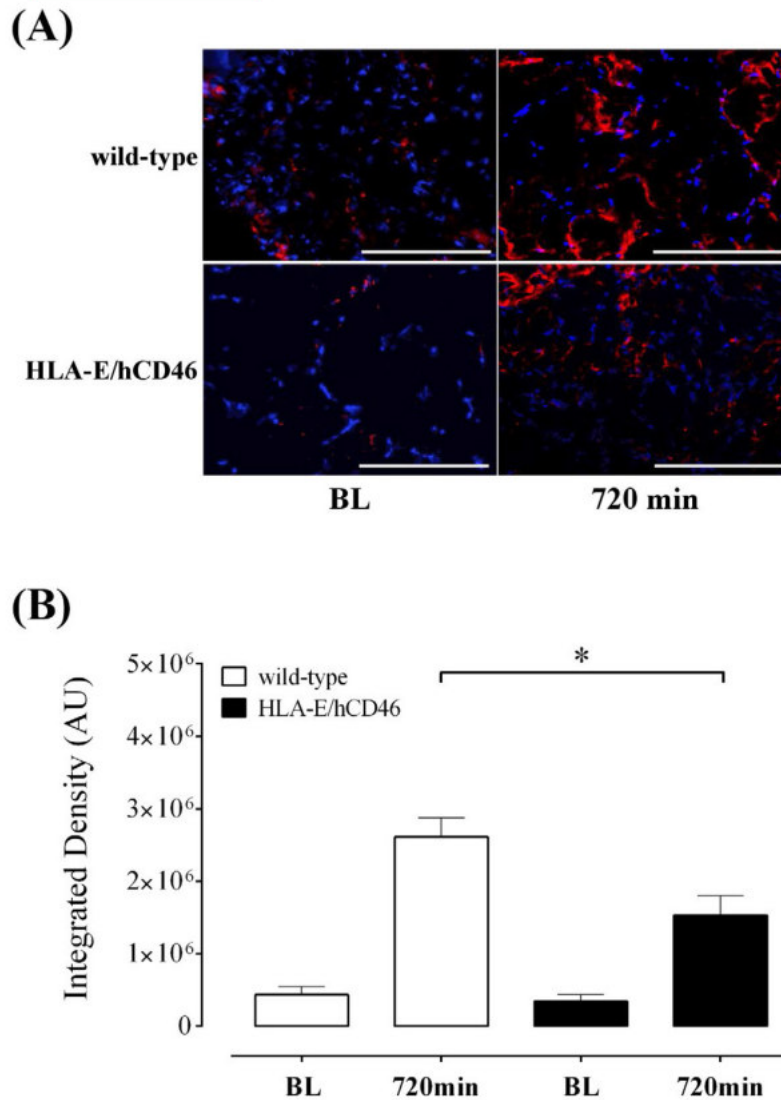


**FIGURE 3** Recruitment of human NK cells in pig muscle tissue. Muscle biopsies from wt and HLA-E/hCD46 tg pig limbs were obtained at BL and at the end-point (720 minutes) of the xenoperfusions and snap-frozen until analysis. NK cells were stained using the specific NK cell surface marker NKp46 followed by secondary goat anti-mouse Alexa Fluor<sup>®</sup> 546 (red), whereas nuclei were revealed with DAPI (blue). (A), Representative images from biopsies taken at BL and end-point in wt and HLA-E/hCD46 double tg limbs are shown. White bars correspond to 75  $\mu$ m. (B), Quantification of fluorescence intensity of integrated density (y-axis) analyzed by ImageJ software on non-manipulated raw TIFF images (11 different fields for each type of limbs, wt and tg, at end-point and 5 different fields at BL). Data shown as mean + SEM, and two-way ANOVA followed by multiple comparisons showed \* significant differences  $P < .05$  between groups

complement deposition and endothelial cell activation, as shown by E-selectin and VCAM-1 expression, and preserved endothelial integrity, as shown by heparin sulfate proteoglycan and VE-cadherin staining. Compared to wt limbs, HLA-E/hCD46 tg porcine tissue was partially protected from tissue damage and xenoperfusion-induced apoptosis, as demonstrated in muscle biopsies at the end-point (720 minutes). Furthermore, the release of inflammatory porcine cytokines, including IL-1 $\beta$ , IL-6, IL-8, and thrombin anti-thrombin complexes, into the plasma, was lower when HLA-E/hCD46 limbs were perfused.<sup>35</sup>

In the present study, we show that the numbers of circulating hCD45 cells rapidly decreased during xenoperfusions. Further characterization of the fate of hCD45 subpopulations by flow cytometry revealed a faster removal of NK cells from the circulation at early time points during perfusion of wt limbs, as compared to HLA-E/hCD46 tg limb perfusions. These findings were corroborated by the analysis of end-point muscle biopsies, demonstrating a lower density of NK cell infiltration in HLA-E/hCD46 tg limbs. In the latter experiments, the cellular marker to characterize human NK cells infiltrating pig



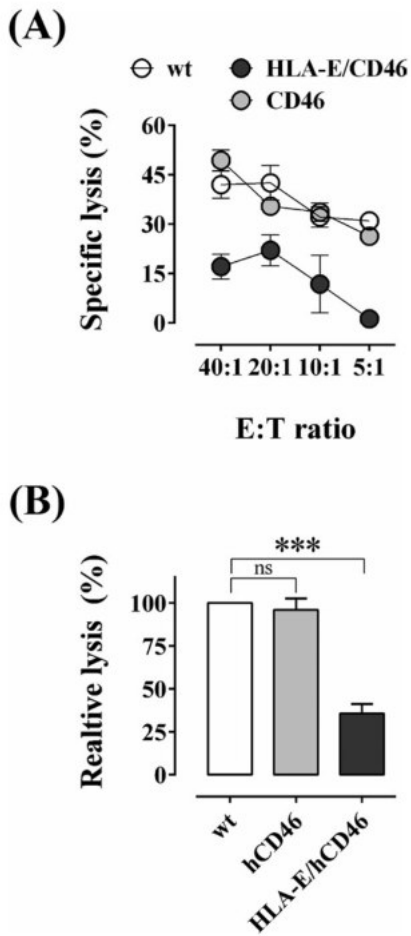


**FIGURE 4** HLA-E expression but not hCD46 expression on pig endothelial cells provides partial protection against xenogeneic human NK cytotoxicity in vitro. (A), Porcine endothelial cells (pEC) derived from wt; hCD46 and HLA-E/hCD46 tg animals were labeled and used as target cells in 2 h non-radioactive Delfia cytotoxicity assays using polyclonal human NK cell lines as effector cells. Data of 1 representative experiment are presented at different effector to target (E:T) ratios showing mean values  $\pm$  SD of triplicates. Specific target cell lysis was calculated by subtracting background lysis of target cells in the absence of effector cells and the maximum release (100%) induced by detergent (Triton X-100) according to the formula provided in the material and methods. (B), Pooled data from 3 independent experiments with mean  $\pm$  SEM are shown; one-way ANOVA revealed a \*\*\* highly significant difference,  $P < .005$ , of the relative inhibition of NK lysis against HLA-E/hCD46 tg pEC target cells as compared to wt pEC

tissues was carefully chosen. The conventional NK cell marker CD56 was immediately discarded as it is expressed in muscle tissue, and there might be cross-reactivity between species. NKp46 (NCR1) is by far the best tissue NK cell marker reported in the literature,<sup>43</sup> and a protocol to stain snap-frozen tissue is available. In general, all NK cells express NKp46; at least 80% are NKp46<sup>bright</sup> and the other 20% NKp46<sup>dull</sup>. As to NKG2A and NKG2D, tissue staining protocols have

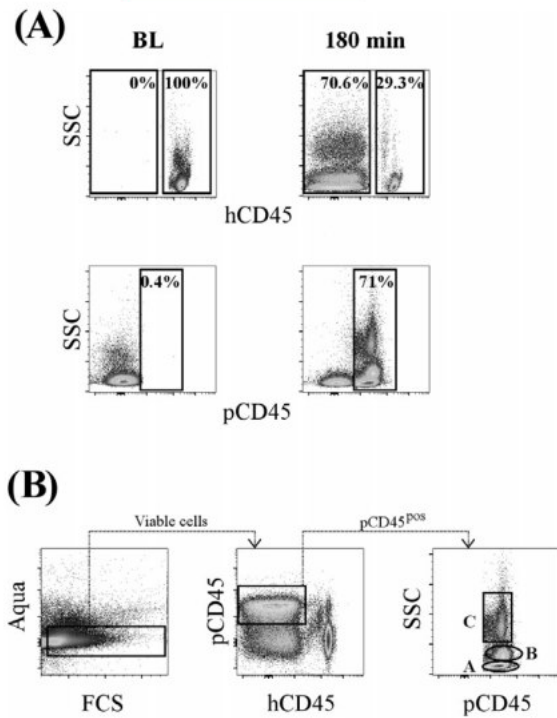


**FIGURE 5** Pig cells are released into the circulation during xenoperfusion. Whole blood samples were taken at different time points during xenoperfusion; peripheral blood mononuclear cells (PBMC) were isolated and stained for viability followed by monoclonal antibody staining. (A), Representative plots of pig CD45 (pCD45) and human CD45 (hCD45) vs side scatter (SSC) are shown for the analysis of PBMC coming from the same experiment isolated at 2 different time points: baseline (BL) and 180 minutes after starting the xenoperfusion of a HLA-E/hCD46 forelimb. (B), Gating strategy used for flow cytometry analysis of pig marker expression during xenoperfusion at time-point 180 minutes. Cells were first gated for viability by plotting forward scatter (FCS) vs LIVE/DEAD<sup>®</sup> Fixable Aqua Dead Cell stain (left plot). Viable cells were next plotted for hCD45 vs pCD45 to discard cell conjugates and cellular debris and select only pCD45 single positive cells (middle plot). Finally, pCD45 vs SSC plot was generated and pig cells populations defined on the base of their cytometric properties, referred to as population A, B, and C, respectively (right plot), from which different pig markers were further analyzed as shown in Table 2

not been established and they are less specific for NK cells since also expressed on CD8 T cells. Double tissue staining, although of potential interest, was not envisioned for this study due to a lack of established protocols. Finally, a small number of NKp46-positive cells were detected in pig heart biopsies stemming from healthy hearts or myocardial infarction experiments and muscle biopsies taken at the end-point of pig limbs perfused with autologous blood in areas of tissue damage but not in healthy tissues. The anti-NKp46 antibody clone 195314 used for tissue staining demonstrated cross-reactivity with porcine lymphocytes (data not shown). However, the intensity of NKp46<sup>+</sup> staining on damaged tissue was much lower than after

**TABLE 2** Phenotypic characteristics of the pig cell populations appearing during xenoperfusion

| Marker                                  | Associated phenotype, alternative name                   | Population Positive cells, % (SD) |             |             |
|---|--|-----------------------------------|-------------|-------------|
|   |  | A                                 | B           | C           |
| pCD45 <sup>+</sup> vs SSC               | Pig leukocytes, LCA                                      | 47.7 (14.8)                       | 32.8 (10.0) | 14.3 (8.9)  |
| SLA I <sup>+</sup>                      | Pig cells <sup>a</sup>                                   | 87.6 (10.8)                       | 82.6 (10.7) | 57.2 (21.9) |
| CD11b <sup>+</sup>                      | Monocyte/granulocyte, possibly CD11b                     | 2.7 (1.5)                         | 77.5 (10.0) | 74.5 (27.7) |
| pCD172a <sup>+</sup>                    | Myeloid lineage <sup>b</sup> , SIRP <sup>c</sup> or SWC1 | 13.1 (4.3)                        | 88.7 (5.2)  | 99.4 (0.6)  |
| pCD16 <sup>+</sup>                      | TCR3A  | 12.2 (12.3)                       | 83.3 (7.0)  | 53.5 (30.2) |
| pCD14 <sup>+</sup>                      | Monocyte/granulocyte                                     | 2.7 (0.8)                         | 87.3 (7.0)  | 67.6 (27.4) |
| pCD3a                                   | T cell <sup>d</sup>                                      | 21.3 (41.6)                       | 2.9 (4.0)   | 1.6 (1.8)   |
| pCD1a <sup>+</sup>                      | Fraction of B cells <sup>e</sup>                         | 9.1 (3.1)                         | 7.0 (2.6)   | 7.6 (1.8)   |
| pCD16 <sup>+</sup> pCD172a <sup>+</sup> | NK cells <sup>f</sup>                                    | 9.7 (10.9)                        | 1.3 (0.0)   | 0.16 (0.0)  |
| pCD16 <sup>+</sup> pCD172a <sup>+</sup> | Monocytes  | 2.6 (1.6)                         | 82.0 (6.6)  | 55.5 (30.1) |
| pCD106 CD31                             | Endothelial cells <sup>g</sup>                           | 2.1 (0.6)                         | 8.6 (6.5)   | 7.1 (4.7)   |

LCA, leukocyte common antigen.

Flow cytometry analysis of PBMC isolated after 180 minutes of human blood xenoperfusion. Cell populations were gated as described in Figure S8 and percentage of positive cells shown as % (SD). Data obtained from 4 independent experiments (2 wt and 2 tg pig legs).

In bold, parameters used to define populations A, B and C.

<sup>a</sup>Pig cells are SLA I positive with the exception of red blood cells and platelets.

<sup>b</sup>When surface markers looked up in large and complex populations.

<sup>c</sup>When surface marker is looked up in the lymphocyte gate.

<sup>d</sup>When surface markers are looked up in large and complex populations.

xenoperfusions and the numbers of circulating pig NK cells did not differ between wt and tg perfusions (table 2 and data not shown). Thus, our observation in xenoperfusion experiments of significantly lower numbers of NKp46<sup>+</sup> NK cells in muscle biopsies from hCD46/HLA-E transgenic limbs perfused with human blood compared to wt limbs indicates that hCD46/HLA-E expression inhibits human NK cell infiltration predominantly directly and to a minor degree due to the prevention of tissue damage and consequent non-xeno-related pig/human NK cell infiltration. Taken together, HLA-E expression slightly delayed the recruitment and ultimately decreased tissue infiltration of human/porcine NK cells into pig limb tissues after 12 hours of perfusion.

There are several limitations of the current study including the lack of hCD46 single-transgenic forelimb perfusions as controls. However, in vitro data by us and others did not show any effect of CD46 expression on NK cytotoxicity against pEC. Importantly, a recently published ex vivo pig lung xenoperfusion study by Laird et al<sup>20</sup> corroborates our findings by clearly showing physiologically meaningful protection from NK cell-mediated damage by GalTKO.hCD46.HLA-E expression using GalTKO.hCD46 lungs as control. In addition reduced NK cell recruitment was also observed in the Munich heart model.<sup>25,26</sup> Moreover, due to the restricted volume of blood donations, we could not perfuse both wt and HLA-E/hCD46 tg pig limbs in parallel with blood obtained from the same donor. Since the proportion of NK cells within the lymphocyte population (0.61%–16.87%) varies enormously among healthy donors,<sup>46</sup> we analyzed the relative drop of NK cell numbers. For the same reason, quantitative analysis of tissue infiltration by NK cells was difficult to interpret. However, despite the fact that HLA-E/hCD46 tg pig

limbs were in general perfused with blood containing higher numbers of NK cells, we observed less NK cell tissue infiltration using NKp46 staining of frozen sections, although the software used quantifies fluorescence intensity, rather than counting individual NK cells.

By all means, our findings beg the question: Where are these NK cells which disappeared completely from the circulation after 720 minutes of perfusion? In contrast to HLA-G, HLA-E does not affect adhesion of human NK cells to pEC, as shown in static and dynamic adhesion assays.<sup>14,30,35</sup> In addition, we have previously reported that transmigration of human NK cells through pig endothelium depends on hCD49d-pCD106 interactions<sup>47</sup> and on hCD99 interactions with so far unknown ligands expressed by pEC.<sup>48</sup> In light of reduced endothelial cell activation during HLA-E/hCD46 tg compared to wt pig limb xenoperfusion,<sup>35</sup> which was associated with lower expression of pCD106, we hypothesize that human NK cells might adhere to the vascular lining of HLA-E/hCD46 tg pig limbs, but transmigrate to a lesser extent into these tissues. Finally, the relative percentages of human B- and T lymphocytes showed no major differences between wt and HLA-E/hCD46 tg xenoperfusions (data not shown), with a reduction in B cells after 3 hours of perfusion, as reported previously in a model of short-term kidney xenoperfusion.<sup>24</sup>

Although there are major differences in terms of endothelial damage during short-term xenoperfusions reported in the literature, in part because different pig organs were employed,<sup>47,51</sup> and the exact contribution of NK cells is unknown, the expression of HLA-E might reduce endothelial damage by preventing NK cell activation. We cannot directly support this hypothesis with experimental data from our model, since the functional assays originally planned with circulating

NK cells obtained during xenoperfusions could not be performed due to very low NK cell numbers. However, in agreement with previous work,<sup>19,21,22,57,58</sup> human anti-pig NK cytotoxicity assays, performed *in vitro* using pEC derived from tg animals as targets, confirmed that HLA-E provided partial protection, whereas the expression of hCD46 had no effect. Furthermore, since NK cells are able to perform FcR-mediated ADCC and neutrophils/macrophages eliminate antibody-coated cells, differences in xenoreactive antibody levels in the blood donors and differential binding to the tg endothelium might have influenced the results. Previous data of the same study have shown that overall human IgM and IgG natural xenoreactive antibodies bind equally to the endothelia of both, wt and hCD46/HLA-E pig limbs after 12 hours of perfusion.<sup>42</sup> However, since the levels of natural xenantibodies in the donor blood samples were not measured, we cannot exclude that differences might have had an impact on NK cell-mediated ADCC and tissue damage.

To date, most studies have focused on the tissue recruitment of human leukocytes in *ex vivo* xenoperfusion models. Perfusion of pig lungs with human blood, for instance, showed a quick drop in WBC counts,<sup>52,53</sup> in particular for monocytes and neutrophils; both in wt animals,<sup>51,54</sup> but also using genetically modified animals.<sup>52</sup> Similar finding was reported for kidney and liver xenoperfusions.<sup>26,42,43,45</sup> In contrast, scarce information is available concerning the release of pig cells. An early publication indicated that porcine leukocytes, mainly lymphocytes, were released from pig kidneys during buffered-saline perfusion.<sup>14</sup> In addition, an increase in WBC counts was also observed during perfusions of pig hearts, although the nature of this rise was not further characterized.<sup>60</sup> At last, perfusion of pig lungs with different perfusion solutions showed the release of pig T- and B lymphocytes as well as monocytes, macrophages, and dendritic cells.<sup>51</sup> In summary, the nature of porcine cells released during xenoperfusion of different organs remains poorly characterized.

In our model of pig limb perfusion, the total circulating leukocyte counts did not decrease as measured by Sysmex not distinguishing between cells of human and pig origin. In contrast, hCD45 PBMC disappeared rapidly from the circulation, presumably due to recruitment and tissue infiltration. Thus, we hypothesized that pig cells were released into the circulation. Indeed, cells of pig origin were detected in the circulation using species-specific cell markers. First, we speculated that these pig cells might correspond to pEC released upon damage of the endothelium during xenoperfusion. Nonetheless, only a small percentage of these cells were of endothelial origin as shown by pCD106<sup>+</sup>CD31<sup>+</sup> expression. Instead, the large majority of the emerging pig cells expressed various lymphocyte and myeloid markers (CD172a, SIRP $\alpha$ , SWC3). Moreover, they were highly positive for SLA-I and pCD45, indicating that they belonged to the leukocyte lineage.<sup>22,47</sup> Despite flushing of the pig limbs for 5 minutes with hydroxyethyl starch before perfusion, these pig cells might have been released from the marginal vascular pool into the bloodstream by detachment from the endothelial lining. Alternatively, pCD45 cells might have been released from the pig bone marrow, since in contrast to organ perfusions, several bones are present in the pig forelimb model (humerus, radius, ulna, and

metacarpals). Lineage negative immature bone marrow cells might also explain the presence in the lymphocyte gate of approximately 40% SLA-I<sup>+</sup> pig cells that are not accounted for by staining with our antibody panel. In conclusion, the release of pig cells needs further investigation in xenoperfusion models of organs foreseen for clinical transplantation, for example, heart, kidney, or lung. Depending on the phenotype and antigen-presenting properties of these cells, even the release of much lower numbers into the circulation following transplantation has major implications for the development of acquired immune xenoresponses and/or tolerance.<sup>61, 62</sup> The protocols for flushing pig organs prior to perfusion or transplantation in order to remove cells might have to be optimized to minimize xenorejection.

In conclusion, the current work showed that HLA-E/hCD46 double tg pig limb perfusion is characterized by slightly delayed NK cell recruitment and reduced tissue infiltration. In addition, we describe and characterize a cell population of pig origin that was released into the circulation during the limb perfusions.

#### ACKNOWLEDGMENTS

The authors would like to thank to L. Grusz, L. Papadayachi and J. Pimenta for their technical help.

#### CONFLICT OF INTEREST

The authors of this manuscript declare no conflicts of interest to disclosure with the exception of DA who works for Revivicor Inc.

#### AUTHOR CONTRIBUTION

GPY provided research design, performed flow cytometry data acquisition, interpretation of data, and wrote the manuscript; AKB participated blood sampling and immunofluorescence analysis; AP conceptually designed and set-up the flow cytometry experiments and data analysis and drafted of the article; NM contributed with cytotoxicity experiments; MP substantial contribution for flow cytometry data acquisition; DA provided primary cells from human CD46 transgenic pigs for nuclear transfer experiments; EW, NK, AB produced HLA-E/hCD46 pigs and multiengineered pigs; EV and MAC participated in the concept and design of the animal experimentation; HJ and DK participated in performing the animal experimentation; RR participated in the concept and design of the study and critical review; JDS provided research design, participated in interpretation of data and writing of the manuscript, and approved the final submitted version.

#### ORCID

Gisella Puga Yung  <http://orcid.org/0000-0002-2283-7798>

Riccardo Friso  <http://orcid.org/0000-0002-3406-0736>

Robert Rieben  <http://orcid.org/0000-0003-4179-8891>

Jörg D. Seebach  <http://orcid.org/0000-0001-5748-4577>



## REFERENCES

- Cooper DK, Fazzalarab MR, Hara H, et al. The pathobiology of pig to primate xenotransplantation: a historical review. *Xenotransplantation*. 2016;23:83-105.
- Griscaner A, Yamada K, Sykes M. Xenotransplantation: immunological hurdles and progress toward tolerance. *Immunol Rev*. 2017;258:241-253.
- Vadori M, Cozzi E. Immunological challenges and therapies in xenotransplantation. *Cold Spring Harbor Perspect Med*. 2014;4:a015578.
- Satyanarula V, Hara H, Fazzalarab MR, et al. New concepts of immune modulation in xenotransplantation. *Transplantation*. 2011;96:937-945.
- Watzl C. How to trigger a killer: modulation of natural killer cell reactivity on many levels. *Adv Immunol*. 2017;127:137-170.
- Su F, van JA, Oettinger HF, Sachs DH, Filgue AS. Analysis of polymorphism in porcine MHC class I genes: alterations in signals recognized by human cytotoxic lymphocytes. *J Immunol*. 1997;159:2313-2326.
- Kwiatkowski P, Artrip JI, John R, et al. Induction of swine major histocompatibility complex class I molecules on porcine endothelium by tumor necrosis factor- $\alpha$  reduces lysis by human natural killer cells. *Transplantation*. 1999;67:211-218.
- Seebach JD, Courack C, Germana S, et al. HLA-Cw3 expression on porcine endothelial cells protects against xenogeneic cytotoxicity mediated by a subset of human NK cells. *J Immunol*. 1997;159:3655-3661.
- Sasali H, Xu XC, Smith DM, Howard T, Mohanakumar T. HLA-G expression protects porcine endothelial cells against natural killer cell-mediated xenogeneic cytotoxicity. *Transplantation*. 1999;67:311-317.
- Dorfling A, Monk NJ, Lech er RL. HLA-G inhibits the transendothelial migration of human NK cells. *Eur J Immunol*. 2003;33:586-591.
- Forte P, Matter-Reissmann UD, Strasser M, Schneider MK, Seebach JD. Porcine aortic endothelial cells transfected with HLA-G are partially protected from xenogenic human NK cytotoxicity. *Hum Immunol*. 2000;61:1066-1073.
- Matsunami K, Miyagawa S, Nakai R, Murase A, Shirakura R. The possible use of HLA-G1 and G3 in the inhibition of NK cell-mediated swine endothelial cell lysis. *Clin Exp Immunol*. 2003;126:165-172.
- Forte P, Pazmany L, Matter-Reissmann UH, et al. HLA-G inhibits rolling adhesion of activated human NK cells on porcine endothelial cells. *J Immunol*. 2001;167:6032-6038.
- Shar and A, Pate A, Lee JH, et al. Genetically modified HLA class I molecules able to inhibit human NK cells without provoking alloreactive CD8<sup>+</sup> CTLs. *J Immunol*. 2002;168:3266-3274.
- Forte P, Baumann BC, Schneider MK, Seebach JD. HLA-Cw4 expression on porcine endothelial cells reduces cytotoxicity and adhesion mediated by CD158a<sup>+</sup> human NK cells. *Xenotransplantation*. 2009;16:19-26.
- Strong RK, Holmes MA, Li P, et al. HLA-E allelic variants. Correlating differential expression, peptide affinities, crystal structures, and thermal stabilities. *J Biol Chem*. 2003;278:5082-5090.
- Hosseini E, Schwarzer AR, Ghasemzadeh M. Do human eulocyte antigen H polymorphisms influence graft versus leukemia after allogeneic hematopoietic stem cell transplantation? *Exp Hematol*. 2015;43:149-157.
- Sammlers PM, Vignani JP, O'Connor GM, et al. A bird's eye view of NK cell receptor interactions with their MHC class I ligands. *Immunol Rev*. 2015;267:143-166.
- Sasali H, Xu XC, Mohanakumar T. HLA-E and HLA-G expression on porcine endothelial cells inhibit xenoreactive human NK cells through CD94/NKG2-dependent and -independent pathways. *J Immunol*. 1999;163:6301-6305.
- Matsunami K, Miyagawa S, Nakai R, Yamada M, Shirakura R. Modulation of the leader peptide sequence of the HLA-E gene up-regulates its expression and down-regulates natural killer cell-mediated swine endothelial cell lysis. *Transplantation*. 2002;73:1582-1589.
- Crew MD, Cannon MJ, Phanavanh B, Garcia-Dorjes CN. An HLA-E single chain trimer inhibits human NK cell reactivity towards porcine cells. *Mol Immunol*. 2005;42:1205-1214.
- Forte P, Baumann BC, Weiss CI, Seebach JD. HLA-E expression on porcine cells: production from human NK cytotoxicity depends on peptide loading. *Am J Transplant*. 2005;5:2085-2093.
- Litfinfeld HG, Crew MD, Forte P, Baumann BC, Seebach JD. Transgenic expression of HLA-E single chain trimer protects porcine endothelial cells against human natural killer cell-mediated cytotoxicity. *Xenotransplantation*. 2007;14:126-137.
- Weiss CI, Lienfeld BG, Muller S, et al. HLA-E/human beta2-microglobulin transgenic pigs: protection against xenogenic human anti-pig natural killer cell cytotoxicity. *Transplantation*. 2009;87:35-43.
- Imvranovic L, Samaja M, Mollerini R, et al. Early recognition of a discordant xenogenic organ by human circulating lymphocytes. *J Immunol*. 1992;149:1416-1423.
- Khalilou H, Barral D, Walter H, et al. Development of an ex vivo model of pig kidney perfused with human lymphocytes. Analysis of xenogenic cellular reactions. *Surgery*. 2000;128:447-457.
- Ramos A, Vega A, Va G, et al. Immunohistochemical study of a new experimental model of acute cellular xenograft rejection. *Transplant Proc*. 2003;35:960.
- Laird CT, Durdorf L, French BM, et al. Transgenic expression of human leukocyte antigen F attenuates Gal $\alpha$ 1-3Gal $\beta$ 1-4 porcine lung xenograft injury. *Xenotransplantation*. 2017;24. <https://doi.org/10.1111/xen.12294>
- Kubicki N, Laird C, Durdorf L, et al. The effect of human leukocyte antigen-E expression on GalTKO/hCD46 lung xenograft survival and injury in an ex vivo xenoperfusion model. *Xenotransplantation*. 2015;22:193.
- Abichl JM, Bongoni AK, Mayr T, et al. Ex vivo perfusion of a pig Gal knockout, CD46/HLA-F double transgenic pig hearts. *Xenotransplantation*. 2015;22:5164.
- Strisio R, Abichl J, Mayr T, et al. Evaluation of immune activation after ex vivo xenoperfusion of GalTKO/hCD46/HLA-E transgenic pig hearts with human blood. *Xenotransplantation*. 2017;24:1232B. <https://doi.org/10.1111/xen.12328>
- Constantinescu MA, Knal E, Xu X, et al. Preservation of amputated extremities by extracorporeal blood perfusion: a feasibility study in a porcine model. *J Surg Res*. 2011;171:291-299.
- Bongoni AK, Kiermeir D, Schröder J, et al. Transgenic Expression of Human CD46 on Porcine Endothelium: effect on Coagulation and Fibrinolytic Cascades During Ex Vivo Human-to-Pig Limb Xenoperfusions. *Transplantation*. 2015;99:2061-2069.
- Dongon AK, Kiermeir D, Jenn H, et al. Activation of the lectin pathway of complement in pig to human xenotransplantation models. *Transplantation*. 2013;96:791-799.
- Bongoni AK, Kiermeir D, Jenn H, et al. Complement-dependent early immunologic responses during ex vivo xenoperfusion of hCD46/HLA-E double transgenic pig forelimbs with human blood. *Xenotransplantation*. 2014;21:230-241.
- Dongon AK, Kiermeir D, Denoyel E, et al. Porcine extrahepatic vascular endothelial  $\alpha$ - $\alpha$ 1-glycoprotein receptor 1 mediates xenogenic platelet phagocytosis in vitro and in human-to-pig ex vivo xenoperfusion. *Transplantation*. 2015;99:693-701.
- Halama N, Braun M, Kahlert C, et al. Natural killer cells are scarce in colorectal carcinoma tissue despite high levels of chemokines and cytokines. *Clin Cancer Res*. 2011;17:678-689.
- Abramoff MD, Magalhães PJ, Ram SJ. Image processing with ImageJ. *Biophotonics Int*. 2004;11:36-42.
- Schneider CA, Rasband WS, Hirtir KW. NIH Image to ImageJ: 25 years of image analysis. *Nat Methods*. 2012;9:671-675.
- Blumberg P, Haula R, Lovgren J, et al. Time-resolved fluorometric assay for natural killer cell activity using target cells labeled with a fluorochrome enhancing ligand. *J Immunol Methods*. 1996;193:199-206.

41. Saalmüller A. Characterization of swine leukocyte differentiation antigens. *Immunol Today*. 1996;17:352-354.
42. Kirk AD, Heinele JS, Mault JR, Sanfilippo T. Ex vivo characterization of human anti-porcine hyperacute cardiac rejection. *Transplantation*. 1993;56:785-791.
43. Kruse PII, Matta J, Ugojini S, Vyver E. Natural cytotoxicity receptors and their ligands. *Immunol Cell Biol*. 2017;92:221-229.
44. Angeo LS, Danerjee PP, Monaco-Shawver L, et al. Practical NK cell phenotyping and variability in healthy adults. *Immunol Res*. 2015;62:11-156.
45. Schneider MK, Strasser M, Giff UO, et al. Rolling adhesion of human NK cells to porcine endothelial cells mainly relies on CD135/CD136 interactions. *Transplantation*. 2002;73:789-796.
46. Schneider MK, Giff UO, M, Rhymer DM, Anstey MA, Scribner JD. Human leukocyte transmigration across Gal $\alpha$ 1,3Gal negative porcine endothelium is regulated by human CD18 and CD139. *Transplantation*. 2009;87:491-499.
47. Collins BL, Chari RS, Magee JC, et al. Mechanisms of injury in porcine livers perfused with blood of patients with fulminant hepatic failure. *Transplantation*. 1994;58:1162-1171.
48. Chari RS, Collins BL, Magee JC, et al. Brief report: treatment of hepatic failure with ex vivo pig liver perfusion followed by liver transplantation. *N Engl J Med*. 1994;331:234-237.
49. Magnusson S, Strolan V, Mohr J, et al. Blocking of human anti-pig xenoantibodies by soluble Gal $\alpha$ 1-3Gal and Gal $\alpha$ 1-2Gal disaccharides; studies in a pig kidney in vitro perfusion model. *Transpl Int*. 2000;13:102-112.
50. Linke R, Diefenbeck M, Friedrich R, Seehofer D, Hammer C. Monitoring of microhemodynamic changes during ex vivo xenogeneic liver perfusion using intravital microscopy. *Transpl Int*. 1998;11:259-265.
51. Nguyen HN, Azinwadeh AM, Schneider C, et al. Absence of Gal epitope prolongs survival of swine lungs in an ex vivo model of hyperacute rejection. *Xenotransplantation*. 2011;18:94-107.
52. Kim HK, Kim JH, Wl HC, et al. Ascorbic acid inhibits endothelial activation, complement activation, and von Willebrand factor secretion in vitro and attenuates hyperacute rejection in an ex vivo model of pig-to-human pulmonary xenotransplantation. *Xenotransplantation*. 2008;15:246-256.
53. Westal GP, Lavey BJ, Salazar F, et al. Sustained function of genetically modified porcine lungs in an ex vivo model of pulmonary xenotransplantation. *J Heart Lung Transplant*. 2011;32:1123-1130.
54. Durdorf L, Stoddard T, Zhang T, et al. Expression of human CD46 modulates inflammation associated with GalTKO lung xenograft injury. *Am J Transplant*. 2014;14:1030-1035.
55. Fiene AC, Molines TC, Videm V, et al. Compstatin, a peptide inhibitor of C3, prolongs survival of ex vivo perfused pig xenografts. *Xenotransplantation*. 1999;6:52-63.
56. Pascher A, Pohlén C, Storck M, et al. Immunopathological observations after xenogeneic liver perfusions using donor pigs transgenic for human decay-accelerating factor. *Transplantation*. 1997;64:384-391.
57. Pohlén C, Pascher A, Storck M, et al. Transgenic human DAF-expressing porcine livers: their function during hemoperfusion with human blood. *Transpl Int Proc*. 1996;28:770-771.
58. Rees MA, Butler AJ, Chavez-Cartaya G, et al. Prolonged function of extracorporeal hDAF-transgenic pig livers perfused with human blood. *Transplantation*. 2002;73:1194-1202.
59. Magnusson S, Mansson JC, Strolan V, et al. Release of pig leukocytes during pig kidney perfusion and characterization of pig lymphocyte carbohydrate xenoantigens. *Xenotransplantation*. 2003;10:432-445.
60. Lee YJ, Chu CH, Sue SH, Chen IC, Wei J. Efficacy of double filtration plasmapheresis in removing xenoantibodies and prolonging xenograft survival in an ex vivo swine perfusion model. *Transpl Int Proc*. 2012;44:114-115.
61. Roman M, Gorgjmaloska O, Nel D, et al. Comparison between cellular and acellular perfusates for ex vivo lung perfusion in a porcine model. *J Heart Lung Transplant*. 2015;34:976-987.
62. Zuckermann FA, Birns RM, Husmann R, et al. Analyses of murine monoclonal antibodies reactive with porcine CD44 and CD45. *Vet Immunol Immunopathol*. 1994;43:293-305.
63. Ezquerro A, Rivola C, Alvarez R, et al. Porcine myelomonocytic markers and cell populations. *Dev Comp Immunol*. 2009;33:264-296.
64. Prieu Guzyack L, Salmon H. Membrane markers of the immune cells in swine: an update. *Vet Res*. 2008;39:54.
65. Moreli AC. Dendritic cells of myeloid lineage: the masterminds behind acute allograft rejection. *Curr Opin Organ Transplant*. 2014;19:20-27.
66. Tai HC, Zhu X, Lin YJ, et al. Attempted depletion of passenger leukocytes by irradiation in pigs. *J Transplant*. 2011;2011:928759.
67. Wood KJ. Passenger leukocytes and microchimerism: what role in transplant induction? *Transplantation*. 2003;75:175-205.

#### SUPPORTING INFORMATION

Additional Supporting Information may be found online in the supporting information tab for this article.

**How to cite this article:** Puga Yung G, Bongoni AK, Pradier A, et al. Release of pig leukocytes and reduced human NK cell recruitment during ex vivo perfusion of HLA-E/human CD46 double-transgenic pig limbs with human blood. *Xenotransplantation*. 2017;e12357. <https://doi.org/10.1111/xen.12357>



## Paper V

### Multiple genetically modified GTKO/hCD46/HLA-E/h $\beta$ 2–mg porcine hearts are protected from complement activation and natural killer cell infiltration during ex vivo perfusion with human blood.

Jan-Michael Abicht, Riccardo Sfriso, Bruno Reichart, Matthias Längin, Katja Gahle, Gisella L. Puga Yung, Jörg D. Seebach, Robert Rieben, David Ayares, Eckhard Wolf, Nikolai Klymiuk, Andrea Baehr, Alexander Kind, Tanja Mayr, Andreas Bauer

**Status:** Published in *Xenotransplantation*, 2018 Feb 8;e12390

**Contribution:** Performed histological analysis, immunofluorescence staining, and data analysis.

**Background:** In pig-to-human xenotransplantation, interactions between human natural killer cells and porcine endothelial cells result in cytotoxicity. Protection from xenogeneic NK cytotoxicity can be achieved in vitro by the expression of the non-classical human leukocyte antigen-E (HLA-E) on porcine endothelial cells.

**Aim:** To test the effect of GTKO/hCD46/HLA-E expression on xenogeneic, and in particular human NK cell response, using an ex vivo perfusion model of pig hearts with human blood.

**Conclusion:** Co-expression of hCD46 and HLA-E on GTKO background in porcine hearts reduced complement deposition, complement dependent injury, and myocardial NK cell infiltration during perfusion with human blood. This tested combination of genetic modifications may minimize damage from acute human-anti-pig rejection reactions and improve myocardial function after xenotransplantation.

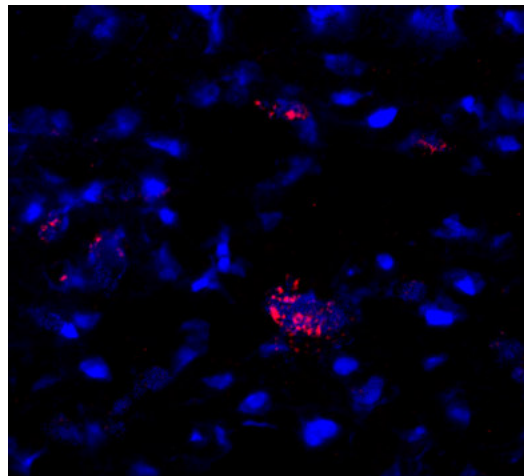


**Figure:** Detail of NKp46 (red) immunofluorescence staining of myocardial tissue.





# Multiple genetically modified GTKO/hCD46/HLA-E/hβ2-mg porcine hearts are protected from complement activation and natural killer cell infiltration during ex vivo perfusion with human blood

Jan-Michael Abicht<sup>1</sup>  | Riccardo Sfriso<sup>2</sup>  | Bruno Reichart<sup>3</sup> | Matthias Längin<sup>1</sup>  | Katja Gahle<sup>1</sup> | Gisella L. Puga Yung<sup>4</sup>  | Jörg D. Seebach<sup>4</sup>  | Robert Rieben<sup>2</sup>  | David Ayares<sup>5</sup> | Eckhard Wolf<sup>6</sup> | Nikolai Klymiuk<sup>6</sup> | Andrea Baehr<sup>6</sup> | Alexander Kind<sup>7</sup> | Tanja Mayr<sup>1</sup> | Andreas Bauer<sup>1</sup>

<sup>1</sup>Department of Anesthesiology, Ludwig Maximilian University, Munich, Germany

<sup>2</sup>Department of Clinical Research, University of Bern, Bern, Switzerland

<sup>3</sup>Translogic Collaborative Research Center 127, Walter Brödel Centre of Experimental Medicine, Ludwig Maximilian University, Munich, Germany

<sup>4</sup>Division of Immunology and Allergy, University Hospital and Faculty of Medicine, University of Geneva, Geneva, Switzerland

<sup>5</sup>Revivicor, Blacksburg, VA, USA

<sup>6</sup>Department of Molecular Animal Breeding and Biotechnology, Ludwig Maximilian University, Munich, Germany

<sup>7</sup>Chair of Livestock Biotechnology, School of Life Sciences Weihenstephan, Technical University of Munich, Munich, Germany

## Correspondence

Jan-Michael Abicht, Department of Anesthesiology, Klinikum der Universität München, Munich, Germany.  
Email: jan.abicht@med.uni-muenchen.de

## Funding information

Deutscher Forschungsgemeinschaft, Grant/Award Number: SFB 127; Swiss National Science Foundation, Grant/Award Number: 310030\_159597\_1

## Abstract

**Background:** In pig-to-human xenotransplantation, early cellular rejection reactions are mediated by natural killer cells (NK cells). Human NK cells are inhibited by HLA-E via CD94/NKG2A receptors. To protect porcine grafts against human NK cell responses, transgenic GTKO pigs expressing hCD46 and HLA-E have been generated. The aim of this study was to test the effect of this genetic modification on xenogenic, and in particular human NK cell response, using an ex vivo perfusion model of pig hearts with human blood.

**Methods:** Cardiopleged and explanted genetically modified (gm) pig hearts (GTKO/hCD46/HLA-E/hβ2-microglobulin) and wild-type (wt) controls (n = 6 each) were reperfused and tested in an 8 hours ex vivo perfusion system using freshly drawn human blood. Cardiac function was evaluated during a 165-minute period in working heart mode. Myocardial damage, antibody deposition, complement activation, and coagulation parameters were evaluated histologically at the end of perfusion. The number of NK cells in the perfusate was determined by flow cytometry at baseline and at 8 hours; tissue infiltration by NK cells was quantified by immunofluorescence microscopy using NKp46 staining of frozen sections.

**Results:** Deposition of IgG ( $1.2 \pm 1 \times 10^7$  vs  $8.8 \pm 2.9 \times 10^6$ ;  $P < .01$ ), IgM ( $4.4 \pm 3.7 \times 10^6$  vs  $1.7 \pm 1.2 \times 10^6$ ;  $P < .01$ ), and the complement activation product C4b/c ( $3.5 \pm 1.3 \times 10^6$  vs  $2.3 \times 10^6 \pm 9.4 \times 10^5$ ;  $P > .01$ ) was lower in gm than wt hearts. NK cell percentages of leukocytes in the perfusate decreased from  $0.94 \pm 0.77\%$  to  $0.21 \pm 0.25\%$  ( $P = .04$ ) during xenoperfusion of wt hearts. In contrast, the ratio of NK cells did not decrease significantly in the gm hearts. In this

**Abbreviations:** Gal, galactose; hCD46, hCD46; gm, genetically modified; GTKO, bilateral knockout of the porcine α-β-galactosyl transferase (GGT4) gene; hCD46, human CD46 complement regulator; HLA-E, human leukocyte antigen E; hβ2-mg, hβ2microglobulin; NK cells, natural killer cells; PAI-1, plasminogen activator inhibitor 1; tPA, tissue plasminogen activator; wt, wild-type.

Meindert Bauer contributed equally.

group, NK cell myocardial infiltration after 480 minutes of perfusion was lower than in wt organs ( $2.5 \pm 3.7 \times 10^4/\text{mm}^2$  vs  $1.3 \pm 1.4 \times 10^5/\text{mm}^2$ ;  $P = .0001$ ). The function of gm hearts was better preserved compared to wt organs, as demonstrated by higher cardiac index during the first 2 hours of ex vivo perfusion.

**Conclusion:** GTKO, hCD46, and HLA-E expression in porcine hearts reduced complement deposition, complement dependent injury, and myocardial NK cell infiltration during perfusion with human blood. This tested combination of genetic modifications may minimize damage from acute human-anti-pig rejection reactions and improve myocardial function after xenotransplantation.

#### KEYWORDS

cardiac xenotransplantation, hCD46, heart, HLA-E, NK cell

## 1 | INTRODUCTION

The shortage of donor organs severely limits allogeneic heart transplantation. Porcine hearts could provide an alternative, but some requirements must be fulfilled before clinical application can become a reality. In addition to non-toxic immunosuppression<sup>1</sup> and safe donor animals clear of disease caused by microorganisms, stable genetically modified (gm) pigs are necessary.

In primates, early immunological responses against wild-type (wt) porcine tissues (hyperacute rejection) are predominantly driven by preformed antibodies against the carbohydrate epitope galactose- $\alpha$ -1,3-galactose (Gal) and subsequent activation of the complement and coagulation cascades. The generation of  $\alpha$ -1,3-galactosyl transferase knockout (GTKO) pigs, whose organs do not present Gal epitopes, was therefore a scientific breakthrough.<sup>2-4</sup> In addition, overexpression of complement regulatory proteins such as human CD46 (membrane cofactor protein) is necessary to inhibit complement activation by non-Gal antibodies (reviewed in Refs [5-7]).

However, early xenogenic reactions are also mediated by various leukocyte subsets, especially natural killer (NK) cells, neutrophils, and monocytes. Human NK cells are able to lyse porcine endothelial cells both directly and by antibody-dependent cellular cytotoxicity following engagement of their Fc $\gamma$ RIII receptor (reviewed in Refs [8-10]).

The activation of NK cells is tightly regulated by a balance between activating and inhibitory receptors. Self MHC class I molecules on healthy, autologous cells represent a major ligand for inhibitory NK receptors.<sup>11</sup> The human inhibitory NK receptor CD94/NKG2A specifically binds to the non-classical MHC class I human leukocyte antigen (HLA)-E.<sup>12</sup> Porcine MHC I proteins (SLA I) do not bind sufficiently to inhibitory receptors on NK cells compared to human MHC I because SLA I cannot efficiently transmit inhibitory signal to human NK cells, which can only be partially overcome by the activation of pig endothelial cells by tumor necrosis factor (TNF) or IL1 in vitro.<sup>13</sup> Porcine cells are therefore recognized as 'dangerous' and killed by human NK cells. However, high expression of HLA-E on porcine endothelial cells can block binding and cytotoxicity of human NK

cells at least partially.<sup>10-15</sup> To achieve this, concomitant expression of human  $\beta$ 2-microglobulin was necessary to produce stable HLA-E expression on porcine endothelial cells.<sup>16-18</sup>

Here, we present results on ex vivo perfusion of GTKO/hCD46/HLA-E/h $\beta$ 2-microglobulin transgenic pig hearts with human blood, supporting the conclusion that these hearts are protected from complement and the human NK cell-mediated responses.

## 2 | MATERIAL AND METHODS

### 2.1 | Animals

Twelve juvenile pigs (German Landrace; body weight  $15.4 \pm 1.2$  kg, heart weight  $77.5 \pm 10.5$  g, blood group O) were used as donors. Six of the animals were transgenic for GTKO/hCD46/HLA-E/h $\beta$ 2-microglobulin (D. Ayares, Revivicor, Blacksburg, USA, and E. Wolf, Molecular Animal Breeding and Biotechnology, Gene Center, LMU Munich, Germany), and six were wt (controls). Anesthesia was conducted with fentanyl ( $10-15$   $\mu\text{g}/\text{kg}$ ) and propofol ( $0.15$   $\mu\text{g}/\text{kg}/\text{min}$ ). The study was carried out according to the European Law on Protection of Animals for Scientific Purposes and was approved by the Government of Upper Bavaria, Germany. All animal experiments were performed according to 3R and ARRIVE guidelines<sup>19</sup> as well as rules set out by the Ludwig Maximilian University, Munich.

### 2.2 | Surgical procedure and the biventricular heart perfusion system

The surgical technique and perfusion system have been previously described in detail.<sup>20</sup> In brief, after cardioplegia with 4°C Bretschneider solution (Custodiol, Dr. F. Köhler, Bensheim, Germany), the hearts were removed and stored in lactated Ringer's solution (Fresenius, Kabi, Bad Homburg, Germany) at 4°C for 150 minutes to simulate an ischemic period that would occur during orthotopic (xeno-)heart transplantation. Superior and inferior venae cavae were ligated. Thereafter, the ascending aorta, the pulmonary artery trunk, and both atria were cannulated and attached to the

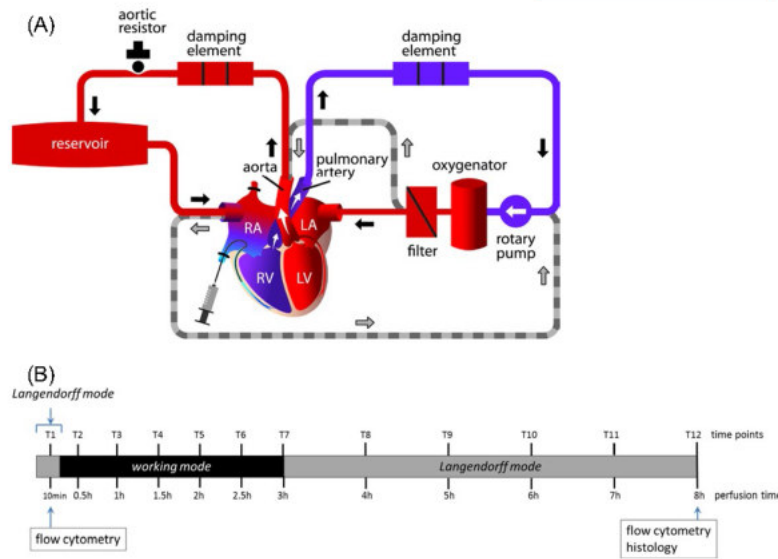


**FIGURE 1** A, The ex vivo perfusion system: during Langendorff perfusion of the heart, extra lines (shown as dashed) are open to pump oxygenated blood with a constant pressure retrograde through the ascending aorta into the coronary arteries. The coronary venous outflow enters the right atrium. The blood is then directed to the rotary pump, the oxygenator, and back to the aorta. During this mode, the heart is beating but non-working, as both ventricles are not filled during diastole. Biventricular working heart mode (dashed lines are closed and the reservoir lifted above the level of the heart): oxygenated blood enters the left atrium, which is ejected from the left ventricle into the ascending aorta (pre- and afterload may be adjusted). From the right atrium and ventricle, blood is ejected into the pulmonary artery trunk; the rotary pump supports blood flow to overcome the resistance of the oxygenator and filter. Perfusate temperature is kept constant by means of a heat exchanger within the oxygenator. B, Experimental design of ten ex vivo perfusion experiments: T0 = begin perfusion without the porcine heart, T1 = start of Langendorff perfusion (beating, non-working mode for altogether 15 min), T2 till T7 = time points of the biventricular, working mode, T8 till T12 = Langendorff perfusion

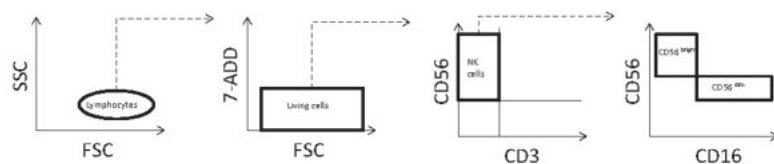
perfusion system (Figure 1A). The perfusion solution consisted of 500 mL freshly drawn human blood, 450 mL hydroxyethyl starch 6% (Volulyte; Fresenius Kabi, Bad Homburg, Germany), 5 mL sodium bicarbonate 8.4%, 0.25 mL calcium gluconate 10%, 5000 IU heparin, and 1 IU of insulin. Activated clotting times of the perfusion solution were longer than 400 seconds.

Human blood donors were six healthy males (4 blood group A; 2 blood group O). Each of them donated blood for the experiments with the gm porcine organs and again 1 month later for control experiments using wt pig hearts. A hollow fiber oxygenator with an incorporated heat exchanger (HILITE 1000; Medos, Stolberg, Germany) maintained a partial O<sub>2</sub> pressure (pO<sub>2</sub>) of 100-150 mm Hg, a pCO<sub>2</sub> of 35-40 mm Hg, and temperature at 36-37°C. Glucose (400 mg/h) and insulin (0.2 IU/h) were added to reach glucose levels in the perfusion solution between 1.2 and 1.4 mg/mL. Bicarbonate was given to keep the base excess between +2 and -2 mEq/L.

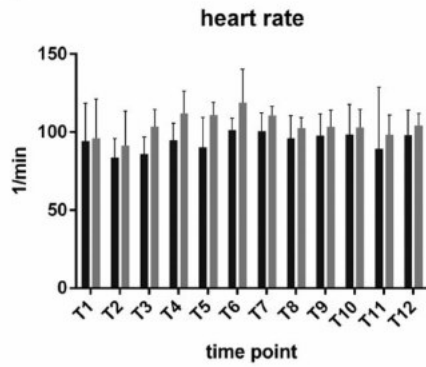
Ex vivo heart perfusion started with 15 minutes of reperfusion in a non-working Langendorff preparation, followed by biventricular working mode. After 3 hours of perfusion, the system was switched back to the Langendorff mode for the final 5 hours, resulting in a total perfusion time of 8 hours. Specimens were collected, and measurements were taken at specific time points (T1-T12; Figure 1B).

Pressure was measured in the ascending aorta, pulmonary artery trunk, and both atria. The catheter in the right atrium also enabled measurement of key parameters in the venous coronary blood, such as lactate, blood gases, and pH. Inline sensors measured the flow/min from the aorta and pulmonary artery (Ultrasonic flow meter UF&B; Cynergy Components Ltd., Dorset, England). The myocardial perfusion index (MPI) was calculated as: (aortic blood flow [mL/min] - pulmonary blood flow [mL/min])/heart weight [g]. The myocardial oxygen (MVO<sub>2</sub>) consumption was measured as: MPI [mL/mg/min] × arterio-venous difference of pO<sub>2</sub> content [mL]. Cardiac index

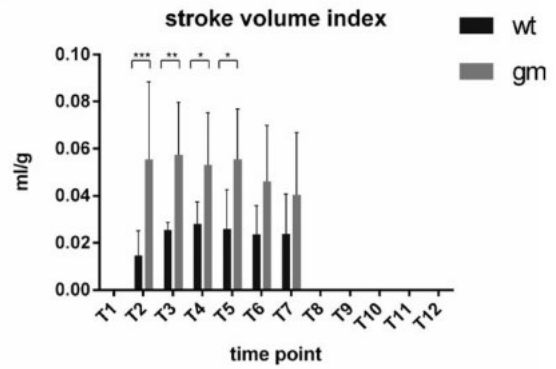
**FIGURE 2** Gating strategy for flow cytometry: identification of natural killer (NK) cells as part of lymphocytes (FS-A vs SS-A), viable (7AAD), CD3-negative and CD56-positive cell population



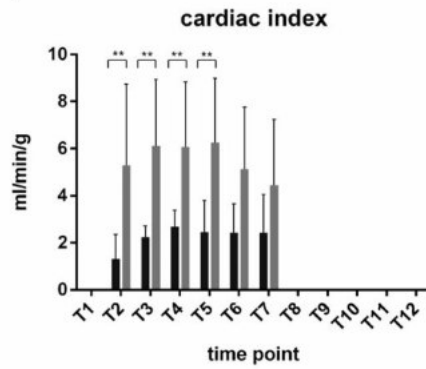
(A)



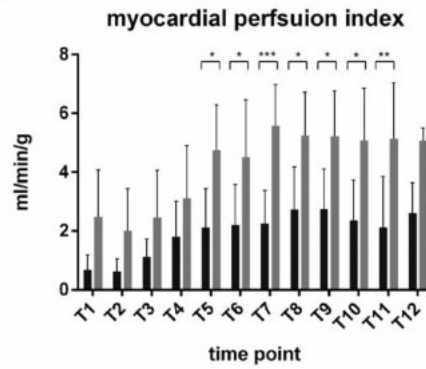
(B)



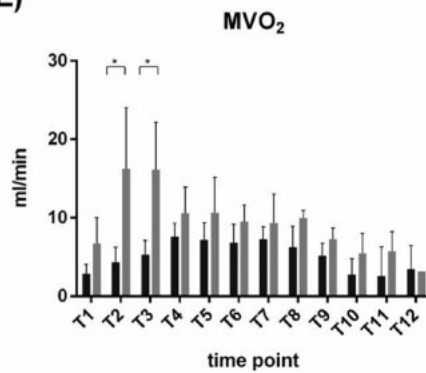
(C)



(D)



(E)



(F)

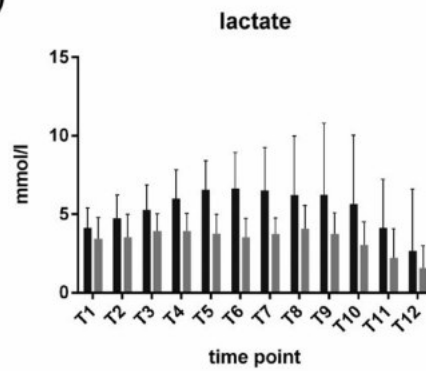




**FIGURE 3** A-C, Hemodynamic parameters of wild-type (wt, n = 6) and genetically modified (gm, n = 6) pig hearts during ex vivo perfusion: heart rates were stable throughout the experiments (wt vs gm non-significant). At several time points during the working heart perfusions (T2-T7), stroke volume index (SVI) and cardiac indices (CI) were significantly better in the gm group: SVI, T2:  $0.055 \pm 0.033$  vs  $0.015 \pm 0.011$  mL/g,  $P < .001$ ; T3:  $0.057 \pm 0.022$  vs  $0.025 \pm 0.003$  mL/g,  $P < .001$ ; T4:  $0.053 \pm 0.022$  vs  $0.028 \pm 0.009$  mL/g,  $P = .006$ ; T5:  $0.056 \pm 0.021$  vs  $0.026 \pm 0.017$  mL/g, all  $P = .001$ ; CI, T2:  $5.28 \pm 3.46$  vs  $1.32 \pm 1.04$  mL/g/min,  $P < .001$ ; T3:  $6.12 \pm 2.83$  vs  $2.24 \pm 0.47$  mL/g/min,  $P < .001$ ; T4:  $6.07 \pm 2.76$  vs  $2.69 \pm 0.69$  mL/g/min,  $P < .001$ ; T5:  $6.27 \pm 2.71$  vs  $2.45 \pm 1.35$  mL/g/min, all  $P < .001$ . D-F, Myocardial perfusion and metabolism. At the following time points, coronary artery blood flows were significantly higher in gm hearts: T6,  $4.7 \pm 1.5$  vs  $2.1 \pm 1.3$  mL/min/g,  $P = .002$ ; T7,  $4.5 \pm 1.9$  vs  $2.2 \pm 1.4$  mL/min/g,  $P = .005$ ; T8,  $5.6 \pm 1.4$  vs  $2.2 \pm 1.1$  mL/min/g,  $P < .001$ ; T9,  $5.2 \pm 1.5$  vs  $2.7 \pm 1.4$  mL/min/g,  $P = .003$ ; T10,  $5.2 \pm 1.5$  vs  $2.7 \pm 1.4$  mL/min/g,  $P = .003$ ; T11,  $5.1 \pm 1.8$  vs  $2.4 \pm 1.4$  mL/min/g,  $P = .002$ ; T12,  $5.1 \pm 1.9$  vs  $2.1 \pm 1.7$  mL/min/g,  $P < .001$ ; during the first 2 h consequently, gm hearts were able to consume more oxygen: T3,  $16.22 \pm 7.81$  vs  $4.32 \pm 1.93$  mL/min/g,  $P < .001$ ; T4:  $16.12 \pm 6.05$  vs  $5.31 \pm 1.79$  mL/min/g;  $P < .001$ . Although the lactate concentrations were lower during the whole observation time in gm hearts, these measurements were not significantly different between the two groups, with the T6 exception. All panels: bars represent means  $\pm$  SD, gm: n = 6, wt: n = 6, \* $P$ -values  $\leq .05$ , \*\* $P \leq .01$ , \*\*\* $P \leq .001$

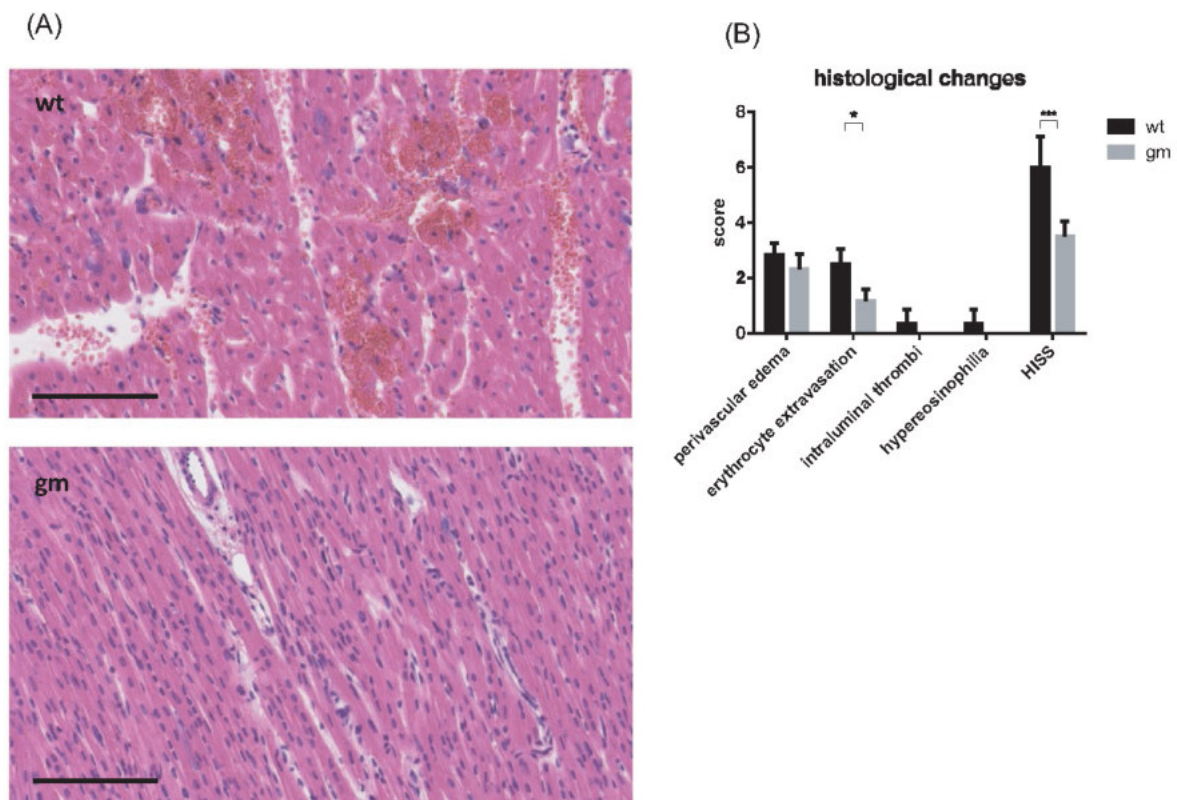


**FIGURE 4** A, H&E-stained samples of the left ventricular wall of wild-type (wt) and genetically modified (gm) porcine hearts after 8 h ex vivo perfusion with human blood eosinophilic infiltration, extracellular edema, and extravasations of erythrocytes are more pronounced in wt hearts. Scale bar = 100  $\mu$ m. B, Histological injury severity score (HISS) was higher in wt histology ( $6 \pm 1.1$ ) compared to gm (3.5  $\pm$  0.5) organs ( $P = .002$ ); bars represent means  $\pm$  SD, gm: n = 6, wt: n = 6, \* $P \leq .05$ , \*\* $P \leq .01$ , \*\*\* $P \leq .001$

(CI) was calculated as: pulmonary blood flow [mL/min]/heart weight [g], stroke volume index (SVI) as: CI [mL/min/g]/heart rate [1/min].

### 2.3 | Edema formation and histology

Porcine hearts were weighed before and after 8 hours of perfusion, and weight gain recorded to quantify edema formation. Myocardial biopsies were formalin-fixed and embedded in paraffin. Sections

(4  $\mu$ m) were cut and either processed immediately or stored at room temperature until further analysis. Hematoxylin-eosin (H&E)-stained sections were scored in a blinded manner for perivascular edema, erythrocyte extravasation, thrombus formation, and eosinophilic infiltration at a scale from 0 to 3 (0 = absent, 1 = scarce, 2 = intermediate and 3 = major pathological changes). The histological injury severity score (HISS) was calculated by summation of these points.

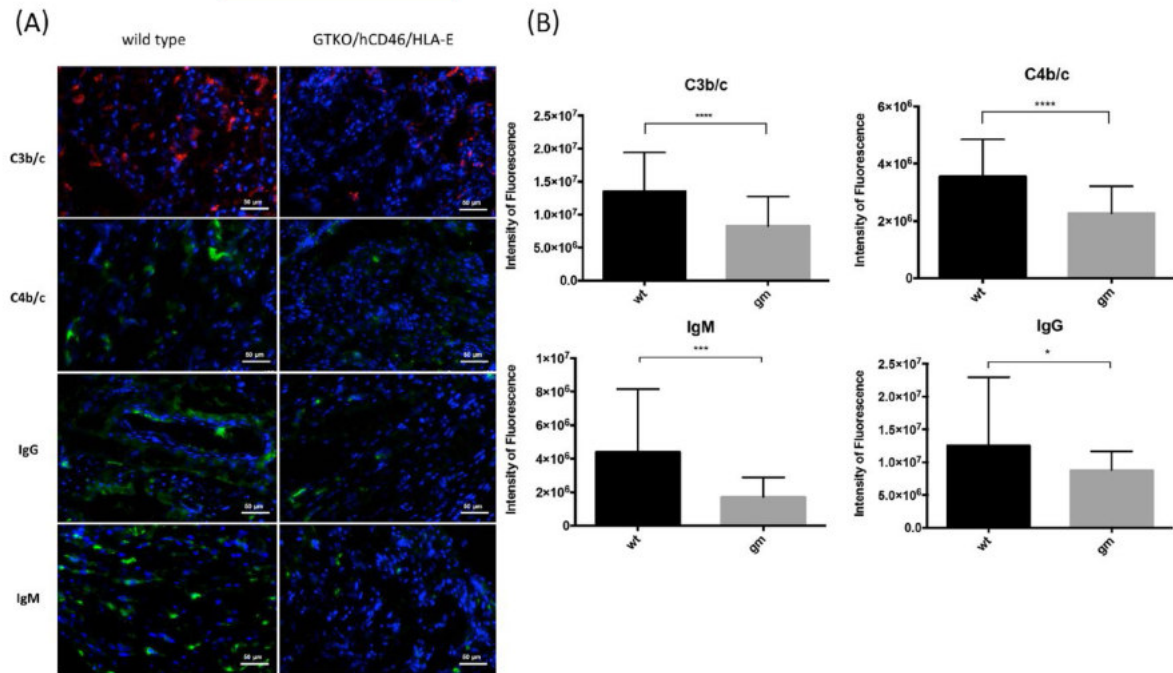


**FIGURE 5** A, Deposition of complement markers and immunoglobulins in myocardial tissues after 480 min xenoperfusion (sample from one wild-type [wt] and one genetically modified [gm] heart). B, Genetically modified myocardial tissues showed lower levels of activated complement components (C3b/c,  $1.4 \times 10^7 \pm 6 \times 10^6$  vs  $8.3 \pm 4.4 \times 10^6$ ; C4b/c,  $3.5 \pm 1.3 \times 10^6$  vs  $2.3 \times 10^6 \pm 9.4 \times 10^5$ ) and IgG ( $1.2 \pm 1 \times 10^7$  vs  $8.8 \pm 2.9 \times 10^6$ ) and IgM ( $4.4 \pm 3.7 \times 10^6$  vs  $1.7 \pm 1.2 \times 10^6$ ). Bars represent means  $\pm$  SD, gm: n = 6, wt: n = 6, \* $P \leq .05$ , \*\* $P \leq .01$ , \*\*\* $P \leq .001$ , \*\*\*\* $P \leq .0001$

## 2.4 | Immunofluorescence staining

Myocardial tissue biopsies were embedded in Tissue-Tek (Sakura Finetek, Zoeterwoude, The Netherlands) and stored frozen at  $-80^\circ\text{C}$ . For immunofluorescence staining,  $5 \mu\text{m}$ -thick cryosections were cut, air-dried for 30–60 minutes, and stored at  $-20^\circ\text{C}$  until further analysis. Cryosections were fixed with ice-cold acetone, hydrated, and stained using either one-step direct or two-step indirect immunofluorescence techniques. The following antibodies were used: rabbit anti-human C3b/c (Dako, Glostrup, Denmark), rabbit anti-human C4b/c-FITC (Dako), goat anti-human IgG-FITC (Sigma-Aldrich Corp., St. Louis MO, USA), goat anti-human IgM-FITC (Sigma), sheep anti-human tissue factor (Affinity biological Inc., Sandhill Drive, Ancaster, ON, Canada), rabbit anti-tPA (tissue-type plasminogen inhibitor, Bioss Inc., Woburn, MA, USA), mouse anti-PAI-1 (plasminogen activator inhibitor 1; Hycult Biotech, Uden, The Netherlands), mouse anti-human NKp46 (R&D Systems Inc., Minneapolis, MN, USA), mouse anti-human CD46 (Hycult Biotech), mouse anti-HLA-E (Biolegend, San Diego, CA, USA), and Bandeiraea simplicifolia isolectin B<sub>4</sub> (BSI-B<sub>4</sub>)-FITC (Sigma). Secondary antibodies were as follows: sheep anti-rabbit IgG-Cy3 (Sigma), donkey anti-sheep IgG-Alexa 488 (ThermoFisher Scientific Inc., Waltham, MA, USA), goat anti-mouse IgG<sub>1</sub>-Alexa 488 (ThermoFisher), and goat anti-mouse-Cy3 (Jackson ImmunoResearch). Nuclei were stained with 4',6-diamidino-2-phenylindole (DAPI; Boehringer,

Roche Diagnostics, Indianapolis, IN, USA). Slides were analyzed using a fluorescence microscope (DM14000B; Leica, Wetzlar, Germany), and fluorescence intensity was quantified using image processing (ImageJ 1.50i, NIH, Bethesda, MD, USA) on unmanipulated TIFF images. All images were collected under the same conditions to allow direct quantification and comparison of fluorescence intensities.

## 2.5 | Flow cytometry

Peripheral blood mononuclear cells (PBMCs) were isolated (Ficoll-Paque Plus; GE Healthcare, Chicago, IL, USA) from blood of the coronary sinus at time points T1 and T12. Samples were prepared for freezing using 95% RPMI (Gibco by Life Technologies, Carlsbad, CA, USA) + 5% HSA (Baxalta Deutschland GmbH, Unterschleißheim, Deutschland) and 80% HSA + 20% DMSO (Sigma-Aldrich Corp., St. Louis, MO, USA) and stored at  $-80^\circ\text{C}$  until analysis.

After thawing, cells were incubated for 30 minutes with fluorescent-labeled antibodies against human CD3 (Biolegend, Pacific Blue), CD16 (BD Bioscience, FITC), and CD56 (Beckman Coulter). 7-AAD (BD Bioscience) was used to mark living cells.

Measurements were made with a Gallios flow cytometer (Beckman Coulter, Inc., Brea, CA, USA). Analysis was performed using FlowJo 10.2 (FlowJo LLC, OR, USA). The gating strategy is shown in Figure 2.

Lactate concentrations in the perfusate increased less in gm hearts (increase at T6:  $-2.4 \pm 1.7$  vs  $+0.3 = 0.6$  mmol/L,  $P = .03$ ; Figure 3F).

### 3.2 | Edema formation and histology

Overall, edema was measured by increase in organ weight over baseline. At the end of the perfusions, control hearts increased from  $94 \pm 13$  to  $142 \pm 28$  g ( $n = 6$ ,  $P < .01$ ), while the gm organs increased from  $61 \pm 8$  to  $76 \pm 15$  g ( $n = 6$ ,  $P < .01$ ). In relative values, gm organs increased by  $25 = 10\%$  and control hearts by  $51 \pm 17\%$  ( $P = .01$ ). Histological analysis (wt and gm  $n = 6$ , Table S2) revealed an average erythrocyte extravasation score of  $1.7 \pm 0.4$  in the gm hearts compared to  $2.5 \pm 0.5$  ( $P < .01$ ) in the controls. Differences in myocardial edema (wt  $2.3 \pm 0.5$  vs gm  $0.28 \pm 0.4$ ;  $P = .24$ ), eosinophilic infiltration (wt  $0.3 \pm 0.5$  vs gm  $0.0 = 0.0$ ;  $P = .45$ ), and thrombus formation infiltration (wt  $0.3 \pm 0.5$  vs gm  $0.0 \pm 0.0$ ;  $P = .45$ ) were not significant. The overall HISS was  $3.5 \pm 0.5$  and  $6 = 1.1$  (gm hearts vs controls,  $P < .01$ ) (Figure 4).

### 3.3 | Verification of transgenic modification in swine hearts

The expression of Gal epitopes, human CD46, and HLA-E was analyzed in tissue samples from control (wt) and transgenic groups (Figure S1). Gal epitopes were not observed in transgenic myocardial tissues, but were clearly evident in wt organs. Transgene expression was detected only in tissues from gm animals.

### 3.4 | Reduction in complement deposition but not fibrinolytic markers in perfused tg hearts

Sample biopsies were stained for complement, coagulation, and fibrinolytic markers (Figure 5) to evaluate other important innate immune factors involved in acute vascular rejection. Deposition of complement activation products (C3b/c and C4b/c) and immunoglobulins (IgG and IgM) was less in the gm group, while fibrinolytic (tPa, PAI-1) and coagulation (TF) markers were not significantly different between wt and gm hearts (Figure 6).

### 3.5 | Reduced number of infiltrated NK cells

Natural killer cells were measured in PBMC samples obtained from the perfusate before and after 8 hours perfusion. The percentage of NK cells present did not change significantly in the gm group, whereas the wt group showed a significant decrease (Figure 7). The presence of NK cells was also assessed in heart biopsies at the end of the perfusion, and the gm group showed significantly lower infiltration as shown in Figure 8.

## 4 | DISCUSSION

Technical advances are streamlining the production of gm pigs faster, making available more lines of potential xenodonor animals with novel

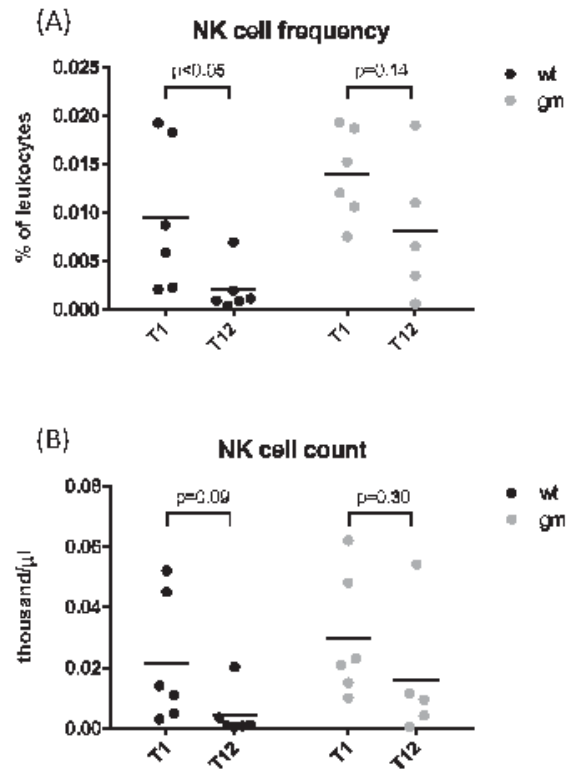


**FIGURE 7** A, natural killer (NK) cells frequency in perfusate at the beginning of ex vivo perfusion (T1) and at the end of the experiment (T12). In the wild-type (wt) hearts, the frequency dropped significantly. The proportion (%) of NK cells among blood lymphocytes was quantified as shown in Figure 2. B, NK cell count calculated as (absolute number of lymphocytes)  $\times$  (frequency of NK cells). Panels A and B (T1: genetically modified [gm];  $n = 6$ , wt:  $n = 6$ ; T12: gm:  $n = 5$ , wt:  $n = 6$ )

genotypes. However, before primate experiments can be conducted, new lines need to be tested in functional models. Our ex vivo perfusion model allows new genetic modifications to be assessed in a working heart situation, similar to models established for lung transplantation.<sup>17,11</sup> Useful comparison with wt control organs, free of immediate hyperacute rejection, is made possible by anticoagulation with heparin and the use of diluted blood as a perfusate to slow tissue damage.

### 4.1 | Model to test Immediate Immune response

In our ex vivo perfusion system,<sup>19</sup> hearts were perfused at a temperature of  $36\text{--}37^\circ\text{C}$  with physiological pre- and afterloads. After 15 minutes reperfusion in Langendorff mode, the system was switched to the biventricular working heart mode to examine myocardial function for a further 165 minutes. Following the experimental design of Bongoni et al,<sup>18</sup> developed for 12 hour limb perfusion, we extended our working heart protocol by 5 hours of perfusion in Langendorff mode. In this way, myocardial perfusion pressure remained stable,



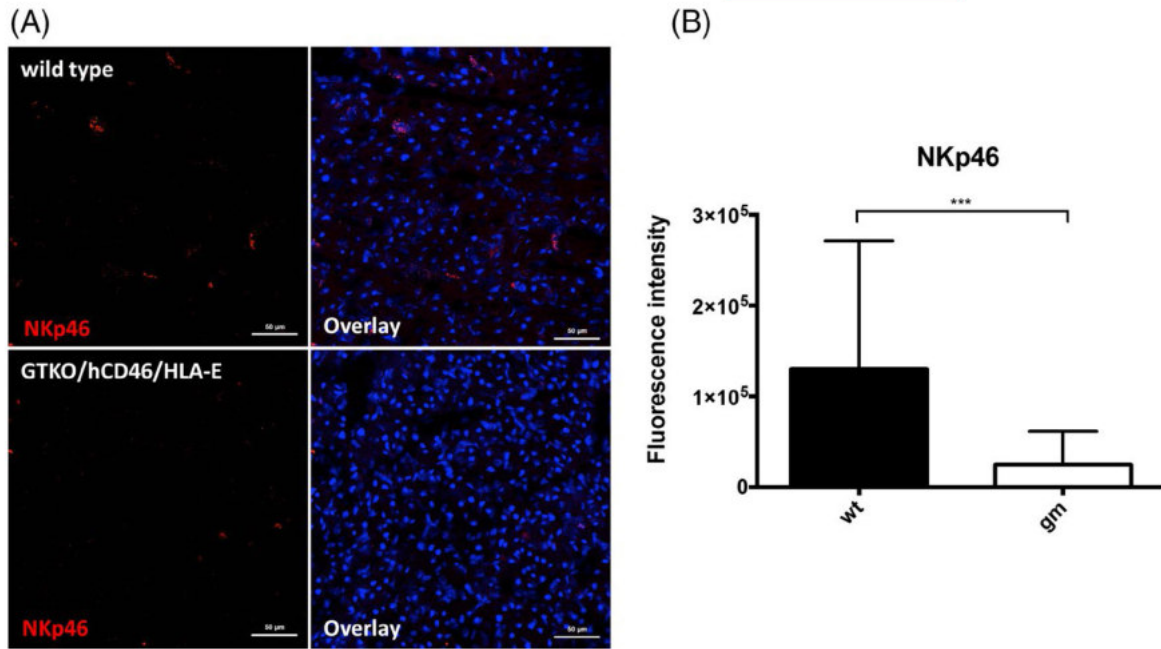


**FIGURE 8** A, All panels: NKp46 staining (red) in myocardial tissues (after 8 h xenoperfusion [samples of one wild-type [wt] and one heart]). Overlay panels: DAPI (blue) was used to visualize the nuclear volume and shape of the tissue section. B, There were fewer NKp46-positive cells in the genetically modified (gm) myocardial tissues: wt  $1.3 \pm 1.4 \times 10^5/\text{mm}^3$  vs gm  $2.5 \pm 3.7 \times 10^4/\text{mm}^3$ ). Bars represent means  $\pm$  SD, gm: n = 6, wt: n = 6, \*\*\* $P \leq .001$

including hearts that would have failed during longer working heart perfusion (Table S1).

During the working heart periods, the left ventricular stroke volume, cardiac indices, and myocardial perfusion of gm hearts were found to be superior to wt organs. The largest differences in function, measured as SVI or MVO<sub>2</sub>, were observed 15 minutes after starting the working heart phase. Laird et al similarly described the greatest functional difference in porcine lungs with and without HLA-E occurred during the first 30 minutes.<sup>22</sup> This immediate effect of suppressing the NK cell-mediated xeno reaction was unexpected and indicated that a shorter experimental design might have been possible.

The lower post-perfusion heart weights of the gm group indicated less edematous changes, and indeed, histological examinations revealed a lower HISS. Thrombotic lesions were not observed in either group due to the high concentration of heparin in the perfusate. These findings are consistent with less antibody deposition (due to GTKO) and less complement activation components (due to hCD46 expression).

The xenoprotective value of HLA-E has been demonstrated in several previous reports. Lilienfeld et al achieved partial protection from human NK cytotoxicity by expressing HLA-E in transfected porcine endothelial cells.<sup>15</sup> In vitro studies with porcine endothelial cells and stable expression of the HLA-E/h $\beta$ 2-microglobulin complex protected against human NK cell-mediated lysis in 80-90% of cases, depending on whether CD94/

NKG2A inhibitory receptors were expressed on NK cells. Also, surface HLA-E/h $\beta$ 2-microglobulin on transgenic porcine endothelial cells inhibited secretion of interferon- $\gamma$  by co-cultured human NK cells.<sup>17</sup>

Bongoni et al showed that combined expression of hCD46/HLA-E in transgenic pig forelimbs perfused ex vivo for 12 hours with warm (32°C) human blood significantly reduced complement-related changes compared to wt.<sup>18</sup> Recently, co-authors of the present study (G. Puga Yung and J.D. Seebach) reported in vitro studies of HLA-E/hCD46 expression in the same ex vivo pig limb xenoperfusion model. NK cytotoxicity against hCD46 single transgenic porcine endothelial cells was not different when compared to wt cells.<sup>23</sup> Similar to the results presented here, NK cell infiltration in the HLA-E/hCD46 gm tissue was less than in wt controls at the end of limb perfusion. Moreover, using an ex vivo pig lung xenoperfusion model with human blood, Laird et al recently reported that transgenic expression of HLA-E limited endothelial damage by preventing NK cell activation and cytotoxicity, resulting in improved pig lung survival and function.<sup>22</sup> That study used the same combination of genetic modifications, GTKO/hCD46/HLA-E, but all positive effects could be ascribed to HLA-E expression because GTKO/hCD46 pig lungs were used as controls.

The lack of such control genotypes meant that we could not quantify the contribution of separate genetic modifications. Therefore, it remains uncertain if the observed differences in myocardial NK cells can be attributed to HLA-E expression. After



8 hours perfusion. GTKO/hCD46/HLA-E/h $\beta$ 2-microglobulin myocardium showed a significantly lower Nkp46 signal than wt, consistent with reduced recruitment or activation of NK cells.<sup>27</sup> In addition to their direct cytotoxic activity, NK cells activate and/or regulate other components of the cellular immune system by secretion of pro-inflammatory cytokines, such as TNF and interferon gamma.<sup>31</sup> In their review, Rieben and Seebach<sup>8</sup> described detrimental links between NK cells and the activated complement system, and complement receptors are present on NK cell surfaces.<sup>26,27</sup> There may thus be synergy between the xenoprotective effects of hCD46 and HLA-E. Furthermore, while direct recognition of Gal epitopes by NK cells independent of antibodies is controversial, endothelial cells derived from GTKO pigs do not diminish direct NK cytotoxicity against porcine (and human) endothelial cells.<sup>26–30</sup>

Maeda et al have also demonstrated that transgenic expression of HLA-E also suppresses the macrophage-mediated cytotoxicity in a xenomodel;<sup>29</sup> this was not specifically analyzed in our study.

Regarding immunological similarity to humans, baboons are generally accepted as recipients in preclinical cardiac xenotransplantation experiments. However, it is difficult to draw conclusions regarding the role of HLA-E from such studies, due to the lack of tools available to characterize non-human primate NK cells, particularly with respect to HLA-E binding.

The tested combination of genetic modifications reduces damage from acute human-anti-pig rejection reactions. However, a large number of different genetical modifications have been made to porcine hearts, and further experiments are needed to identify the favorable combination for preclinical experiments.

## ACKNOWLEDGMENTS

This work was funded by the German Research Foundation (Deutsche Forschungsgemeinschaft, DFG) TRR127. We thank the Walter Brendel Centre for their support. JDS and GPY were supported by the Swiss National Science Foundation (#310030\_159594.1).

## AUTHOR CONTRIBUTIONS

Jan-Michael Abicht, Tanja Mayr, and Andreas Bauer designed the study, conducted experiments, collected and analyzed data, and prepared the manuscript. Bruno Reichart secured funding, analyzed the data, and revised the article. Riccardo Friso contributed histological analysis, immunofluorescence staining, and data analysis. Robert Rieben contributed to the concept and data analysis of the study. Katja Gahle and Matthias Längin conducted experiments and collected data. Gisella Puga Yung and Jörg D. Seebach contributed to the analysis of data and revised the manuscript. David Ayares, Eckhard Wolf, Nikolai Khymniuk, and Andrea Baehr genetically constructed animal breeding. Alexander Kind critically revised the article and approved the final draft.

## DISCLOSURE

David Ayares, Chief Executive Officer, Revivicor, Inc.

## ORCID

Jan-Michael Abicht  <http://orcid.org/0000-0001-7361-1249>

Riccardo Friso  <http://orcid.org/0000-0002-3406-0736>

Matthias Längin  <http://orcid.org/0000-0003-0996-4941>

Gisella L. Puga Yung  <http://orcid.org/0000-0002-2283-7798>

Jörg D. Seebach  <http://orcid.org/0000-0001-5748-4577>

Robert Rieben  <http://orcid.org/0000-0003-4179-8891>

## REFERENCES

- Mohiuddin MM, Singh AK, Corcoran PC, et al. Chimeric 2C10R4 anti-CD40 antibody therapy is critical for long-term survival of GTKO, hCD46, hTBM pig to primate cardiac xenograft. *Nat Commun*. 2016;7:11138.
- Phelps CJ, Koike C, Vaught TD, et al. Production of  $\alpha$ 1,3 galactosyl transferase-deficient pigs. *Science*. 2003;299:411–414.
- Kuwaki K, Tseng YL, Dor HMF, et al. Heart transplantation in baboons using  $\alpha$ 1,3 galactosyltransferase gene knockout pigs as donors: initial experience. *Nat Med*. 2005;11:29–31.
- Yamada K, Yazawa K, Shimizu A, et al. Marked prolongation of porcine renal xenograft survival in baboons through the use of  $\alpha$ 1,3-galactosyltransferase gene knockout donors and the cotransplantation of vascularized thymic tissue. *Nat Med*. 2005;11:32–34.
- Kim DD, Song WC. Membrane complement regulatory proteins. *Clin Immunol*. 2006;118:127–136.
- Pferson RN III, Dorling A, Ayares D, et al. Current status of xenotransplantation and prospects for clinical application. *Xenotransplantation*. 2009;16:263–280.
- Elser D, Ezzelarab M, Hara H, et al. Clinical xenotransplantation: the next medical revolution? *Transpl*. 2012;379:672–681.
- Rieben R, Seebach JD. Xenograft rejection: IgG<sub>1</sub>, complement and NK cells team up to activate and destroy the endothelium. *Trends Immunol*. 2005;26:2–5.
- Schneider MKJ, Seebach JD. Current cellular primate immunoburdens in pig to primate xenotransplantation. *Curr Opin Organ Transplant*. 2006;13:171–177.
- Puga Yung GL, Schneider MKJ, Seebach JD. The role of NK cells in pig-to-human xenotransplantation. *J Immunol Res*. 2017;2017:4627304.
- Randall DH, Vamvakis RF, McMahon CW. Regulation of the natural killer cell receptor repertoire. *Annu Rev Immunol*. 2001;19:291–330.
- García P, Lano M, de Heredia AB, et al. Human T cell receptor mediated recognition of HLA-E. *Eur J Immunol*. 2002;32:936–944.
- Sasaki H, Xu XC, Mohanakumar T. HLA-E and HLA-G expression on porcine endothelial cells inhibit xenoreactive human NK cells through CD94/NKG2 – dependent and independent pathways. *J Immunol*. 1999;163:6301–6305.
- Matsunami K, Miyagawa S, Nakai R, Yamada M, Shirakura R. Modulation of the leader peptide sequence of the HLA-E gene up-regulates its expression and down-regulates natural killer cell-mediated syngeneic endothelial cell lysis. *Transplantation*. 2002;74:1582–1589.
- Lienfeld BG, Crew MD, Forte P, Daumann DC, Seebach JD. Transgenic expression of HLA-E single chain trimer protects

- porcine endothelial cells against human natural killer cell-mediated cytotoxicity. *Xenotransplantation*. 2007;14:126-137.
16. Ulbrecht M, Courturier A, Martinuzzi S, et al. Cell surface expression of HLA-E: interaction with human beta2-microglobulin and allelic differences. *Eur J Immunol*. 1999;29:537-547.
  17. Weiss EH, Littenfeld BG, Müller S, et al. HLA-E/human p2-microglobulin transgenic pigs: protection against xenogeneic human anti-pig natural killer cell cytotoxicity. *Transplantation*. 2009;87:35-43.
  18. Dongon AK, Khermeir D, Jenn H, et al. Complement-dependent early immunologic responses during ex vivo xenotransplantation of hCD46/HLA-E double-transgenic pig forelimbs with human blood. *Xenotransplantation*. 2014;21:230-243.
  19. Kilkenny C, Browne WJ, Cuthill IC, Emerson M, Altman DG. Improving bioscience research reporting: the ARRIVE guidelines for reporting animal research. *PLoS Biol*. 2010;8:e1000412.
  20. Abicht JM, Mayr TA, Janch J, et al. Large animal biventricular working heart perfusion system with low priming volume-comparison between in vivo and ex vivo cardiac function. *Thorac Cardiovasc Surg*. 2016;66:071-082.
  21. Havris DG, Quinn KJ, French BM, et al. Meta-analysis of the independent and cumulative effects of multiple genetic modifications on pig lung xenograft performance during ex vivo perfusion with human blood. *Xenotransplantation*. 2015;22:102-111.
  22. Laird CT, Burdorf L, French DM, et al. Transgenic expression of human leukocyte antigen-E attenuates GalKO:hCD46 porcine lung xenograft injury. *Xenotransplantation*. 2017;24:e12297.
  23. Puga-Yung G, Dongon AK, Pradier A, et al. Release of pig leukocytes and reduced human NK cell recruitment during ex vivo perfusion of HLA-E/human CD46 double-transgenic pig limbs with human blood. *Xenotransplantation*. 2017;25:e12357.
  24. Campos C, López N, Pera A, et al. Expression of NKp30, NKp46 and DNAM-1 activating receptors on resting and IL-2 activated NK cells from healthy donors according to CMV serostatus and age. *Biogerontology*. 2015;16:671-683.
  25. Schuster IS, Couderl JD, Amelonon CH, Duggl-Esposti MA. "Natural regulators": NK cells as modulators of T cell immunity. *Front Immunol*. 2016;7:235.
  26. Klein F, D'Kerio L, Yefrem F. Contribution of CR3, CD11b/CD18 to cytotoxicity by human NK cells. *Mol Immunol*. 1990;27:1343-1347.
  27. Lovic G, Vaagg JT, Dassen F, Szpirer C, Ryan JC, Rostad H. Characterization and molecular cloning of rat C1gRp, a receptor on NK cells. *Eur J Immunol*. 2000;30:3355-3362.
  28. Baumann BC, Schneider MK, Littenfeld BG, et al. Endothelial cells derived from pigs lacking Gal(alpha1,3)Gal no reduction of human leukocyte adhesion and natural killer cell cytotoxicity. *Transplantation*. 2005;79:1067-1072.
  29. Baumann BC, Forti P, Hawley RJ, Richen R, Schneider MK, Seibach JD. Lack of galactose-alpha-1,3-galactose expression on porcine endothelial cells prevents complement-induced lysis but not direct xenogeneic NK cytotoxicity. *J Immunol*. 2004;172:6460-6467.
  30. Christiansen D, Moulthouris E, MI and J, Zingoni A, Santoni A, Samliri MS. Recognition of a carbohydrate xenopeptide by human NKR1A (CD161). *Xenotransplantation*. 2006;13:440-446.
  31. Sheikh S, Parhar R, Kwasi A, et al. Alpha gal independent dual recognition and activation of xenogeneic endothelial cells and human naive natural killer cells. *Xenotransplantation*. 2009;70:917-928.
  32. He Z, Hirnfeld C, Kimmig Bransch M, Islam KB, Hogerström J. Aberrant expression of alpha-Gal on primary human endothelium does not confer susceptibility to NK cell cytotoxicity or increased NK cell adhesion. *Eur J Immunol*. 2004;34:1185-1195.
  33. Horvath Antillano JA, Porter CM, Bloom ET. Human NK cells can lyse porcine endothelial cells independent of their expression of Gal(alpha1,3)-Gal and ICling is enhanced by activation of either effector or target cells. *Xenotransplantation*. 2006;13:118-127.
  34. Maeda A, Kawamura T, Ueno T, Usui N, Eguchi H, Miyagawa S. The suppression of inflammatory macrophage-mediated cytotoxicity and proinflammatory cytokine production by transgenic expression of HLA-E. *Transl Immunol*. 2013;29:76-81.

#### SUPPORTING INFORMATION

Additional Supporting Information may be found online in the supporting information tab for this article.

**How to cite this article:** Abicht J-M, Sfriso R, Reichart B, et al. Multiple genetically modified GTKO/hCD46/HLA-E/h $\beta$ 2-ming porcine hearts are protected from complement activation and natural killer cell infiltration during ex vivo perfusion with human blood. *Xenotransplantation*. 2018:e12390. <https://doi.org/10.1111/xen.12390>

## Paper VI

### Consistent success in life supporting porcine cardiac xenotransplantation

Matthias Längin, Tanja Mayr, Bruno Reichart, Sebastian Michel, Stefan Buchholz, Sonja Guethoff, Alexey Dashkevich, Andrea Baehr, Stefanie Egerer, Andreas Bauer, Maks Mihalj, Alessandro Panelli, Lara Issl, Jiawei Ying, Ann Kathrin Fresch, Fabian Werner, Isabelle Lutzmann, Stig Steen, Trygve Sjöberg, Audrius Paskevicius, Liao Qiuming, Riccardo Sfriso, Robert Rieben, Maik Dahlhoff, Barbara Kessler, Elisabeth Kemter, Katharina Klett, Rabea Hinkel, Christian Kupatt, Almuth Falkenau, Simone Reu, Reinhard Ellgass, Rudolf Herzog, Uli Binder, Günter Wich, Arne Skerra, David Ayares, Alexander Kind, Uwe Schönmann, Franz-Josef Kaup, Christian Hagl, Eckhard Wolf, Nikolai Klymiuk, Paolo Brenner, Jan-Michael Abicht

**Status:** Accepted for publication in *Nature*

**Contribution:** Performed immunofluorescence and anti-nonGal antibody analysis

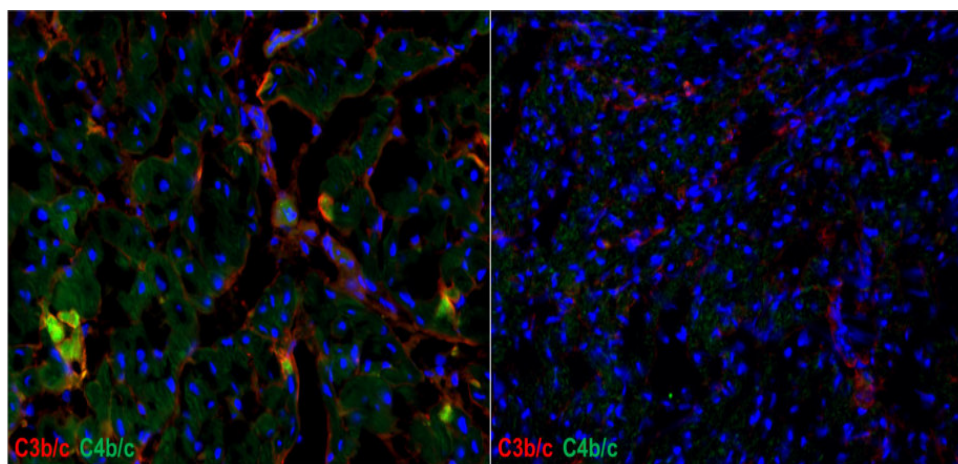


**Figure:** Complement deposition (C3b/c and C4b/c) on myocardial tissue. Group I (left) and Group III (right).

**Background:** Heart transplantation is the only cure for patients with terminal cardiac failure, but the supply of allogeneic donor organs falls far short of the clinical need. For the last 25 years, xenotransplantation of genetically modified pig hearts has been discussed as a potential alternative, but consistent long-term life supporting function of porcine cardiac xenografts in non-human primates has not been achieved.

**Aim:** To achieve long term survival (>90 days) of GTKO/hCD46/hTM transgenic porcine heart transplanted orthotopically into baboons and bring xenotransplantation closer to the clinical application.

**Conclusion:** Non-ischemic cold perfusion of the hearts combined with effective counteraction of post-transplantation growth ensured long-term orthotopic xenograft function in baboons, the most stringent preclinical xenotransplantation model. Consistent life-supporting function of xeno-hearts for up to five months is a milestone on the way to clinical cardiac xenotransplantation.

1 **Consistent success in life supporting porcine cardiac xenotransplantation**

2

3 Matthias Längin<sup>1,2#</sup>, Tanja Mayr<sup>1,2#</sup>, Bruno Reichart<sup>2\*</sup>, Sebastian Michel<sup>3</sup>, Stefan Buchholz<sup>3</sup>,  
4 Sonja Guethoff<sup>2,3</sup>, Alexey Dashkevich<sup>3</sup>, Andrea Baehr<sup>4</sup>, Stefanie Egerer<sup>4</sup>, Andreas Bauer<sup>1</sup>,  
5 Maks Mihalj<sup>3</sup>, Alessandro Panelli<sup>2</sup>, Lara Issl<sup>2</sup>, Jiawei Ying<sup>2</sup>, Ann Kathrin Fresch<sup>2</sup>, **Ines**  
6 **Buttgereit<sup>2</sup>, Maren Mokolke<sup>2</sup>, Julia Radan<sup>2</sup>**, Fabian Werner<sup>1</sup>, Isabelle Lutzmann<sup>2</sup>, Stig Steen<sup>5</sup>,  
7 Trygve Sjöberg<sup>5</sup>, Audrius Paskevicius<sup>5</sup>, Liao Qiuming<sup>5</sup>, Riccardo Sfriso<sup>6</sup>, Robert Rieben<sup>6</sup>,  
8 Maik Dahlhoff<sup>4</sup>, Barbara Kessler<sup>4</sup>, Elisabeth Kemter<sup>4</sup>, Katharina Klett<sup>7,8,9</sup>, Rabea Hinkel<sup>7,8,9</sup>,  
9 Christian Kupatt<sup>7,9</sup>, Almuth Falkenau<sup>10</sup>, Simone Reu<sup>11</sup>, Reinhard Ellgass<sup>3</sup>, Rudolf Herzog<sup>3</sup>,  
10 Uli Binder<sup>12</sup>, Günter Wich<sup>13</sup>, Arne Skerra<sup>14</sup>, David Ayares<sup>15</sup>, Alexander Kind<sup>16</sup>, Uwe  
11 Schönmann<sup>17</sup>, Franz-Josef Kaup<sup>17</sup>, Christian Hagl<sup>3</sup>, Eckhard Wolf<sup>4</sup>, Nikolai Klymiuk<sup>4</sup>, Paolo  
12 Brenner<sup>2,3§</sup> & Jan-Michael Abicht<sup>1,2§</sup>

13

14 <sup>1</sup>Department of Anaesthesiology, University Hospital, LMU Munich, Munich, Germany

15 <sup>2</sup>Transregional Collaborative Research Center 127, Walter Brendel Centre of Experimental  
16 Medicine, LMU Munich, Munich, Germany

17 <sup>3</sup>Department of Cardiac Surgery, University Hospital, LMU Munich, Munich, Germany

18 <sup>4</sup>Institute of Molecular Animal Breeding and Biotechnology, Gene Center, LMU Munich,  
19 Germany

20 <sup>5</sup>Department of Cardiothoracic Surgery, Lund University and Skåne University  
21 Hospital, Lund, Sweden

22 <sup>6</sup>Department for BioMedical Research (DMBR), University of Bern, Switzerland

23 <sup>7</sup>I. Medizinische Klinik, Klinikum Rechts der Isar, TUM, Munich, Germany

24 <sup>8</sup>Institute for Cardiovascular Prevention (IPEK), LMU Munich, Germany

25 <sup>9</sup>DZHK (German Center for Cardiovascular Research), partner site Munich Heart Alliance,  
26 Munich, Germany

27 <sup>10</sup>Institute of Veterinary Pathology, LMU Munich, Munich, Germany

28 <sup>11</sup>Institute of Pathology, Medical Faculty, LMU Munich, Munich, Germany

29 <sup>12</sup>XL-protein GmbH, Freising, Germany

30 <sup>13</sup>Wacker-Chemie AG, Munich, Germany

31 <sup>14</sup>Munich Center for Integrated Protein Science (CIPS-M) and Lehrstuhl für Biologische  
32 Chemie, School of Life Sciences Weihenstephan, Technical University of Munich, Germany

33 <sup>15</sup>Revivicor, Blacksburg, VA, USA

34 <sup>16</sup>Chair of Livestock Biotechnology, School of Life Sciences Weihenstephan, Technical  
35 University of Munich, Germany

36 <sup>17</sup>German Primate Centre, Göttingen, Germany

37 <sup>#,§</sup>authors contributed equally to this work.

38

39 \* Corresponding author:

40 Prof. Dr. Bruno Reichart

41 Walter Brendel Centre of Experimental Medicine, LMU Munich

42 Marchioninistraße 27

43 81377 Munich, Germany

44 Tel ++49 89 4400 73727

45 Fax ++49 89 2180 76503

46 [bruno.reichart@med.uni-muenchen.de](mailto:bruno.reichart@med.uni-muenchen.de)

47 **Heart transplantation is the only cure for patients with terminal cardiac failure, but the**  
48 **supply of allogeneic donor organs falls far short of the clinical need** <sup>1-3</sup>.  
49 **Xenotransplantation of genetically modified pig hearts has been discussed as a potential**  
50 **alternative** <sup>4</sup>. **Genetically multi-modified pig hearts lacking  $\alpha$ Gal epitopes (GTKO) and**  
51 **expressing human membrane cofactor protein (hCD46) and human thrombomodulin**  
52 **(hTM) have survived for up to 945 days after heterotopic abdominal transplantation in**  
53 **baboons** <sup>5</sup>. **This model demonstrated long-term acceptance of discordant xenografts with**  
54 **safe immunosuppression but did not predict their life supporting function. In spite of 25**  
55 **years of extensive research, the maximum survival of a baboon after heart replacement**  
56 **with a porcine xenograft was only 57 days and this was achieved only once** <sup>6</sup>. **Here we**  
57 **show that GTKO/hCD46/hTM pig hearts require specific perfusion preservation and**  
58 **post-transplantation growth control to ensure long-term orthotopic xenograft function**  
59 **in baboons, the most stringent preclinical xenotransplantation model. Consistent life-**  
60 **supporting function of xeno-hearts for up to 195 days is a milestone on the way to**  
61 **clinical cardiac xenotransplantation** <sup>7</sup>.

62

63 **Xenotransplantation of genetically multi-modified pig hearts (GTKO/hCD46/hTM; blood**  
64 **group 0) was performed** using the clinically approved “Shumway’s” orthotopic technique <sup>8</sup>.  
65 Fourteen captive-bred baboons (*Papio anubis*, blood groups B and AB) served as recipients.  
66 All recipients received basic immunosuppression, similar to that described by Mohiuddin <sup>5</sup>:  
67 induction therapy included mycophenolate-mofetil (MMF), methylprednisolone (MP), anti-  
68 CD20 Ab, anti-thymocyte-globulin, and the monkey-specific anti-CD40 mouse/rhesus  
69 chimeric IgG4 mAb (clone 2C10R4) <sup>9</sup> or our own humanized anti-CD40L PASylated Fab <sup>10</sup>.  
70 Maintenance therapy consisted of MMF and MP tapered down, and anti-CD40 mAb or anti-

71 CD40L PASylated Fab (Extended Data Table 1). Post-operative treatment of the recipients  
72 has been described elsewhere <sup>11</sup>.

73 In group I (n = 5), donor organs were preserved with two clinically approved crystalloid  
74 solutions (4°C Custodiol HTK or Belzer’s UW solution), each given once after cross-  
75 clamping the ascending aorta and before excision of the porcine donor organ. The hearts were  
76 kept in plastic bags filled with ice-cold solution and surrounded by ice cubes (static  
77 preservation).

78 The results of group I were disappointing. Despite short ischemic preservation times ( $123 \pm 7$   
79 min), survival times were only one day (n = 3), 3 days and 30 days (Fig. 1a). The four short-  
80 term survivors were successfully weaned from cardiopulmonary bypass (CPB), and three  
81 extubated, but all were lost due to severe systolic left heart failure in spite of high dose  
82 intravenous catecholamines (Extended Data Fig. 1). This so-called “perioperative cardiac  
83 xenograft dysfunction (PCXD)” <sup>12</sup> has been observed in 40 to 60 % of the orthotopic cardiac  
84 xenotransplantation experiments described in the literature <sup>4</sup>. The only 30-day survivor  
85 (cardiac preservation with Belzer’s UW-solution) gradually developed left ventricular (LV)  
86 myocardial hypertrophy and stiffening, resulting in progressive diastolic LV failure associated  
87 with increased serum levels of troponin T, an indicator of myocardial damage (Fig. 1b).  
88 Increased serum bilirubin levels (Fig. 1c) and several other clinical-chemical parameters  
89 (Table 1) indicated associated terminal liver disease. Upon necropsy, marked cardiac  
90 hypertrophy (Fig. 1e) with thickened LV myocardium and a decreased LV cavity became  
91 evident (Fig. 1f).

92 To reduce the incidence of PCXD observed in group I, we explored new ways to improve  
93 xenograft preservation. In group II (n = 4), the same IS regime as in group I was used, but the  
94 pig hearts were preserved with an 8°C oxygenated albumin-containing hyperoncotic  
95 cardioplegic solution containing nutrition, hormones and erythrocytes <sup>13</sup>. From explantation



96 until transplantation, the organs were continuously perfused and oxygenated by a heart  
97 perfusion system. During implantation surgery, the hearts were intermittently perfused every  
98 15 minutes until the aortic clamp was opened at the end of transplantation<sup>13</sup>.

99 After non-ischemic continuous organ perfusion ( $206 \pm 43$  min), all four baboons in group II  
100 could easily be weaned from CPB, showing graft function superior to group I, and required  
101 less catecholamine support (Extended Data Fig. 1). No organ was lost due to PCXD. One  
102 experiment had to be terminated on the fourth postoperative day due to a technical failure; the  
103 other three animals lived for 18, 27 and 40 days (Fig. 1a). Echocardiography during the  
104 experiments revealed increasing hypertrophy of the LV myocardium as measured by LV mass  
105<sup>14,15</sup> (Fig. 1d), LV stiffening and decreasing LV filling volumes (Extended Data Fig. 2a). Graft  
106 function remained normal throughout the experiments, but diastolic relaxation gradually  
107 deteriorated (Supplementary Video 1a). Troponin T levels were consistently above normal  
108 range and increased markedly at the end of each experiment (Table 1; Fig. 1b);  
109 simultaneously platelet counts decreased while LDH increased (Table 1; Extended Data Fig. 3  
110 a, b), suggesting thrombotic microangiopathy as described for heterotopic abdominal cardiac  
111 xenotransplantation<sup>5,16</sup>. In addition, secondary liver failure developed: increasing serum  
112 bilirubin concentrations (Fig. 1c) and decreased prothrombin-ratio and cholinesterase  
113 indicated reduced liver function, while increased serum activities of alanine-aminotransferase  
114 (ALT) and aspartate-aminotransferase (AST) pointed to liver damage (Table 1). At necropsy,  
115 the weight of group II hearts had more than doubled (on average 259%) compared to the time  
116 point of transplantation. Histology confirmed myocardial cell hypertrophy (Fig. 1j, k) and  
117 revealed multifocal myocardial necrosis, thromboses, and immune cell infiltration (Fig. 1h  
118 left); in the liver, multifocal cell necroses were observed (Fig. 1h right). Taken together, these  
119 alterations are consistent with diastolic pump failure and subsequent congestive liver damage  
120 resulting from massive cardiac overgrowth. Immunofluorescence analyses of the myocardium

121 and plasma levels of non-Gal xenoreactive antibodies <sup>17</sup> did not indicate humoral graft  
122 rejection (Fig. 2, Extended Data Fig. 4).

123 To prevent diastolic heart failure, we investigated means of preventing cardiac hypertrophy.  
124 The following modifications were made for group III (n = 5): recipients were weaned from  
125 cortisone at an early stage and received antihypertensive treatment (pigs have a lower systolic  
126 pressure than baboons, ~80 vs. ~120 mmHg) and additional temsirolimus medication to  
127 counteract cardiac overgrowth. After heart perfusion times of  $219 \pm 30$  min, all five animals  
128 were easily weaned from CPB, comparable to group II (Extended Data Fig. 1). None of the  
129 recipients in group III showed PCXD, all reached a steady state with good heart function after  
130 four weeks. One recipient (#10) developed recalcitrant pleural effusions due to occlusion of  
131 the thoracic lymph duct and was thus euthanized after 51 days. Two recipients (#11, #12)  
132 lived in good health for three months until euthanasia, according to the study protocol. In  
133 these three recipients, echocardiography revealed no increase in LV mass (Fig. 1d); graft  
134 function remained normal with no signs of diastolic dysfunction (Extended Data Fig. 2b;  
135 Supplementary Video 1b). Biochemical parameters of heart and liver functions, as well as  
136 LDH levels and platelet counts, were normal or only slightly altered throughout the  
137 experiments (Table 1, Fig. 1b, c; Extended Data Fig. 3a,b), consistent with normal histology  
138 (Fig. 1i). Histology of LV myocardium showed no signs of hypertrophy (Fig. 1j, k), and  
139 Western blot analysis of myocardium revealed phosphorylation levels of mTOR lower than  
140 non-transplanted age-matched control hearts (Fig. 1l). Similar to group II, there were no signs  
141 of humoral graft rejection in group III (Fig. 2, Extended Data Fig. 4).

142 The study protocol for group III was extended aiming at a graft survival of 6 months. The last  
143 two recipients in this group (#13, #14) were allowed to survive in good general condition for  
144 195 and 182 days, with no major changes of platelet counts, and serum LDH and bilirubin  
145 levels (Fig. 1a; Extended Data Fig. 3a, b). Intravenous temsirolimus treatment was

146 discontinued on day 175 and on day 161. Up to this point, systolic and diastolic heart function  
147 was normal (Supplementary Video 1c). Thereafter, increased growth of the cardiac graft was  
148 observed in both recipients (Fig. 1d), emphasising the importance of mTOR inhibition in the  
149 orthotopic xenogeneic heart xenotransplantation model. Similar to the changes observed in  
150 group II, the smaller recipient #13 developed signs of diastolic dysfunction associated with  
151 elevated serum levels of troponin T and beginning congestive liver damage (increased serum  
152 ALT and AST levels, decreased prothrombin-ratio and cholinesterase); platelet counts  
153 remained within normal ranges (Table 1, Fig. 1b, c; Extended Data Fig. 3a, b). Histology  
154 confirmed hepatic congestion and revealed multifocal myocardial necroses without immune  
155 cell infiltrations or signs of thrombotic microangiopathy. In the larger recipient #14, who had  
156 to be euthanized simultaneously with companion #13, the consequences of cardiac  
157 overgrowth were minimal.

158 Consistent survival of life-supporting pig hearts in non-human primates for at least three  
159 months meets for the first time preclinical efficacy requirements for the initiation of clinical  
160 xenotransplantation trials as suggested by an advisory report of the International Society of  
161 Heart and Lung Transplantation <sup>7</sup>.

162 Two steps were key to success:

163 **(1) Non-ischemic porcine heart preservation.** Group I xeno-hearts that underwent ischemic  
164 static myocardial preservation with crystalloid solutions (as used for clinical allogeneic  
165 procedures) showed PCXD in four of five cases, necessitating large amounts of  
166 catecholamines. This phenomenon is clearly similar to “cardiac stunning”, known since the  
167 early days of cardiac surgery, and does not represent hyperacute rejection <sup>4</sup>. In contrast, in  
168 groups II and III (non-ischemic porcine heart preservation by perfusion) <sup>13</sup>, all nine recipients  
169 came off CPB easily since their cardiac outputs remained unchanged compared to baseline.  
170 The short-term results achieved in these groups were excellent even by clinical standards.

171 **(2) Prevention of detrimental xenograft overgrowth.** Previous pig-to-baboon kidney and  
172 lung transplantation experiments have suggested that growth of the graft depends more on  
173 intrinsic factors than on stimuli from the recipient such as growth hormones<sup>18</sup>. The massive  
174 cardiac hypertrophy in our group II recipients indicates a more complex situation. Notably, a  
175 transplanted heart in this group showed 62% greater weight gain than the non-transplanted  
176 heart of a sibling in the same time span (Extended Data Fig. 2c).

177 In group III, cardiac overgrowth was successfully counteracted by a combination of  
178 treatments: i) decreasing the baboon's blood pressure to match the lower porcine levels; ii)  
179 tapering cortisone at an early stage - it can cause hypertrophic cardiomyopathy in early life in  
180 humans<sup>19</sup>; and iii) using the sirolimus prodrug temsirolimus to mitigate myocardial  
181 hypertrophy. Sirolimus compounds are known to control the complex network of cell growth  
182 by inhibiting both mTOR kinases<sup>20</sup>. There is clinical evidence that sirolimus treatment can  
183 attenuate myocardial hypertrophy, and improve diastolic pump function<sup>21,22</sup>, and also  
184 ameliorate rare genetic overgrowth syndromes in humans<sup>23</sup>. In addition to the effects of  
185 human thrombomodulin expression in the graft<sup>5,24</sup>, temsirolimus treatment may prevent the  
186 formation of thrombotic microangiopathic lesions even further by reducing collagen induced  
187 platelet aggregation and by destabilizing platelet aggregates formed under shear stress  
188 conditions<sup>25</sup>.

189 In summary, our study demonstrates that consistent long-term life-supporting orthotopic  
190 xenogeneic heart transplantation in the most relevant preclinical model is feasible, paving the  
191 way to clinical translation of xenogeneic heart transplantation.

192

193

194  
195  
196  
197  
198  
199  
200  
201  
202  
203  
204  
205  
206  
207  
208  
209  
210  
211  
212  
213  
214  
215  
216  
217  
218  
219  
220  
221  
222  
223  
224  
225  
226  
227  
228  
229  
230  
231  
232  
233  
234  
235  
236  
237  
238  
239  
240  
241  
242  
243  
244  
245

References

- 1 Lund, L. H. *et al.* The Registry of the International Society for Heart and Lung Transplantation: Thirty-fourth Adult Heart Transplantation Report-2017; Focus Theme: Allograft ischemic time. *The Journal of heart and lung transplantation : the official publication of the International Society for Heart Transplantation* **36**, 1037-1046, doi:10.1016/j.healun.2017.07.019 (2017).
- 2 Rossano, J. W. *et al.* The Registry of the International Society for Heart and Lung Transplantation: Twentieth Pediatric Heart Transplantation Report-2017; Focus Theme: Allograft ischemic time. *The Journal of heart and lung transplantation : the official publication of the International Society for Heart Transplantation* **36**, 1060-1069, doi:10.1016/j.healun.2017.07.018 (2017).
- 3 Eurotransplant. Annual Report 2016. 104 (Eurotransplant International Foundation, 2017).
- 4 Mohiuddin, M. M., Reichart, B., Byrne, G. W. & McGregor, C. G. A. Current status of pig heart xenotransplantation. *International journal of surgery (London, England)* **23**, 234-239, doi:10.1016/j.ijsu.2015.08.038 (2015).
- 5 Mohiuddin, M. M. *et al.* Chimeric 2C10R4 anti-CD40 antibody therapy is critical for long-term survival of GTKO.hCD46.hTBM pig-to-primate cardiac xenograft. *Nature communications* **7**, 11138, doi:10.1038/ncomms11138 (2016).
- 6 Byrne, G. W., Du, Z., Sun, Z., Asmann, Y. W. & McGregor, C. G. Changes in cardiac gene expression after pig-to-primate orthotopic xenotransplantation. *Xenotransplantation* **18**, 14-27, doi:10.1111/j.1399-3089.2010.00620.x (2011).
- 7 Cooper, D. K. *et al.* Report of the Xenotransplantation Advisory Committee of the International Society for Heart and Lung Transplantation: the present status of xenotransplantation and its potential role in the treatment of end-stage cardiac and pulmonary diseases. *The Journal of heart and lung transplantation : the official publication of the International Society for Heart Transplantation* **19**, 1125-1165 (2000).
- 8 Lower, R. R. & Shumway, N. E. Studies on orthotopic homotransplantation of the canine heart. *Surgical forum* **11**, 18-19 (1960).
- 9 Lowe, M. *et al.* A novel monoclonal antibody to CD40 prolongs islet allograft survival. *American journal of transplantation : official journal of the American Society of Transplantation and the American Society of Transplant Surgeons* **12**, 2079-2087, doi:10.1111/j.1600-6143.2012.04054.x (2012).
- 10 Binder, U. & Skerra, A. PASylation®: A versatile technology to extend drug delivery. *Current Opinion in Colloid & Interface Science* **31**, 10-17, doi:<https://doi.org/10.1016/j.cocis.2017.06.004> (2017).
- 11 Mayr, T. *et al.* Hemodynamic and perioperative management in two different preclinical pig-to-baboon cardiac xenotransplantation models. *Xenotransplantation* **24**, doi:10.1111/xen.12295 (2017).
- 12 Byrne, G. W. & McGregor, C. G. Cardiac xenotransplantation: progress and challenges. *Current opinion in organ transplantation* **17**, 148-154, doi:10.1097/MOT.0b013e3283509120 (2012).
- 13 Steen, S., Paskevicius, A., Liao, Q. & Sjoberg, T. Safe orthotopic transplantation of hearts harvested 24 hours after brain death and preserved for 24 hours. *Scandinavian cardiovascular journal : SCJ* **50**, 193-200, doi:10.3109/14017431.2016.1154598 (2016).
- 14 Devereux, R. B. *et al.* Echocardiographic assessment of left ventricular hypertrophy: comparison to necropsy findings. *The American journal of cardiology* **57**, 450-458 (1986).
- 15 Lang, R. M. *et al.* Recommendations for chamber quantification: a report from the American Society of Echocardiography's Guidelines and Standards Committee and the Chamber Quantification Writing Group, developed in conjunction with the European Association of Echocardiography, a branch of the European Society of Cardiology. *Journal of the American*

- 246 *Society of Echocardiography : official publication of the American Society of*  
247 *Echocardiography* **18**, 1440-1463, doi:10.1016/j.echo.2005.10.005 (2005).
- 248 16 Kuwaki, K. *et al.* Heart transplantation in baboons using alpha1,3-galactosyltransferase gene-  
249 knockout pigs as donors: initial experience. *Nature medicine* **11**, 29-31, doi:10.1038/nm1171  
250 (2005).
- 251 17 Azimzadeh, A. M. *et al.* Development of a consensus protocol to quantify primate anti-non-  
252 Gal xenoreactive antibodies using pig aortic endothelial cells. *Xenotransplantation* **21**, 555-  
253 566, doi:10.1111/xen.12125 (2014).
- 254 18 Tanabe, T. *et al.* Role of intrinsic (graft) versus extrinsic (host) factors in the growth of  
255 transplanted organs following allogeneic and xenogeneic transplantation. *American journal*  
256 *of transplantation : official journal of the American Society of Transplantation and the*  
257 *American Society of Transplant Surgeons* **17**, 1778-1790, doi:10.1111/ajt.14210 (2017).
- 258 19 Lesnik, J. J., Singh, G. K., Balfour, I. C. & Wall, D. A. Steroid-induced hypertrophic  
259 cardiomyopathy following stem cell transplantation in a neonate: a case report. *Bone*  
260 *marrow transplantation* **27**, 1105-1108, doi:10.1038/sj.bmt.1703029 (2001).
- 261 20 Saxton, R. A. & Sabatini, D. M. mTOR Signaling in Growth, Metabolism, and Disease. *Cell* **168**,  
262 960-976, doi:10.1016/j.cell.2017.02.004 (2017).
- 263 21 Imamura, T. *et al.* Everolimus attenuates myocardial hypertrophy and improves diastolic  
264 function in heart transplant recipients. *International heart journal* **57**, 204-210,  
265 doi:10.1536/ihj.15-320 (2016).
- 266 22 Paoletti, E. mTOR inhibition and cardiovascular diseases: cardiac hypertrophy.  
267 *Transplantation* **102**, S41-S43, doi:10.1097/tp.0000000000001691 (2018).
- 268 23 Manning, B. D. Game of TOR - the target of rapamycin rules four kingdoms. *The New England*  
269 *journal of medicine* **377**, 1297-1299, doi:10.1056/NEJMcibr1709384 (2017).
- 270 24 Wuensch, A. *et al.* Regulatory sequences of the porcine THBD gene facilitate endothelial-  
271 specific expression of bioactive human thrombomodulin in single- and multitransgenic pigs.  
272 *Transplantation* **97**, 138-147, doi:10.1097/TP.0b013e3182a95cbc (2014).
- 273 25 Aslan, J. E., Tormoen, G. W., Loren, C. P., Pang, J. & McCarty, O. J. S6K1 and mTOR regulate  
274 Rac1-driven platelet activation and aggregation. *Blood* **118**, 3129-3136, doi:10.1182/blood-  
275 2011-02-331579 (2011).

276

277

278 **Supplementary Information** is available in the online version of the paper

279

280 **Acknowledgments** We thank the Walter Brendel Centre of Experimental Medicine, Munich  
281 for support and provision of facilities, especially U. Pohl, M. Shakarami and all animal care  
282 takers. Financial support was provided by the German Research Foundation (Deutsche  
283 Forschungsgemeinschaft, DFG) TRR 127. We acknowledge Keith Reimann (Non-Human  
284 Primate Reagent Resource, MassBiologics of the University of Massachusetts Medical  
285 School, Boston, MA, USA) for providing CD40 mAb for the experiments.

286

287 **Author contributions** B.R., P.B., T.M, M.L. and J.A. conceived and led the study; M.L.,  
288 T.M., B.R., R.E., R.Her., S.G., S.B., S.M., A.Bau., F.W., M.M., A.Pan., L.I., Y.J., A.K.F.,  
289 L.Q., C.H., I.L., **I.B., M.M., J.R.**, P.B., and J.A. performed the experiments and collected  
290 samples; S.S., T.S., A.Pas., and L.Q. performed non-ischemic heart preservation; M.L.,  
291 A.Pan., A.Bau., and J.A. performed haemodynamic and echocardiographic analyses; R.S., and  
292 R.R. provided immunological analyses; E.K., K.K., R.Hin., and C.K. performed  
293 histochemical analyses; M.D. and E.W. provided protein analysis; A.F., and S.R. performed  
294 necropsy and histological analyses with contribution of T.M. and A.Pan.; M.L., T.M., B.R.,  
295 R.S., R.R., R.Hin., M.D., and J.A. analyzed the data; A.Bae., S.E., B.K., D.A., E.W., and  
296 N.K. provided genetically multi-modified donor pigs; U.S. and F.-J.K. provided non-human  
297 primates; U.B., G.W., and A.S developed PASylated anti-CD40L Fab; B.R., M.L., T.M., and  
298 J.A. wrote the manuscript; A.K., A.S., R.R., S.S., R.Hin., P.B. and E.W. reviewed and edited  
299 the manuscript.

300

301 **Author Information** Reprints and permissions information is available at  
302 [www.nature.com/reprints](http://www.nature.com/reprints). The authors declare competing financial and non-financial  
303 interests: details are available in the online version of the paper. Readers are welcome to  
304 comment on the online version of the paper. Correspondence and requests for materials  
305 should be addressed to B.R. ([bruno.reichart@med.uni-muenchen.de](mailto:bruno.reichart@med.uni-muenchen.de)).

306



307 **Tables**

| Experiment          | Group I                 | Group II                |                         |                         | Group III                               |                     |                     |                     |                     | Reference  |
|---------------------|-------------------------|-------------------------|-------------------------|-------------------------|---|---------------------|---------------------|---------------------|---------------------|------------|
|                     | # 3                     | # 6                     | # 8                     | # 9                     | # 10                                    | # 11                | # 12                | # 13                | # 14                |            |
| Bilirubin (mg/dl)   | 1.2                     | 0.9                     | 2.7                     | 4.5                     | 0.3                                     | 0.2                 | 0.2                 | 0.2                 | 0.2                 | ≤ 1.2      |
| AST (U/l)           | 646                     | 896                     | 792                     | 354                     | 101                                     | 27                  | 23                  | 63                  | 28                  | ≤ 49       |
| PR (%)              | 30                      | 6                       | 6                       | 6                       | 101                                     | 96                  | 117                 | 26                  | 99                  | 70 - 130   |
| CHE (kU/l)          | 1.6                     | 1.6                     | 1.4                     | 1.1                     | 2.1                                     | 9.4                 | 14.4                | 7.3                 | 7.2                 | 4.6 - 11.5 |
| Trop T (hs) (ng/ml) | 0.233                   | 0.660                   | 1.460                   | 1.470                   | 0.218                                   | 0.037               | 0.018               | 0.556               | 0.140               | ≤ 0.014    |
| CK total (U/l)      | 654                     | 636                     | 1017                    | 953                     | 3053                                    | 143                 | 66                  | 461                 | 96                  | ≤ 189      |
| LDH (U/l)           | 3252                    | 6853                    | 2842                    | 1627                    | 436                                     | 311                 | 511                 | 962                 | 497                 | ≤ 249      |
| Platelets (G/L)     | 99                      | 101                     | 65                      | 29                      | 216                                     | 202                 | 128                 | 271                 | 303                 | 150 - 300  |
| Survival (d)        | 30                      | 18                      | 27                      | 40                      | 51                                      | 90                  | 90                  | 195                 | 182                 |            |
| Causes of death     | heart and liver failure | heart and liver failure | heart and liver failure | heart and liver failure | SCV thrombosis, thoracic duct occlusion | elective euthanasia | elective euthanasia | elective euthanasia | elective euthanasia |            |

308

309 **Table 1: Serum levels of liver and heart enzymes, platelet counts and prothrombin ratio**  
 310 **at the end of experiments that lasted longer than two weeks (right column: normal**  
 311 **reference values).** Group I and II animals exhibited pathological biochemical findings  
 312 corresponding to heart and liver failure; platelet counts were low and LDH was elevated. By  
 313 contrast, most parameters remained close to, or within, normal ranges in animals of group III.  
 314 The baboon in experiment #10 had to be euthanized because of severe pleural effusions due to  
 315 superior caval vein (SCV) thrombosis and thoracic lymph duct occlusion. The animals in  
 316 experiments #11 and #12 were electively terminated after reaching the study endpoint of 90  
 317 days but showed no signs of cardiac or liver dysfunction. Experiments #13 and #14 **were**  
 318 **electively terminated after six months; recipient #13 showed signs of beginning heart and**  
 319 **liver dysfunction.**

320

321

322 **Figures**

323 **Figure 1: Laboratory parameters, survival, necropsy and histology after orthotopic**  
324 **xenotransplantation. a**, Kaplan-Meier curve of survival of groups I (black; n = 5 animals), II  
325 (red; n = 4 animals) and III (magenta; n = 5 animals); two-sided log-rank test, p = 0.0007. **b -**  
326 **c**, Serum concentrations of high sensitive cardiac troponin T (b) and bilirubin (c). **d**, LV  
327 masses of xeno-hearts #9 (group II), #11 and #13 (both group III); note increased graft growth  
328 after discontinuation of temsirolimus (arrow). **e-g**, Front view of #3 (group I, e) and transverse  
329 cuts of the porcine donor (left) and the baboons' own hearts (right) of #3 (f) and #11 (g). Note  
330 extensive LV hypertrophy and reduction of LV cavity of the donor organ of #3 in contrast to  
331 #11. **h-i**, HE stainings of donor LV myocardium (left) and recipient liver (right); scale bars =  
332 100  $\mu$ m. #9 (h) myocardium: multifocal cell necroses with hypereosinophilia, small vessel  
333 thromboses, moderate interstitial infiltration of lymphocytes, neutrophils and macrophages;  
334 liver: multifocal centrilobular cell vacuolisations and necroses, multifocal intralesional  
335 haemorrhages. #11 (i) myocardium: sporadic infiltrations of lymphocytes, multifocal minor  
336 interstitial oedema; liver: small vacuolar degeneration of hepatocytes (lipid type. **j**, WGA-  
337 stained myocardial sections of a sham operated porcine heart (co, left), #9 (centre) and #11  
338 (right); scale bar = 50  $\mu$ m. e-j, n = 4, groups I/II; n = 3, group III; n = 1, control; one  
339 representative biological sample for group I/II, group III and control (l) is shown. **k**,  
340 Quantitative analysis of myocyte cross-sectional areas; mean $\pm$ s.d., p values as indicated, one-  
341 way ANOVA with Holm-Sidak's multiple comparisons test (n = 3 biologically independent  
342 samples with 5-8 measurements each). **l**, Western blot analysis of myocardium from #11 and  
343 #12: reduced mTOR phosphorylation compared with age-matched control samples. n = 2,  
344 group III; n = 2, controls. For gel source data, see Supplementary Figure 1.

345

346

347 **Figure 2: Quantitative evaluation of antibodies, complement and fibrin in myocardial**  
348 **tissue and serum levels of non-Gal xenoreactive antibodies. a-e**, Quantitative evaluation of  
349 fluorescence intensities (**n = 9 biologically independent samples with 5-10 measurements** per  
350 experiment; for representative images see Extended Data Figure 3). IgM (**a**), IgG (**b**), C3b/c  
351 (**c**), C4b/c (**d**), and fibrin (**e**). Colour code: group I (**#3**), black; group II (**#6, #8, #9**), red;  
352 group III (**#11-#14**), magenta. C3b/c and C4b/c values are compared to those of controls (**co**)  
353 measured in a healthy pig heart; bars indicate mean $\pm$ s.d. **j, k**, Levels of xenoreactive non-Gal  
354 IgM and IgG antibodies in baboon plasma; antibody binding to GTKO/hCD46/hTM porcine  
355 aortic endothelial cells (PAEC) was analysed by FACS. Values are expressed as median  
356 fluorescence intensity. **#4, #6, #9, and #10** had received anti-CD40L PASylated Fab, the  
357 others anti-CD40 mAb. Plasma from **a baboon** who rejected a heterotopically intrathoracic  
358 transplanted pig heart served as positive control (**co**, grey).

359

360

361 **Methods**

362 Animals: Experiments were carried out between February 2015 and August 2018. Fourteen  
363 juvenile pigs of cross-bred genetic background (German Landrace and Large White, blood  
364 group 0) served as donors for heart xenotransplantation. All organs were homozygous for  
365 alpha 1,3-galactosyltransferase knockout (GTKO), and heterozygous transgenic for hCD46  
366 and human thrombomodulin (hTM)<sup>24</sup> (Revivicor, Blacksburg, VA, USA and Institute of  
367 Molecular Animal Breeding and Biotechnology, LMU Munich, Munich, Germany).  
368 Localisation and stability of hCD46/hTM expression were verified post-mortem by  
369 immunohistochemistry (Extended Data Fig. 5). Donor heart function and absence of valvular  
370 defects were evaluated 7 days prior to transplantation by echocardiography. Fourteen male  
371 captive-bred baboons (*Papio anubis*, blood groups B and AB) were used as recipients  
372 (German Primate Centre, Göttingen, Germany).

373 The study was approved by the local authorities and the Government of Upper Bavaria. All  
374 animals were treated in compliance with the Guide for the Care and Use of Laboratory  
375 Animals (US National Institutes of Health and German Legislation).

376 Anaesthesia and Analgesia: Baboons were premedicated by intramuscular injection of  
377 ketamine hydrochloride 6-8 mg/kg (Ketavet<sup>®</sup> 100 mg/mL; Pfizer Deutschland GmbH, Berlin,  
378 Germany) and 0.3-0.5 mg/kg midazolam (Midazolam-ratiopharm<sup>®</sup>; ratiopharm GmbH, Ulm,  
379 Germany). General anaesthesia was induced with an intravenous bolus of 2.0-2.5 mg/kg  
380 propofol (Propofol<sup>®</sup>-Lipuro 2%; B. Braun Melsungen AG, Melsungen, Germany) and 0.05  
381 mg fentanyl (Fentanyl-Janssen 0.5 mg; Janssen-Cilag GmbH, Neuss, Germany), and  
382 maintained with propofol (0.16±0.06 mg/kg/min) or sevoflurane (1-2 Vol% endexpiratory;  
383 Sevorane, AbbVie Germany GmbH & Co. KG, Wiesbaden, Germany) and bolus  
384 administrations of fentanyl (6-8 µg/kg, repeated every 45 min) as described elsewhere<sup>11</sup>.  
385 Continuous infusion of fentanyl, ketamine hydrochloride and metamizole (Novaminsulfon-

386 ratiopharm<sup>®</sup> 1 g/2 mL; ratiopharm GmbH, Ulm, Germany) was applied post-operatively to  
387 ensure analgesia.

388 Donor heart explantation and preservation: Pigs were premedicated by intramuscular injection  
389 of ketamine hydrochloride 10-20 mg/kg, azaperone 10 mg/kg (Stresnil<sup>®</sup> 40 mg/ml; Lilly  
390 Deutschland GmbH, Bad Homburg, Germany) and atropine sulphate (Atropinsulfat B. Braun  
391 0.5 mg; B. Braun Melsungen AG, Melsungen, Germany). General anaesthesia was induced  
392 with an intravenous bolus of 20 mg propofol and 0.05 mg fentanyl and maintained with  
393 propofol (0.12 mg/kg/min) and bolus administrations of fentanyl (2.5 µg/kg, repeated every  
394 30 min).

395 After median sternotomy and heparinisation (500 IU/kg), a small cannula was inserted into  
396 the ascending aorta, which was then cross-clamped distal of the cannula. In group I, the heart  
397 was cardiopleged with a single dose of 20 ml/kg crystalloid cardioplegic solution at 4°C:  
398 experiments #2, #4 and #5 received Custodiol HTK solution (Dr. F. Köhler Chemie GmbH,  
399 Bernsheim, Germany), experiments #1 and #3 Belzer's UW solution (Preservation Solutions  
400 Inc., Elkhorn, WI, USA). The appendices of the right and left atrium were opened for  
401 decompression. The heart was then excised, submersed in cardioplegic solution and stored on  
402 ice.

403 In groups II and III, hearts were preserved as described by Steen et al.<sup>13</sup>, using 3.5 L of an  
404 oxygenated albumin-containing hyperoncotic cardioplegic nutrition solution with hormones  
405 and erythrocytes at a temperature of 8°C in a portable extracorporeal heart preservation  
406 system consisting of a pressure- and flow-controlled roller pump, an O<sub>2</sub>/CO<sub>2</sub> exchanger, a  
407 leukocyte filter, an arterial filter and a cooler/heater unit.

408 After aortic cross-clamping, the heart was perfused with 600 ml preservation medium, then  
409 excised and moved into the cardiac preservation system. A large cannula was introduced into  
410 the ascending aorta and the mitral valve made temporarily incompetent to prevent left

411 ventricular dilation; the superior caval vein was ligated, inferior caval vein, pulmonary artery  
412 and pulmonary veins were however left open for free outlet of perfusate. The heart was  
413 submersed in a reservoir filled with cold perfusion medium and antegrade coronary perfusion  
414 commenced via the already placed aortic cannula. The perfusion pressure was regulated at  
415 precisely 20 mmHg. During implantation, the heart was intermittently perfused for 2 min  
416 every 15 min.

417 Implantation technique: The recipient's thorax was opened at the midline. Unfractionated  
418 heparin (500 IU/kg; Heparin-Natrium-25000-ratiopharm, ratiopharm GmbH) was given and  
419 the heart-lung machine connected, using both caval veins and the ascending aorta. CBP  
420 commenced and the recipient cooled (30°C in group I, 34°C in groups II and III). After cross-  
421 clamping the ascending aorta, the recipient's heart was excised at the atrial levels, both large  
422 vessels were cut. The porcine donor heart was transplanted applying Shumway's and Lower's  
423 technique <sup>8</sup>.

424 A wireless telemetric transmitter (Data Sciences International, St. Paul, MN, USA) was  
425 implanted in a subcutaneous pouch in the right medioclavicular line between the 5th and 6th  
426 rib. Pressure probes were inserted into the ascending aorta and the apex of the left ventricle,  
427 an ECG lead was placed in the right ventricular wall.

428 Immunosuppressive regimen, anti-inflammatory and additive therapy: Immunosuppression  
429 was based on Mohiuddin's regimen <sup>5</sup>, with C1 esterase inhibitor instead of cobra venom  
430 factor for complement inhibition (Extended Data Table 1). Induction consisted of anti-CD20  
431 Ab (Mabthera; Roche Pharma AG, Grenzach-Wyhlen, Germany), ATG (Thymoglobuline,  
432 Sanofi-Aventis Germany GmbH, Frankfurt, Germany), and either anti-CD40 mAb  
433 (mouse/rhesus chimeric IgG4 clone 2C10R4, NIH Non-human Primate Reagent Resource,  
434 Mass Biologicals, Boston, MA, USA; courtesy of Keith Reimann; experiments #1-3, #5, #7,  
435 #8, #11-14) or humanised anti-CD40L PASylated Fab (XL-protein GmbH, Freising, Germany

436 and Wacker-Chemie, München, Germany; experiments #4, #6, #9, #10). Maintenance  
437 immunosuppression consisted of MMF (CellCept, Roche, Basle, Switzerland; trough level 2-  
438 3 µg/ml), either anti-CD40 mAb (experiments #1-3, #5, #7, #8, #11-14) or anti-CD40L  
439 PASylated Fab (experiments #4, #6, #9, #10), and methylprednisolone (Urbasone soluble,  
440 Sanofi-Aventis Germany GmbH, Frankfurt, Germany). Anti-inflammatory therapy included  
441 IL6-receptor antagonist (RoActemra, Roche Pharma AG, Grenzach-Wyhlen, Germany), TNF-  
442 alpha inhibitor (Enbrel, Pfizer Pharma GmbH, Berlin, Germany) and IL1-receptor antagonist  
443 (Kineret, Swedish Orphan Biovitrum GmbH, Martinsried, Germany). Additive therapy:  
444 acetylsalicylic acid (Aspirin, Bayer Vital GmbH, Leverkusen, Germany), unfractionated  
445 heparin (Heparin-Natrium-25000-ratiopharm, ratiopharm GmbH, Ulm, Germany), C1 esterase  
446 inhibitor (Berinert, CSL Behring GmbH, Hattersheim, Germany), ganciclovir (Cymevene,  
447 Roche Pharma AG, Grenzach-Wyhlen, Germany), cefuroxime (Cefuroxim Hikma, Hikma  
448 Pharma GmbH, Martinsried, Germany) and epoetin beta (NeoRecormon 5000IU, Roche  
449 Pharma AG, Grenzach-Wyhlen, Germany).

450 Starting from 10 mg/kg/d, methylprednisolone was tapered down 1 mg/kg every 10 days in  
451 group I and II; in group III, methylprednisolone was tapered down to 0.1 mg/kg within 19  
452 days. Also in group III, temsirolimus (Torisel, Pfizer Pharma GmbH, Berlin, Germany) was  
453 added to the maintenance immunosuppression, administered as daily i.v. short infusions  
454 aiming at rapamycin trough levels of 5-10 ng/ml. Group III also received continuous i.v.  
455 antihypertensive medication with enalapril (Enahexal, Hexal AG, Holzkirchen, Germany) and  
456 metoprolol tartrate (Beloc i.v., AstraZeneca GmbH, Wedel, Germany), aiming at mean  
457 arterial pressures of 80 mmHg and a heart rate of 100 bpm.

458 Haemodynamic measurements: After induction of general anaesthesia, a central venous  
459 catheter (Arrow International, Reading, PA, USA) was inserted in the left jugular vein and an  
460 arterial catheter (Thermodilution Pulsioath; Pulsion Medical Systems, Munich, Germany) in



461 the right femoral artery. Cardiac output and stroke volume were assessed by transpulmonary  
462 thermodilution and indexed to the body surface area of the recipient using the formula  
463  $0.083 * \text{kg}_{\text{body weight}}^{0.639}$ . Measurements were taken after induction of anaesthesia and 60  
464 minutes after termination of CPB in steady state and recorded with PiCCOWin software  
465 (Pulsion Medical Systems, Munich, Germany). All data were processed with Excel  
466 (Microsoft, Redmond, Washington, USA) and analysed with GraphPad Prism 7.0 (GraphPad  
467 Software Inc., San Diego, California, USA).

468 Quantification of LV mass, LV mass increase and FS: Transthoracic echocardiographic  
469 examinations were carried out under analgosedation at regular intervals using an HP Sonos  
470 7500 (HP Inc., Palo Alto, CA, USA) and a Siemens Acuson X300 (Siemens AG, Munich,  
471 Germany); midpapillary short axis views were recorded. At end-diastole and end-systole, LV  
472 diameters (LVEDD, LVESD), diastolic and systolic interventricular (IVSd, IVSs), posterior  
473 wall thicknesses (PWd, PWs) were measured; the mean of three measurements was used for  
474 further calculations and visualisation (Excel and PowerPoint, Microsoft, Redmond,  
475 Washington, USA).

476 LV mass was calculated using formula 1, relative LV mass increase and LV FS using  
477 formulas 2 and 3<sup>14,15</sup>.

478 (1)  $\text{LV mass (g)} = 0.8(1.04([\text{LVEDD} + \text{IVSd} + \text{PWd}]^3 - [\text{LVEDD}]^3)) + 0.6$

479 (2)  $\text{LV mass increase (\%)} = ([\text{LV mass}_{\text{end}} / \text{LV mass}_{\text{start}}] - 1)100$

480 (3)  $\text{FS (\%)} = ([\text{LVEDD} - \text{LVESD}] / \text{LVEDD})100$

481 Necropsy and histology: Necropsies and histology were performed at the Institute of  
482 Veterinary Pathology and the Institute of Pathology (LMU Munich). Specimen were fixed in  
483 formalin, embedded in paraffin and plastic, sectioned and haematoxylin-eosin (HE) stained.

484 Histochemical analysis: Cryosections (8  $\mu\text{m}$ ) were generated using standard histological  
485 techniques. Myocyte size was quantified as cross-sectional area. 8  $\mu\text{m}$  thick cardiac sections  
486 of the left ventricle were stained with Alexafluor647-conjugated wheat germ agglutinin (Life  
487 Technologies) and the nuclear dye 4',6-diamidino-2-phenylindole (DAPI, Life Technologies).  
488 Images were acquired with a 63x objective using a Leica TCS SP8 confocal microscope;  
489 SMASH software (MATLAB, <https://de.mathworks.com/products/matlab.html>) was used to  
490 determine the average cross-sectional area of cardiomyocytes in one section (200-300 cells  
491 per section and 5-8 sections per heart).

492 Immunofluorescence staining: Myocardial tissue biopsies were embedded in Tissue-Tek  
493 (Sakura Finetek, Zoeterwoude, The Netherlands) and stored frozen at  $-80^{\circ}\text{C}$ . For  
494 immunofluorescence staining, 5  $\mu\text{m}$  cryosections were cut, air dried for 30 to 60 min and  
495 stored at  $-20^{\circ}\text{C}$  until further analysis. The cryosections were fixed with ice-cold acetone,  
496 hydrated and stained using either one-step direct or two-step indirect immunofluorescence  
497 techniques. The following antibodies were used: rabbit anti-human C3b/c (Dako, Glostrup,  
498 Denmark), rabbit anti-human C4b/c-FITC (Dako), goat anti-pig IgM (AbD Serotec, Hercules  
499 CA, USA), **goat anti-human IgG-FITC (Sigma Aldrich, St.Louis, MO, USA)**, rabbit anti-  
500 human fibrinogen-FITC (Dako). Secondary antibodies were donkey anti-goat IgG-Alexa 488  
501 (Thermo Fischer Scientific, MA, USA), sheep anti-rabbit Cy3 (Sigma-Aldrich). Nuclear  
502 staining was performed using DAPI (Boehringer, Roche Diagnostics, Indianapolis, IN, USA).  
503 The slides were analysed using a fluorescence microscope (DM14000B; Leica, Wetzlar,  
504 Germany). **Five to ten immunofluorescence pictures per each marker were acquired randomly  
505 and the fluorescence intensity was quantified using ImageJ software, version 1.50i  
506 (<https://imagej.nih.gov/ij/>), on unmanipulated TIFF images.** All pictures were taken under the  
507 same conditions to allow correct quantification and comparison of fluorescence intensities.

508 Assessment of anti-non-Gal antibody levels: Plasma levels of anti-non-Gal baboon IgM and  
509 IgG antibodies were measured by flow cytometry following the consensus protocol published  
510 by Azimzadeh et al. <sup>17</sup>. Briefly, GTKO/hCD46/hTM porcine aortic endothelial cells (PAEC)  
511 were harvested and suspended at  $2 \times 10^6$  cells/ml in staining buffer (PBS+1%BSA). Plasma  
512 samples were heat-inactivated at 56°C for 30 min and diluted 1/20 in staining buffer. PAEC  
513 were incubated with diluted baboon plasma for 45 minutes at 4°C. Cells were then washed  
514 with cold staining buffer and incubated with goat anti-human IgM-RPE (Southern Biotech,  
515 Birmingham, USA) or goat anti-human IgG-FITC (Thermo Fischer) for 30 minutes at 4°C.  
516 After rewashing with cold staining buffer, cells were resuspended in PBS, acquired on FACS  
517 LSRII (BD Biosciences, New Jersey, USA) and analysed using FlowJo analysis software for  
518 detection of mean fluorescence intensity (MFI) in the FITC channel or in the RPE channel.  
519 Data were then plotted using Prism 7 (Graphpad software, Inc.).

520 Western blot analysis: For protein extraction, heart samples were homogenised in Laemmli  
521 sample buffer, and protein content estimated using the bicinchoninic acid (BCA, Merck,  
522 Darmstadt, Germany) protein assay. 20 µg total protein was separated by 10% SDS-PAGE  
523 and transferred to PDVF membranes (Millipore, Billerica, USA) by electroblotting.  
524 Membranes were washed in Tris-buffered saline solution with 0.1% Tween-20 (Merck) (TBS-  
525 T) and blocked in 5% w/v fat-free milk powder (Roth, Karlsruhe, Germany) for 1 h at room  
526 temperature. Membranes were then washed again in TBS-T and incubated in 5% w/v BSA  
527 (Roth) of the appropriate primary antibody overnight at 4°C. The following antibodies were  
528 used: rabbit anti-human pmTOR (#5536; Cell Signaling, Frankfurt, Germany), rabbit anti-  
529 human mTOR (#2983; Cell Signaling), and rabbit anti-human GAPDH (#2118; Cell  
530 Signaling). After washing, membranes were incubated in 5% w/v fat-free milk powder with a  
531 horseradish peroxidase labelled secondary antibody (goat anti-rabbit IgG; #7074; Cell  
532 Signaling) for 1 h at room temperature. Bound antibodies were detected using an enhanced  
533 chemiluminescence detection reagent (ECL Advance Western Blotting Detection Kit, GE

534 Healthcare, Munich, Germany) and appropriate X-ray films (GE Healthcare). After detection,  
535 membranes were stripped (2% SDS, 62.5 mM Tris/HCl, pH 6.7, 100 mM  $\beta$ -mercaptoethanol)  
536 for 30 min at 70°C and incubated with an appropriate second antibody.

537 Immunohistochemical staining: Myocardial tissue was fixed with 4% formalin overnight,  
538 paraffin embedded and 3  $\mu$ m sections were cut and dried. Heat-induced antigen retrieval was  
539 performed in Target Retrieval solution (#S1699, Dako) in boiling water bath for 20 min for  
540 hCD46 and in citrate buffer, pH 6.0, in a steamer for 45 min for hTM, respectively.  
541 Immunohistochemistry was performed using the following primary antibodies: **mouse anti-**  
542 **human CD46 monoclonal antibody** (#HM2103, Hycult Biotech, Plymouth Meeting, PA,  
543 USA) and **mouse anti-human thrombomodulin monoclonal antibody** (sc-13164, Santa Cruz,  
544 Dallas, Texas, USA). Secondary antibody was biotinylated AffiniPure goat anti-mouse IgG  
545 (#115-065-146, Jackson ImmunoResearch, West Grove, PA, USA). Immunoreactivity was  
546 visualized using 3,3-diaminobenzidine tetrahydrochloride dihydrate (DAB) (brown colour).  
547 Nuclear counterstaining was done with haemalum (blue colour).

548 Statistical analysis: For survival data, Kaplan-Meier curves were plotted and the Mantel-Cox  
549 log-rank test used to determine significant differences between groups. For haemodynamic  
550 data, statistical significance was determined using unpaired and paired two-sided Student's t-  
551 test as indicated; data presented as single measurements with bars as group medians. For  
552 histochemical analysis, one-way ANOVA with Holm-Sidak's multiple comparisons was used  
553 to determine statistical significance; data presented as mean $\pm$ s.d.;  $p < 0.05$  was considered  
554 significant.

555 Data availability statement: The data that support the findings of this study are available from  
556 the corresponding author upon reasonable request.

557

558 **Extended Data Tables**

559 **Extended Data Table 1: Immunosuppressive regimen, anti-inflammatory and additive**  
560 **therapy with corresponding doses and timing intervals.** Immunosuppression was based on  
561 Mohiuddin's regimen<sup>5</sup>, with C1 esterase inhibitor instead of cobra venom factor for  
562 complement inhibition. Starting from 10 mg/kg/d, methylprednisolone was tapered down 1  
563 mg/kg every 10 days in group I and II; in group III, methylprednisolone was tapered down to  
564 0.1 mg/kg within 19 days. **In group III, temsirolimus was added to the maintenance**  
565 **immunosuppression, administered as daily infusions (rapamycin trough levels: 5-10 ng/ml).**  
566 **Group III animals also received continuous antihypertensive medication (enalapril,**  
567 **metoprolol tartrate).** Ab, antibody; mAb, monoclonal Ab; ATG, anti-thymocyte globulin;  
568 CMV, Cytomegalovirus; Fab, fragment antigen binding; IgG4, immunoglobulin G4; IL,  
569 interleukin; i.v., intravenous; MMF, mycophenolate mofetil; PASylated, conjugated with a  
570 long structurally disordered Pro/Ala/Ser amino acid chain; s.c., subcutaneous; TNF $\alpha$ , tumour  
571 necrosis factor  $\alpha$ .

572

573 **Extended Data Figures**

574 **Extended Data Figure 1: Haemodynamic data, measured by transpulmonary**  
575 **thermodilution and post-operative catecholamine support.** Measurements were taken after  
576 induction of anaesthesia (before CPB) and 60 minutes after termination of CPB (after CPB).  
577 Donor hearts of group I (black) received crystalloid cardioplegia, donor hearts of groups II  
578 (red) and III (magenta) were preserved with continuous cold hyperoncotic perfusion; data  
579 presented as scatter plots with **mean $\pm$ s.d.; n = 14 animals, two-sided** paired and unpaired t-  
580 tests, **p-values as indicated. a, stroke volume index** and **b, cardiac index** before and after CPB.  
581 Both parameters decreased in group I and were lower in group I after CPB than **in** group II  
582 and III. **c, Dosages of catecholamines** 60 minutes after termination of CPB and **d, durations of**

583 post-operative vasopressive and inotropic support. **Animals in** group I required more  
584 noradrenaline and epinephrine than **those in** group II and III. Animals in group I required  
585 inotropic support with epinephrine for a longer time.

586

587 **Extended Data Figure 2: Graphics of LV sizes during diastole (left) and systole (right),**  
588 **derived from transthoracic echocardiography. a,** Experiment #9 (group II, survival 40  
589 days): LV mass had increased by 303% on day 38, LV function was severely impaired due to  
590 myocardial hypertrophy and decreased LV filling volume. LV FS were 32% and 14% on day  
591 1 and 38. **b,** Experiment #11 (group III, survival 90 days): in contrast to experiment #9, LV  
592 mass had increased by only 22% on day 82, LV function was preserved. LV FS were 27% and  
593 34% on day 1 and 82. **c,** Pig 5157 (control, donor sibling of experiment #9): LV mass had  
594 increased by 187% on day 33, LV Function was preserved. LV FS were 32% and 41% on day  
595 1 and 33. Compared to experiment #9 (a), the LV had grown less in size, and showed no  
596 hypertrophy.

597

598 **Extended Data Figure 3: Additional laboratory parameters. a - b,** Serum concentrations  
599 of lactate dehydrogenase (a) and platelet counts (b) in animals of groups I (black), II (red) and  
600 III (magenta). At the end of experiments in groups I and II, platelet counts decreased while  
601 LDH increased. Group III animals did not show these alterations.

602

603 **Extended Data Figure 4: Immunofluorescent staining of myocardial tissue. a-d,**  
604 Immunofluorescent stainings of myocardial sections from group I (#3; left row), group II (#9;  
605 middle row), and group III (#11, right row) for IgM (a), IgG (b), C3b/c (c; red), C4b/c (c;  
606 green), and fibrin (d); nuclei stained with DAPI (blue); scale bars = 25  $\mu$ m. n = 1, group I; n =

607 3, group II; n = 5, group III; one representative biological sample per group is shown.

608

609 **Extended Data Figure 5: Immunohistochemistry of post-mortem myocardial specimen**  
610 **(experiments #1-14). a-b,** Expression of human membrane cofactor protein (hCD46) **(a)** and  
611 human thrombomodulin (hTM) **(b)** was **consistent** in all donor organs; **scale bar = 50µm. n =**  
612 **14, GTKO/hCD46/hTM pigs; n = 1, wild-type pig (control). Biological samples from all**  
613 **animals are shown.**

614

#### 615 **Supplementary Information**

616 **Supplementary Video 1: Transthoracic echocardiographic midpapillary short axis views**  
617 **of porcine grafts after cardiac xenotransplantation. a,** Experiment #9 (group II, **day 30**):  
618 increased LV wall thickness and reduced LV filling volume indicating myocardial  
619 hypertrophy. LV function was impaired. **b,** Experiment #11 (group III, **day 57**): normal LV  
620 wall thickness and normal LV filling volume. LV function was preserved. **c,** Experiment **#14**  
621 (group III, **day 180**): **increased LV wall thickness, but** normal LV filling volume. LV function  
622 was preserved. **a-c, n = 4, groups I/II; n = 5, group III; one representative video from groups**  
623 **I/II and two representative videos from animals of group III at different time points are**  
624 **shown.**

625

#### 626 **Supplementary Figure 1: Gel Source data**

627

Figure 1

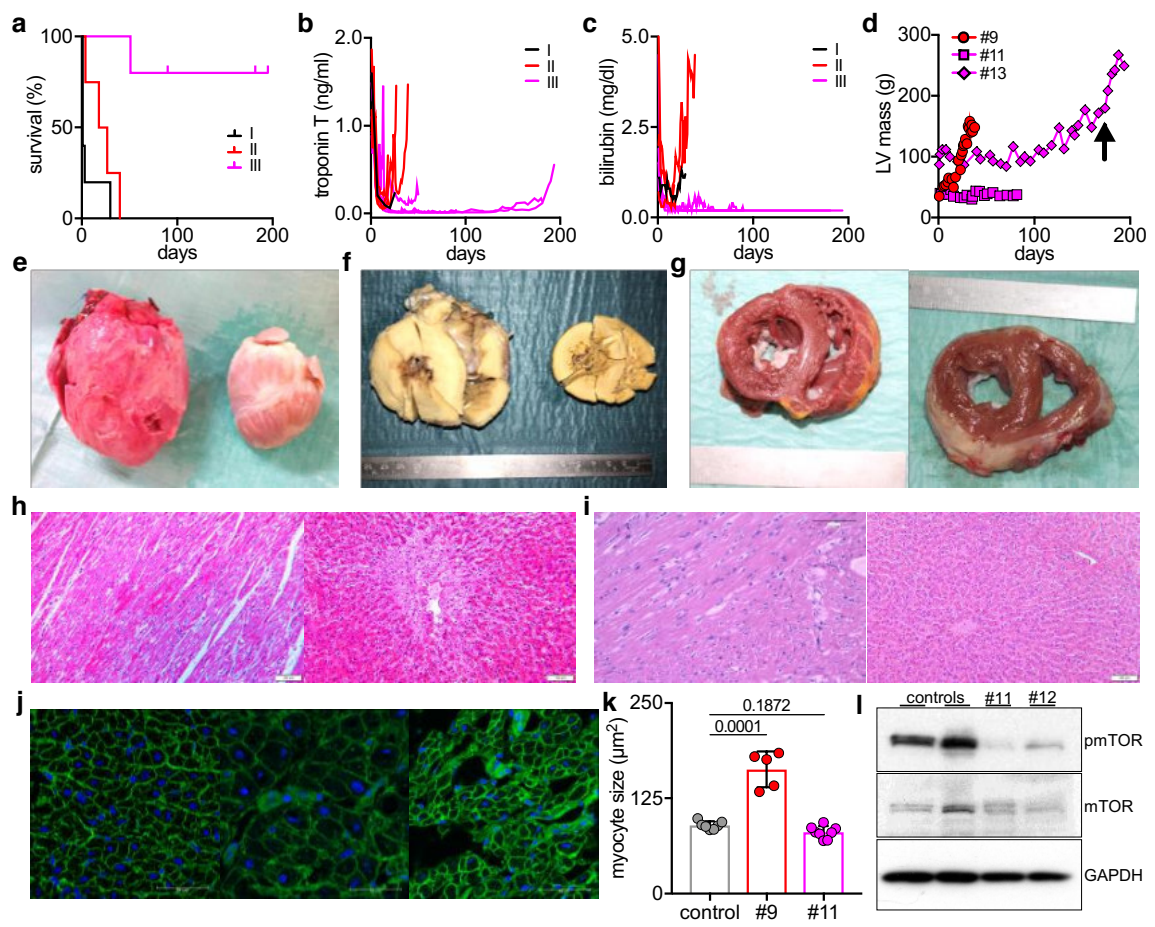
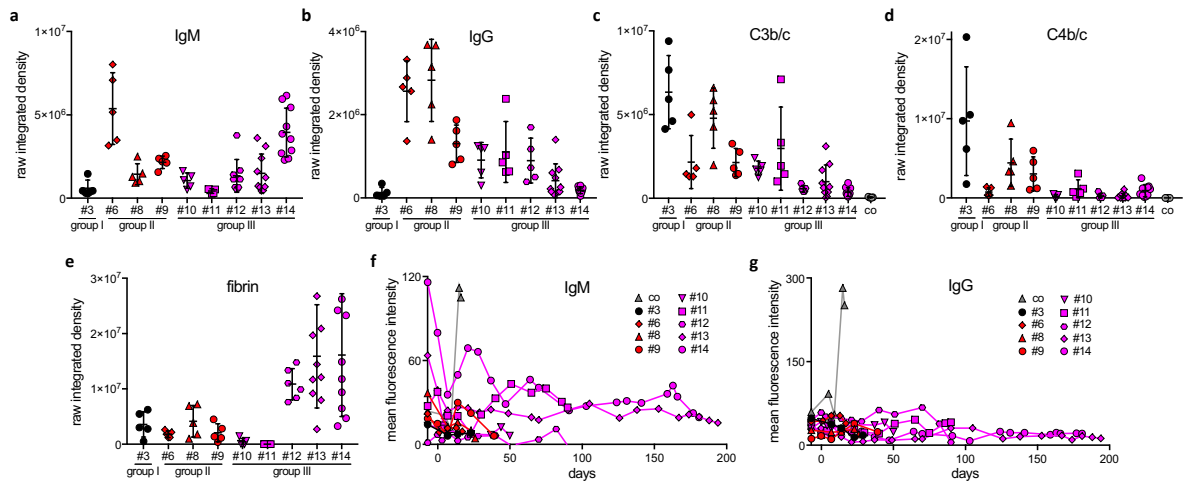




Figure 2

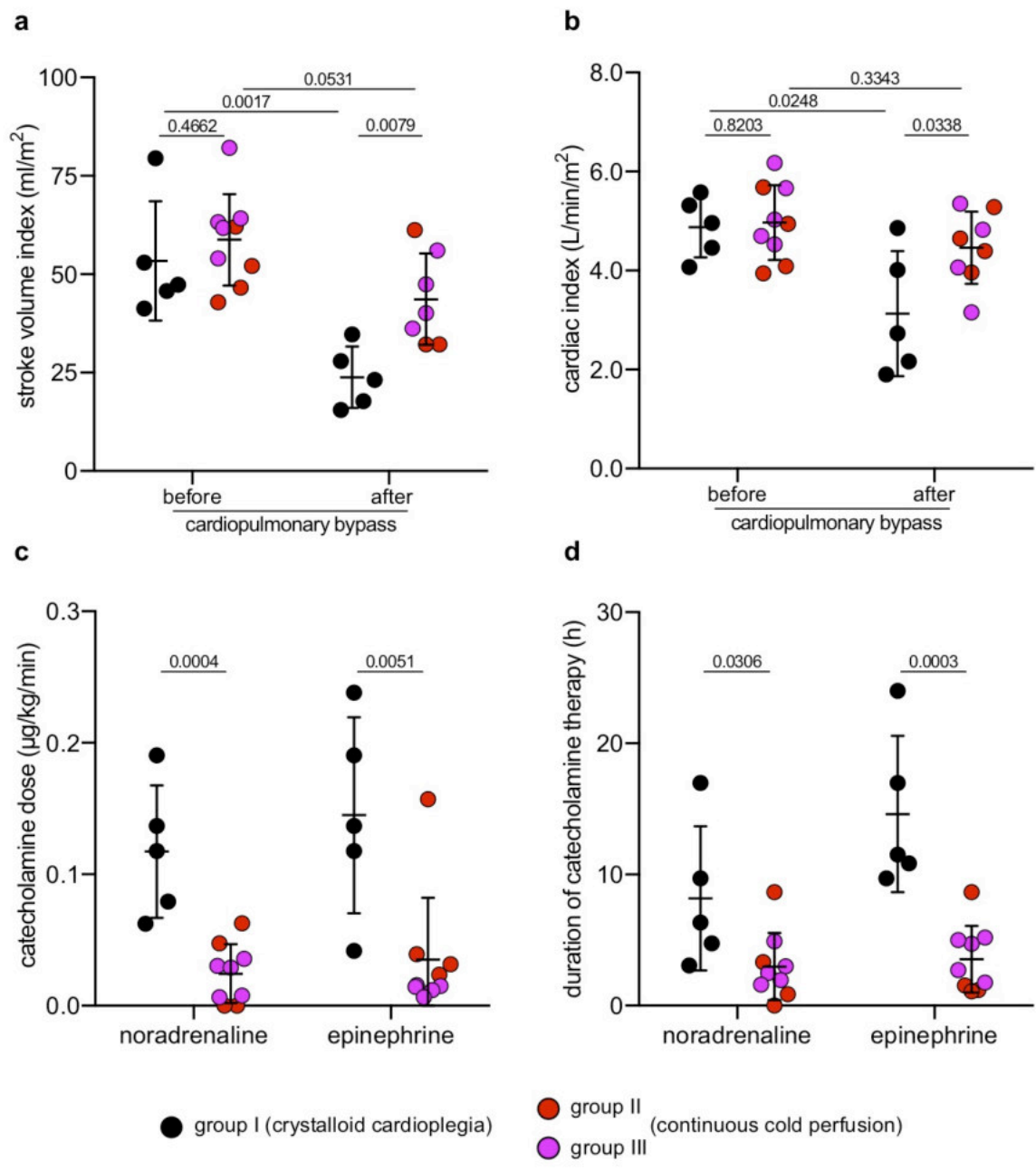


Extended Data Table 1

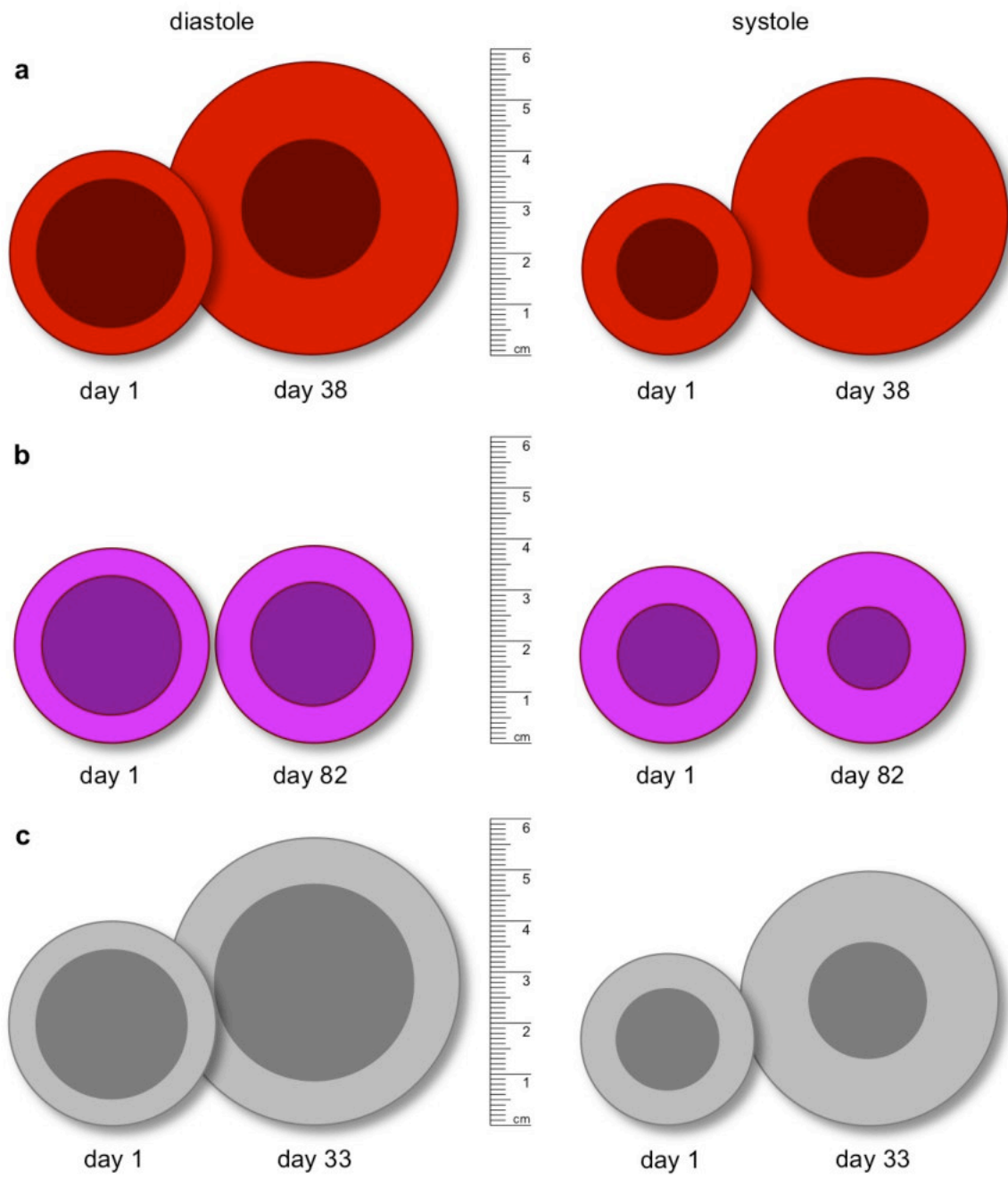
| Agent   | Dose  | Timing                             |
|---|---|------------------------------------|
| Induction                                     |   |                                    |
| anti-CD20 Ab                                  | 19 mg kg <sup>-1</sup> , i.v. short infusion                              | days -7, 0, 7 and 14               |
| ATG   | 5 mg kg <sup>-1</sup> , continuously i.v.                                 | days -2 and -1                     |
| anti-CD40 mAb or<br>anti-CD40L PASylated Fab* | 50 mg kg <sup>-1</sup> or 20 mg kg <sup>-1</sup> ;<br>i.v. short infusion | days -1 and 0                      |
| Maintenance                                   |   |                                    |
| MMF   | 40 mg kg <sup>-1</sup> , continuously i.v.                                | daily, started on day -2           |
| anti-CD40 mAb or<br>anti-CD40L PASylated Fab* | 50 mg kg <sup>-1</sup> or 20 mg kg <sup>-1</sup><br>i.v. short infusion   | days 3, 7, 10, 14, 19, then weekly |
| methylprednisolone                            | 10 mg kg <sup>-1</sup> , bolus i.v.                                       | daily, tapered down                |
| Anti-inflammatory therapy                     |   |                                    |
| IL6-receptor antagonist                       | 8 mg kg <sup>-1</sup> , short infusion i.v.                               | monthly                            |
| TNF $\alpha$ inhibitor                        | 0.7 mg kg <sup>-1</sup> , bolus s.c.                                      | weekly                             |
| IL1-receptor antagonist                       | 1.3 mg kg <sup>-1</sup> , bolus s.c. or i.v.                              | daily                              |
| Additive therapy                              |   |                                    |
| acetylsalicylic acid                          | 2 mg kg <sup>-1</sup> , bolus i.v.  | daily                              |
| unfractionated heparin                        | 20-40 U kg <sup>-1</sup> h <sup>-1</sup> , continuously i.v.              | daily, started on day 5            |
| C1 esterase inhibitor                         | 17.5 U kg <sup>-1</sup> , i.v. short infusion                             | days 0, 1, 7 and 14                |
| ganciclovir                                   | 5 mg kg <sup>-1</sup> , continuously i.v.                                 | daily                              |
| cefuroxim                                     | 50 mg kg <sup>-1</sup> , continuously i.v.                                | daily, prophylaxis from day 0 to 5 |
| epoetin beta                                  | 2,000 U, bolus s.c. or i.v.   | days -7, 0 and if necessary        |

\*anti-CD40 mAb: #1-3, #5, #7-8, #11-14; anti-CD40L PASylated Fab: #4, #6, #9, #10

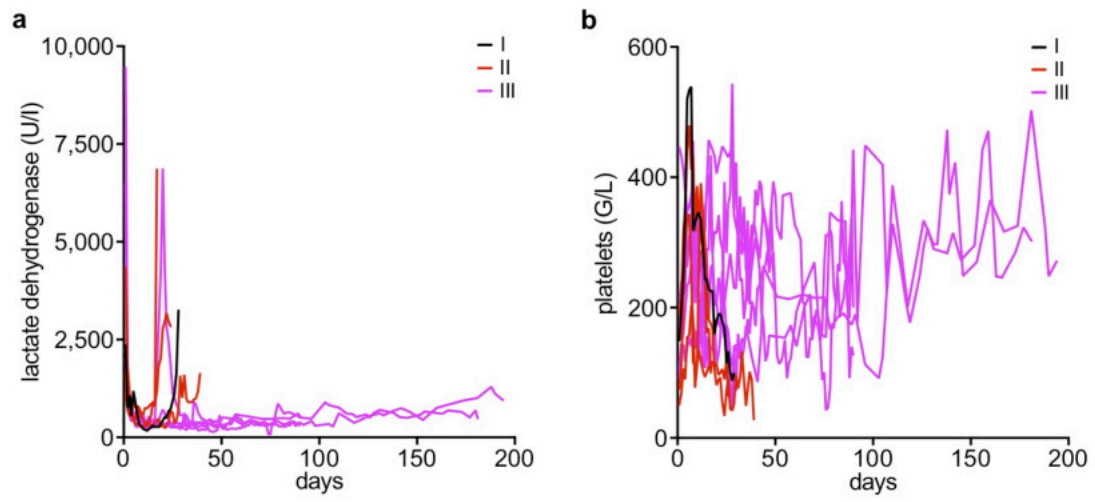
Extended Data Figure 1



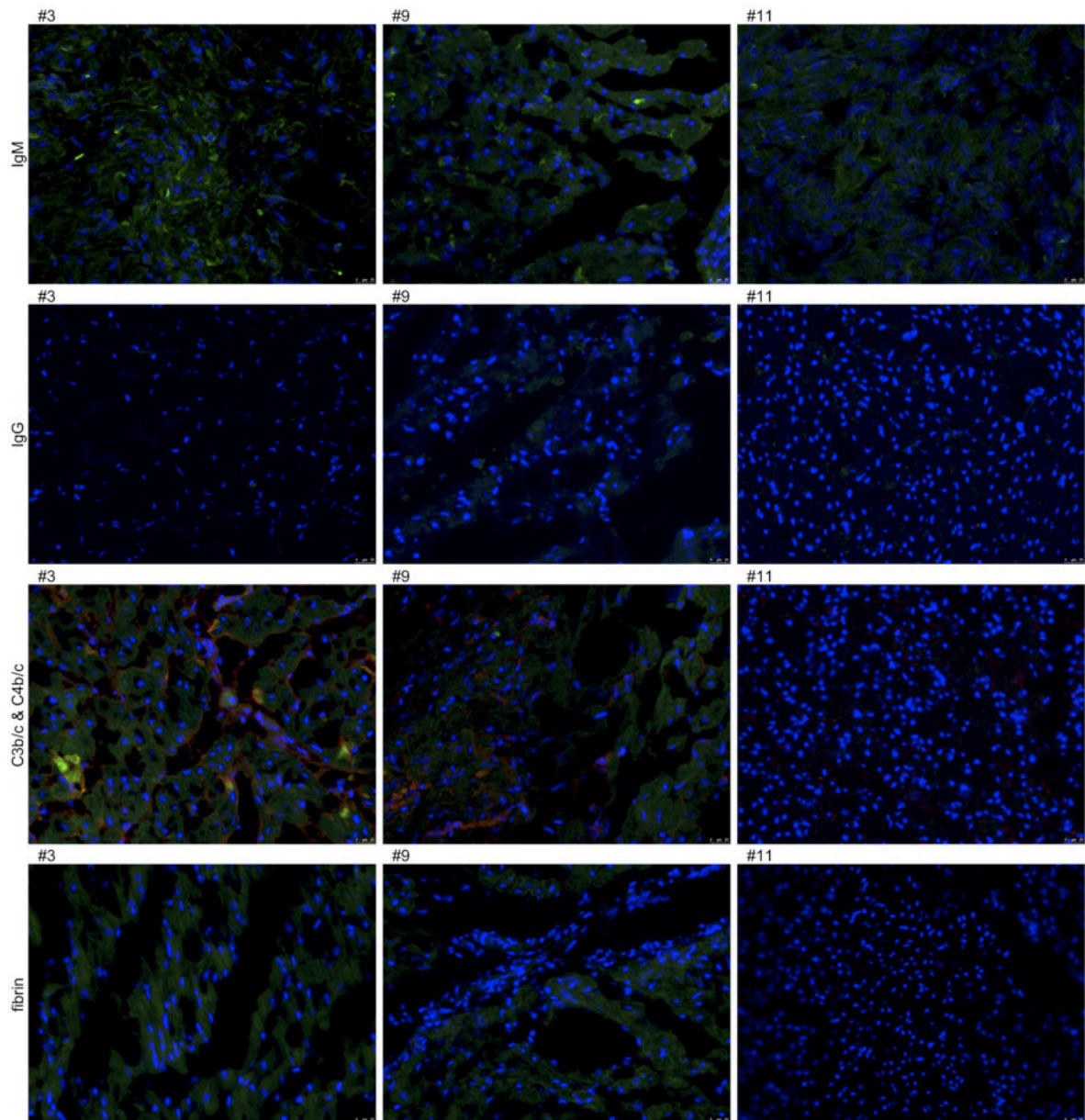
Extended Data Figure 2



Extended Data Figure 3

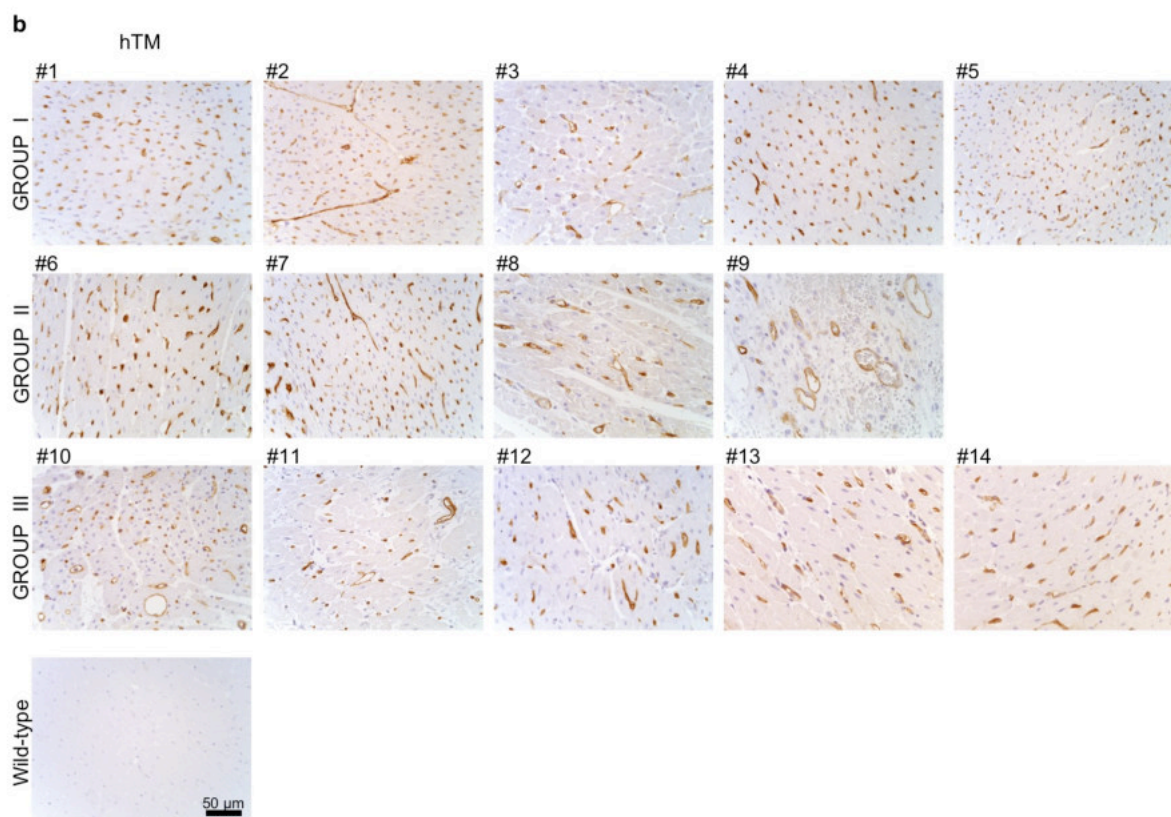
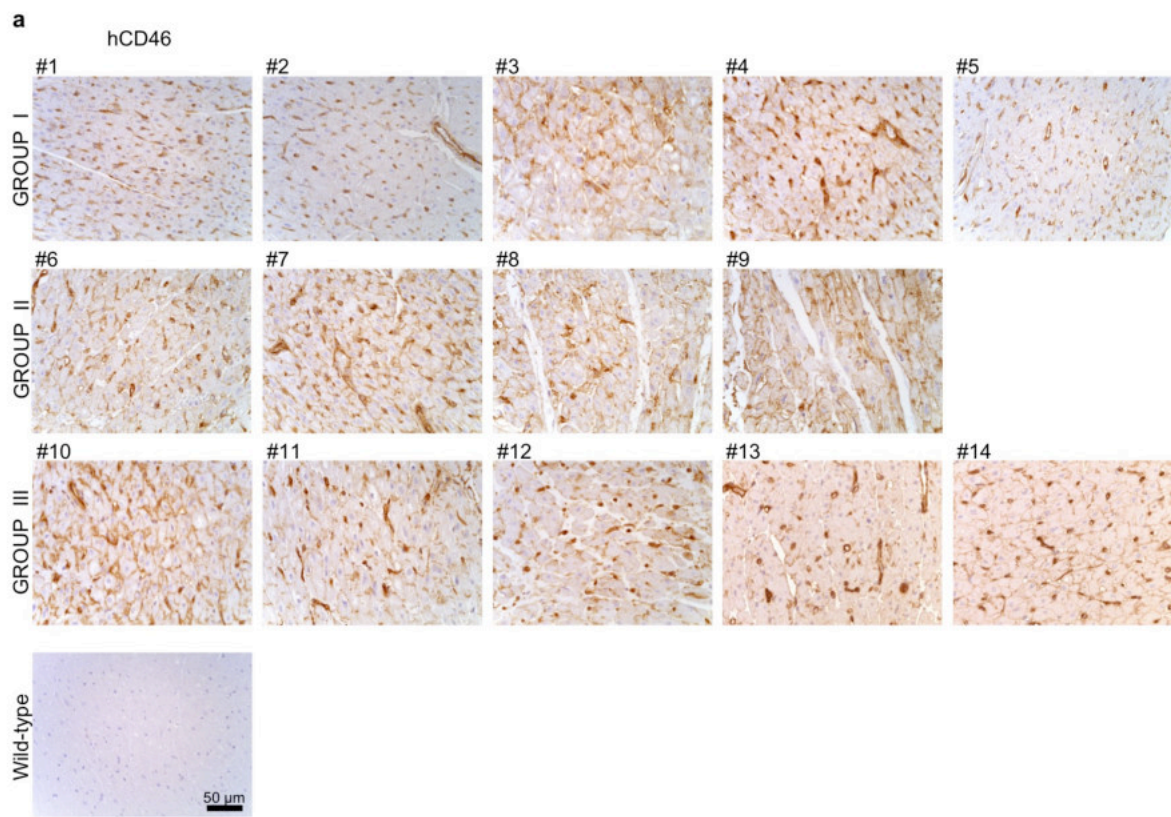


Extended Data Figure 4





# Extended Data Figure 5







## Overall discussion and outlook

Pig-to-human xenotransplantation may provide a solution to the shortage of organ donors. However, molecular incompatibilities and immunological mechanisms responsible for xenograft rejection need to be understood and overcome in order to pave the way for clinical application. Genetic manipulations of the organ donor together with a clinically compatible immunosuppressive regimen are leading to considerable advancements in the prolongation of graft survival in pre-clinical pig to non-human primate models. However, endothelial cell activation followed by graft intravascular thrombosis, thrombocytopenia and consumptive coagulopathy in the recipient are typical outcomes of acute vascular rejection which currently represents a major obstacle.

*In vitro* models which allow to mimic (xenogeneic) activation of EC as well as to study their natural anti-inflammatory and anticoagulant properties are fundamental not only in xenotransplantation research but also in other clinical conditions.

Culturing porcine EC on the surface of microcarrier beads (Paper I) permitted to increase the surface-to-volume ratio allowing to exploit the physiological properties of EC when incubated with non-anticoagulated human blood. Furthermore, a novel *in vitro* microfluidic model (Paper II) was established. EC were cultured in round section microchannels and exposed to physiological flow and shear stress in a closed recirculating system. A time- and volume-dependent increase of EC activation (E-selectin) and complement deposition (C3b/c) was observed. Complement inhibitors such as C1 INH, APT070, and DXS showed to prevent activation of complement and EC in a xenotransplantation setting.

Other studies (Paper IV and Paper V) showed that combined overexpression of hCD46 and HLA-E guaranteed protective effects when pig limbs or porcine hearts were *ex vivo* perfused with heparinized, whole human blood. No hyperacute rejection was observed in both studies. Furthermore, inhibition of the terminal pathway of complement by blocking the central complement proteins C3b and C4b and a greater protection against NK cells binding to xenogeneic tissue was demonstrated. The model allowed to assess NK cell migration after 8 hours of perfusion and it might be

a helpful tool to further assess the role of other transgenes in preventing delayed cellular rejection.

In collaboration with Munich, pre-clinical orthotopic pig-to-baboon cardiac xenotransplantation experiments were performed using GTKO/hCD46/hTM transgenic pigs (Paper VI). Increase of plasma anti-nonGal antibody levels due to rejection was not observed. The complement and coagulation activation were efficiently controlled by the genetic modification of donor pigs. This, combined with the optimized non-ischemic organ preservation techniques, the immunosuppressive regimen and the anti-inflammatory treatments contributed to the prolonged survival of the transplanted porcine organs beyond 180 days.

The extremely rapid development of genetically engineered pigs will probably bring clinical xenotransplantation closer to reality in the near future. However, it is hard to estimate the exact number and combination of genetic modifications necessary for a successful xenotransplantation. In this view, we propose to use our *in vitro* microfluidic model for testing of genetically modified EC and to provide fundamental data which can help to identify the best, organ-specific combination of transgenes to be used in the future pre-clinical pig-to-baboon experiments.

Besides that, the study of the endothelial glycocalyx and the interactions with important plasma proteins – such as C1 inhibitor, superoxide dismutase, antithrombin III, fibroblast growth factor, vascular endothelial growth factor – might reveal interesting molecular insights into the compatibility or incompatibility between porcine endothelial cell glycocalyx and human plasma proteins allowing for a better understanding of its role in acute vascular rejection. Preliminary results showed that in our *in vitro* microfluidic system normal humans serum induces strong shedding of the endothelial glycocalyx<sup>38</sup> and as a consequence the anti-coagulant and anti-inflammatory properties of the EC are lost. Prevention of glycocalyx shedding in xenotransplantation will certainly help to prevent endothelial cell activation and the consequent inflammation and coagulation activation which are typical hallmarks of the acute vascular rejection.

## Acknowledgments

I would like to acknowledge all the people who have helped me throughout my PhD. First of all, I would like to express my utmost gratitude to my supervisor Prof. Dr. Robert Rieben for giving me the opportunity to start my scientific career with an amazing PhD full of collaborations, congresses, travels and results. Thanks to his guidance, motivation, advices and constant support he contributed a lot to completing my thesis.

I am also grateful to Prof. Dr. Jörg Seebach and Dr. Ruth Lyck who accepted to be my co-supervisor and mentor, respectively. I would like to thank Prof. Dr. Emanuele Cozzi from the University of Padua for having kindly accepted to assess my thesis as external co-referee.

I greatly appreciated the help and constant support from all the lab members: Dr. Adriano Taddeo, Alain Despont, Oliver Steck, Jane Shaw, Yvonne Roschi and Uyen Vo as well as the former colleagues, namely Dr. Shengye Zhang, Dr. Mai Abdelhafez, Dr. Dzhuliya Dzhonova and Pavan Garimella.

Furthermore, I would like to thank the many collaborators who helped me with my work and gave me a great opportunity to actively contribute to their research, particularly Dr. Jan-Michael Abicht, Dr. Matthias Längin, Prof. Dr. Bruno Reichart, Dr. Nikolai Klymiuk, Prof. Dr. Eckhard Wolf, Dr. Andrea Bähr, Dr. Annegret Wünsch, from Munich for their support in providing all the transgenic cells for my experiments, tissue biopsies and plasma samples from *ex vivo* xenoperfusion studies as well as from preclinical xenotransplantation experiments.

Last but not least, I wish to thank my family and especially a huge thank to my wife Martina. I will be forever indebted to her. She was always there to support and to motivate me with patience and love during my studies as well as in our day to day life.

Finally, I would like to thank everybody who was important to the success of this thesis, as well as to express my apologies if I have not mentioned all of them.



# Riccardo Sfriso

## Curriculum Vitae

Born on December 27, 1988 in Chioggia, Italy  
Swiss B permit

Email: [riccardo.sfriso@dbmr.unibe.ch](mailto:riccardo.sfriso@dbmr.unibe.ch)

ORCID: 0000-0002-3406-0736



### Education

2015 – 2018                      PhD in Biomedical Sciences, University of Bern  
2008 – 2014                      PharmD, Chemistry and Pharmaceutical Technologies,  
University of Padova

### Working experience

2015 – 2018                      PhD student in Biomedical Sciences, University of Bern  
2008 – 2014                      MSc student thesis internship, Department of  
Pharmaceutical and Pharmacological Sciences, University  
of Padova (Italy)

### Awards

2018                                ICS Travel Award for the XXVII International Complement  
Workshop 2018, Santa Fe (New Mexico)  
2017                                TTS-IXA Travel Award for the 14<sup>th</sup> Congress of the  
International Xenotransplantation Association 2017,  
Baltimore (USA)  
2016                                ICS Poster Award at the XXVI International Complement  
Workshop 2016, Kanazawa (JPN)

### Research Grants

2018                                Johanna Dürmüller-Bol Foundation (24'532 CHF)

## **Teaching**

- Practical courses in biomedical research (Wahlpraktikum) for MD students
- Tutoring Master theses for students in biomedical sciences
- Tutoring Bachelor and Master theses for students of Molecular Life Sciences
- Tutoring "Matura projects" within the program for the promotion of young scientists of the Swiss Academy of Science
- Immunology Practical courses for BSc students of the Natural Life Sciences Faculty, University of Bern.

## **Contribution to Scientific Peer-Review**

Journal: Xenotransplantation

## **Memberships**

The Transplantation Society

International Xenotransplantation Association

Swiss Transplantation Society

International Complement Society

## Publications

1. Längin M, Mayr T, Michel S, Buchholz S, Guethoff S, Dashkevich A, Bähr A, Egerer S, Bauer A, Mihalj M, Panelli A, Issl L, Ying J, Fresch AK, Werner F, Lutzmann I, Steen S, Sjöberg T, Paskevicius A, Liao Q, **Sfriso R**, Rieben R, et al. Consistent success in life supporting porcine cardiac xenotransplantation. Nature. Accepted for publication.
2. **Sfriso R**, Zhang S, Bichsel C, Steck O, Despont A, Guenat O, Rieben R. 3D artificial round section micro- vessels to investigate endothelial cells under physiological flow conditions. Sci Rep 2018 Apr 12; 8(1):5898. doi:10.1038/s41598-018-24273-7
3. Abicht J-M, **Sfriso R**, Reichart B, et al. Multiple genetically modified GTKO/hCD46/HLA-E/h $\beta$ 2–mg porcine hearts are protected from complement activation and natural killer cell infiltration during ex vivo perfusion with human blood. Xenotransplantation. 2018; e12390.
4. Puga Yung G, Bongoni A, Pradier A, Madelon N, Papaserafeim M, **Sfriso R**, et al. Release of pig leukocytes and reduced human NK cell recruitment during ex vivo perfusion of HLA-E/human CD46 double- transgenic pig limbs with human blood. Xenotransplantation. 2017; e12357
5. **Sfriso R**, Bongoni A, Banz Y, Klymiuk N, Wolf E, Rieben R. Assessment of the anticoagulant and anti- inflammatory properties of endothelial cells using 3D cell culture and non-anticoagulated whole blood. J Vis Exp. 2017 Sep 5;(127): e56227–7
6. Di Liddo R, Bertalot T, Schuster A, Schrenk S, Müller O, Apfel J, Reischmann P, Rajendran S, **Sfriso R**, et al. Fluorescence-based gene reporter plasmid to track canonical Wnt signaling in ENS inflammation. Am J Physiol Gastrointest Liver Physiol. American Physiological Society; 2016 Mar 15; 310(6):G337–46

## Book chapters

1. **Sfriso R**, Rieben R. 3D cell culture models for the assessment of anticoagulant and anti-inflammatory properties of endothelial cells. (Chapter 7) *Methods in Molecular Biology*. Springer Nature.

## Published abstracts

1. **Sfriso R.**, Rieben R., Imaging of porcine endothelial glycocalyx by confocal microscopy and assessment of its shedding by human serum in an in vitro microfluidic model of pig-to-human xenotransplantation, *Vasa* vol. 47/Supplement 100. Oct. 2018
2. **Sfriso R.**, Steck O., Fisher K., Schnieke A., and Rieben R., Reduced complement deposition on multitransgenic porcine fibroblasts in a xeno-microfluidic model, *Mol. Immunol.*, vol. 102, pp. 211–212, Oct. 2018.
3. **Sfriso R.**, Abdelhafez M., and Rieben R., Allogeneic complement activation in vitro using porcine aortic endothelial cells and porcine serum, *Mol. Immunol.*, vol. 102, p. 212, Oct. 2018.
4. **Sfriso R.**, Abicht J. M., Längin M., Mayr T., Reichart B., and Rieben R., Prevention of complement-mediated rejection in pig-to-baboon cardiac xenotransplantation, *Mol. Immunol.*, vol. 102, p. 212, Oct. 2018.
5. **Sfriso R.**, Steck O., Fischer K, et al., Multitransgenic porcine fibroblasts are protected from immunoglobulin binding and complement deposition in a xeno-microfluidic model, *Transplantation*, vol. 102, p. S106, Jul. 2018.
6. **Sfriso R.** and Rieben R., Real time high-resolution imaging of porcine endothelial glycocalyx shedding by human serum in an in vitro microfluidic model of pig-to-human xenotransplantation, *Transplantation*, vol. 102, p. S741, Jul. 2018.



7. **Sfriso, R.**, Abicht J., Mayr T., et al. Evaluation of innate immune activation after ex vivo xenoperfusion of GTKO/Hcd46/HLA- E transgenic pig hearts with human blood. *Xenotransplantation* 24, 5 (2017)
8. **Sfriso, R.**, Steck O., Rieben R. 3D artificial blood vessels to study acute vascular rejection in xenotransplantation. *Xenotransplantation* 24, 5 (2017)
9. Wünsch A., Kameritsch P., **Sfriso R.**, Bähr A., et al. Monitoring the activation status of endothelial cells by a genetically encoded calcium-sensor. *Xenotransplantation* 24, 5 (2017)
10. Rieben, R., **Sfriso R.**, Abicht J., et al. Assessment of complement and NK cell activation in GalTKO/hCD46/HLA-E porcine hearts ex vivo xenoperfused with human blood. *Mol. Immunol.* 89, 207 (2017)
11. **Sfriso R.**, Steck O., Bähr A., et al. In vitro assessment of xenogeneic complement and endothelial cell activation using a microvascular flow model. *Mol. Immunol.* 89, 209 (2017)
12. **Sfriso R.**, Klymiuk N., Wünsch A., et al. Activation of complement and coagulation in xenotransplantation: Effect of growth hormone receptor knockout on porcine aortic endothelial cells. *Immunobiology* 221, 1174–1175 (2016)
13. **Sfriso R.**, Zhang S., Bichsel C. A., Guenat O. T. & Rieben R. A vessel-like microfluidic system to study complement and coagulation in the context of xenotransplantation. *Immunobiology* 221, 1175 (2016)
14. **Sfriso R.**, Garimella P., Puga Yung G., et al. Functional Evaluation of Immortalized Porcine Endothelial Cells in a Whole Blood Clotting Assay. *Transplantation* 99, S106–S106 (2015)

## Oral Presentations and Invited lectures

- 16-20 Sep 2018 "Prevention of complement-mediated rejection in pig-to-baboon cardiac xenotransplantation". XXVII International Complement Workshop, Santa Fe (New Mexico)
- 02-05 July 2018 "Multitransgenic Porcine Fibroblasts are Protected from Immunoglobulin Binding and Complement Deposition in a Xeno-Microfluidic Model". International Congress of the Transplantation Society, Madrid (ESP).
- 05 March 2018 "A 3D Microvascular Flow System to Investigate Pig to Human Xenotransplantation in Vitro". Seminar. Theodor Kocher Institute, University of Bern
- 11-13 Oct 2017 "Multitransgenic Porcine Fibroblasts are Protected from Immunoglobulin Binding and Complement Deposition in a Xeno-Microfluidic Model". SFB TRR 127 Meeting, San Servolo, Venice (ITA).
- 20-23 Sep 2017 "Evaluation of Innate Immune Activation After Ex Vivo Xenoperfusion of GTKO/hCD46/HLA-E Transgenic Pig Hearts with Human Blood".  
  
"3D Artificial Blood Vessels to Study Acute Vascular Rejection in Xenotransplantation". 14th International Xenotransplantation Association (IXA) Congress in Baltimore, Maryland, (USA)
- 02-04 May 2017 "A 3D Microvascular Flow System to Investigate Pig to Human Xenotransplantation in Vitro". SFB TRR 127 Spring Meeting in Göttingen (DE).
- 18-23 Aug 2016 "Growth Hormone Receptor Knockout on Porcine Aortic Endothelial Cells: Effect on Complement and Coagulation".

International Congress of the Transplantation Society, Hong Kong.

15-19 Nov 2015 "Functional Evaluation of Immortalized Porcine Endothelial Cells in a Whole Blood Clotting Assay". International Xenotransplantation Joint congress, Melbourne (AUS).

28-30 Sept 2015 "Porcine Aortic Immortalized Endothelial Cells: Characterization and Evaluation of the Anticoagulant Phenotype in a Whole Blood Clotting Assay." 8th Minisymposium on Xenotransplantation, Freising (DE).



## **Declaration of Originality**

**Last name, first name:** Sfriso Riccardo

**Matriculation number:** 14-140-719

I hereby declare that this thesis represents my original work and that I have used no other sources except as noted by citations.

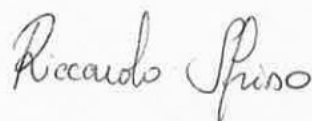
All data, tables, figures and text citations which have been reproduced from any other source, including the internet, have been explicitly acknowledged as such.

I am aware that in case of non-compliance, the Senate is entitled to withdraw the doctorate degree awarded to me on the basis of the present thesis, in accordance with the "Statut der Universität Bern (Universitätsstatut; UniSt)", Art. 69, of 7 June 2011.

**Place, date**

Bern, 26.10.2018

**Signature**

A handwritten signature in cursive script that reads "Riccardo Sfriso".